

**Biological Treatment of Perchlorate and Nitrate Contaminated  
Drinking Water**  
– Optimization of System Performance Using Microbial Community  
Characterization

by

**Xu Li**

A dissertation submitted in partial fulfillment  
Of the requirements for the degree of  
Doctor of Philosophy  
(Environmental Engineering)  
in The University of Michigan  
2008

Doctoral Committee:

Professor Lutgarde M. Raskin, Co-Chair  
Associate Professor Eberhard F. Morgenroth, Co-Chair, University of Illinois  
Professor Peter Adriaens  
Assistant Professor Chuan Wu Xi  
Professor Laurie A. Achenbach, Southern Illinois University  
Jess C. Brown, Carollo Engineers

© Xu Li

---

2008

**Dedication**

致亲人和挚友

**To Family and Good Friends.**

## **Acknowledgements**

I first would like to thank Lutgarde Raskin, my Ph.D. advisor, who provided the guidance and academic framework from which I was able to learn and grow. She demonstrated how to be a good researcher in many ways. I would also like to thank my co-advisor Eberhard Morgenroth, who gave me support both before and after I left the University of Illinois. I also owe appreciation to my committee members, Jess Brown, Laurie Achenbach, Chuanwu Xi, and Peter Adriaens, for their valuable input during my research.

I would like to thank my colleagues and friends at the University of Illinois and the University of Michigan: Young-Chul Choi, Toshio Shimada Beltran, Zhi Zhou, Sudini Padmasiri, Dominic Frigon, Aurelio Briones, Chuanwu Xi, Tara Jackson, Giridhar Upadhyaya, Wangki Yuen, Lynn Williams, Andrew Henderson and others. Special thanks to Young-Chul, Chuanwu, and Rocky, who shared their wisdom with me and helped me start my research. Another special thank you to Tara, who has been a good friend to me in many ways. For those I have unintentionally omitted, I appreciate the opportunity to work with you, and your support will never be forgotten.

I would also like to thank Tom Yavaraski, for his assistant in instrument analysis, and Peter Adriaens and Jeremy Semrau, for access to equipment. Part of the work was the result of collaborative efforts with people at Carollo Engineers. I would like to thank Gregorio Estevao and Axel Etori for the pilot-scale reactor performance data.

To mom and dad – I cannot express in words how blessed I feel about having you as parents. You were wonderful role models to me, and you have supported me in every

way a person can be supported. To other family members – you are part of my daily life more than you know and I love you all.

I would also like to acknowledge the funding sources: U.S. National Science Foundation (BES-0123342) and U.S. Department of Defense (ESTCP ER-0554).

## Table of Contents

Dedication.....	ii
Acknowledgements.....	iii
List of Tables.....	viii
List of Figures.....	ix
List of Appendices.....	xiv
Abstract.....	xv
Chapter 1 Introduction, Objectives, and Strategies .....	1
1.1 Perchlorate Contamination and Treatment Technologies.....	1
1.2 Perchlorate Reducing Bacteria.....	5
1.3 Microbial Communities in Engineered Systems.....	7
1.4 Objectives .....	9
1.5 Research Strategies .....	11
1.6 Figures.....	13
1.7 References.....	14
Chapter 2 Quantitative rRNA-Targeted Solution-Based Hybridization Assay	
Using Peptide Nucleic Acid Molecular Beacons.....	21
2.1. Introduction.....	21
2.2. Materials and Methods.....	24
2.2.1 PNA MBs.....	24
2.2.2 RNA Extractions.....	25
2.2.3 Hybridizations.....	26
2.2.4 Data Analysis.....	28
2.2.5 Detection Limit.....	29
2.3. Results.....	29
2.3.1 Response of PNA MB in the Absence of rRNA.....	29
2.3.2 Hybridization Kinetics.....	30
2.3.3 Optimization of Hybridization Conditions .....	32
2.3.4 Detection Limit .....	35
2.3.5 Spike-in Experiment .....	35
2.3.6 Environmental Samples .....	35
2.4. Discussion.....	36
2.5. Tables.....	42
2.6. Figures.....	45
2.7. References.....	55

Chapter 3	Effects of Increases in Backwash Frequency and Intensity on Reactor Performance and Microbial Community Structure in a Biofilm Reactor .....	61
3.1.	Introduction.....	61
3.2.	Materials and Methods.....	64
3.2.1.	Reactor Operation .....	64
3.2.2.	Data Analyses on Reactor Performance .....	65
3.2.3.	Extracellular and Intracellular DNA Extractions and Protein Assay.....	66
3.2.4.	Clone Library .....	66
3.2.5.	Phylogenetic Analyses.....	67
3.2.6.	Real-time PCR Primer Design and Reaction Conditions .....	68
3.2.7.	Real-time PCR Standard Curves.....	69
3.3.	Results.....	71
3.3.1.	eDNA .....	71
3.3.2.	Microbial Community.....	72
3.3.3.	Real-time PCR Standard Curves.....	73
3.3.4.	Daily Weak Backwash Experiment .....	74
3.3.5.	Daily Strong Backwash Experiment.....	76
3.4.	Discussion.....	77
3.5.	Tables.....	81
3.6.	Figures.....	85
3.7.	References.....	96
Chapter 4	Effects of Phosphorus Addition on Reactor Performance and Microbial Communities of Biologically Active Carbon (BAC) Reactors for Drinking Water Treatment .....	101
4.1.	Introduction.....	101
4.2.	Materials and Methods.....	103
4.2.1.	Reactor Operation .....	103
4.2.2.	Chemical Measurements.....	105
4.2.3.	Clone Library .....	106
4.2.4.	Microbial Sequence Analyses.....	107
4.2.5.	Real-Time PCR.....	108
4.3.	Results.....	110
4.3.1.	Bench- and Pilot-scale BAC Reactor Performance .....	110
4.3.2.	Microbial Communities in the Bench- and Pilot-scale BAC Reactors....	111
4.3.3.	Comparison of Microbial Community Structures.....	112
4.3.4.	Microbial Population Dynamics in the Bench-scale BAC .....	113
4.4.	Discussion.....	114
4.5.	Tables.....	118
4.6.	Figures.....	122
4.7.	References.....	131
Chapter 5	Operation of a Biologically Active Carbon Reactor to Treat Nitrate and Perchlorate Contaminated Drinking Water.....	136
5.1	Introduction.....	136

5.2	Materials and Methods.....	139
5.2.1	Intermittent Electron Donor Addition Experiment.....	139
5.2.2	Adsorption Isotherm Experiment.....	140
5.2.3	Mass Balance Calculation.....	141
5.2.4	Disinfection Experiment.....	142
5.3	Results.....	143
5.3.1	Intermittent Electron Donor Addition.....	143
5.3.2	Adsorption Isotherm.....	145
5.3.3	Calculation on Formation of Storage Materials and Overall Mass Balance.....	146
5.3.4	Inactivation Kinetics.....	147
5.4	Discussion.....	148
5.5	Figures.....	151
5.6	References.....	157
Chapter 6	Conclusions and Future Research.....	160
6.1	Conclusions.....	160
6.2	Future Research.....	163
	Appendices.....	166



## List of Tables

Table 2.1. Specificity, coverage, and sequences of the PNA MBs Dmonas0121 and Dsoma0848 <sup>1</sup> . .....	42
Table 2.2. Target sites in the 16S rRNA of target and non-target species included in this study for the PNA MBs Dmonas0121 and Dsoma0848. ....	43
Table 2.3. Summary of hybridization conditions for various experiments <sup>1</sup> . ....	44
Table 3.1. Sequence, coverage, specificity, and annealing temperature for each primer set designed in this study.....	81
Table 3.2. Target and non-target used in the characterization of each real-time PCR primer set, and the amplification efficiencies for each real-time PCR primer set. ....	82
Table 3.3. Relative abundance of bacterial population determined using clone library sequence analyses in biomass samples collected on Day 0 of the weak backwash experiment (total of 182 clones) and Day 5 of the strong backwash experiment (total of 184 clones). <sup>1</sup> .....	83
Table 3.4. Values of $p$ estimating the similarity between the two bacterial clone libraries using $\int$ -LIBSHUFF.....	84
Table 4.1. Sequences and annealing temperatures of the real-time PCR primer sets used in this study.....	118
Table 4.2. Phylogenetic affiliation of the clones in the four clone libraries (%). ....	119
Table 4.3. Values of $p$ estimating the similarity between the two bacterial clone libraries using $\int$ -LIBSHUFF.....	120
Supplemental Table 4.1. Sequence, coverage, specificity, and annealing temperature for each primer set used in this study. ....	122

## List of Figures

- Figure 1.1. Correlation among reactor operation, microbial community, and reactor performance. Reactor operation determines reactor performance by impacting the structure and function of the microbial community inside a bioreactor (dark solid arrows). Without microbial knowledge, when reactor performance drops, adjustment in reactor operation will be made using a trial and error approach (light dashed arrow). With knowledge on microbial communities, more accurate guidance can be provided for reactor operation adjustment (light solid arrow).....13
- Figure 2.1. Non-specific opening of PNA MB Dsoma0848 due to the increases in hybridization temperature and formamide concentration in hybridization buffers. No rRNA was included in this experiment. ....45
- Figure 2.2. A sample plot showing the kinetics of the hybridizations of PNA MB Dsoma0848 to target and non-target 16S rRNA in the presence of 10 mM NaCl. The points are experimental data points, and the lines are curve fit based on a pseudo-first-order reaction model simulated in KaleidaGraph. The numbers in parentheses indicate the number of mismatches between 16S rRNA and PNA MB. The  $R^2$  values of the three curves in this figure ranged from 0.986 to 0.993.....46
- Figure 2.3 The effects of NaCl concentrations in hybridization buffers on final net fluorescence signals (a) and apparent rate constants (b) from hybridizations of PNA MB Dsoma0848 to target and non-target 16S rRNA. Mean values of duplicates are reported and the error bars represent the range of the duplicates. The numbers in parentheses indicate the number of mismatches between 16S rRNA and PNA MB. ....47
- Figure 2.4. Melting profiles of the hybridizations of PNA MB Dsoma0848 with its target and non-target 16S rRNAs. The numbers in parentheses indicate the number of mismatches between 16S rRNA and PNA MB. The experiment was repeated and similar profiles were obtained (data shown in Supplemental Figure 2.1). ....48
- Figure 2.5. Melting profiles of the hybridizations of PNA MB Dsoma0848 with the 16S rRNAs of its target, non-target, and an artificial mixture containing equal amounts of target and non-target. The numbers in parentheses indicate the number of mismatches between 16S rRNA and PNA MB. The experiment was repeated and similar profiles were obtained (data shown in Supplemental Figure 2.2).....49
- Figure 2.6. Melting profiles of the hybridizations of PNA MB Dmonas0121 with its target and non-target 16S rRNAs. The numbers in parentheses

	indicate the number of mismatches between 16S rRNA and PNA MB. ....	50
Figure 2.7.	Effect of formamide concentration at 25°C on the net fluorescence signals from the hybridizations of PNA MB Dmonas0121 with its target and non-target 16S rRNAs. Mean values of duplicates are reported and the error bars represent the range of the duplicates. The numbers in parentheses represent the number of mismatch between 16S rRNA and PNA MB.....	51
Figure 2.8.	Net fluorescence signals from the hybridizations of PNA MB Dsoma0848 with a series consisting of various amounts of target 16S rRNA ( <i>D. suillum</i> ) spiked to RNA extracted from an environmental sample and with a series of samples containing only target 16S rRNA corresponding to the amounts of 16S rRNA target in the first series. ....	52
Figure 3.1.	The ratios of eDNA to total DNA in biomass samples collected from the daily weak backwash (grey) and daily strong backwash experiments (dark). For the sample from Day 1 of the daily strong backwash experiment, the eDNA extracts likely were contaminated with iDNA: about 12.6% of the iDNA ended up in the eDNA extract. The ratio for this specific sample was not included in the reported average percentages in the text. The insert shows the relative abundances for the three dominant genera for the iDNA and “eDNA” extracts for the sample from Day 1 of the daily strong backwash experiment.....	85
Figure 3.2.	A phylogenetic tree of the clones that were closely associated with the three major bacterial genera present in the biofilm reactor. “Day 0” and “Day 5” refer to Day 0 of the daily weak backwash experiment and Day 5 of the daily strong backwash experiment, respectively. The numbers in parentheses are the numbers of clones.....	86
Figure 3.3.	Rarefaction curves indicating bacterial 16S rRNA richness within the two clone libraries. The dashed line represents 1:1, indicating infinite diversity. The table lists the bacterial 16S rRNA sequence diversity indices. OTUs were defined as groups of sequences sharing 95% 16S rRNA sequence identity. The estimates of phylotype richness were calculated according to the abundance-based coverage estimate (ACE) and the bias-corrected Chao1 estimator. The Shannon-Weiner diversity index and the Inverse Simpson’s diversity index, which consider species richness as well as evenness, were also calculated. ....	87
Figure 3.4.	Standard curves for the primer sets designed for <i>Dechloromonas</i> , <i>Zoogloea</i> , and <i>Curvibacter</i> clones, and the standard curve for the bacterial primer set.....	88
Figure 3.5.	The effluent DO (top row) and perchlorate (bottom row) concentrations during the daily weak backwash experiment (left column) and the daily strong backwash experiment (right column).	

	(■) Effluent DO level; (□) Initial DO removal; (●) Effluent perchlorate concentration; (○) Initial perchlorate reduction rate. ....	89
Figure 3.6.	Protein measurements (top row) and the relative abundance of the three major bacterial genera in total bacterial population (bottom row) during the daily weak (left column) and strong (right column) backwash experiments. Trendlines: (solid) <i>Dechloromonas</i> ; (dashed) <i>Zoogloea</i> ; (dotted) <i>Curvibacter</i> . ....	90
Figure 4.1.	Schematics of both the bench- and the pilot-scale biological drinking water treatment systems. ....	122
Figure 4.2.	Reactor performance of the bench-scale BAC reactor (A) and the pilot-scale BAC reactor (B). ....	123
Figure 4.3.	Fractions of the four subclasses of the <i>Proteobacteria</i> in the bench- and pilot-scale BAC reactors before and after phosphorus addition. ....	124
Figure 4.4.	Phylogenetic tree of perchlorate reducing bacteria in the two systems before and after phosphorus addition. The two numbers in each parenthesis represent the numbers of the clones before and after phosphorus addition. ....	125
Figure 4.5.	Rarefaction curves indicating bacterial 16S rRNA richness within clone libraries from the bench- and the pilot-scale BAC reactors before and after phosphorus addition. The dashed line represents 1:1, indicating infinite diversity. The table lists the bacterial 16S rRNA sequence diversity indices. OTUs were defined as groups of sequences sharing 95% 16S rRNA sequence identity. The estimates of phylotype richness were calculated according to the abundance-based coverage estimate (ACE) and the bias-corrected Chao1 estimator. The Shannon-Weiner diversity index and the Inverse Simpson's diversity index, which take into account species richness and evenness, were also calculated. ....	126
Figure 4.6.	Changes in relative abundance of <i>Dechloromonas</i> spp. (A) and <i>Azospira</i> spp. (B) in the bacterial community of the bench-scale BAC reactor relative to the day that phosphorus was added (Day 0). ....	127
Figure 5.1.	A sample figure showing the nitrate concentration profiles with simulated curves using an exponential decay model. ....	151
Figure 5.2.	Nitrate and perchlorate removal rates as functions of electron donor in the batch tests. The wet weight of BAC particles added to each batch test was identical. ....	152
Figure 5.3.	Results of effluent nitrate, perchlorate, and acetic acid from the intermittent electron donor addition experiment. For simplicity, influent and effluent DO levels, which respectively remained at 7 mg/L and below the detection limit throughout the experiment, were not included in the figure. ....	153
Figure 5.4.	Adsorption isotherm for acetic acid adsorption on GAC (pH 7.40-7.65). The curve is constructed based on Equation 3. ....	154
Figure 5.5.	Breakdown of source (positive values) and sink (negative values) of acetic acid within one feast and one famine stage in the intermittent	

	electron donor addition experiment. Values of acetic acid corresponding to PHB formation/consumption are balanced values. ....	155
Figure 5.6.	Inactivation kinetics of BAC reactor effluent using ( $C_{\text{monochloramine}}=4$ mg/L, pH=8, at 20°C). The curve corresponds to Equation 4. The reported data points are the averages of four replicates. ....	156
Supplemental Figure 2.1.	Melting profiles of the hybridizations of PNA MB Dsoma0848 with its target and non-target 16S rRNAs. The numbers in parentheses indicate the number of mismatches between 16S rRNA and PNA MB. ....	53
Supplemental Figure 2.2.	Melting profiles of the hybridization of PNA MB Dsoma0848 with the 16S rRNA of its target, non-target, and an artificial mixture containing equal amounts of target and non-target. The numbers in parentheses indicate the number of mismatches between 16S rRNA and PNA MB. ....	54
Supplemental Figure 3.1.	Characterization on primer sets with various annealing temperatures: (A) Dchm0991F/1146R, (B) Zoog0487F/0627R, and (C) Curvib1001F/1107R. Filled symbols: target. Open symbols: non-target. The numbers of mismatches of the non-targets are listed in Table 3.2. ....	91
Supplemental Figure 3.2.	An electrophoresis gel image of real-time PCR products using the Dchm0991F/1146R primer set. Lane 1: DNA ladder; Lane 2 and 3: <i>Dechloromonas</i> (target) and <i>Zoogloea</i> (non-target) with an annealing temperature of 58.4°C; Lane 4 and 5: <i>Dechloromonas</i> (target) and <i>Zoogloea</i> (non-target) with an annealing temperature of 64.7°C. ....	92
Supplemental Figure 3.3.	Representative melting curves for the targets and non-targets of the three real-time PCR primer sets designed in this study: (A) Dchm0991F/1146R ( $T_m=86.90\pm 0.15^\circ\text{C}$ for <i>Dechloromonas</i> , N/A for <i>Zoogloea</i> ); (B) Zoog0487F/0627R ( $T_m=86.63\pm 0.18^\circ\text{C}$ for <i>Zoogloea</i> , $T_m=86.36\pm 0.17^\circ\text{C}$ for <i>Curvibacter</i> , $T_m=87.10\pm 0.17^\circ\text{C}$ for <i>Dechloromonas</i> ); (C) Curvib1001F/1107R ( $T_m=85.93\pm 0.21^\circ\text{C}$ for <i>Curvibacter</i> , $T_m=86.50\pm 0.16^\circ\text{C}$ for <i>Zoogloea</i> ). The numbers in parentheses are the numbers of mismatches with the corresponding primers. The averages and standard deviations were from n replicates (n>10). ....	93
Supplemental Figure 3.4.	The effluent DO (top row) and perchlorate (bottom row) concentrations during the daily weak backwash experiment (left column) and the daily strong backwash experiment (right column), which were replicate experiments of the ones in Figure 3.5. (■) Effluent DO level; (●) Effluent perchlorate concentration. These plots were reproduced from the work by Choi and coworkers (Choi et al., 2007). ....	94
Supplemental Figure 3.5.	Fractions of three major bacterial genera in total bacterial population during the weak (A) and strong (B) backwash	

experiments. Trendlines: (solid) <i>Dechloromonas</i> ; (dashed) <i>Zoogloea</i> ; (dotted) <i>Curvibacter</i> .....	95
Supplemental Figure 4.1. The schematic of the entire pilot-scale system in California. The pilot-scale BAC reactor included in this work is one of the two FXB Bioreactors in the schematic. ....	128
Supplemental Figure 4.2 Characterizations on the primer sets for <i>Dechloromonas</i> (A) and <i>Azospira</i> (B). The numbers in parentheses represents the numbers of mismatches of each template with the corresponding forward and reverse primers, respectively. For the non-targets, at some annealing temperatures the PCR reaction did not generated enough fluorescence to pass the threshold, therefore, the corresponding $C_{\text{threshold}}$ value was not available.....	129
Supplemental Figure 4.3. Standard curves for the primer sets designed for <i>Dechloromonas</i> and <i>Azospira</i> , and for the bacterial primer set. Error bars represent standard deviation from triplicates. ....	130

## List of Appendices

Appendix A	Effect of Backwashing on Perchlorate Removal in Fixed Bed Biofilm Reactors .....	166
Appendix B	Chemisorption of Oxygen Onto Activated Carbon Can Enhance the Stability of Biological Perchlorate Reduction in Fixed Bed Biofilm Reactors.....	178
Appendix C	Membrane Hybridization Results.....	189
Appendix D	Characterizations of PNA MB Probes Using 16S rRNA and Whole Cells .....	196
Appendix E	Microbial Community Analysis of a Biologically Active Carbon Reactor Operated for Perchlorate Removal .....	206
Appendix F	Bench-Scale BAC .....	216
Appendix G	Curriculum Vitae.....	218

## ABSTRACT

Among many strategies to solve water quality problems, environmental biotechnology provides attractive solutions to remove contaminants from drinking water sources in more sustainable ways than traditional methods. In this dissertation, efforts were presented to optimize and apply biologically active carbon (BAC) reactors to remove inorganic contaminants (i.e., perchlorate and nitrate) from groundwater and synthetic groundwater. The optimization strategies included promoting biological activity by adding phosphorus, utilizing the activated carbon adsorption capacity and an intracellular storage mechanism to control effluent electron donor residual, and controlling microbial contamination by disinfecting reactor effluent with monochloramine. In order to study the perchlorate reducing bacterial populations inside bioreactors, a solution-based hybridization assay using peptide nucleic acid molecular beacon probes was developed to quantify 16S ribosomal RNA of *Dechloromonas* and *Azospira*. In addition, molecular techniques such as clone library and real time polymerase chain reaction were applied to monitor specific microbial populations in BAC reactors after changes in various reactor operating conditions. With the knowledge obtained from the microbial studies, the correlation among reactor operation, microbial community, and reactor performance was elucidated. The use of environmental biotechnology, complemented by molecular studies of the microbial communities involved, as demonstrated in this dissertation, provides a promising avenue to mitigate a variety of water quality problems.



# Chapter 1

## Introduction, Objectives, and Strategies

### 1.1 Perchlorate Contamination and Treatment Technologies

During the past decade, perchlorate has been detected in more than 25 states in the United States and affected the drinking water supplies of millions of people (Gullick et al., 2001; Motzer, 2001). Perchlorate is introduced to the environment through human activity (Urbansky, 2002; Wilkin et al., 2007) and natural processes (Dasgupta et al., 2005; Rao et al., 2007). Because it is a competitive inhibitor of the process by which iodide is absorbed by the thyroid (Greer et al., 2002), perchlorate is on U.S. EPA's drinking water contaminant candidate list (US-EPA, 2008) and is regulated by a number of states at concentrations ranging from 1 to 18  $\mu\text{g/L}$  (US-EPA, 2005).

Abiotic and biological treatment methods have been developed to remove perchlorate from water (Xu et al., 2003). Abiotic treatment options, such as ion exchange (Venkatesh et al., 2000; Gu et al., 2001), membrane filtration (Urbansky and Schock, 1999), activated carbon adsorption (Chen et al., 2005), and zero valent iron nanoparticle mediated reduction (Xiong et al., 2007), rely on physical and/or chemical processes to remove perchlorate from water. In comparison, biological treatment relies on perchlorate

reducing bacteria (PRB) to convert perchlorate to non-toxic chloride (Coates and Achenbach, 2004), and has been proven successful in various reactor configurations (Nerenberg et al., 2002; Brown et al., 2003; Min et al., 2004). Compared to their abiotic counterparts, biological treatment systems can achieve consistent perchlorate removal without generating concentrated waste streams, which require further treatment (Brown et al., 2002; Xu et al., 2003). In addition, biological treatment processes generally are less costly (Brown et al., 2005), although recent reductions in the price of ion exchange resins may make the economics of these two categories of competing technologies more comparable (Roquebert et al., 2000). Another attractive feature of biological treatment is its potential to simultaneously remove multiple contaminants, such as chromate, selenate, and dichloromethane (Nerenberg and Rittmann, 2004).

Biological perchlorate removal from drinking water can be practiced in various reactor configurations, such as fixed-bed bioreactors (Brown et al., 2003; Min et al., 2004), fluidized-bed bioreactors (Greene and Pitre, 2000; McCarty and Meyer, 2005), and membrane biofilm bioreactors (Nerenberg et al., 2002; Nerenberg et al., 2008). The biomass in these bioreactors resides primarily in biofilms. Compared to the other reactor configurations, fixed-bed bioreactors are easy to implement and relatively simple to operate. Various fixed-bed bioreactors employ different types of biofilm attachment materials: sorptive attachment materials such as granular activated carbon (GAC) (Brown et al., 2003; Choi et al., 2008), and nonsorptive attachment materials such as sand (Min et al., 2004) and glass beads (Choi et al., 2007).

Among various fixed-bed bioreactor designs, fixed-bed bioreactors using GAC as biofilm attachment materials, the so-called fixed-bed biologically active carbon (BAC)

systems, have the following advantages in treating contaminated drinking water. First, for many drinking water treatment plants that employ GAC filters for advanced drinking water treatment, no extra construction is needed to convert them to BAC systems. In fact, many GAC filters are operated biologically by allowing microbial growth on GAC surface. Second, the adsorption capacity of the GAC surface provides an effective means to remove contaminants that are not biodegradable (Weber, 1974). Furthermore, contaminants that are toxic or inhibitory to microbial activities can be adsorbed, so that the microbes grown on GAC are exposed to much lower concentrations of such contaminants (Ehrhardt and Rehm, 1985; Choi et al., 2008).

The benefits of operating fixed-bed BAC reactors (or BAC filters) in drinking water treatment have been recognized for a few decades, and fixed-bed BAC reactors have been studied extensively (Rittmann and Snoeyink, 1984). In the past, BAC filters, usually following a pre-ozonation step, have been studied for their potential to remove contaminants that cannot be efficiently removed in conventional processes (Servais et al., 1987). Such contaminants include taste/odor/color causing compounds (Nerenberg et al., 2000; Rittmann et al., 2002; Elhadi et al., 2004), biodegradable dissolved organic carbon (BDOC) (Kim et al., 1997; Nishijima and Speitel, 2004), and inorganic contaminants, such as ammonia (Andersson et al., 2001), nitrate (Kapoor and Viraraghavan, 1997), bromate (Kirisits et al., 2001), and metals (Knoppert et al., 1980).

The performance of fixed-bed bioreactors can be affected, among other parameters, by temperature (Moll et al., 1999; Andersson et al., 2001), temporary shutdown (Niquette et al., 1998), and backwash (Liu et al., 2001; Tranckner et al., 2008). In the study by Andersson and co-workers, ammonia removal reached up to 90% when

the water temperature varied from 4 to 10°C, whereas less than 30% of ammonia was removed when the water temperature was below 4°C. Regular backwashing is necessary for the continuous operation of fixed-bed bioreactors, and the operating procedure for backwashing affects reactor performance (Hozalski and Bouwer, 1998). For example, if backwash water contains chlorine, when other operating parameters are not optimal, the reactor performance will be impaired (Liu et al., 2001). In addition, backwash intensity and frequency can also affect reactor performance as well as the microbial communities involved (Choi et al., 2007). Choi and coworkers performed a preliminary study on this topic, and further investigation is needed.

So far, most bench- and pilot-scale studies on biological drinking water treatment have only focused on removing the contaminants of interest, but neglected other characteristics of effluent quality that might have been affected by the biological treatment processes. For example, studies on biological drinking water treatment rarely discuss microbial characteristics of reactor effluents or develop approaches to control possible microbial contamination. In fact, microbes from biological treatment processes can end up in reactor effluents and cause microbial contamination of finished water, which is a concern that needs to be addressed. Another example is the lack of investigation on optimization of electron donor addition to biological treatment systems. External electron donor is required for many biological drinking water treatment processes. An optimized electron donor addition strategy should meet the need to promote biological activity in bioreactors and at the same time minimize electron donor residual in reactor effluents. These biological and chemical characteristics of effluent quality are critical in evaluating biological drinking water treatment. Brown recognized

the need for more characterizations of reactor effluents and initiated a study to develop post-treatments for a BAC reactor for perchlorate removal (Brown, 2002). The impact of BAC systems on the overall quality of finished drinking water deserves further study.

## 1.2 Perchlorate Reducing Bacteria

Perchlorate reducing bacteria (PRB) can utilize perchlorate as an electron acceptor and reduce it to chlorate using perchlorate reductase (Kengen et al., 1999). Then, PRB can further reduce chlorate to chlorite using (per)chlorate reductase. In the last step, chlorite is converted to chloride and molecular oxygen by chlorite dismutase (van Ginkel et al., 1996). This pathway allows engineered systems containing PRB to remove perchlorate from water and convert perchlorate to non-toxic chloride.

PRB that have been isolated so far are phylogenetically diverse and consist of members within the *Alpha-*, *Beta-*, and *Epsilonproteobacteria* (Wallace et al., 1996; Achenbach et al., 2001; Coates and Achenbach, 2004). Among the identified PRB, three PRB genera *Dechloromonas*, *Dechlorosoma*, and *Dechlorospirillum* have been detected repeatedly in natural and engineered systems (Coates et al., 1999; Waller et al., 2004; Nozawa-Inoue et al., 2005; Zhang et al., 2005; Bardiya and Bae, 2008; Choi et al., 2008). It needs to be mentioned that the type strain of the genus *Dechlorosoma*, *D. suillum*, had been identified as a later subjective synonym of *Azospira oryzae* (Tan and Reinhold-Hurek, 2003). Therefore, previous *Dechlorosoma* spp. have been reclassified under the genus *Azospira*, even though the genus name *Dechlorosoma* was used extensively in earlier literature.

PRB are not only phylogenetically diverse, but also functionally diverse. In addition to perchlorate, most PRB can use oxygen and nitrate as electron acceptors with the preferred order of oxygen, nitrate, and perchlorate (Coates and Achenbach, 2004). The presence of multiple electron acceptors in solution affects biological perchlorate reduction by pure cultures in different ways. For example, the species *Dechlorosoma suillum* did not reduce perchlorate until nitrate was completely removed in a medium containing equal moles of the two electron acceptors (Chaudhuri et al., 2002). In contrast, *Dechloromonas agitata* could not use nitrate as a sole electron acceptor (Bruce et al., 1999), but could simultaneously conduct complete perchlorate reduction and partial denitrification from nitrate to nitrite (Chaudhuri et al., 2002), presumably because nitrate can be co-reduced by (per)chlorate reductase (Coates and Achenbach, 2006). Different from the case of *D. agitata*, separately induced pathways for chlorate and nitrate reduction were discovered in the strain *Dechlorosoma* sp. KJ (Xu et al., 2004). In addition to the genera *Dechloromonas* and *Dechlorosoma*, other PRB species were also studied. *Citrobacter* spp. preferred perchlorate as an electron acceptor over nitrate (Bardiya and Bae, 2004). Strain GR-1 grown on perchlorate could not reduce nitrate (Rikken et al., 1996); however, perchlorate reductase purified from this strain had a higher activity in reducing nitrate than reducing perchlorate (Kengen et al., 1999), which left questionable whether GR-1 contained a separate nitrate reductase when grown on nitrate. *Pseudomonas chloritidismutans* could use chlorate and oxygen as electron acceptors, but not nitrate, perchlorate, or bromate (Wolterink et al., 2002). Interestingly, although *P. chloritidismutans* did not grow on bromate, its cytoplasmic chlorate reductase could reduce bromate (Wolterink et al., 2003).

PRB species have also been studied for their maximum specific growth rates, which can vary significantly from species to species. For example, with acetate as the sole electron donor, *Dechlorosoma* sp. KJ exhibited an increasing maximum specific growth rates in the order of perchlorate < chlorate  $\approx$  oxygen (i.e., 0.14, 0.26 and 0.27 h<sup>-1</sup>) for the three electron acceptors. The order for *Dechloromonas* sp. PDX was perchlorate = chlorate < oxygen (i.e., 0.21, 0.21 and 0.28 h<sup>-1</sup>) (Logan et al., 2001). In contrast, when acetate was again used as the sole electron donor, the *Dechloromonas* isolates from a contaminated site had much lower maximum specific growth rates for perchlorate (i.e., 0.067 and 0.085 h<sup>-1</sup>) than the corresponding values reported by Logan and co-workers (Waller et al., 2004).

Most of the studies on PRB were conducted on pure cultures. In natural or engineered systems, however, PRB co-exist with other microbial species and form microbial communities in these environments. The environments interact with the microbial communities, and therefore have a profound impact on the microbial populations in the communities. In engineered systems, it is of critical importance to correlate system operating conditions (i.e., environments), the biomass in the systems (i.e., microbial communities), and system performance.

### **1.3 Microbial Communities in Engineered Systems**

To maximize the beneficial effects of microbial communities in engineered systems, it is important to study the structure and function of these microbial communities (Briones and Raskin, 2003; Curtis et al., 2003; Curtis and Sloan, 2004; Rittmann et al., 2006).

Microbial community structures have been commonly studied using molecular techniques targeting 16S ribosomal RNA (rRNA) or 16S rRNA genes (Amann et al., 1995). These 16S rRNA based techniques have been used to identify, quantify, and visualise specific microbial populations in complex microbial communities (Theron and Cloete, 2000). Among a suite of molecular techniques, we selected to construct clone libraries to allow 16S rRNA gene sequence analyses for identification of the microbial populations in our systems (Suzuki et al., 1997), and performed quantitative real time polymerase chain reaction (PCR) to study the dynamics of selected populations during reactor operation (Lie and Petropoulos, 1998). Microbial community functions can be assessed using various strategies. The potential functions of a microbial community can be assessed by targeting the genes that encode the enzymes involved in the functions. For example, PCR based techniques have been developed to target chlorite dismutase and perchlorate reductase genes (Bender et al., 2004; Nozawa-Inoue et al., 2008), both encoding key enzymes in biological perchlorate removal. In engineered systems, the functions of microbial communities can also be described using reactor performance data, such as COD removal (Fernandez et al., 1999), nitrate removal (Krauter et al., 2005), accumulation of volatile fatty acids (Hashsham et al., 2000), and specific gas production in anaerobic digesters (McMahon et al., 2001).

Microbial community studies have been applied to a number of systems that were capable of biological perchlorate reduction, such as fixed bed biofilm reactors (Zhang et al., 2005), membrane biofilm reactors (Nerenberg et al., 2008), a bioreactor containing indigenous wetland sediment (Krauter et al., 2005), and perchlorate-contaminated soils (Waller et al., 2004; Nozawa-Inoue et al., 2005). Among these studies, two provided



some quantitative information about PRB populations. Zhang et al. employed fluorescence *in situ* hybridization (FISH) and observed that *Dechloromonas* spp. primarily resided at the surface of the biofilm in their fixed-bed bioreactor, while *Dechlorosoma* spp. resided at the bottom of the biofilm. Nerenberg et al., who provided hydrogen as the sole electron donor to membrane biofilm reactors, observed that the relative abundance of *Dechloromonas* spp. increased with the influent perchlorate concentrations. Since only few studies have quantitatively linked microbial community structure to function in systems designed for biological perchlorate removal, additional work is needed to fill this gap.

## **1.4 Objectives**

The objectives of this study are (i) to optimize biofilm reactor operation using knowledge obtained from microbial community characterization and (ii) to study the potential of fixed-bed biofilm reactors to produce high quality drinking water from water sources contaminated with perchlorate and nitrate. The work associated with the first objective should be of interest to biological process engineers who want to gain better control of their engineered systems (Curtis et al., 2003). The outcome of the research performed in the context of the second objective will benefit the development and evaluation of biological drinking water treatment technologies for perchlorate and nitrate removal specifically, but also will benefit the field of biological drinking water treatment in general (Brown, 2007).

To achieve the first objective, the correlation among reactor operation, microbial community, and reactor performance needs to be elucidated. Microbial community characterization should be used to not only *explain* the performance of bioreactors but also to *guide* the operation of the biological units. As illustrated in Figure 1.1, reactor operation determines reactor performance by influencing the structure and function of the microbial community involved (dark solid arrows). In other words, microbial communities inside bioreactors respond to changes in reactor operation, and consequently the microbial responses determine the reactor performance. Without understanding the correlation, when reactor performance deteriorates, changes in reactor operation are usually made based on a trial and error approach (light dashed arrow). With the knowledge obtained from microbial community characterization, reactor operation can be adjusted consistent with this knowledge (light solid arrow).

For the second objective, overall water quality, including not only the concentrations of nitrate and perchlorate, but also the concentrations of other chemical and microbial components in reactor effluents, needs to be evaluated. The drinking water industry needs to adhere to strict regulations. Therefore, in order to evaluate if biological treatment processes can be an effective and reliable approach for drinking water treatment, overall treatment performance, focusing on both target contaminants and possible side effects from biological treatment, needs to be considered and studied.

## 1.5 Research Strategies

First, a quantitative hybridization assay to monitor PRB populations in microbial communities was developed. The hybridization assay was designed to target the 16S rRNA of PRB populations, because the level of 16S rRNA can reflect the abundance of the active portion of the populations. Different from commonly used hybridization techniques for 16S rRNA quantification, such as FISH and membrane hybridization, the new method was a solution-based hybridization assay. To develop this assay, peptide nucleic acid molecular beacon probes were designed and characterized for two perchlorate reducing bacterial genera.

Second, fixed-bed biofilm reactors were built to remove perchlorate and nitrate from drinking water. For these bioreactors, backwash and nutrient addition were selected as the operating conditions to study the correlation among reactor operation, microbial community, and reactor performance. The microbial communities involved were characterized using the newly developed solution-based hybridization assay and other molecular techniques.

Third, the overall quality of bioreactor effluents was analyzed with respect to nitrate and perchlorate as well as other chemical and microbial characteristics. Efforts were made to minimize electron donor residual and control potential microbial contamination in reactor effluents.

This dissertation consists of six chapters. Chapter 1 provides a general introduction to the work, presents the objectives, and lists the research strategies that were applied to achieve the objectives. Chapters 2 – 5 are written as stand-alone-studies for publication as peer-reviewed journal papers. In addition to the introduction in

Chapter 1, each of these chapters provides an introduction with literature review relevant to the topics covered in the respective chapters. Chapter 2 presents the development and evaluation of the solution-based hybridization assay using peptide nucleic acid molecular beacon probes. Chapter 3 describes the effects of backwash frequency and intensity on reactor performance as well as on microbial community structures of a bench-scale fixed-bed biofilm reactor. Chapter 4 discusses the effects of nutrient addition on reactor performance and microbial community structures of two fixed-bed BAC reactors, one bench- and one pilot-scale reactor. Chapter 5 presents efforts made to minimize electron donor residual in reactor effluents and to control microbial contamination by disinfecting reactor effluents. Overall conclusions and future research are presented in Chapter 6. Tables, figures, and references are listed at the end of each chapter.

## 1.6 Figures

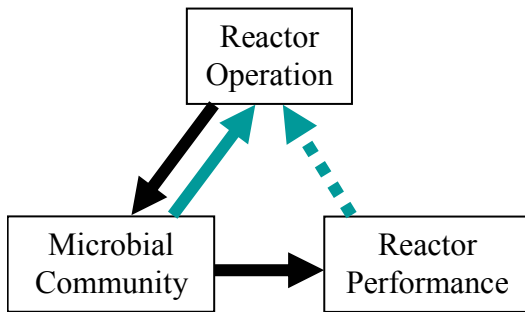


Figure 1.1. Correlation among reactor operation, microbial community, and reactor performance. Reactor operation determines reactor performance by impacting the structure and function of the microbial community inside a bioreactor (dark solid arrows). Without microbial knowledge, when reactor performance drops, adjustment in reactor operation will be made using a trial and error approach (light dashed arrow). With knowledge on microbial communities, more accurate guidance can be provided for reactor operation adjustment (light solid arrow).

## 1.7 References

- Achenbach, L.A., Michaelidou, U., Bruce, R.A., Fryman, J. and Coates, J.D. (2001) *Dechloromonas Agitata* Gen. Nov., Sp Nov and *Dechlorosoma Suillum* Gen. Nov., Sp Nov., Two Novel Environmentally Dominant (Per)Chlorate-Reducing Bacteria and Their Phylogenetic Position. *International Journal of Systematic and Evolutionary Microbiology* 51, 527-533.
- Amann, R.I., Ludwig, W. and Schleifer, K.H. (1995) Phylogenetic Identification and in-Situ Detection of Individual Microbial-Cells without Cultivation. *Microbiological Reviews* 59(1), 143-169.
- Andersson, A., Laurent, P., Kihn, A., Prevost, M. and Servais, P. (2001) Impact of Temperature on Nitrification in Biological Activated Carbon (Bac) Filters Used for Drinking Water Treatment. *Water Research* 35(12), 2923-2934.
- Bardiya, N. and Bae, J. (2004) Role of *Citrobacter Amalonaticus* and *Citrobacter Farmeri* in Dissimilatory Perchlorate Reduction. *Journal of Basic Microbiology* 44(2), 88-97.
- Bardiya, N. and Bae, J.H. (2008) Isolation and Characterization of *Dechlorospirillum Anomalous* Strain Jb116 from a Sewage Treatment Plant. *Microbiological Research* 163(2), 182-191.
- Bender, K.S., Rice, M.R., Fugate, W.H., Coates, J.D. and Achenbach, L.A. (2004) Metabolic Primers for Detection of (Per) Chlorate-Reducing Bacteria in the Environment and Phylogenetic Analysis of Cld Gene Sequences. *Applied and Environmental Microbiology* 70(9), 5651-5658.
- Briones, A. and Raskin, L. (2003) Diversity and Dynamics of Microbial Communities in Engineered Environments and Their Implications for Process Stability. *Current Opinion in Biotechnology* 14(3), 270-276.
- Brown, J. (2002) Abiotic and Biotic Perchlorate Removal in an Activated Carbon Filter, University of Illinois, Urbana-Champaign.
- Brown, J. (2007) Biological Drinking Water Treatment: Benefiting from Bacteria. *The Bridge* 37(4).
- Brown, J.C., Anderson, R.D., Min, J.H., Boulos, L., Prasifka, D. and Juby, G.J.G. (2005) Fixed Bed Biological Treatment of Perchlorate-Contaminated Drinking Water. *Journal American Water Works Association* 97(9), 70-81.
- Brown, J.C., Snoeyink, V.L. and Kirisits, M.J. (2002) Abiotic and Biotic Perchlorate Removal in an Activated Carbon Filter. *Journal American Water Works Association* 94(2), 70-79.

- Brown, J.C., Snoeyink, V.L., Raskin, L. and Lin, R. (2003) The Sensitivity of Fixed-Bed Biological Perchlorate Removal to Changes in Operating Conditions and Water Quality Characteristics. *Water Research* 37(1), 206-214.
- Bruce, R., Achenbach, L. and Coates, J. (1999) Reduction of (Per)Chlorate by a Novel Organism Isolated from Paper Mill Waste. *Environmental Microbiology* 1(4), 319-329.
- Chaudhuri, S.K., O'Connor, S.M., Gustavson, R.L., Achenbach, L.A. and Coates, J.D. (2002) Environmental Factors That Control Microbial Perchlorate Reduction. *Applied and Environmental Microbiology* 68(9), 4425-4430.
- Chen, W.F., Cannon, F.S. and Rangel-Mendez, J.R. (2005) Ammonia-Tailoring of Gac to Enhance Perchlorate Removal. II: Perchlorate Adsorption. *Carbon* 43(3), 581-590.
- Choi, Y.C., Li, X., Raskin, L. and Morgenroth, E. (2007) Effect of Backwashing on Perchlorate Removal in Fixed Bed Biofilm Reactors. *Water Research* 41(9), 1949-1959.
- Choi, Y.C., Li, X., Raskin, L. and Morgenroth, E. (2008) Chemisorption of Oxygen onto Activated Carbon Can Enhance the Stability of Biological Perchlorate Reduction in Fixed Bed Biofilm Reactors. *Water Research* 42(13), 3425-3434.
- Coates, J.D. and Achenbach, L.A. (2004) Microbial Perchlorate Reduction: Rocket-Fuelled Metabolism. *Nature Reviews Microbiology* 2(7), 569-580.
- Coates, J.D. and Achenbach, L.A. (2006) *The Microbiology of Perchlorate Reduction and Its Bioremediative Application*, Springer.
- Coates, J.D., Michaelidou, U., Bruce, R.A., O'Connor, S.M., Crespi, J.N. and Achenbach, L.A. (1999) Ubiquity and Diversity of Dissimilatory (Per)Chlorate-Reducing Bacteria. *Applied and Environmental Microbiology* 65(12), 5234-5241.
- Curtis, T.P., Head, I.M. and Graham, D.W. (2003) Theoretical Ecology for Engineering Biology. *Environmental Science & Technology* 37(3), 64a-70a.
- Curtis, T.P. and Sloan, W.T. (2004) Prokaryotic Diversity and Its Limits: Microbial Community Structure in Nature and Implications for Microbial Ecology. *Current Opinion in Microbiology* 7(3), 221-226.
- Dasgupta, P.K., Martinelango, P.K., Jackson, W.A., Anderson, T.A., Tian, K., Tock, R.W. and Rajagopalan, S. (2005) The Origin of Naturally Occurring Perchlorate: The Role of Atmospheric Processes. *Environmental Science & Technology* 39(6), 1569-1575.
- Ehrhardt, H.M. and Rehm, H.J. (1985) Phenol Degradation by Microorganisms Adsorbed on Activated Carbon. *Applied Microbiology and Biotechnology* 21(1-2), 32-36.
- Elhadi, S.L.N., Huck, P.M. and Slawson, R.M. (2004) Removal of Geosmin and 2-Methylisoborneol by Biological Filtration. *Water Science and Technology* 49(9), 273-280.

Fernandez, A., Huang, S.Y., Seston, S., Xing, J., Hickey, R., Criddle, C. and Tiedje, J. (1999) How Stable Is Stable? Function Versus Community Composition. *Applied and Environmental Microbiology* 65(8), 3697-3704.

Greene, M.R. and Pitre, M.P. (2000) Perchlorate in the Environment. Urbansky, E.T. (ed), pp. 241-256, Kluwer Academic/Plenum Publishers, New York.

Greer, M.A., Goodman, G., Pleus, R.C. and Greer, S.E. (2002) Health Effects Assessment for Environmental Perchlorate Contamination: The Dose Response for Inhibition of Thyroidal Radioiodine Uptake in Humans. *Environmental Health Perspectives* 110(9), 927-937.

Gu, B.H., Brown, G.M., Maya, L., Lance, M.J. and Moyer, B.A.A. (2001) Regeneration of Perchlorate (ClO<sub>4</sub><sup>-</sup>)-Loaded Anion Exchange Resins by a Novel Tetrachloroferrate (FeCl<sub>4</sub><sup>-</sup>) Displacement Technique. *Environmental Science & Technology* 35(16), 3363-3368.

Gullick, R.Q., Lechvallier, M.W. and Barhorst, T.A.S. (2001) Occurrence of Perchlorate in Drinking Water Sources. *Journal American Water Works Association* 93(1), 66-77.

Hashsham, S.A., Fernandez, A.S., Dollhopf, S.L., Dazzo, F.B., Hickey, R.F., Tiedje, J.M. and Criddle, C.S. (2000) Parallel Processing of Substrate Correlates with Greater Functional Stability in Methanogenic Bioreactor Communities Perturbed by Glucose. *Applied and Environmental Microbiology* 66(9), 4050-4057.

Hozalski, R.M. and Bouwer, E.J. (1998) Deposition and Retention of Bacteria in Backwashed Filters. *Journal American Water Works Association* 90(1), 71-85.

Kapoor, A. and Viraraghavan, T. (1997) Nitrate Removal from Drinking Water - Review. *Journal of Environmental Engineering-Asce* 123(4), 371-380.

Kengen, S.W.M., Rikken, G.B., Hagen, W.R., van Ginkel, C.G. and Stams, A.J.M. (1999) Purification and Characterization of (Per)Chlorate Reductase from the Chlorate-Respiring Strain Gr-1. *Journal of Bacteriology* 181(21), 6706-6711.

Kim, W.H., Nishijima, W., Shoto, E. and Okada, M. (1997) Pilot Plant Study on Ozonation and Biological Activated Carbon Process for Drinking Water Treatment. *Water Science and Technology* 35(8), 21-28.

Kirisits, M.J., Snoeyink, V.L., Inan, H., Chee-Sanford, J.C., Raskin, L. and Brown, J.C. (2001) Water Quality Factors Affecting Bromate Reduction in Biologically Active Carbon Filters. *Water Research* 35(4), 891-900.

Knoppert, P.L., Oskam, G. and Vreedenburgh, E.G.H. (1980) An Overview of European Water-Treatment Practice. *Journal American Water Works Association* 72(11), 592-599.



- Krauter, P., Daily, B., Dibley, V., Pinkart, H. and Legler, T. (2005) Perchlorate and Nitrate Remediation Efficiency and Microbial Diversity in a Containerized Wetland Bioreactor. *International Journal of Phytoremediation* 7(2), 113-128.
- Lie, Y.S. and Petropoulos, C.J. (1998) Advances in Quantitative PCR Technology: 5' Nuclease Assays. *Current Opinion in Biotechnology* 9(1), 43-48.
- Liu, X.B., Huck, P.M. and Slawson, R.M. (2001) Factors Affecting Drinking Water Biofiltration. *Journal American Water Works Association* 93(12), 90-101.
- Logan, B., Zhang, H., Mulvaney, P., Milner, M., Head, I. and Unz, R. (2001) Kinetics of Perchlorate- and Chlorate-Respiring Bacteria. *Applied and Environmental Microbiology* 67(6), 2499-2506.
- McCarty, P.L. and Meyer, T.E. (2005) Numerical Model for Biological Fluidized-Bed Reactor Treatment of Perchlorate-Contaminated Groundwater. *Environmental Science & Technology* 39(3), 850-858.
- McMahon, K.D., Stroot, P.G., Mackie, R.I. and Raskin, L. (2001) Anaerobic Codigestion of Municipal Solid Waste and Biosolids under Various Mixing Conditions - Ii: Microbial Population Dynamics. *Water Research* 35(7), 1817-1827.
- Min, B., Evans, P.J., Chu, A.K. and Logan, B.E. (2004) Perchlorate Removal in Sand and Plastic Media Bioreactors. *Water Research* 38(1), 47-60.
- Moll, D.M., Summers, R.S., Fonseca, A.C. and Matheis, W. (1999) Impact of Temperature on Drinking Water Biofilter Performance and Microbial Community Structure. *Environmental Science & Technology* 33(14), 2377-2382.
- Motzer, W.E. (2001) Perchlorate: Problems, Detection, and Solutions. *Environmental Forensics* 2(4), 301-311.
- Nerenberg, R., Kawagoshi, Y. and Rittmann, B.E. (2008) Microbial Ecology of a Perchlorate-Reducing, Hydrogen-Based Membrane Biofilm Reactor. *Water Research* 42(4-5), 1151-1159.
- Nerenberg, R. and Rittmann, B.E. (2004) Hydrogen-Based, Hollow-Fiber Membrane Biofilm Reactor for Reduction of Perchlorate and Other Oxidized Contaminants. *Water Science and Technology* 49(11-12), 223-230.
- Nerenberg, R., Rittmann, B.E. and Najm, I. (2002) Perchlorate Reduction in a Hydrogen-Based Membrane-Biofilm Reactor. *Journal American Water Works Association* 94(11), 103-114.
- Nerenberg, R., Rittmann, B.E. and Soucie, W.J. (2000) Ozone/Biofiltration for Removing Mib and Geosmin. *Journal American Water Works Association* 92(12), 85-+.

- Niquette, P., Prevost, M., Servais, P., Beaudet, J.F., Coallier, J. and Lafrance, P. (1998) Shutdown of Bac Filters: Effects on Water Quality. *Journal American Water Works Association* 90(12), 53-61.
- Nishijima, W. and Speitel, G.E. (2004) Fate of Biodegradable Dissolved Organic Carbon Produced by Ozonation on Biological Activated Carbon. *Chemosphere* 56(2), 113-119.
- Nozawa-Inoue, M., Jien, M., Hamilton, N.S., Stewart, V., Scow, K.M. and Hristova, K.R. (2008) Quantitative Detection of Perchlorate-Reducing Bacteria by Real-Time PCR Targeting the Perchlorate Reductase Gene. *Applied and Environmental Microbiology* 74(6), 1941-1944.
- Nozawa-Inoue, M., Scow, K.M. and Rolston, D.E. (2005) Reduction of Perchlorate and Nitrate by Microbial Communities in Vadose Soil. *Applied and Environmental Microbiology* 71(7), 3928-3934.
- Rao, B., Anderson, T.A., Orris, G.J., Rainwater, K.A., Rajagopalan, S., Sandvig, R.M., Scanlon, B.R., Stonestrom, D.A., Walvoord, M.A. and Jackson, W.A. (2007) Widespread Natural Perchlorate in Unsaturated Zones of the Southwest United States. *Environmental Science & Technology* 41(13), 4522-4528.
- Rikken, G.B., Kroon, A.G.M. and vanGinkel, C.G. (1996) Transformation of (Per)Chlorate into Chloride by a Newly Isolated Bacterium: Reduction and Dismutation. *Applied Microbiology and Biotechnology* 45(3), 420-426.
- Rittmann, B.E., Hausner, M., Löffler, F., Love, N.G., Muyzer, G., Okabe, S., Oerther, D.B., Peccia, J., Raskin, L. and Wagner, M. (2006) A Vista for Microbial Ecology and Environmental Biotechnology. *Environmental Science & Technology* 40(4), 1096-1103.
- Rittmann, B.E. and Snoeyink, V.L. (1984) Achieving Biologically Stable Drinking-Water. *Journal American Water Works Association* 76(10), 106-114.
- Rittmann, B.E., Stilwell, D., Garside, J.C., Amy, G.L., Spangenberg, C., Kalinsky, A. and Akiyoshi, E. (2002) Treatment of a Colored Groundwater by Ozone-Biofiltration: Pilot Studies and Modeling Interpretation. *Water Research* 36(13), 3387-3397.
- Roquebert, V., Booth, S., Cushing, R.S., Crozes, G. and Hansen, E. (2000) Electrodialysis Reversal (Edr) and Ion Exchange as Polishing Treatment for Perchlorate Treatment. *Desalination* 131(1-3), 285-291.
- Servais, P., Billen, G. and Hascoet, M.C. (1987) Determination of the Biodegradable Fraction of Dissolved Organic-Matter in Waters. *Water Research* 21(4), 445-450.
- Suzuki, M.T., Rappe, M.S., Haimberger, Z.W., Winfield, H., Adair, N., Strobel, J. and Giovannoni, S.J. (1997) Bacterial Diversity among Small-Subunit Rrna Gene Clones and Cellular Isolates from the Same Seawater Sample. *Applied and Environmental Microbiology* 63(3), 983-989.

- Tan, Z. and Reinhold-Hurek, B. (2003) *Dechlorosoma Suillum* Achenbach Et Al. 2001 Is a Later Subjective Synonym of *Azospira Oryzae* Reinhold-Hurek and Hurek 2000. *International Journal of Systematic and Evolutionary Microbiology* 53, 1139-1142.
- Theron, J. and Cloete, T.E. (2000) Molecular Techniques for Determining Microbial Diversity and Community Structure in Natural Environments. *Critical Reviews in Microbiology* 26(1), 37-57.
- Tranckner, J., Wricke, B. and Krebs, P. (2008) Estimating Nitrifying Biomass in Drinking Water Filters for Surface Water Treatment. *Water Research* 42(10-11), 2574-2584.
- Urbansky, E.T. (2002) Perchlorate as an Environmental Contaminant. *Environmental Science and Pollution Research* 9(3), 187-192.
- Urbansky, E.T. and Schock, M.R. (1999) Issues in Managing the Risks Associated with Perchlorate in Drinking Water. *Journal of Environmental Management* 56(2), 79-95.
- US-EPA (2005) State Perchlorate Advisory Levels and Other Resources, [http://www.epa.gov/fedfac/documents/perchlorate\\_links.htm](http://www.epa.gov/fedfac/documents/perchlorate_links.htm).
- US-EPA (2008) Drinking Water Contaminant Candidate List 3 US-EPA, <http://www.epa.gov/safewater/ccl/ccl3.html>.
- van Ginkel, C.G., Rikken, G.B., Kroon, A.G.M. and Kengen, S.W.M. (1996) Purification and Characterization of Chlorite Dismutase: A Novel Oxygen-Generating Enzyme. *Archives of Microbiology* 166(5), 321-326.
- Venkatesh, K.R., Cobe, E.R., Jennings, D.L. and Wagner, N.J. (2000) Process for the Removal and Destruction of Perchlorate and Nitrate from Aqueous Streams, U.S. patent 6,066,257, U.S.A.
- Wallace, W., Ward, T., Breen, A. and Attaway, H. (1996) Identification of an Anaerobic Bacterium Which Reduces Perchlorate and Chlorate as *Wolinella Succinogenes*. *Journal of Industrial Microbiology* 16(1), 68-72.
- Waller, A., Cox, E. and Edwards, E. (2004) Perchlorate-Reducing Microorganisms Isolated from Contaminated Sites. *Environmental Microbiology* 6(5), 517-527.
- Weber, W.J. (1974) Adsorption Processes. *Pure and Applied Chemistry* 37(3), 375-392.
- Wilkin, R.T., Fine, D.D. and Burnett, N.G. (2007) Perchlorate Behavior in a Municipal Lake Following Fireworks Displays. *Environmental Science & Technology* 41(11), 3966-3971.
- Wolterink, A.F.W.M., Jonker, A.B., Kengen, S.W.M. and Stams, A.J.M. (2002) *Pseudomonas Chloritidismutans* Sp Nov., a Nondenitrifying, Chlorate-Reducing

Bacterium. *International Journal of Systematic and Evolutionary Microbiology* 52, 2183-2190.

Wolterink, A.F.W.M., Schiltz, E., Hagedoorn, P.L., Hagen, W.R., Kengen, S.W.M. and Stams, A.J.M. (2003) Characterization of the Chlorate Reductase from *Pseudomonas Chloritidismutans*. *Journal of Bacteriology* 185(10), 3210-3213.

Xiong, Z., Zhao, D.Y. and Pan, G. (2007) Rapid and Complete Destruction of Perchlorate in Water and Ion-Exchange Brine Using Stabilized Zero-Valent Iron Nanoparticles. *Water Research* 41(15), 3497-3505.

Xu, J., Song, Y., Min, B., Steinberg, L. and Logan, B. (2003) Microbial Degradation of Perchlorate: Principles and Applications. *Environmental engineering Science* 20(5), 405-422.

Xu, J., Trimble, J., Steinberg, L. and Logan, B. (2004) Chlorate and Nitrate Reduction Pathways Are Separately Induced in the Perchlorate-Respiring Bacterium *Dechlorosoma* Sp K<sub>j</sub> and the Chlorate-Respiring Bacterium *Pseudomonas* Sp P<sub>da</sub>. *Water Research* 38(3), 673-680.

Zhang, H., Logan, B.E., Regan, J.M., Achenbach, L.A. and Bruns, M.A. (2005) Molecular Assessment of Inoculated and Indigenous Bacteria in Biofilms from a Pilot-Scale Perchlorate-Reducing Bioreactor. *Microbial Ecology* 49(3), 388-398.

## Chapter 2

### Quantitative rRNA-Targeted Solution-Based Hybridization Assay Using Peptide Nucleic Acid Molecular Beacons

#### 2.1. Introduction

Accurate quantification of specific populations in complex microbial communities is important in many areas of microbiology. Today, real-time PCR based techniques are often used for this purpose (Suzuki et al., 2000). Other PCR based techniques, such as denaturing gradient gel electrophoresis (Muyzer, 1999) and terminal restriction fragment length polymorphism (Marsh, 1999), have also been used to study microbial population dynamics, but they are less suitable as quantitative techniques (von Wintzingerode et al., 1997). Oligonucleotide probe based microbial quantification methods that do not rely on PCR usually target the small-subunit rRNA, and include quantitative membrane hybridization, quantitative fluorescence *in situ* hybridization (FISH), and phylogenetic microarrays. While membrane hybridization has been used successfully to study microbial population dynamics in a variety of complex microbial systems (Raskin et al., 1994; Zheng et al., 2006), this technique is time consuming and labor intensive. Quantitative FISH also has been used effectively to quantify microbial populations (Pernthaler et al., 2003; Zhou et al., 2007). However, in some applications, traditional

FISH methods do not provide satisfactory quantitative results, because of poor cell permeability for oligonucleotide probes (Carr et al., 2005), low accessibility of target sites in rRNA (Fuchs et al., 1998), or poor sensitivity when the cellular rRNA content is low (Hahn et al., 1992). Microarray techniques have the potential to quantify rRNA extracted from environmental samples (El Fantroussi et al., 2003), but reproducibility and specificity issues have not been addressed satisfactorily (Small et al., 2001; Pozhitkov et al., 2007).

Peptide nucleic acid (PNA) oligomer probes were studied for their hybridization properties for the first time about 15 years ago (Egholm et al., 1993). PNA differs from DNA in that it contains an electro-neutral polypeptide backbone, while DNA includes a negatively charged sugar-phosphate backbone (Nielsen et al., 1994). The neutral backbone results in hybridization characteristics unique to PNA probes. For example, compared with traditional DNA probes, PNA probes bind stronger to target nucleic acids (Egholm et al., 1993) and are less dependent on the salt concentration used when hybridized to target DNA oligonucleotides (Kuhn et al., 2002). Furthermore, their hybridization kinetics are less affected by the secondary structure of target nucleic acids (Armitage, 2003). These characteristics have allowed successful applications of PNA probes in various fields of microbiology (Worden et al., 2000; Oliveira et al., 2002; Chandler and Jarrell, 2003; Brehm-Stecher et al., 2005).

Apart from PNA-conferred improvements in probe composition, novel probe chemistries have also been devised for both DNA- and PNA-based probes. These include molecular beacons (MBs) (Tyagi and Kramer, 1996; Xi et al., 2003), adjacent fluorescence resonance energy transfer (FRET) probes (Cardullo et al., 1988; Tsuji et al.,

2000), light-up probes (Svanvik et al., 2000; Privat et al., 2001), and quenched autoligation (QUAL) probes (Sando and Kool, 2002a; 2002b). The first DNA MB probes were developed by Tyagi and Kramer (Tyagi and Kramer, 1996). A DNA MB contains a probe sequence complementary to the target region of nucleic acids and a stem structure consisting of a few nucleotides complementary to each other allowing the DNA MB to form a stem-loop structure. A fluorophore is attached to one end of the DNA MB, while a quencher is bound to the other end. When no target nucleic acid is present, DNA MBs remain in their stem-loop configuration and the proximity of the quencher to the fluorophore results in limited or no fluorescence. When DNA MB probes bind to target nucleic acids, the stem-loop structure opens, resulting in an increase in the distance between fluorophore and quencher, and fluorescence can be detected. Thus, DNA MB probes only fluoresce upon hybridization to target nucleic acids, allowing a solution-based hybridization format (Tyagi and Kramer, 1996). Hybridizations with DNA MBs exhibit several other advantages, such as low background signal (Marras et al., 2006), high specificity (Bonnet et al., 1999), and high sensitivity (Vet et al., 1999). Because of these characteristics, DNA MB probes have shown to be advantageous in applications in real-time PCR (Vet et al., 1999; Petersen et al., 2004), visualization of mRNA in living cells (Bratu et al., 2003), and detection of nucleic acids in array techniques (Yao and Tan, 2004; Bockisch et al., 2005), but have been less successful in quantifying rRNA in solution-based hybridizations (Xi et al., 2003).

PNA MB probes were developed to make use of the advantages of both PNA probes and the structure of MBs (Ortiz et al., 1998; Seitz, 2000). Different from DNA MBs, which contain a stem-loop structure, PNA MBs consist of only a loop structure.

The stemless loop structure of PNA MBs simplifies probe design. PNA MBs are hydrophobic, and therefore, tend to fold to minimize surface area in aqueous solution (Seitz, 2000). In addition, the electrostatic interaction between two oppositely charged amino acids at each end may help bring the fluorophore and quencher in close proximity. So far, most of the studies on PNA MBs have focused on the hybridization of PNA MBs to DNA oligonucleotides (Kuhn et al., 2001; Kuhn et al., 2002) or PCR products (Petersen et al., 2004), except for a few studies in which 16S rRNA was used as targets in PNA MB hybridization (Coull et al., 2001; Xi et al., 2003; Xi et al., 2005). Even though PNA MBs are considerably more expensive than DNA MBs and are only available from one authorized vendor (Panagene, Daejeon, Korea), the use of PNA MBs in solution-based rRNA-targeted hybridizations showed much promise in a previous study (Xi et al., 2003). However, more work to evaluate reaction kinetics and hybridization specificity is needed before this technique can be used as a quantitative tool with environmental samples.

The present study addresses how probe sequence and hybridization conditions affect the kinetics of hybridization of PNA MBs to 16S rRNA, how well PNA MBs can differentiate target and non-target 16S rRNA, and affirms the potential of PNA MB hybridization as a quantitative assay in environmental studies.

## **2.2. Materials and Methods**

### **2.2.1 PNA MBs**

PNA MBs were designed in this study to target 16S rRNA of bacterial species within the genera *Dechloromonas* (S-G-Dmonas-0121-a-A-18, hereafter referred to as PNA MB



Dmonas0121) and *Dechlorosoma* (S-G-Dsoma-0848-a-A-17, hereafter referred to as PNA MB Dsoma0848). Note that the type strain of the genus *Dechlorosoma*, *Dechlorosoma suillum* DSM 13638T, is almost identical to the type strain of the genus *Azospira*, *Azospira oryzae* 6a3T, indicating that *D. suillum* is a later subjective synonym of *A. oryzae* (Tan and Reinhold-Hurek, 2003). The two PNA MBs both contain the fluorophore tetramethylrhodamine (TAMRA) and the quencher DABCYL [4-(4-dimethylaminophenylazo)-benzoic acid]. The specificity, coverage, and sequences of the two PNA MBs are provided in Table 2.1. Sequences of the target sites in the 16S RNAs of target and non-target species used in this study are presented in Table 2.2. A third PNA MB was designed to target the bacterial domain (S-D-Bact-0338-a-A-18, hereafter referred to as Bact0338) (Xi et al., 2003). All three PNA MBs were synthesized by Applied Biosystems (Foster City, CA) at the time. Upon receipt, PNA MBs were suspended in distilled deionized water (ddH<sub>2</sub>O) at a concentration of 50  $\mu$ M, and stored in polypropylene vials at -80°C in the dark. These stock solutions were heated to 50°C for 10 min to ensure homogeneous solutions prior to preparing 10 fold dilutions to serve as working stocks. Working stocks were stored at -20°C in the dark.

### 2.2.2 RNA Extractions

Bacterial cultures *Dechloromonas agitata* and *D. suillum* were purchased from the Deutsche Sammlung von Mikroorganismen und Zellkulturen GmbH (DSMZ; DSM 13637 and 13638, respectively), and *Methylophilus methylotrophus* and *Marinospirillum minutulum* were purchased from the American Type Culture Collection (ATCC; ATCC 53528 and 19193, respectively). Each of the four cultures was grown for 42 h in 10 mL

of its recommended growth medium, then 200  $\mu$ L of each culture was transferred to 200 mL of the growth medium. To reach their mid exponential growth phase, *D. agitata* and *D. suillum* were grown aerobically at 30°C in DSMZ medium #1 for 14 and 18 h, respectively, *M. methylotrophus* was grown aerobically at 30°C in ATCC medium #1545 for 78 h, and *M. minutulum* was grown aerobically at 26°C in ATCC marine broth 2216 for 56 h. The environmental sample used in the spike-in experiment was collected from a laboratory-scale anaerobic bioreactor (Zheng et al., 2006). The environmental samples used to compare PNA MB hybridization results with clone library results were collected from a laboratory-scale biologically active carbon (BAC) reactor (Li et al.).

Total RNA was extracted from centrifuged cell pellets using a phenol-chloroform-isoamyl alcohol extraction procedure (Stahl et al., 1988), and the RNA was resuspended in ddH<sub>2</sub>O and stored at -80°C. The concentrations of nucleic acids in the RNA extracts were measured spectrophotometrically using a NanoDrop ND1000 (NanoDrop Technologies, Wilmington, DE) at a wavelength of 260 nm. Furthermore, the quality of the RNA extracts was evaluated using polyacrylamide gel electrophoresis (JULE Biotechnologies Inc., Milford, CT) and images of the gels were analyzed using a Kodak Molecular Imaging Software (version 4.0.3K1, Rochester, NY). The concentration of the 16S rRNA in each extract was calculated as the product of the total nucleic acid concentration estimated spectrophotometrically and the mass ratio of 16S rRNA to total nucleic acid obtained from the gel image analyses.

### **2.2.3 Hybridizations**

The hybridization buffer composition and hybridization condition for PNA MB Bact0338

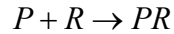
were adopted from the study by Xi *et al.* (Xi *et al.*, 2003). The hybridization buffer used for PNA MBs Dmonas0121 and Dsoma0848 was modified from the same study and contained 25 mM Tris-HCl and 10 mM NaCl, except for specific experiments as described below. In the experiments testing various salt concentrations, hybridization buffers contained NaCl with final concentrations ranging from 0 to 500 mM. In the experiments using formamide for stringency control, hybridization buffers contained formamide ranging from 0 to 90% (v/v). In the experiments for which environmental samples were used, hybridization conditions were adopted from the characterization experiments in this study or the study by Xi and coworkers (Xi *et al.*, 2003). Detailed hybridization conditions for all experiments are summarized in Table 2.3.

Experiments to study the non-specific opening of PNA MB (i.e., response of PNA MB in the absence of rRNA), hybridization kinetics of PNA MB, and effects of formamide on hybridization stringency were performed in Costar standard 96-well microplates with black walls and clear bottoms (Corning 3651, Corning Incorporated, Corning, NY). Fluorescence signals in these experiments were measured using a Bio-Tek Synergy HT multi-detection microplate reader (Winooski, VT) and expressed in relative fluorescence units (RFUs). Experiments to determine optimal hybridization temperatures (melting curve experiments), detection limit, and experiments with environmental samples were conducted in an Eppendorf ThermoStat Plus (Hamburg, Germany) for temperature control. Fluorescence signals in these experiments were measured using a NanoDrop ND3300 (NanoDrop Technologies, Wilmington, DE) and expressed in RFUs.

#### 2.2.4 Data Analysis

Net RFUs for hybridization of PNA to 16S rRNA were calculated as the differences between the RFUs obtained with samples containing only PNA MB and RFUs from mixtures containing also 16S rRNA.

A pseudo-first-order model was used to fit the kinetic curves (Podell et al., 1991) for the formation of hybrids (PR) between PNA MB probes (P) and target 16S rRNA (R).



$$\frac{d[PR]}{dt} = -\frac{d[R]}{dt} = k_u[R] \quad (1)$$

where  $t$  is time,  $[R]$  is the concentration of target 16S rRNA in solution,  $[PR]$  is the concentration of hybrids, and  $k_u$  is the pseudo-first-order rate constant. This model assumes that the concentration of PNA MBs remains constant during hybridization. The assumption was satisfied by providing PNA MBs in 20-fold excess of 16S rRNA (Table 2.3). Integration of Equation (1) yields:

$$\frac{[R]_t}{[R]_0} = \exp(-k_u t) \quad (2)$$

where,  $[R]_t$  and  $[R]_0$  are the 16S rRNA concentrations at time  $t$  and time zero, respectively. Then the equation can be converted to:

$$\frac{[R]_0 - [R]_t}{[R]_0} = 1 - \exp(-k_u t) \quad (3)$$

and further:

$$\frac{[PR]_t}{[PR]_\infty} = 1 - \exp(-k_u t) \quad (4)$$

where  $[PR]_t$  and  $[PR]_\infty$  are the hybrid concentrations at time  $t$  and at time infinity, respectively. The value of  $[PR]_t$  was measured in units of RFU. The values of  $[PR]_\infty$

and  $k_u$  were simulated using the curve-fitting function in the software Kaleidagraph (Synergy Software, Reading, PA). The two parameters,  $[PR]_\infty$  and  $k_u$ , provided information on the final hybridization signal and the apparent rate constant, respectively. The values of the apparent rate constants were subject to statistical analyses in Microsoft Excel using 2-way analyses of variance (2-way ANOVA) with 16S rRNA sequence as one independent variable and NaCl concentration as the other independent variable. In this study, the units for the pseudo-first-order apparent rate constant are  $\text{RFU} \times \text{min}^{-1} \times \text{M}^{-1}$ . If RFU is converted to molarity, the units simplify to  $\text{min}^{-1}$ .

### 2.2.5 Detection Limit

The detection limit of the PNA MB hybridization assay was determined using a standard procedure (EPA, 1999) with seven replicates for each 16S rRNA concentration included in the experiment (Table 2.3). In brief, measurement results from seven replicates were calculated for standard deviation ( $s$ ), a critical  $t$ -value was obtained using a degree of freedom of 6 and a confidence level of 99% ( $t_{6, 0.99}$ ), and method detection limit ( $MDL$ ) was calculated as

$$MDL = t_{6,0.99} \times s \quad (5)$$

## 2.3. Results

### 2.3.1 Response of PNA MB in the Absence of rRNA

Before optimizing the stringency of hybridization between PNA MB and 16S rRNA by varying hybridization temperatures and formamide concentrations in hybridization

buffers, the response of PNA MB to these two approaches in the absence of target or non-target nucleic acid was evaluated. The PNA MB Dsoma0848 exhibited substantial fluorescence without binding to target nucleic acids at high temperatures (>40°C for 50% formamide and >50°C for 30% formamide) and at all temperatures in 70% formamide (Figure 2.1). The fluorescence signals are due to the opening of the loop structure of the PNA MB, a process referred to as non-specific opening of PNA MB hereafter.

The effect of formamide on the non-specific opening of PNA MB is more substantial than that of temperature (Figure 2.1). For example, a formamide concentration of 70% resulted in higher fluorescence signals at low temperatures than a formamide concentration of 30% at high temperatures. In addition, an increase in temperature did not promote further non-specific opening of PNA MB in the presence of 70% formamide. Because of the different patterns of fluorescence signals associated with the non-specific opening of PNA MB, this non-specific opening was monitored for all experiments in this study by including a control containing only PNA MB for each hybridization condition. The fluorescence signals due to the non-specific opening of PNA MB were subtracted from the fluorescence signals of samples containing 16S rRNA, and the resulting values are reported as net fluorescence signals using net relative fluorescence units (net RFUs).

## **2.3.2 Hybridization Kinetics**

### *2.3.2.1. Kinetics of hybridization to target and non-target 16S rRNA*

Prior to the determination of optimal hybridization conditions, the kinetic properties of hybridizations of PNA MB were studied with various 16S rRNA sequences and in

hybridization buffers of various NaCl concentrations. Five hundred fmol (1 fmol equals  $10^{-15}$  mole) of one target 16S rRNA (*D. suillum*) and two non-target 16S rRNAs (*M. minutulum* and *M. methylotrophus*) were used in each hybridization reaction with 10,000 fmol of PNA MB Dsoma0848 (Table 2.3). This 20-fold excess of PNA MB to target and non-target 16S rRNA resulted in hybridization reactions that exhibited pseudo-first-order kinetics, as indicated in Figure 2.2 with good agreement between the simulation curves and the experimental data points. Hybridization of PNA MB Dsoma0848 to its target 16S rRNA (*D. suillum*) resulted in the highest final net fluorescence signals among the three hybridizations. Unexpectedly, the final signal of the hybridization to the 16S rRNA with four mismatches (*M. methylotrophus*) was higher than that from the hybridization to the 16S rRNA with one mismatch (*M. minutulum*). This phenomenon was also observed for some hybridization conditions in other kinetic experiments (Figure 2.3a). In addition, the hybridization of PNA MB Dsoma0848 to non-target 16S rRNAs exhibited faster kinetics and reached equilibrium faster than the hybridization to target 16S rRNA (Figure 2.2).

#### 2.3.2.2. *Effects of NaCl Concentration on Hybridization Kinetics*

The effects of monovalent cation concentration (i.e., sodium) on the kinetics of hybridization of PNA MB to 16S rRNA were studied by plotting final net fluorescence signals and apparent rate constants for various NaCl concentrations (Figure 2.3). As the NaCl concentration increased, final net fluorescence signals dropped substantially in hybridizations with both target and non-target 16S rRNA (Figure 2.3a). The maximum difference between the final net fluorescence signals for target and non-targets was

obtained at a NaCl concentration of 10 mM (Figure 2.3a). Therefore, a NaCl concentration of 10 mM was chosen for subsequent experiments.

The apparent rate constants also decreased as the NaCl concentration increased (Figure 2.3b). In addition, the apparent rate constants for the target were lower than those of the non-targets at all the NaCl concentrations tested, although this difference was not statistically significant. In the 2-way ANOVA tests, NaCl concentration – an independent variable – appeared to have a significant effect on the apparent rate constants ( $p < 0.05$ ). In contrast, 16S rRNA sequence – the other independent variable – did not have a significant effect on the apparent rate constant ( $p = 0.24$ ). The interaction between the two independent variables was not significant either ( $p = 0.99$ ). The slower overall kinetics of the hybridization with target rRNA did not allow elimination of signal from non-target using a kinetic approach.

### **2.3.3 Optimization of Hybridization Conditions**

#### *2.3.3.1. Melting Curves*

Melting curves of the hybridizations of PNA MB Dsoma0848 with 16S rRNAs showed that at the lowest hybridization temperature of 22°C, target 16S rRNA (*D. suillum*) exhibited a higher net fluorescence signal than non-target 16S rRNAs with one and four mismatches (*M. minutulum* and *M. methylotrophus*, respectively) (Figure 2.4). Consistent with the order of final hybridization signals presented in the kinetic experiments (Figure 2.2 and Figure 2.3a), the net fluorescence signal from *M. methylotrophus* (four mismatches) was higher than that from *M. minutulum* (one mismatch) at 22°C and subsequent temperatures evaluated. As the temperature was



increased, the net fluorescence signals of all three melting curves increased slightly, then decreased. Between 64 and 70°C, the three melting curves reached their minimum values. At about 68°C, the net fluorescence signal from *M. minutulum* was zero and the signal from *M. methylotrophus* was low. Hence, 68°C was selected as the optimal hybridization temperature for PNA MB Dsoma0848.

After reaching minimum values, the net fluorescence signals increased for all three melting curves until the end of the experiment (Figure 2.4). Such a phenomenon has not been reported in other studies with PNA MBs. Since the data in Figure 2.4 were reported in units of net RFUs, it is likely that the presence of rRNA molecules – regardless of sequence – facilitated the non-specific openings of PNA MBs at high temperatures.

To confirm the optimal hybridization temperature and demonstrate that elimination of signals from non-target rRNA can be achieved in mixed cultures at optimized hybridization conditions, an artificial mixture containing equal amounts of 16S rRNA from target and non-target with one mismatch (*D. suillum* and *M. minutulum*, respectively) was hybridized with PNA MB Dsoma0848 (Figure 2.5). At the optimized hybridization temperature of 68°C, the net fluorescence signal from non-target 16S rRNA with one mismatch was zero. The net fluorescence signals from the target and the artificial mixture were nearly identical, confirming that the non-target 16S rRNA did not contribute to signal. Thus, after optimization of hybridization conditions, PNA MBs can be used to quantify target 16S rRNA in samples containing mixtures of rRNA, such as environmental samples. In addition, the fluorescence signal at 68°C in the melting curve experiment started at 22°C (Figure 2.4) was similar to the fluorescence signal at 68°C in

the melting curve experiment started at 60°C (Figure 2.5), which verified that the 2 min time period was sufficient for the hybridization to reach equilibrium after each increase in temperature (Table 2.3).

A similar melting curve experiment was conducted for PNA MB Dmonas0121 with its target 16S rRNA (*D. agitata*) and non-target 16S rRNAs with two and four mismatches (*M. methylotrophus* and *D. suillum*, respectively) (Figure 2.6). Typical melting profiles were observed for target and non-target 16S rRNAs. For the range of hybridization temperatures tested, the net fluorescence signals for non-targets were never completely eliminated (Figure 2.6), even when formamide was added at 10 and 20% to the hybridization buffers (data not shown). Therefore, hybridizations with PNA MB Dmonas0121 may result in substantial false-positive signals, especially for environmental samples containing low-abundance target populations. Hence, the addition of formamide to hybridization buffers at a broad range of percentages was evaluated in order to minimize signals from non-target rRNA.

#### 2.3.3.2. *Stringency Control using Formamide*

The experiment performed to optimize the formamide concentration in the hybridization buffer for PNA MB Dmonas0121 resulted in typical sigmoidal shaped curves for both target 16S rRNA and non-target 16S rRNA with two mismatches (*D. agitata* and *M. methylotrophus*, respectively) (Figure 2.7). However, for formamide concentrations above approximately 40%, the net fluorescence signals were negative.

#### **2.3.4 Detection Limit**

The detection limit of the hybridization assay using PNA MB Dsoma0848 was determined to be approximately 1.6 nM of 16S rRNA at the optimized hybridization condition (i.e., hybridization temperature of 68°C with no formamide in the hybridization buffer) (data not shown).

#### **2.3.5 Spike-in Experiment**

The hybridization assay using PNA MB Dsoma0848 allowed quantification of target 16S rRNA spiked at different concentrations to RNA extracted from an environmental sample. The hybridization response of PNA MB Dsoma0848 was linear over the range of 0 to 30% of relative abundance for the 16S rRNA spiked to the RNA extract from an environmental sample and for the corresponding target 16S rRNA alone (i.e., 0 – 43 fmol of target 16S rRNA; Figure 2.8). However, the environmental RNA extracts spiked with the different concentrations of target 16S rRNA resulted in higher hybridization signals.

#### **2.3.6 Environmental Samples**

Two PNA MB hybridization assays using Dsoma0848 and Bact0338 were used to quantify the 16S rRNA from *Dechlorosoma* spp. and the total bacterial population in two biomass samples collected from a laboratory-scale BAC reactor, which was operated for nitrate and perchlorate removal from groundwater. After normalizing the results from Dsoma0848 with the results from Bact0338 (data on individual standard curves not shown), it was determined that *Dechlorosoma* spp. accounted for 10.5 and 36.4% of the bacterial community in the two biomass samples. In comparison, 16S rRNA gene clone

libraries indicated the relative abundances of *Dechlorosoma* spp. were 0.6 and 10.1% in these two biomass samples, respectively (Li et al.).

## 2.4. Discussion

In order to evaluate PNA MB hybridization as a tool to quantify specific 16S rRNA in environmental samples, hybridization kinetics and hybridization specificity were studied. Non-specific opening of PNA MBs was observed at stringent hybridization conditions, making it necessary to include a control containing only PNA MB in each experiment. Despite the increase in net fluorescence signal at high temperatures in melting curves, hybridizations at optimal temperatures can eliminate false-positive signals from non-target rRNAs, differing in only one base from target rRNA (Figure 2.4 and Figure 2.5).

The kinetics of hybridization reactions depend on both forward and reverse reactions (i.e., association and dissociation processes). Solid surface hybridizations with linear DNA and PNA probes have been used to study association and dissociation rates. For example, using immobilized linear DNA oligonucleotide probes, Livshits and Mirzabekov demonstrated that the association rate constant was the same for target and non-target DNA (Livshits and Mirzabekov, 1996), and Dai et al. showed that non-targets exhibited higher dissociation rate constants than targets, which resulted in faster overall kinetics for non-target (Dai et al., 2002). In contrast, immobilized linear PNA probes generally exhibited higher association rate constants and lower dissociation rate constants for targets than for non-targets (Jensen et al., 1997). Unlike solid surface hybridizations, the solution-based hybridizations in this study do not allow separate analyses of

association and dissociation processes. Based on conclusions presented by Jensen and coworkers (Jensen et al., 1997), we suggest that the lower apparent rate constants in the hybridizations with target 16S rRNA (Figure 2.2 and Figure 2.3b) were the result of lower dissociation rate constants for target 16S rRNA.

The lower apparent rate constants for the hybridization of PNA MB with target 16S rRNAs demonstrated it was not feasible to use a kinetic approach to eliminate false-positive fluorescence signals due to non-specific hybridization. Therefore, other approaches, such as optimizing hybridization temperature and formamide concentration in the hybridization buffer, were used to control hybridization specificity for the PNA MBs Dmonas0121 and Dsoma0848. Before these approaches were tested, the salt concentration in the hybridization buffer was optimized.

Because 16S rRNAs were used as target molecules, the NaCl concentration in the hybridization buffer affected not only the hybridization between PNA MB Dsoma0848 and target molecules, but also the secondary structures of the rRNA molecules. High salt concentrations (i.e., high ionic strength) in hybridization buffers favor the formation of RNA secondary structure and make the target sites in rRNA less accessible (Tinoco and Bustamante, 1999). A study on hybridizations between linear PNA probes and double-stranded DNA (ds DNA) oligonucleotide targets revealed that the initial association rates dropped as the NaCl concentrations increased from 20 to 50 mM (Kuhn et al., 1998). Unlike ds DNA oligonucleotides, 16S rRNAs exhibit higher-order structure, thus it was important to compare hybridization results for different NaCl concentrations.

It should be noted that the hybridization condition used in the kinetic experiments did not correspond to the optimized hybridization condition. As indicated above, the

objectives of these experiments were to compare the kinetics of hybridizations of PNA MB to target and to non-target 16S rRNAs, evaluate the effects of NaCl concentrations on PNA MB hybridization kinetics, and choose a NaCl concentration for experiments thereafter. Previous studies have evaluated the kinetics of hybridizations of PNA MB and DNA MB to target and non-target DNA oligonucleotides (Kuhn et al., 2002) and target 16S rRNA (Xi et al., 2003). To our knowledge, this is the first study evaluating the effects of rRNA sequence and hybridization buffers on the kinetics of hybridizations of PNA MB to 16S rRNA.

The hybridization optimization experiments, with varying hybridization temperatures and formamide concentrations in hybridization buffers, indicated the two PNA MB probes designed in this study required different optimization strategies (Figure 2.4 - Figure 2.7). A third PNA MB, Bact0338, previously designed and characterized by Xi and coworkers (Xi et al., 2003), was also included in our study. Xi et al. defined the optimal formamide concentration as the condition that maximized the difference between the fluorescence signal of a hybridization reaction and the fluorescence signal of the control reaction only containing PNA MB. They demonstrated that hybridization at the optimized condition allowed differentiation of target and non-target 16S rRNAs when their abundances were comparable. However, unpublished data from our study showed that the optimal hybridization condition defined in that study (Xi et al., 2003) resulted in significant false-positive signals when the relative abundance of target 16S rRNA was low in an artificial mixture. Therefore, in the current study, melting curve experiments were conducted for PNA MB probe Bact0338 with target and non-target 16S rRNAs to determine a condition that minimized signal from non-targets. Unexpectedly, PNA MB

Bact0338 exhibited melting profiles completely different from those shown in Figure 2.4 and Figure 2.6: the net fluorescence signals from both target and non-target 16S rRNAs increased with hybridization temperatures (data not shown). Thus, we conclude that each newly designed PNA MB needs to be carefully characterized and may require different stringency control strategies.

The difference between the two series in Figure 2.8 may be attributed to the presence of target 16S rRNA in the environmental sample. The environmental sample was collected from an anaerobic bioreactor, and the genus *Dechlorosoma* contains heterotrophic facultative anaerobic respiring bacteria (Achenbach et al., 2001). Alternatively, the difference may be the result of non-specific hybridization and/or non-specific opening of PNA MB due to binding to environmental substances in the samples. This possible non-specific hybridization signal corresponded to about 5% of the total signal. In this experiment, we decided to spike RNA extracted from a pure culture of a target strain into RNA extracted from an environmental sample, rather than spiking target cells into an environmental sample followed by RNA extraction. This latter approach may overestimate the sensitivity of the method, because target cells grown in rich medium likely have higher levels of 16S rRNA than cells in environmental samples (Kerkhof and Ward, 1993).

The relative abundance values of *Dechlorosoma* spp. determined with the 16S rRNA targeted PNA MB hybridization assay and with the 16S rRNA gene targeted clone library method were different. Both methods provided results that could be qualitatively linked to the performance of the bioreactor: the increase of *Dechlorosoma* spp. with time was consistent with improved perchlorate removal in the bioreactor. Although the results

obtained with the two methods differed substantially, such differences are not unusual, especially when methods subject to PCR biases are involved (Acinas et al., 2005). It should also be noted that the target biomarker for the two methods were different: the solution-based hybridization assay targets 16S rRNA, whereas the clone library method targets 16S rRNA genes. Others have shown substantial differences when such quantitative results were compared (Gonzalez et al., 2000; Brinkmeyer et al., 2003).

We observed that PNA MB in the absence of rRNA produced substantial fluorescence signals at high temperatures or high formamide concentrations (Figure 2.1). Bonnet et al. proposed a three-conformational model for DNA MB probes (Bonnet et al., 1999). The authors demonstrated that there were three conformations of structured DNA MB: DNA MBs hybridized to RNA molecules, free DNA MBs that do not contribute to fluorescence signals, and randomly coiled free DNA MBs that fluoresce. According to Bonnet et al., the third conformation usually occurs at high temperatures when hybrids between probe and target nucleic acid have melted and the stem structure of DNA MB is broken. In the current study, although the structure of PNA MBs is different from that of DNA MBs, it is reasonable to speculate that the majority of PNA MBs are present in a coiled free form at high temperatures. The observed increases in net fluorescence signals in the presence of target and non-target rRNAs (Figure 2.4 - Figure 2.5) suggest that rRNA molecules, independent of sequence, facilitate the formation of the coil free PNA MB.

The negative values in net fluorescence signals (Figure 2.4 - Figure 2.7) may result from a quenching effect of nucleic acids on fluorophores. A study by Wang and coworkers suggested a quenching effect on TAMRA, the same dye used in the PNA MBs



Dmonas0121 and Dsoma0848, when the dye is in proximity of a guanosine near the target site (Wang et al., 2004). In the current study, the fluorescence signals were reported in net fluorescence signals, the difference between the signals from controls containing only PNA MB and the signals from corresponding samples also containing rRNA molecules. Because the quenching effect is absent in the controls, the subtraction caused negative signals in the net fluorescence signals. It was noticed that the negative net fluorescence signals were more evident in the formamide experiment (Figure 2.7) than in the melting curve experiments (Figure 2.4 - Figure 2.6). This might be related to the fact that formamide is more efficient in causing non-specific opening of PNA MB than temperature in controls (Figure 2.1). Future studies should focus on designing new PNA MBs that maintain their loop structure even at stringent conditions when target rRNA is not present.

## 2.5. Tables

Table 2.1. Specificity, coverage, and sequences of the PNA MBs Dmonas0121 and Dsoma0848<sup>1</sup>.

PNA MB	# of sequences with perfect match	# of targets in database <sup>2</sup>	Specificity <sup>3</sup>	Coverage <sup>4</sup>	Sequences (N-terminus to C-terminus)
Dmonas0121	61	58	33/61	33/58	TAMRA-E-AAGGTACGTTCCGATACA-K-K-DABCYL
Dsoma0848	29	22	20/29	20/22	TAMRA-E-TAGCTGCGGTACTAAAA-K-K-DABCYL

<sup>1</sup> Information on specificity and coverage was obtained through the Ribosomal Database Project II (RDP II) on May 22<sup>nd</sup> 2006 (Cole et al., 2005).

<sup>2</sup> The number of targets in database is defined as the total number of sequences in RDP database that belong to either *Dechloromonas* or *Dechlorosoma*.

<sup>3</sup> Specificity = “Number of target sequences with perfect match to each PNA MB” / “Number of sequences with perfect match to each PNA MB”.

<sup>4</sup> Coverage = “Number of target sequences with perfect match to each PNA MB” / “The number of targets in the RDP database”.

Table 2.2. Target sites in the 16S rRNA of target and non-target species included in this study for the PNA MBs Dmonas0121 and Dsoma0848.

Species <sup>1</sup>	Dmonas0121 <sup>2</sup> (5'-3')	Dsoma0848 <sup>2</sup> (5'-3')
<i>Dechloromonas agitata</i>	-UGUAUCGGAACGUACCUU-	
<i>Dechlorosoma suillum</i> <sup>3</sup>	-U <u><b>CA</b></u> AUCGGAACGUAC <u><b>CA</b></u> -	-UUUUAGUACCGCAGCUA-
<i>Methylophilus methylotrophus</i>	-U <u><b>A</b></u> AUCGGAACGU <u><b>G</b></u> CCUU-	- <u><b>CA</b></u> <u><b>U</b></u> <u><b>G</b></u> A <u><b>A</b></u> CGCAGCUA-
<i>Marinospirillum minutulum</i>		-UUUUAGUA <u><b>A</b></u> CGCAGCUA-

<sup>1</sup> The first three species belong to the *Betaproteobacteria*, and *M. minutulum* belongs to the *Gammaproteobacteria*.

<sup>2</sup> The bold underlined nucleotides indicate the mismatches to the PNA MBs presented in Table 2.1.

<sup>3</sup> The name *Dechlorosoma suillum* is a subjective synonym of the name *Azospira oryzae* (Tan and Reinhold-Hurek, 2003).

Table 2.3. Summary of hybridization conditions for various experiments<sup>1</sup>.

	<b>Non-specific Opening of PNA MB</b>	<b>Kinetic Experiment</b>	<b>Melting Curve Experiments</b> (including pure cultures & an artificial mixture)	<b>Formamide Experiment</b>	<b>Detection Limit Experiment</b>	<b>Spike-in Experiment</b>	<b>Environmental Sample Experiment<sup>7</sup></b>
16S rRNA (fmol)	No RNA added	500	7.5 <sup>2,3</sup>	400	0, 4.5, 6, and 7.5 ( <i>D. suillum</i> )	(100 + <i>n</i> ) and <i>n</i> <sup>6</sup>	250
PNA MB (fmol)	3,750 (Dsoma0848)	10,000 (Dsoma0848)	150 (Dsoma0848 and Dmonas0121)	5,000 (Dmonas0121)	150 (Dsoma0848)	500 (Dsoma0848)	500 (Dsoma0848)
Sample Vol (μL)	220	220	1.5	250	1.5	1.5	1.5
Hybridization condition	30, 50, and 70% formamide in hybridization buffers, hybridized at temp from 25 to 90°C with 5°C steps.	25°C, no formamide.	Hybridizations took place at a starting temp, then the hybridization temp increased in a step wise manner <sup>4</sup> .	0 - 90% of formamide in hybridization buffers, and hybridized at 25°C.	68°C <sup>5</sup> for 100 min.	68°C <sup>5</sup> for 100 min.	68°C <sup>5</sup> for 100 min.
Instrument	Microplate	Microplate	NanoDrop	Microplate	NanoDrop	NanoDrop	NanoDrop

<sup>1</sup> In nearly all experiments for PNA MBs Dmonas0121 and Dsoma0848, hybridization buffers contained 25 mM Tris-HCl and 10 mM NaCl. In the experiments testing various salt concentrations, the final NaCl concentrations in hybridization buffers varied from 0 to 500 mM. In the experiments using formamide to control hybridization stringency, the hybridization buffers contained 0 – 90% formamide.

<sup>2</sup> 0.1% (v/v) diethyl pyrocarbonate (Sigma-Aldrich, St. Louis, MO) was added to minimize RNA degradation in all melting curve experiments.

<sup>3</sup> In the experiments using pure cultures, each 1.5 μL sample contained 7.5 fmol of target or non-target 16S rRNA. In the experiment with artificial mixtures of 16S rRNA, each 1.5 μL of the mixture contained 7.5 fmol of target 16S rRNA (*D. suillum*) and 7.5 fmol of non-target 16S rRNA (*M. minutulum*).

<sup>4</sup> The melting curve experiments with pure cultures started at 22°C for 100 min, then the temperature was increased with 3°C steps until 91°C. The melting curve experiment with an artificial mixture started at 60°C for 100 min, then the temperature was increased with 2 and 3°C steps until 81°C. In both experiments, fluorescence signals were measured 2 min after each increase in temperature.

<sup>5</sup> The hybridization temperature 68°C (in 0% formamide hybridization buffer) was determined experimentally, Figure 2.4 and Figure 2.5.

<sup>6</sup> In the first series of rRNA mixtures, 100 fmol aliquots of 16S rRNA from an environmental sample (Zheng et al., 2006) were spiked with *n* fmol of target 16S rRNA from *D. suillum* resulting in various 16S rRNA percentages equal to  $n/(100+n)$  (i.e., 0, 1, 2.5, 5, 10, 20, and 30%). In the second series, only *n* fmol of target 16S rRNA from *D. suillum* were used, corresponding to the amounts of 16S rRNA target in the first series.

<sup>7</sup> The Environmental Sample Experiment also involved the use of PNA MB Bact0338. Hybridization buffer composition and hybridization condition for Bact0338 were reported in Ref (Xi et al., 2003).

## 2.6. Figures

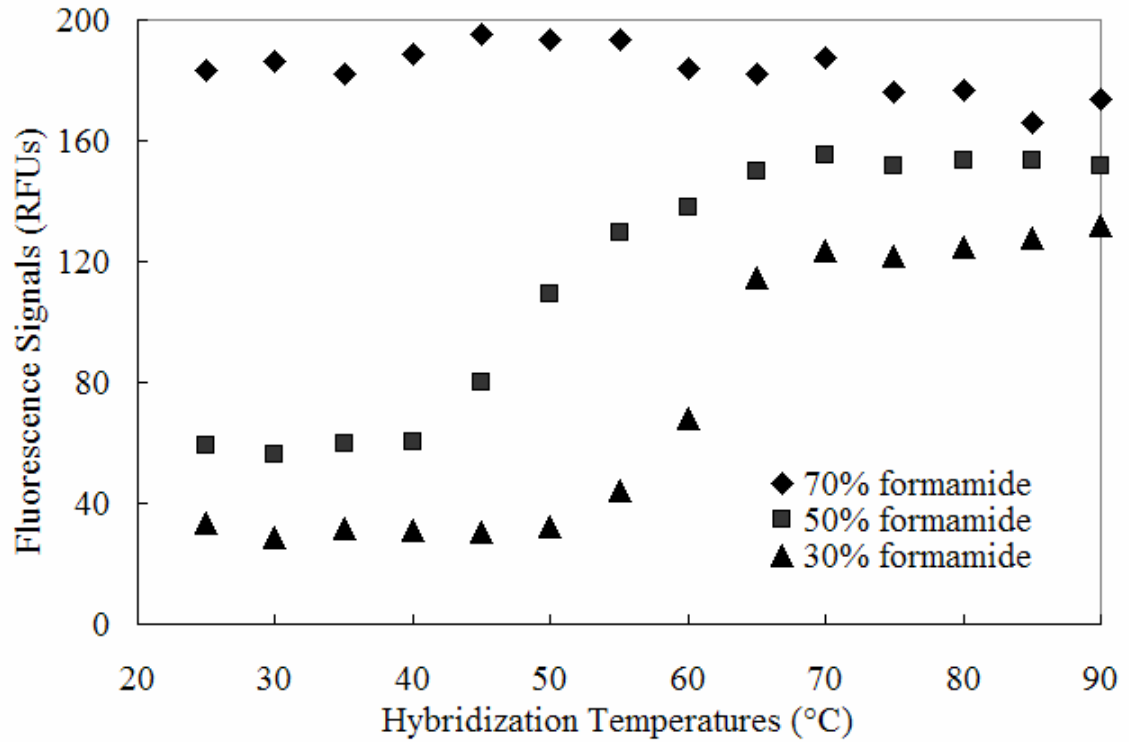


Figure 2.1. Non-specific opening of PNA MB Dsoma0848 due to the increases in hybridization temperature and formamide concentration in hybridization buffers. No rRNA was included in this experiment.

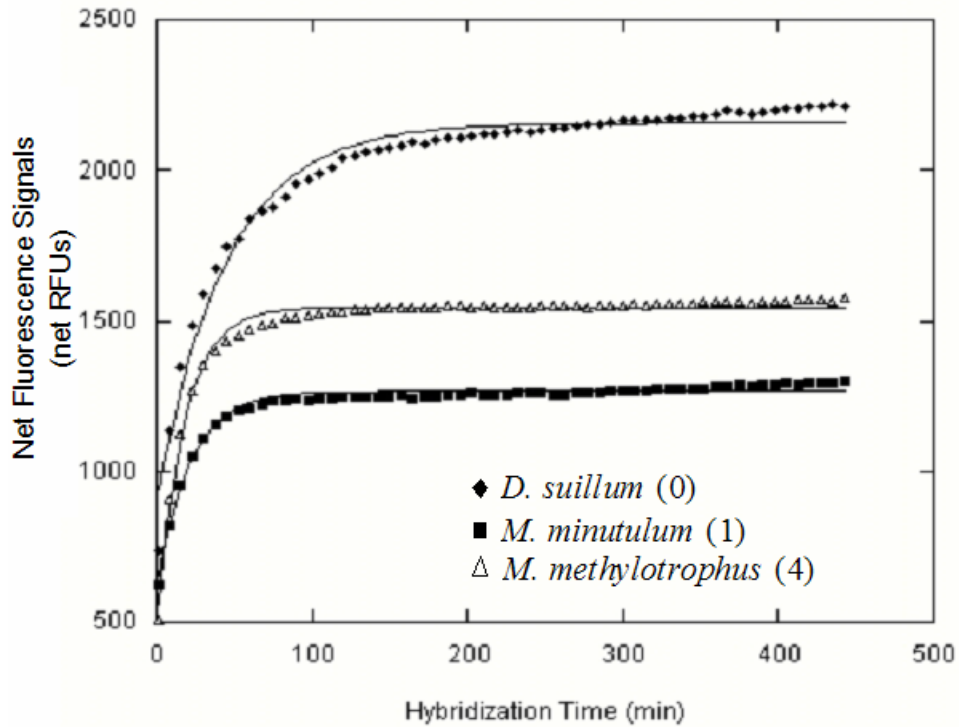


Figure 2.2. A sample plot showing the kinetics of the hybridizations of PNA MB Dsoma0848 to target and non-target 16S rRNA in the presence of 10 mM NaCl. The points are experimental data points, and the lines are curve fit based on a pseudo-first-order reaction model simulated in KaleidaGraph. The numbers in parentheses indicate the number of mismatches between 16S rRNA and PNA MB. The  $R^2$  values of the three curves in this figure ranged from 0.986 to 0.993.

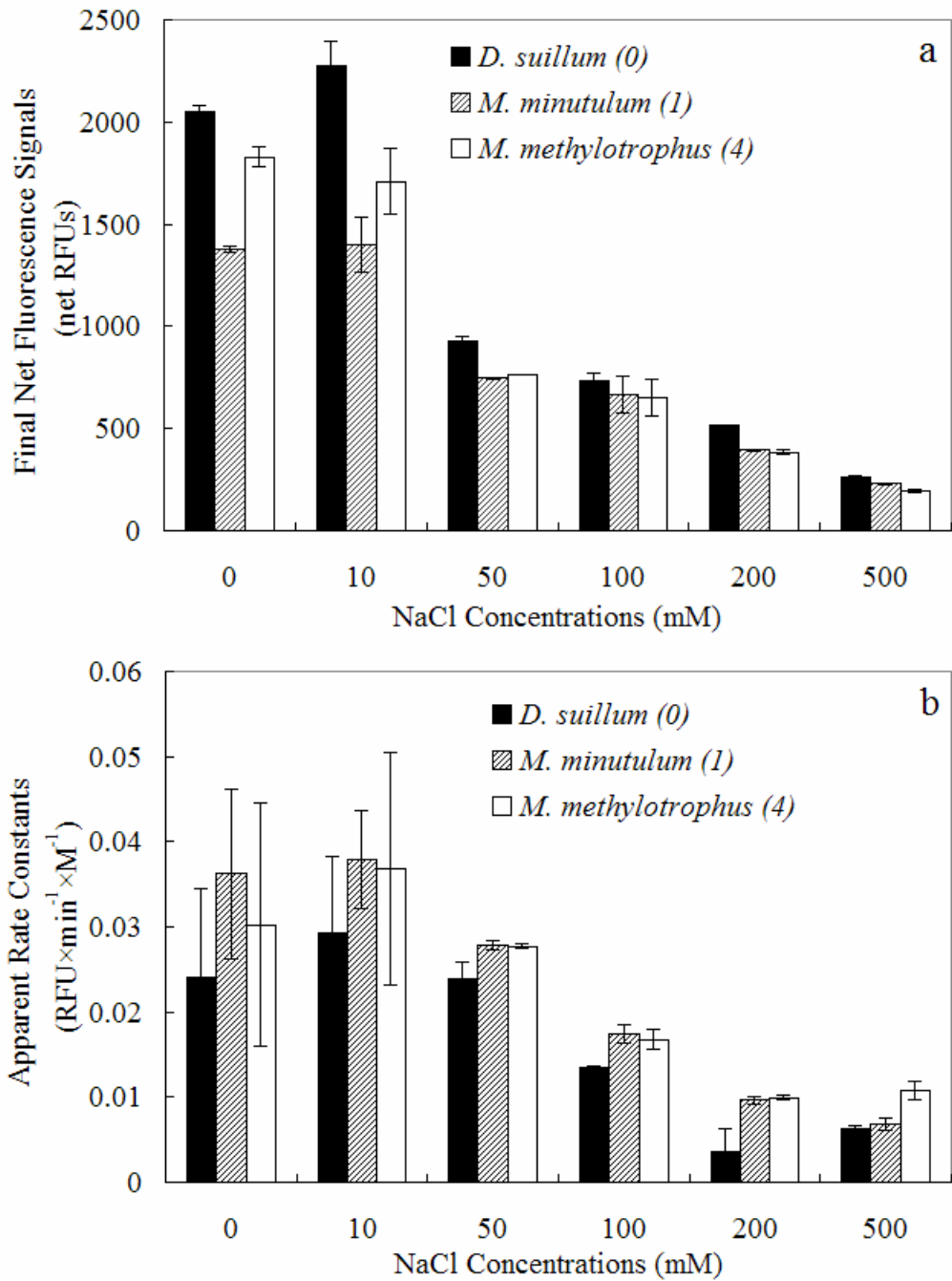


Figure 2.3 The effects of NaCl concentrations in hybridization buffers on final net fluorescence signals (a) and apparent rate constants (b) from hybridizations of PNA MB Dsoma0848 to target and non-target 16S rRNA. Mean values of duplicates are reported and the error bars represent the range of the duplicates. The numbers in parentheses indicate the number of mismatches between 16S rRNA and PNA MB.

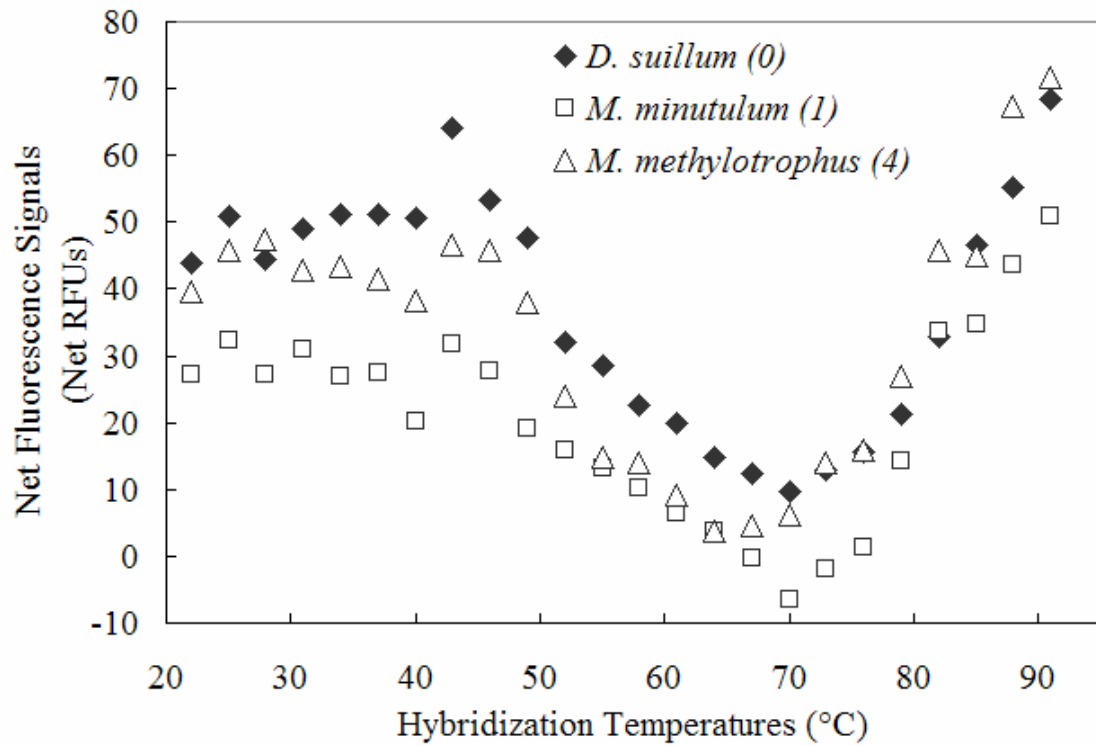


Figure 2.4. Melting profiles of the hybridizations of PNA MB Dsoma0848 with its target and non-target 16S rRNAs. The numbers in parentheses indicate the number of mismatches between 16S rRNA and PNA MB. The experiment was repeated and similar profiles were obtained (data shown in Supplemental Figure 2.1).



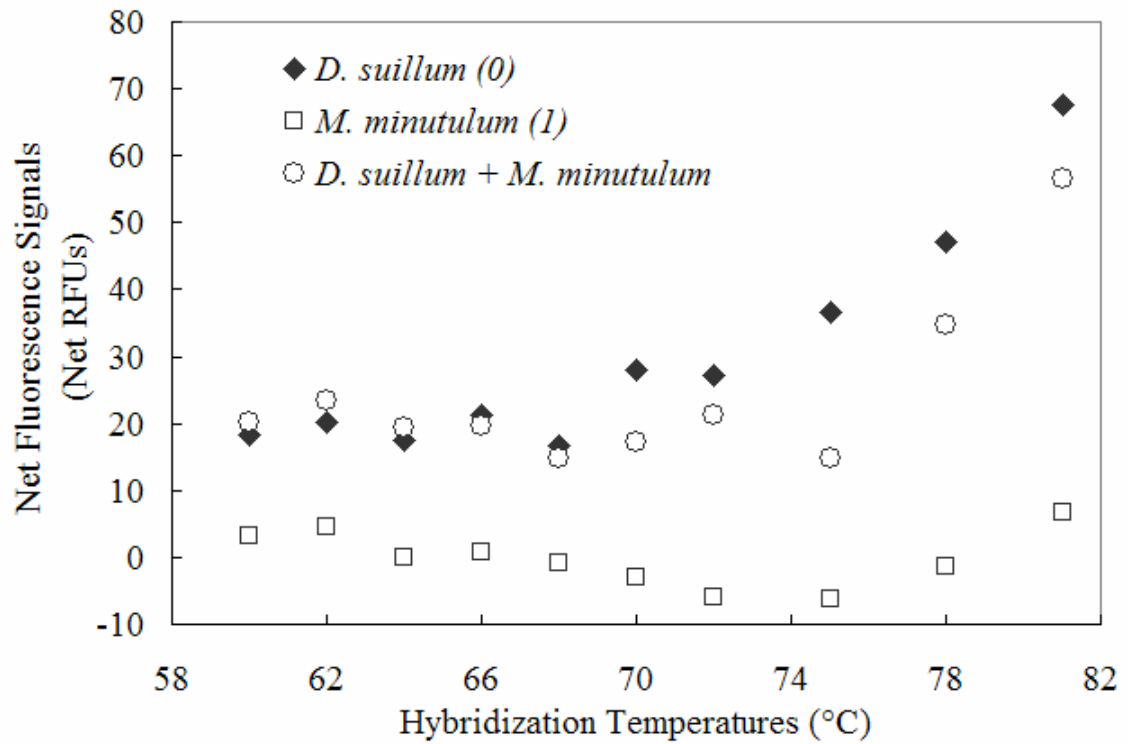


Figure 2.5. Melting profiles of the hybridizations of PNA MB Dsoma0848 with the 16S rRNAs of its target, non-target, and an artificial mixture containing equal amounts of target and non-target. The numbers in parentheses indicate the number of mismatches between 16S rRNA and PNA MB. The experiment was repeated and similar profiles were obtained (data shown in Supplemental Figure 2.2).

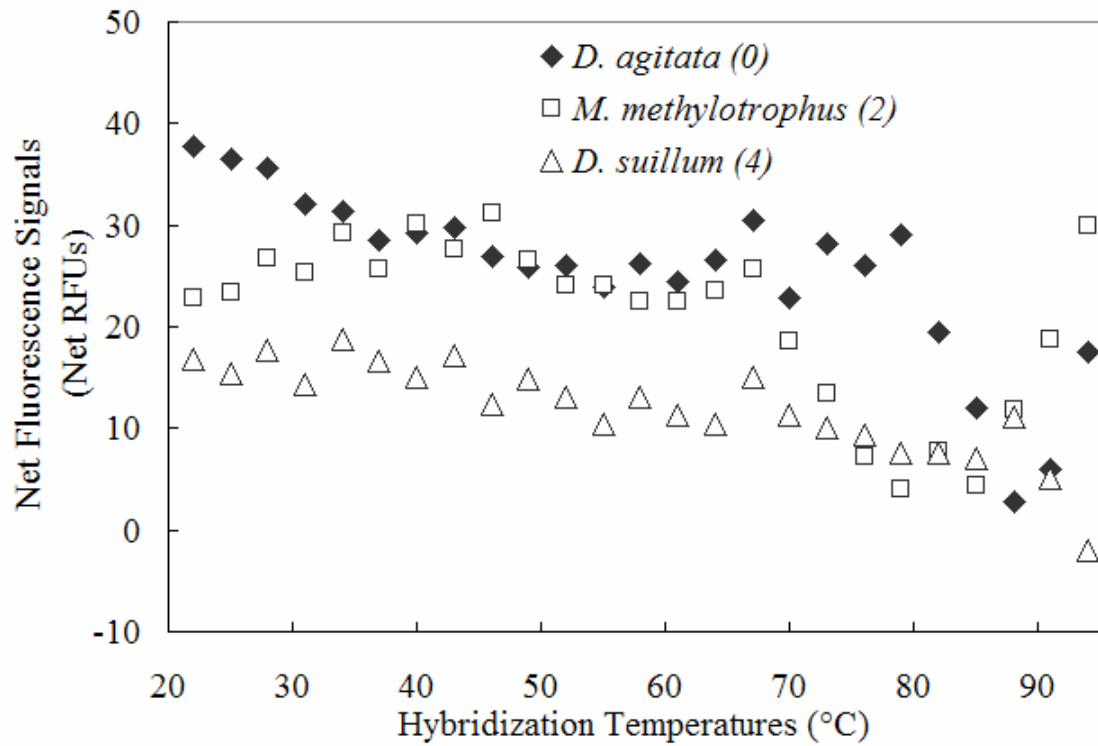


Figure 2.6. Melting profiles of the hybridizations of PNA MB Dmonas0121 with its target and non-target 16S rRNAs. The numbers in parentheses indicate the number of mismatches between 16S rRNA and PNA MB.

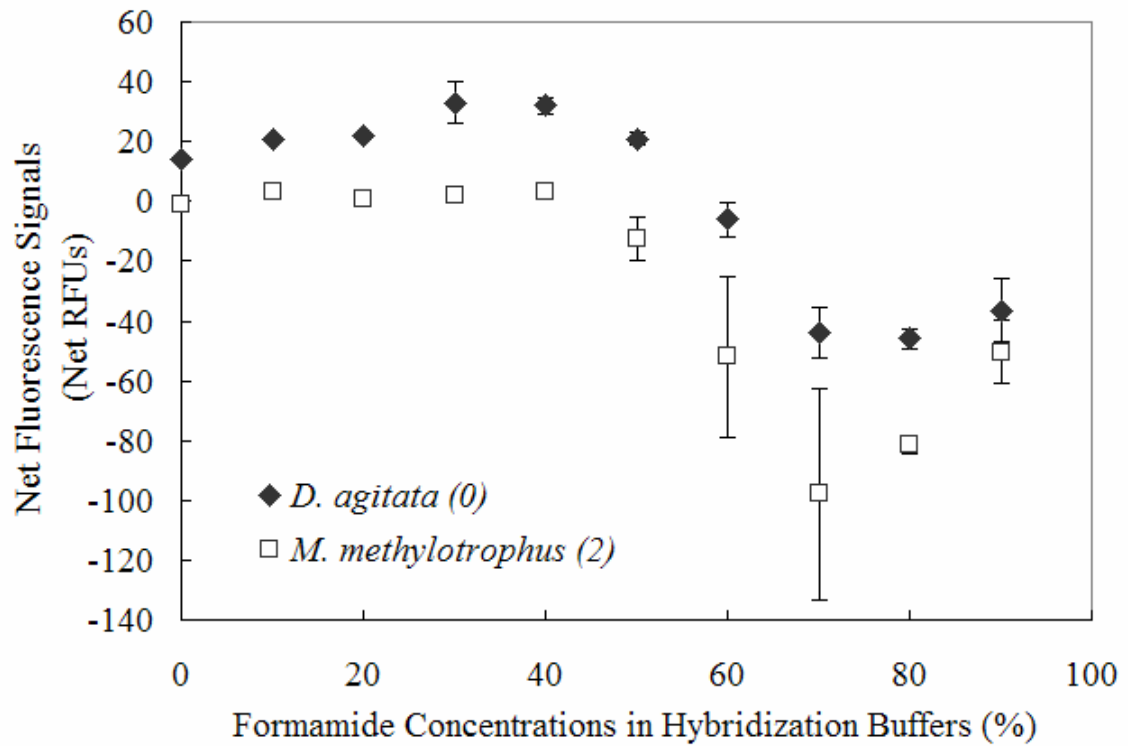


Figure 2.7. Effect of formamide concentration at 25°C on the net fluorescence signals from the hybridizations of PNA MB Dmonas0121 with its target and non-target 16S rRNAs. Mean values of duplicates are reported and the error bars represent the range of the duplicates. The numbers in parentheses represent the number of mismatch between 16S rRNA and PNA MB.

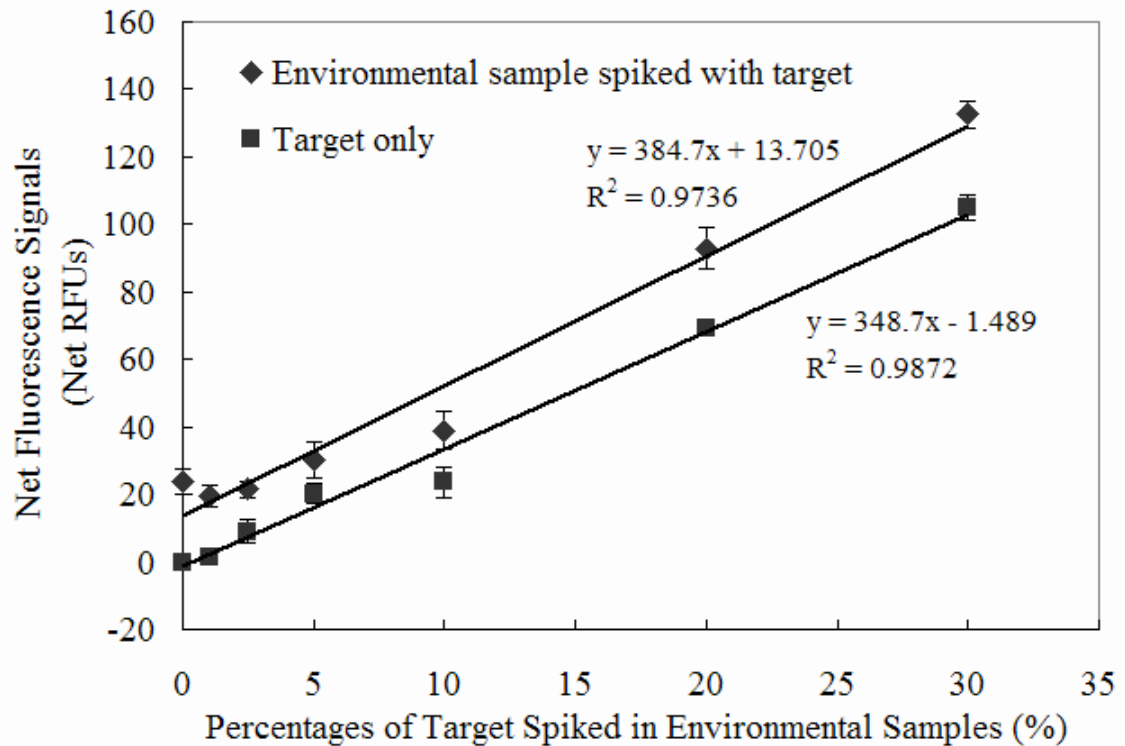
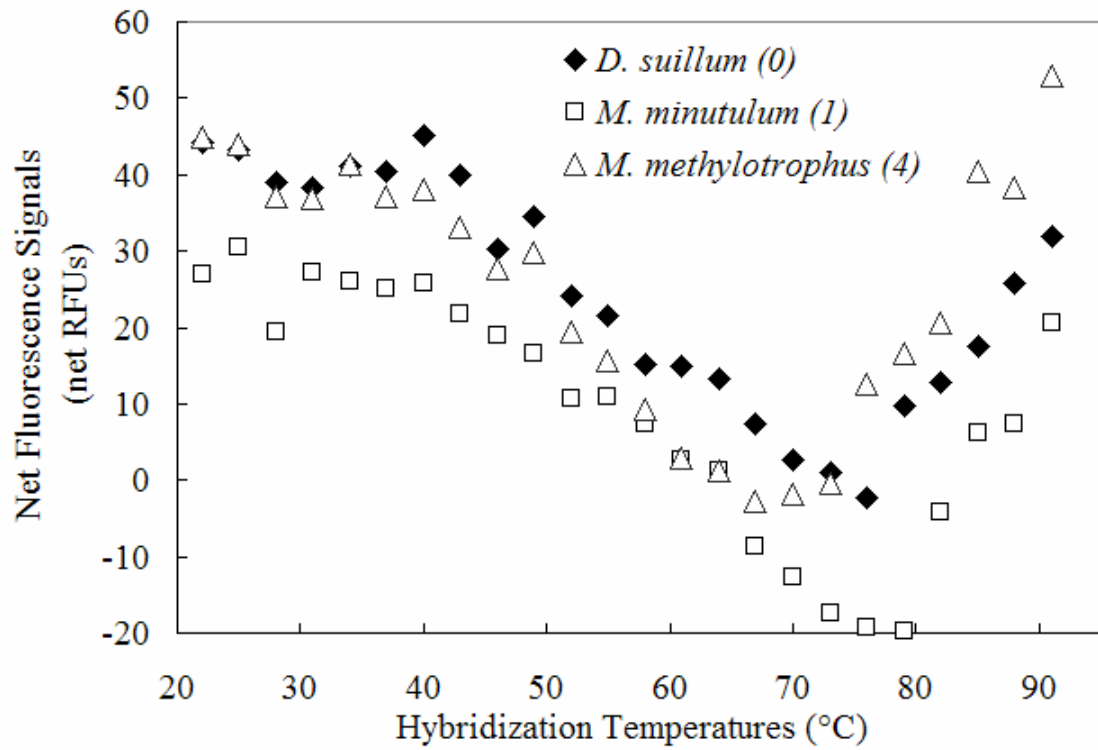
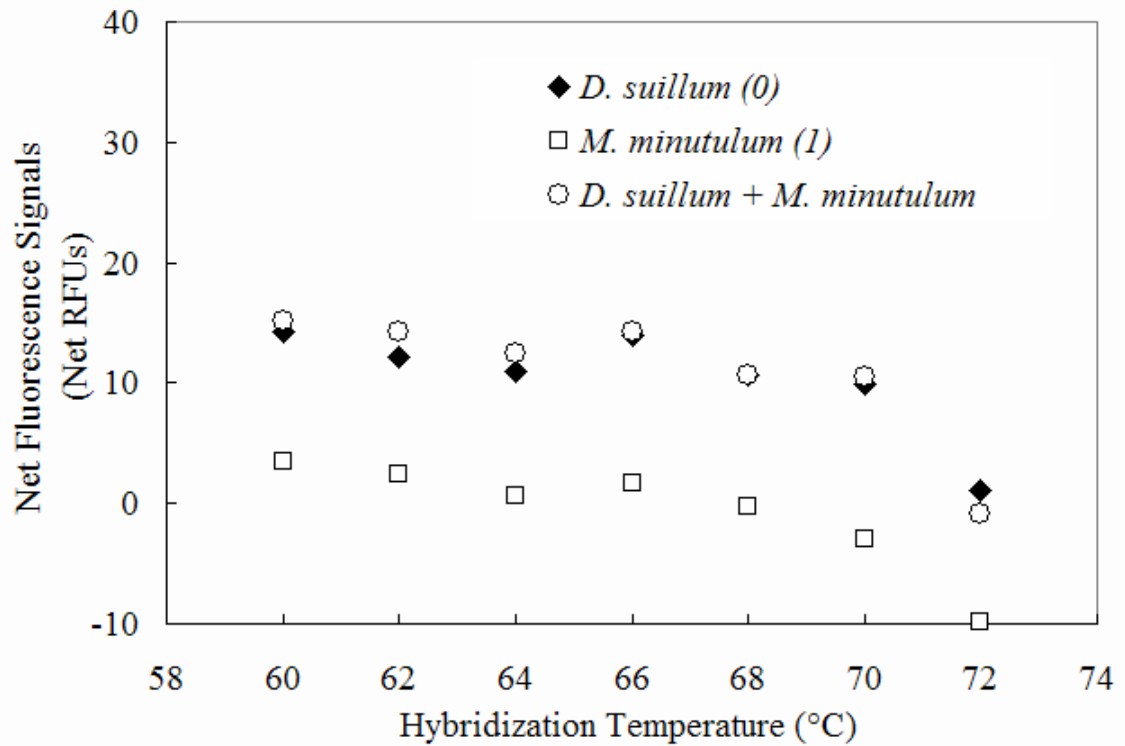


Figure 2.8. Net fluorescence signals from the hybridizations of PNA MB Dsoma0848 with a series consisting of various amounts of target 16S rRNA (*D. suillum*) spiked to RNA extracted from an environmental sample and with a series of samples containing only target 16S rRNA corresponding to the amounts of 16S rRNA target in the first series. The error bars represent standard deviations of five replicates.



Supplemental Figure 2.1. Melting profiles of the hybridizations of PNA MB Dsoma0848 with its target and non-target 16S rRNAs. The numbers in parentheses indicate the number of mismatches between 16S rRNA and PNA MB.



Supplemental Figure 2.2. Melting profiles of the hybridization of PNA MB Dsoma0848 with the 16S rRNA of its target, non-target, and an artificial mixture containing equal amounts of target and non-target. The numbers in parentheses indicate the number of mismatches between 16S rRNA and PNA MB.

## 2.7. References

Achenbach, L.A., Michaelidou, U., Bruce, R.A., Fryman, J. and Coates, J.D. (2001) *Dechloromonas Agitata* Gen. Nov., Sp Nov and *Dechlorosoma Suillum* Gen. Nov., Sp Nov., Two Novel Environmentally Dominant (Per)Chlorate-Reducing Bacteria and Their Phylogenetic Position. *International Journal of Systematic and Evolutionary Microbiology* 51, 527-533.

Acinas, S.G., Sarma-Rupavtarm, R., Klepac-Ceraj, V. and Polz, M.F. (2005) Pcr-Induced Sequence Artifacts and Bias: Insights from Comparison of Two 16s Rrna Clone Libraries Constructed from the Same Sample. *Applied and Environmental Microbiology* 71(12), 8966-8969.

Armitage, B.A. (2003) The Impact of Nucleic Acid Secondary Structure on Pna Hybridization. *Drug Discovery Today* 8(5), 222-228.

Bockisch, B., Grunwald, T., Spillner, E. and Bredehorst, R. (2005) Immobilized Stem-Loop Structured Probes as Conformational Switches for Enzymatic Detection of Microbial 16s Rrna. *Nucleic Acids Research* 33(11), -.

Bonnet, G., Tyagi, S., Libchaber, A. and Kramer, F.R. (1999) Thermodynamic Basis of the Enhanced Specificity of Structured DNA Probes. *Proceedings of the National Academy of Sciences of the United States of America* 96(11), 6171-6176.

Bratu, D.P., Cha, B.J., Mhlanga, M.M., Kramer, F.R. and Tyagi, S. (2003) Visualizing the Distribution and Transport of Mrnas in Living Cells. *Proceedings of the National Academy of Sciences of the United States of America* 100(23), 13308-13313.

Brehm-Stecher, B.F., Hyldig-Nielsen, J.J. and Johnson, E.A. (2005) Design and Evaluation of 16s Rrna-Targeted Peptide Nucleic Acid Probes for Whole-Cell Detection of Members of the Genus *Listeria*. *Applied and Environmental Microbiology* 71(9), 5451-5457.

Brinkmeyer, R., Knittel, K., Jurgens, J., Weyland, H., Amann, R. and Helmke, E. (2003) Diversity and Structure of Bacterial Communities in Arctic Versus Antarctic Pack Ice. *Applied and Environmental Microbiology* 69(11), 6610-6619.

Cardullo, R.A., Agrawal, S., Flores, C., Zamecnik, P.C. and Wolf, D.E. (1988) Detection of Nucleic-Acid Hybridization by Nonradiative Fluorescence Resonance Energy-Transfer. *Proceedings of the National Academy of Sciences of the United States of America* 85(23), 8790-8794.

Carr, E.L., Eales, K., Soddell, J. and Seviour, R.J. (2005) Improved Permeabilization Protocols for Fluorescence in Situ Hybridization (Fish) of Mycolic-Acid-Containing Bacteria Found in Foams. *Journal of Microbiological Methods* 61(1), 47-54.

- Chandler, D.P. and Jarrell, A.E. (2003) Enhanced Nucleic Acid Capture and Flow Cytometry Detection with Peptide Nucleic Acid Probes and Tunable-Surface Microparticles. *Analytical Biochemistry* 312(2), 182-190.
- Cole, J.R., Chai, B., Farris, R.J., Wang, Q., Kulam, S.A., McGarrell, D.M., Garrity, G.M. and Tiedje, J.M. (2005) The Ribosomal Database Project (Rdp-Ii): Sequences and Tools for High-Throughput Rna Analysis. *Nucleic Acids Research* 33, D294-D296.
- Coull, J.M., Gildea, B.D. and Hyldig-Nielsen, J.J. (2001) *Methods, Kits and Compositions Pertaining to Pna Molecular Beacons*, Boston Probes, Inc., USA.
- Dai, H.Y., Meyer, M., Stepaniants, S., Ziman, M. and Stoughton, R. (2002) Use of Hybridization Kinetics for Differentiating Specific from Non-Specific Binding to Oligonucleotide Microarrays. *Nucleic Acids Research* 30(16), -.
- Egholm, M., Buchardt, O., Christensen, L., Behrens, C., Freier, S.M., Driver, D.A., Berg, R.H., Kim, S.K., Norden, B. and Nielsen, P.E. (1993) Pna Hybridizes to Complementary Oligonucleotides Obeying the Watson-Crick Hydrogen-Bonding Rules. *Nature* 365(6446), 566-568.
- El Fantroussi, S., Urakawa, H., Bernhard, A.E., Kelly, J.J., Noble, P.A., Smidt, H., Yershov, G.M. and Stahl, D.A. (2003) Direct Profiling of Environmental Microbial Populations by Thermal Dissociation Analysis of Native Rnas Hybridized to Oligonucleotide Microarrays. *Applied and Environmental Microbiology* 69(4), 2377-2382.
- EPA (1999) Protocol for Epa Approval of New Methods for Organic and Inorganic Analytes in Wastewater and Drinking Water, Epa 821-B-98-003, U.S. EPA, Washington DC.
- Fuchs, B.M., Wallner, G., Beisker, W., Schwiipp, I., Ludwig, W. and Amann, R. (1998) Flow Cytometric Analysis of the in Situ Accessibility of Escherichia Coli 16s Rna for Fluorescently Labeled Oligonucleotide Probes. *Applied and Environmental Microbiology* 64(12), 4973-4982.
- Gonzalez, J.M., Simo, R., Massana, R., Covert, J.S., Casamayor, E.O., Pedros-Alio, C. and Moran, M.A. (2000) Bacterial Community Structure Associated with a Dimethylsulfoniopropionate-Producing North Atlantic Algal Bloom. *Applied and Environmental Microbiology* 66(10), 4237-4246.
- Hahn, D., Amann, R.I., Ludwig, W., Akkermans, A.D.L. and Schleifer, K.H. (1992) Detection of Microorganisms in Soil after Insitu Hybridization with Ribosomal-Rna-Targeted, Fluorescently Labeled Oligonucleotides. *Journal of General Microbiology* 138, 879-887.
- Jensen, K.K., Orum, H., Nielsen, P.E. and Norden, B. (1997) Kinetics for Hybridization of Peptide Nucleic Acids (Pna) with DNA and Rna Studied with the Biacore Technique. *Biochemistry* 36(16), 5072-5077.



- Kerkhof, L. and Ward, B.B. (1993) Comparison of Nucleic-Acid Hybridization and Fluorometry for Measurement of the Relationship between Rna/DNA Ratio and Growth-Rate in a Marine Bacterium. *Applied and Environmental Microbiology* 59(5), 1303-1309.
- Kuhn, H., Demidov, V.V., Coull, J.M., Fiandaca, M.J., Gildea, B.D. and Frank-Kamenetskii, M.D. (2002) Hybridization of DNA and Pna Molecular Beacons to Single-Stranded and Double-Stranded DNA Targets. *Journal of the American Chemical Society* 124(6), 1097-1103.
- Kuhn, H., Demidov, V.V., Frank-Kamenetskii, M.D. and Nielsen, P.E. (1998) Kinetic Sequence Discrimination of Cationic Bis-Pnas Upon Targeting of Double-Stranded DNA. *Nucleic Acids Research* 26(2), 582-587.
- Kuhn, H., Demidov, V.V., Gildea, B.D., Fiandaca, M.J., Coull, J.C. and Frank-Kamenetskii, M.D. (2001) Pna Beacons for Duplex DNA. *Antisense & Nucleic Acid Drug Development* 11(4), 265-270.
- Li, X., Upadhyaya, G., Yuen, W., Brown, J., Morgenroth, E. and Raskin, L. Addition of Phosphorus to Bac Reactors Improves Reactor Performances by Promoting the Growth of *Dechloromonas* Spp. And *Dechlorosoma* Spp. In preparation
- Livshits, M.A. and Mirzabekov, A.D. (1996) Theoretical Analysis of the Kinetics of DNA Hybridization with Gel-Immobilized Oligonucleotides. *Biophysical Journal* 71(5), 2795-2801.
- Marras, S.A.E., Tyagi, S. and Kramer, F.R. (2006) Real-Time Assays with Molecular Beacons and Other Fluorescent Nucleic Acid Hybridization Probes. *Clinica Chimica Acta* 363(1-2), 48-60.
- Marsh, T.L. (1999) Terminal Restriction Fragment Length Polymorphism (T-Rflp): An Emerging Method for Characterizing Diversity among Homologous Populations of Amplification Products. *Current Opinion in Microbiology* 2(3), 323-327.
- Muyzer, G. (1999) Dgge/Tgge a Method for Identifying Genes from Natural Ecosystems. *Current Opinion in Microbiology* 2(3), 317-322.
- Nielsen, P.E., Egholm, M. and Buchardt, O. (1994) Peptide Nucleic-Acid (Pna) - a DNA Mimic with a Peptide Backbone. *Bioconjugate Chemistry* 5(1), 3-7.
- Oliveira, K., Procop, G.W., Wilson, D., Coull, J. and Stender, H. (2002) Rapid Identification of *Staphylococcus Aureus* Directly from Blood Cultures by Fluorescence in Situ Hybridization with Peptide Nucleic Acid Probes. *Journal of Clinical Microbiology* 40(1), 247-251.
- Ortiz, E., Estrada, G. and Lizardi, P.M. (1998) Pna Molecular Beacons for Rapid Detection of Pcr Amplicons. *Molecular and Cellular Probes* 12(4), 219-226.

- Pernthaler, J., Pernthaler, A. and Amann, R. (2003) Automated Enumeration of Groups of Marine Picoplankton after Fluorescence in Situ Hybridization. *Applied and Environmental Microbiology* 69(5), 2631-2637.
- Petersen, K., Vogel, U., Rockenbauer, E., Nielsen, K.V., Kolvraa, S., Bolund, L. and Nexø, B. (2004) Short Pna Molecular Beacons for Real-Time Pcr Allelic Discrimination of Single Nucleotide Polymorphisms. *Molecular and Cellular Probes* 18(2), 117-122.
- Podell, S., Maske, W., Ibanez, E. and Jablonski, E. (1991) Comparison of Solution Hybridization Efficiencies Using Alkaline Phosphatase-Labeled and P-32 Labeled Oligodeoxynucleotide Probes. *Molecular and Cellular Probes* 5(2), 117-124.
- Pozhitkov, A.E., Stedtfeld, R.D., Hashsham, S.A. and Noble, P.A. (2007) Revision of the Nonequilibrium Thermal Dissociation and Stringent Washing Approaches for Identification of Mixed Nucleic Acid Targets by Microarrays. *Nucleic Acids Research* 35(9), -.
- Privat, E., Melvin, T., Asseline, U. and Vigny, P. (2001) Oligonucleotide-Conjugated Thiazole Orange Probes As "Light-Up" Probes for Messenger Ribonucleic Acid Molecules in Living Cells. *Photochemistry and Photobiology* 74(4), 532-541.
- Raskin, L., Stromley, J.M., Rittmann, B.E. and Stahl, D.A. (1994) Group-Specific 16s Ribosomal-Rna Hybridization Probes to Describe Natural Communities of Methanogens. *Applied and Environmental Microbiology* 60(4), 1232-1240.
- Sando, S. and Kool, E.T. (2002a) Imaging of Rna in Bacteria with Self-Ligating Quenched Probes. *Journal of the American Chemical Society* 124(33), 9686-9687.
- Sando, S. and Kool, E.T. (2002b) Quencher as Leaving Group: Efficient Detection of DNA-Joining Reactions. *Journal of the American Chemical Society* 124(10), 2096-2097.
- Seitz, O. (2000) Solid-Phase Synthesis of Doubly Labeled Peptide Nucleic Acids as Probes for the Real-Time Detection of Hybridization. *Angewandte Chemie-International Edition* 39(18), 3249-+.
- Small, J., Call, D.R., Brockman, F.J., Straub, T.M. and Chandler, D.P. (2001) Direct Detection of 16s Rna in Soil Extracts by Using Oligonucleotide Microarrays. *Applied and Environmental Microbiology* 67(10), 4708-4716.
- Stahl, D.A., Flesher, B., Mansfield, H.R. and Montgomery, L. (1988) Use of Phylogenetically Based Hybridization Probes for Studies of Ruminant Microbial Ecology. *Applied and Environmental Microbiology* 54(5), 1079-1084.
- Suzuki, M.T., Taylor, L.T. and DeLong, E.F. (2000) Quantitative Analysis of Small-Subunit Rna Genes in Mixed Microbial Populations Via 5'-Nuclease Assays. *Applied and Environmental Microbiology* 66(11), 4605-4614.

- Svanvik, N., Westman, G., Wang, D.Y. and Kubista, M. (2000) Light-up Probes: Thiazole Orange-Conjugated Peptide Nucleic Acid for Detection of Target Nucleic Acid in Homogeneous Solution. *Analytical Biochemistry* 281(1), 26-35.
- Tan, Z. and Reinhold-Hurek, B. (2003) *Dechlorosoma Suillum* Achenbach Et Al. 2001 Is a Later Subjective Synonym of *Azospira Oryzae* Reinhold-Hurek and Hurek 2000. *International Journal of Systematic and Evolutionary Microbiology* 53, 1139-1142.
- Tinoco, I. and Bustamante, C. (1999) How Rna Folds. *Journal of Molecular Biology* 293(2), 271-281.
- Tsuji, A., Koshimoto, H., Sato, Y., Hirano, M., Sei-Iida, Y., Kondo, S. and Ishibashi, K. (2000) Direct Observation of Specific Messenger Rna in a Single Living Cell under a Fluorescence Microscope. *Biophysical Journal* 78(6), 3260-3274.
- Tyagi, S. and Kramer, F.R. (1996) Molecular Beacons: Probes That Fluoresce Upon Hybridization. *Nature Biotechnology* 14(3), 303-308.
- Vet, J.A.M., Majithia, A.R., Marras, S.A.E., Tyagi, S., Dube, S., Poiesz, B.J. and Kramer, F.R. (1999) Multiplex Detection of Four Pathogenic Retroviruses Using Molecular Beacons. *Proceedings of the National Academy of Sciences of the United States of America* 96(11), 6394-6399.
- von Wintzingerode, F., Gobel, U.B. and Stackebrandt, E. (1997) Determination of Microbial Diversity in Environmental Samples: Pitfalls of Pcr-Based Rna Analysis. *FEMS Microbiology Reviews* 21(3), 213-229.
- Wang, L., Gaigalas, A.K., Blasic, J. and Holden, M.J. (2004) Spectroscopic Characterization of Fluorescein- and Tetramethylrhodamine-Labeled Oligonucleotides and Their Complexes with a DNA Template. *Spectrochimica Acta Part a-Molecular and Biomolecular Spectroscopy* 60(12), 2741-2750.
- Worden, A.Z., Chisholm, S.W. and Binder, B.J. (2000) In Situ Hybridization of *Prochlorococcus* and *Synechococcus* (Marine Cyanobacteria) Spp. With Rna-Targeted Peptide Nucleic Acid Probes. *Applied and Environmental Microbiology* 66(1), 284-289.
- Xi, C.W., Balberg, M., Boppart, S.A. and Raskin, L. (2003) Use of DNA and Peptide Nucleic Acid Molecular Beacons for Detection and Quantification of Rna in Solution and in Whole Cells. *Applied and Environmental Microbiology* 69(9), 5673-5678.
- Xi, C.W., Raskin, L. and Boppart, S.A. (2005) Evaluation of Microfluidic Biosensor Development Using Microscopic Analysis of Molecular Beacon Hybridization Kinetics. *Biomedical Microdevices* 7(1), 7-12.
- Yao, G. and Tan, W.H. (2004) Molecular-Beacon-Based Array for Sensitive DNA Analysis. *Analytical Biochemistry* 331(2), 216-223.

Zheng, D., Angenent, L.T. and Raskin, L. (2006) Monitoring Granule Formation in Anaerobic Upflow Bioreactors Using Oligonucleotide Hybridization Probes. *Biotechnology and Bioengineering* 94(3), 458-472.

Zhou, Z., Pons, M.N., Raskin, L. and Zilles, J.L. (2007) Automated Image Analysis for Quantitative Fluorescence in Situ Hybridization with Environmental Samples. *Applied and Environmental Microbiology* 73(9), 2956-2962.

## **Chapter 3**

### **Effects of Increases in Backwash Frequency and Intensity on Reactor Performance and Microbial Community Structure in a Biofilm Reactor**

#### **3.1. Introduction**

Biofilm reactor technology provides a new avenue for drinking water treatment, and has demonstrated to be effective in removing a range of contaminants from source waters (Urfer et al., 1997; Min et al., 2004; Nerenberg and Rittmann, 2004). A key component in further advancing the technology is to elucidate the correlation among reactor operation, reactor performance, and microbial community structure/function (Briones and Raskin, 2003; Curtis et al., 2003). In this study, a fixed-bed biofilm reactor designed to remove perchlorate from drinking water was studied to illustrate such correlation. Perchlorate is an endocrine disruptor with several adverse health effects (Greer et al., 2002) and has been detected in many drinking water sources (Urbansky, 2002). Perchlorate is on U.S. EPA's drinking water contaminant candidate list (US-EPA, 2008) and is regulated by a number of states in the U.S. (CA-DHS, 2005; US-EPA, 2005; MA-DEP, 2006) at various levels ranging from 1 to 18  $\mu\text{g/L}$ .

In recent years, fixed-bed biofilm reactors have been evaluated for the removal of perchlorate from drinking water (Miller and Logan, 2000; Brown et al., 2003; Choi et al., 2007). Regular reactor backwashing is necessary to allow continued operation of these bioreactors (Hozalski and Bouwer, 1998). During normal operation, the biofilm support medium in fixed-bed reactors remains stationary, as opposed to fluidized bed reactors in which the support medium is fluidized. As water passes through the stationary bed, particulates including microbial cell aggregates accumulate in void space and cause clogging. Backwashing, the passing of a flow of water or a mixture of water and air in the opposite direction of the regular flow, removes particulate matter and resolves bioreactor clogging (Ahmad et al., 1998). Backwashing removes most loosely attached biofilms and a fraction of tightly attached biofilms (Servais et al., 1991), depending on the backwash intensity. Backwashing with high intensity may cause too much biomass loss and impair reactor performance (Lahav et al., 2001). Backwashing with low intensity may lead to insufficient removal of clogging, quick pressure buildup during operation, and consequently more frequent backwashes. Backwash frequency is usually determined experimentally by monitoring pressure buildup caused by clogging across the reactor.

Recently, the effects of backwash frequency and intensity on reactor performance were studied with two fixed-bed biofilm reactors operated to remove perchlorate from drinking water (Choi et al., 2007). In that study, after the backwash frequency was increased from monthly to daily, reactor performance first decreased and then recovered. In contrast, after the backwash intensity was increased, daily strong backwashes caused performance failure. The difference in responses likely rooted in the way microbial

communities, especially perchlorate reducing bacterial populations, responded to the changes in backwash procedure.

Perchlorate reducing bacteria (PRB) can utilize perchlorate as an electron acceptor and convert it to chloride (Coates and Achenbach, 2004). PRB described so far mainly belong to three genera *Dechloromonas*, *Azospira*, and *Dechlorospirillum* (Coates et al., 1999; Waller et al., 2004). For most PRB, oxygen is a preferred electron acceptor over perchlorate (Coates and Achenbach, 2004). Hence, to allow perchlorate removal by bioreactors, oxygen needs to be removed by PRB and/or other aerobic bacteria before biological perchlorate reduction can start (Xu et al., 2003). Therefore, simultaneous studies of PRB and other aerobic bacteria are crucial in studying engineered systems designed to remove perchlorate.

In this study, correlations among reactor operation (i.e., backwash frequency and intensity), reactor performance (i.e., dissolved oxygen and perchlorate removal), and microbial community shifts (i.e., relative abundance of PRB and other aerobic bacteria) were investigated. The microbial community structure was first determined using clone library analyses targeting 16S rRNA genes and then the major bacterial populations were monitored using quantitative real-time polymerase chain reaction (PCR). The results show how different bacterial populations responded to different backwash parameters, and provide insights in designing backwash strategies for fixed-bed biofilm systems.

## 3.2. Materials and Methods

### 3.2.1. Reactor Operation

The reactor configuration, influent composition, operating conditions, and backwash procedures were similar to the ones reported in an earlier study (Choi et al., 2007). In brief, a bench-scale fixed-bed biofilm reactor with an inner diameter of 2.4 cm and a height of 24 cm was filled with 1-mm diameter glass beads (empty bed volume of 63.4 mm<sup>3</sup>). Influent was pumped into the bottom of the glass bead reactor at a flow rate ( $Q_{\text{influent}}$ ) of 2.7 mL/min, resulting in an empty bed contact time of 23.4 min. A recirculation loop ( $Q_{\text{recirculation}}=5\times Q_{\text{influent}}$ ) was installed to the reactor to approximate a completely mixed mode of the bulk solution inside the reactor. The influent contained two electron acceptors: 3 mg/L dissolved oxygen (DO) and 50 µg/L perchlorate. A phosphate buffer solution with a final concentration of 0.5 mM maintained the pH inside the reactor at 7.5, and it served as phosphorus source along with 0.15 mg/L NH<sub>4</sub>Cl as N as nitrogen source. Based on stoichiometric calculations (Rittmann and McCarty, 2001) with an assumed net yield value of 0.4 g COD<sub>biomass</sub>/g COD<sub>acetate</sub>, 2 mg/L of acetate as C was needed to serve as the sole electron donor. These operating parameters were defined as the baseline operating condition for this system. In a “weak backwash”, reactor content was stirred in 100-mL of previously collected reactor effluent in a 600-mL beaker with a 7.5 cm long magnetic stir bar at 75 revolutions per minute (RPM) for 1 min, and then the supernatant was decanted. In a “strong backwash”, the reactor content was stirred in 125 mL previously collected effluent at 150 RPM twice for 1 min each time, with supernatant decanting and new effluent replenishment between these periods. The reactor was backwashed about once a month before the daily weak backwash experiment



started. Six days after the daily weak backwash experiment, the daily strong backwash experiment was conducted.

Influent and effluent DO concentrations were measured using WTW multi340 meters with Cellox325 sensors in WTW D201 flow cells (WTW Inc., Weilheim, Germany) connected to the inlet and outlet of the reactor. All other chemical parameters were measured according to Standard Methods (American Public Health Association (APHA), 1992). Perchlorate was measured using an ion chromatograph system (Dionex ICS-2000, Sunnyvale, CA) according to EPA Standard Method 314.1. An AS-16 analytical column and an AG-16 guard column were used, while the eluent was 65 mM KOH. The detection limits for DO and perchlorate were 0.01 mg/L and 1 µg/L, respectively.

### **3.2.2. Data Analyses on Reactor Performance**

The effluent DO and perchlorate concentration profiles were fitted using polynomial trendlines in Microsoft Excel. The  $R^2$  values for the fitted perchlorate concentration profiles ranged from 0.906 to 0.978 for the daily weak backwash experiment and 0.808 to 0.971 (with an outlier of 0.492 for Day 5) for the daily strong backwash experiment. The initial perchlorate reduction rates were calculated by taking derivatives of the simulated curves at time zero. The  $R^2$  values for the simulated DO concentration profiles ranged from 0.854 to 0.978 for Day 1-3 in the daily weak backwash experiment, and 0.936 and 0.963 for Day 3 and 5 in the daily strong backwash experiment. The initial DO removal was calculated using the influent DO concentration (i.e., 3 mg/L) and subtracting the fitted effluent DO concentrations at time zero.

### **3.2.3. Extracellular and Intracellular DNA Extractions and Protein Assay**

For clone library construction, biomass samples were collected from the glass bead reactor on Day 0 of the daily weak backwash experiment and Day 5 of the strong backwash experiment. Total DNA was extracted from these two biomass samples using FastDNA SPIN Kit (Qbiogene Inc., Irvine, CA). For quantitative real-time PCR measurements, biomass samples were collected at each of the 11 backwash events. Extracellular DNA (eDNA) was separated from cellular materials and extracted by following a published protocol (Corinaldesi et al., 2005). Intracellular DNA (iDNA) was extracted by following a protocol modified from the one by Griffiths and coworkers (Griffiths et al., 2000). All DNA extracts were quantified using a NanoDrop ND1000 (NanoDrop Technology, Wilmington, DE), and their qualities were evaluated by electrophoresis on a 1% agarose gel. Protein measurements were conducted using a protein assay kit (Bio-Rad, Hercules, CA).

### **3.2.4. Clone Library**

16S rRNA genes were amplified in triplicate using the PCR on a Mastercycler (Eppendorf International, Hamburg, Germany) with the forward primer 8F (5'-AGA GTT TGA TCC TGG CTC AG-3') and the reverse primer 1492R (5'-GG[C/T] TAC CTT GTT ACG ACT T-3') (Dojka et al., 1998; Richardson et al., 2002). The composition of the PCR solutions and the conditions of the PCR reactions were adopted from the work by Dojka and coworkers (Dojka et al., 1998). The PCR reaction involved 30 cycles and started with 12 min of denaturation at 94°C and ended with a final extension at 72°C for 12 min. Each cycle consisted of denaturation at 94°C for 1 min, annealing at 50°C for 45

s, and extension at 72°C for 2 min. Pooled PCR products from triplicates were purified by electrophoresis on a 1% agarose gel and extracted using the MinElute Gel Extraction Kit (QIAGEN Inc., Valencia, CA). Purified PCR products were cloned into TOPO vectors (Invitrogen Inc., Carlsbad, CA), and transformed into chemically competent *Escherichia coli*. The transformed *E. coli* cells were plated on Luria-Bertani agar that contained 50 µg/mL kanamycin and were incubated at 37°C overnight. Colonies were randomly picked and used to inoculate three 96-well microplates. Two of the three 96-well microplates in glycerol stocks were sent to the Genomic Center at Washington University (St. Louis, MO) for sequencing.

### **3.2.5. Phylogenetic Analyses**

A total of 768 clones (eight 96-well microplates, two for each library) were sequenced using vector primers T3 and T7. Nucleotide sequences were analyzed and edited using BioEdit (Hall, 1999). Closely related sequences identified via the Ribosomal Database Project (RDP) (Cole et al., 2007) was aligned using ClustalW (Chenna et al., 2003) for bacterial 16S rRNA genes. The phylogenetic tree was based on a region of the 16S rRNA gene of ca. 600 bp starting at the 8F primer region and was created based on the evolutionary history inferred using the neighbor-joining method (Saitou and Nei, 1987) and the evolutionary distance computed using the Jukes-Cantor methods (Jukes and Cantor, 1969) incorporated in the software program MEGA (Tamura et al., 2007). The percentages of replicate trees in which the associated taxa clustered together in the bootstrap test (1000 replicates) are shown next to the branches (Felsenstein, 1985). There were a total of 500 sites in the final dataset used to build the phylogenetic tree.

Operational taxonomic units (OTUs) were defined as clones that shared 95% identity in 16S rRNA genes (Fields et al., 2005). OTUs, diversity statistics, and rarefaction curves were calculated using DOTUR (Schloss and Handelsman, 2005). The similarities of the bacterial 16S rRNA gene clone libraries were evaluated using  $\beta$ -LIBSHUFF (Schloss et al., 2004).

### **3.2.6. Real-time PCR Primer Design and Reaction Conditions**

Real-time PCR primer sets were designed based on representative sequences of the clones of interests (i.e., *Dechloromonas*, *Zoogloea*, and *Curvibacter*) using the Primer3 program (Rozen and Skaletsky, 2000) made available by Integrated DNA Technologies ([www.idtdna.com](http://www.idtdna.com)) and were synthesized by Invitrogen (Carlsbad, CA). The lengths of the amplicons using the three primer sets ranged from 106 to 155 bp. The specificities of the designed primer sets were manually verified using the Probe Match function of RDP (Cole et al., 2007), while the coverage of the designed primer sets were evaluated against the clones of interest in relevant clone libraries (Table 3.1). The specificities of the designed primer sets were further characterized with various ranges of annealing temperatures using the gradient PCR function of the real-time PCR thermocycler Mastercycler *realplex* system (Eppendorf International, Hamburg, Germany) (Supplemental Figure 3.1). The selected annealing temperatures for the three designed primer sets could differentiate the fluorescence signals between equal amounts of target and non-target templates ( $10^6$  copies per  $\mu\text{L}$ ) by at least 15  $C_{\text{threshold}}$  units (Supplemental Figure 3.1 and Table 3.1). The specificities of the primer sets were also tested by electrophoresis on 1% agarose gels to verify the sizes of the amplicons (Supplemental

Figure 3.2) and by monitoring the melting temperatures from melting curves on target and non-target templates (Supplemental Figure 3.3). The real-time PCR primer set Bact1369F/1492R for quantifying total bacteria was adopted from Suzuki and coworkers (Suzuki et al., 2000).

All real-time PCR experiments were performed using a RealMasterMix SYBR Green Kit (Eppendorf International, Hamburg, Germany), which has a self-adjusting chelating mechanism to control the  $Mg^{2+}$  concentration. The reaction mixtures in 25  $\mu$ L final volume contained 11.25  $\mu$ L of 2.5X RealMasterMix SYBR Green solution (including 0.05 U/ $\mu$ L HotMaster *Taq* DNA Polymerase, 10 mM magnesium acetate, 1.0 mM dNTPs, and 2.5X SYBR Green solution), 150 nM of forward and reverse primers, Sigma water (Sigma-Aldrich, St. Louis, MO), and  $10^6$  copies of target/non-target template or 10 ng of DNA template from environmental samples. All quantification experiments included Sigma water as a non-template control to assure identification of false positives. As suggested in the manual of the RealMasterMix SYBR Green kit, amplification involved one cycle of 95°C for 10 min for initial denaturation and then 40 cycles of 95°C for 15 s followed by annealing at the temperatures reported in Table 3.1 for 20 s and extension at 68°C for 30 s. Detection of SYBR fluorescence was set at the extension step of each cycle. Melting profiles were collected after 40 cycles of amplification to check the specificity of the amplification.

### **3.2.7. Real-time PCR Standard Curves**

Target and non-target templates were plasmid DNA extracted from clones obtained from the clone libraries constructed in the current study using QIAprep Miniprep Kit

(QIAGEN Inc., Valencia, CA) and quantified using NanoDrop ND1000. The target templates contained the representative sequences based on which corresponding primer sets were designed, while the non-target templates contained sequences with the *least* number of mismatches with the designed primer sets in the relevant clone libraries (Table 3.2). Dilutions of purified *E. coli* plasmid DNA containing the 16S rRNA genes of *Dechloromonas*, *Zoogloea*, and *Curvibacter* were used as standards for real-time PCR in the quantification of specific populations. The plasmid DNA concentrations (copy # per  $\mu\text{L}$ ) were calculated using the following equation

$$\begin{aligned} \text{plasmid DNA concentration} \left[ \frac{\text{copy}}{\mu\text{L}} \right] &= (\text{plasmid DNA concentration} \left[ \frac{\text{ng}}{\mu\text{L}} \right]) \times \frac{1}{(3956 + 1484) \times 607.4 + 157.9} \left[ \frac{\text{nmol}}{\text{ng}} \right] \\ &\times \left( \frac{1 \text{ mol}}{10^9 \text{ nmol}} \right) \times \left( \frac{6.023 \times 10^{23} \text{ copy}}{\text{mol}} \right) \end{aligned}$$

where 3956 and 1484 are the lengths of the pCR<sup>®</sup>4-TOPO vector (Invitrogen Corporation, Carlsbad, CA) and PCR insert, the constants of 607.4 and 157.9 were obtained for the calculation of the molecular weight of double stranded DNA ([www.ambion.com](http://www.ambion.com)).

The slope, the y-intercept, and the  $R^2$  values in Table 3.2 were obtained from the standard curves, which were constructed from triplicate measurements for each real-time PCR primer set. The amplification efficiencies were calculated using the equation,

$$E = 10^{(-1/\text{slope})} - 1$$

where  $E$  is the efficiency of the real-time PCR reaction with a maximum value of 1, and the slope is the slope of the standard curve.

To enumerate target copy numbers in environmental samples, standard curves were measured in triplicate on each 96-well microplates to avoid discrepancies across microplates. The relative abundance values of the three genera were calculated using the copy number of each genus divided by the copy number of the total bacterial population.

### 3.3. Results

#### 3.3.1. eDNA

Extracellular DNA (eDNA) is deemed important for biofilm studies because of its high abundance in certain natural environments (Steinberger et al., 2002; Corinaldesi et al., 2005) and its sequence similarity to intracellular DNA in multi-species biofilms developed from pure cultures (Steinberger and Holden, 2005). We investigated if the presence of eDNA would affect 16S rRNA gene sequence analyses and the quantification of total DNA extracted for the biofilm reactor operated in the current study. The mass ratios of eDNA to total DNA for the biomass samples, collected in the two sets of backwash experiments (i.e., daily weak and daily strong backwash experiments), are presented in Figure 3.1. The average amount of eDNA reported as a percentage of the total DNA was  $22.2 \pm 8.9\%$  for the two backwash experiments ( $n=10$ , excluding the sample on Day 1 of the daily strong backwash experiment), while the average percentages were  $20.6 \pm 4.6\%$  ( $n=6$ ) and  $24.8 \pm 13.7\%$  ( $n=4$ ) for the daily weak and daily strong backwash experiments, respectively. Statistical analysis showed no significant difference between the two sets ( $p=0.610$ ), which indicated that the microbial community inside the glass bed reactor contained similar percentages of eDNA under minor and major disturbances (i.e., weak and strong backwashes).

Real-time PCR results showed that eDNA extracts from the biofilm reactor did not contain 16S rRNA sequences that were amplifiable by the four primer sets used in this study (data not shown). Among the four primer sets, three were designed to target the three dominant bacterial genera in the reactor (Table 3.1 and below), and the other was a bacterial primer set (Suzuki et al., 2000). The only exception was the eDNA

extract from Day 1 of the daily strong backwash experiment, which was amplified by all four primer sets (insert in Figure 3.1). This eDNA extract likely was contaminated with intracellular DNA (iDNA), because real-time PCR results showed the relative abundances of the three targeted genera (i.e., *Dechloromonas*, *Zoogloea*, and *Curvibacter*) in this eDNA extract to be very similar to those in the corresponding iDNA extract (insert in Figure 3.1). Since the eDNA samples did not contain sequences that were amplifiable with the four PCR primer sets, separate analyses of eDNA and iDNA were not pursued for the clone library and subsequent real-time PCR experiments.

### **3.3.2. Microbial Community**

Two clone libraries were constructed to study the microbial community in the bioreactor: one for the biomass sample collected on Day 0 of the daily weak backwash experiment, and one for the biomass sample collected on Day 5 of the daily strong backwash experiment (Table 3.3). In both libraries, the *Betaproteobacteria* were most abundant class. In the first clone library, the two most abundant bacterial genera were *Dechloromonas* and *Zoogloea*, comprising 13.2 and 26.4% of the total bacterial population, respectively. The corresponding values dropped to 2.7 and 13.6% in the second library. The most abundant genus in the second library was *Curvibacter* accounting for 50.0% of the total bacterial population. Using the Library Comparison function on RDP, it was determined that the changes in relative abundance of these three bacterial genera between the two libraries were significant ( $p < 0.01$  in all three cases). Therefore, the relative abundances of these three genera were monitored using real-time PCR throughout the two daily backwash experiments (below).



A phylogenetic tree was constructed for the clones that belonged to the three genera in both clone libraries (Figure 3.2). Clones associated with *Dechloromonas* in both clone libraries clustered together and were closely related to *Dechloromonas* sp. HZ and *Dechloromonas* sp. JM. The clones associated with *Zoogloea* and *Curvibacter* in both libraries also clustered together.

Genus level analyses revealed changes in the overall community structure before and after the daily backwash experiments. In Figure 3.3, the Chao 1 and ACE indices increased from 60 and 75 to 81 and 92, respectively, indicating the microbial richness increased during the backwash experiments. In contrast, the Shannon-Weiner and Inverse Simpson's microbial diversity indices decreased from 2.77 and 11.51 to 2.40 and 4.73, respectively, likely due to the decrease in the evenness of the bacterial community. The rarefaction curves in Figure 3.3 showed that the bacterial richness at the genus level was similar before and after the backwash experiments. Table 3.3 shows that the microbial compositions of the two clone libraries were different. This observation was statistically supported by the results generated using  $\beta$ -LIBSHUFF (Table 3.4,  $p < 0.05$  in all comparisons), indicating the two clone libraries originated from significantly different microbial communities.

### **3.3.3. Real-time PCR Standard Curves**

The annealing temperatures reported in Table 3.1 were determined experimentally for each real-time PCR primer set designed in this study (Supplemental Figure 3.1). The standard curve constructed for each primer set (Figure 3.4) was linear between  $C_{\text{threshold}}$  and Log Target Concentration using units of gene copy # per  $\mu\text{L}$ :  $R^2$  values ranged from

0.993 to 0.995 (Table 3.2). Among the four primer sets used, Bact1369F/1492R had the narrowest linear range: the  $C_{\text{threshold}}$  values for the standards of  $10^1$  and  $10^2$  copies per  $\mu\text{L}$  fell outside the linear range and thus were not included in the standard curve. The linear ranges covered all the measurements from unknown samples. The high y-intercept value for Bact1369F/1492R indicates a lower detection limit at a given cycle number (Ritalahti et al., 2006). In addition, the amplification efficiencies for the four primer sets ranged from 0.627 (Bact1369F/1492R) to 0.952 (Dchm0991F/1146R).

#### **3.3.4. Daily Weak Backwash Experiment**

Before the daily weak backwash experiment, the reactor was backwashed once every month and was able to consistently remove dissolved oxygen (DO) and perchlorate to below their respective detection limits (data not shown). After the weak backwash on Day 0, there were minimum disturbances in reactor performance with respect to effluent DO and perchlorate concentrations (Figure 3.5 A and B). Immediately after the weak backwash on Day 1, the effluent DO concentration started at about 0.5 mg/L and then dropped to 0.04 mg/L at the end of the day. During the next four days, the effluent DO concentration immediately after each backwash decreased: from about 0.5 mg/L on Day 2 to about 0.05 mg/L on Day 5. At the same time, the duration of low effluent DO level in each backwash cycle increased every day. To better illustrate the improvement of reactor performance in terms of lowering effluent DO concentration along the course of the experiment, initial DO removal was plotted in Figure 3.5 A. It is clear from the trendline that there was an improvement in the reactor performance since Day 1.

A similar trend was noticed for the effluent perchlorate profiles (Figure 3.5 B). On Day 1, the effluent perchlorate concentration immediately after the weak backwash was close to the influent perchlorate concentration (i.e., 50 µg/L), then decreased throughout the day. Similar patterns repeated for subsequent daily weak backwashes. To better illustrate the perchlorate removal trend, the initial slopes of the curves fitted to the effluent perchlorate profiles, defined as “Initial Perchlorate Reduction Rates” immediately after each weak backwash, were calculated and plotted. It is clear from the trendline in Figure 3.5 B that the reactor’s ability to remove perchlorate also improved throughout the daily weak backwash experiment.

The amount of biomass removed was the highest for Day 0 of the daily weak backwash experiment, because the reactor had been backwashed only once a month before the start of this backwash experiment and had accumulated a large amount of biomass (Figure 3.6 A). The amount of biomass removed during both experiments varied somewhat, however, the averages of the two sets of backwash experiments (excluding Day 0 of the daily weak backwash experiments) were not significantly different ( $p=0.588$ , Figure 3.6 A and C).

The three abundant bacterial populations responded differently to the daily weak backwashes according to real-time PCR results, as shown in Figure 3.6 B. The relative abundance of *Dechloromonas* first decreased from 27.3% on Day 0 to 2.5% on Day 3, and then increased to 12.1% on Day 5. The relative abundance of *Zoogloea* first increased from 26.7% on Day 0 to 36.1% on Day 2, and then decreased to 15.6% on Day 5. The relative abundance of *Curvibacter* increased from 19.8% on Day 0 to 40.3% on Day 5. The relative abundances of these three populations on Day 0 determined by real-

time PCR (i.e., 27.3, 26.7, and 19.8%, respectively) were in reasonable agreement with the corresponding values determined in the clone library analyses (i.e., 13.2, 26.4, and 7.7% respectively, Table 3.3).

### **3.3.5. Daily Strong Backwash Experiment**

The bioreactor was not backwashed for six days after the daily weak backwash experiment. At the end of the six days, the reactor exhibited consistent complete removal of DO and perchlorate (data not shown). Then, the microbial community was exposed to strong backwashes for five consecutive days. The increase in backwash intensity dramatically affected reactor performance (Figure 3.5 C and D). Immediately after the strong backwash on Day 1, the effluent DO concentration was 0.01 mg/L and remained low throughout the day. For the next few days, the effluent DO concentration immediately after each backwash increased as the experiment proceeded, except for Day 4. After the strong backwash on Day 4, the effluent DO concentration remained 0.01 mg/L throughout the day, likely due to malfunctioning of the DO probe (the effluent DO concentrations during Day 4 could not have been lower than those during Day 1; also, the results of a replicate experiment presented in Supplemental Figure 3.4 indicated a decreasing trend of DO removal similar to Figure 3.5 C). The trendline shown in Figure 3.5 C demonstrates a deteriorating ability of the microbial community to consume DO.

A decreasing ability to remove perchlorate was also observed during the daily strong backwash experiment. The effluent perchlorate concentration immediately after each daily strong backwash was close to the influent perchlorate concentration (i.e., 50  $\mu\text{g/L}$ , Figure 3.5 D). The reactor was able to achieve complete perchlorate removal at the

end of Day 1. Starting on Day 2, the ability of the reactor to remove perchlorate deteriorated. On Day 5, the effluent perchlorate concentration remained at a level close to the influent perchlorate concentration throughout the day. The trendline in Figure 3.5 D confirmed that the ability of the reactor to remove perchlorate had decreased.

Similar to the daily weak backwash experiment, the three major bacterial genera responded differently to the strong backwashes as determined by real-time PCR (Figure 3.6 D). The relative abundance of *Dechloromonas* decreased from 7.0% on Day 1 to 0.5% on Day 5. The relative abundance of *Zoogloea* first slightly increased from 9.0% to 14.3% during the first two days, and then decreased to 2.4% on Day 5. The relative abundance of *Curvibacter* increased from 60.9% on Day 1 to 97.5% on Day 5. The relative abundances of *Dechloromonas* and *Zoogloea* on Day 5 measured with real-time PCR (i.e., 0.5 and 2.4%, respectively) were lower than the corresponding values obtained through clone library analyses (i.e., 2.7 and 13.6%, respectively, Table 3.3). For the relative abundance of *Curvibacter*, the value measured using real-time PCR (i.e., 97.5%) was substantially higher than the corresponding value determined through clone library analysis (i.e., 50.0%).

### **3.4. Discussion**

Three real-time PCR primer sets, targeting strains that belong to the genera *Dechloromonas*, *Zoogloea*, and *Curvibacter*, were designed based on the sequence information of the corresponding clones in the 16S rRNA gene clone libraries, instead of from the sequence information available in public databases. Thus, the designed primers

are not strictly genus-specific primers. In other words, these primers only target a subpopulation of each genus that was relevant to the bioreactor operated in the current study. Such design requires lower stringency on primer coverage, and warrants higher specificity. Thus, it is not surprising that even the closest non-targets for some designed primers had more than seven mismatches (Table 3.2). The primer sets were characterized to obtain optimized annealing temperatures for the real-time PCR experiments using known concentrations of plasmids containing target and non-target sequences. The real-time PCR results showed good correlation with the clone library analyses, except for the *Curvibacter* population on Day 5 of the daily strong backwash experiment.

The DNA samples used for the microbial analyses were extracted from the biomass removed during each backwash. The biomass remaining in the reactor after backwash was not sampled, because the size of the reactor was small and repeated sampling would have significantly changed the amount of biofilm in the reactor.

*Dechloromonas* spp. and *Azospira* spp. were the only known PRB detected in the reactor. The dominance of *Dechloromonas* in perchlorate reducing systems has been shown by other studies in which acetate was used as the sole electron donor (Zhang et al., 2005; Choi et al., 2008). In the phylogenetic analyses, the *Dechloromonas*-like clones from the reactor clustered together, and were found to be closely related to *Dechloromonas* sp. HZ and *Dechloromonas* sp. JM, both of which are PRB and can utilize acetate as an electron donor (Logan et al., 2001; Zhang et al., 2002). Other PRB species, such as *Dechlorospirillum* spp. and *Azospirillum* spp., which were isolated from various natural and engineered systems (Waller et al., 2004; Bardiya and Bae, 2008), were not present in the reactor.

The presence of *Zoogloea* spp. in the biofilm reactor is not surprising, as members of the genus have been characterized as slime formers in engineered systems (Dias and Bhat, 1964; Rossellomora et al., 1995). *Zoogloea* spp. are aerobic (Unz, 1984; Xie and Yokota, 2006) and thus utilized DO as their electron acceptor in the current system. The genus *Curvibacter* has been described only recently (Ding and Yokota, 2004), and knowledge about the ecological function of *Curvibacter* spp. is limited, except that they have been detected in freshwater (Ding and Yokota, 2004), Antarctic coastal waters (Gentile et al., 2006), and activated sludge (Thomsen et al., 2007). *Curvibacter* spp. were the most abundant population at the end of the strong backwash experiment (Figure 3.6 D and Table 3.3). Considering that *Curvibacter* spp. can also use oxygen as their electron acceptor (Ding and Yokota, 2004), and the oxygen removal efficiency was low at the end of the strong backwash experiment (Figure 3.5 C), we speculate that the *Curvibacter* spp. in the reactor did not play a significant role in lowering DO levels.

Both reactor performance and PRB population abundance recovered from the disturbance imposed by increased backwash frequency. After the backwash frequency was increased from once a month to once a day, reactor performance in terms of perchlorate removal dropped initially. During the rest of the daily weak backwash experiment, reactor performance improved continuously (Figure 3.5 B). In the meantime, the relative abundance of *Dechloromonas* spp. showed a down-and-up trend (Figure 3.6 B), different from the continuous improvement of reactor performance. The discrepancy in the trends of the relative abundance of PRB and perchlorate removal indicates that bacterial population(s) other than *Dechloromonas* spp. impacted perchlorate removal efficiency. Such bacterial population(s) likely affected perchlorate removal by lowering

DO, the competing electron acceptor, in the bioreactor. In contrast, neither the reactor performance nor the PRB population recovered from the increase in backwash intensity. Reactor performance in terms of perchlorate removal and the relative abundance of *Dechloromonas* spp. continuously dropped during the daily strong backwash experiment (Figure 3.5 D and Figure 3.6 D).

The daily weak and strong backwash experiments were repeated during a related study, and biomass samples collected were subject to real-time PCR analyses (Supplemental Figure 3.4 previously published in (Choi et al., 2007) and Supplemental Figure 3.5). The trends in DO and perchlorate removal efficiencies obtained in this related study were similar to those observed in the current study, although some differences in microbial community shifts were observed (Supplemental Figure 3.5 and Figure 3.6).

In conclusion, after a minor disturbance in reactor operation, such as an increase in backwash frequency, the PRB population (i.e., *Dechloromonas* spp.) was able to recover, and reactor performance (i.e., perchlorate removal) improved gradually. In comparison, after a major disturbance in reactor operation, such as an increase in backwash intensity, *Dechloromonas* spp. failed to adjust to the change, *Curvibacter* spp. became the dominant population, and consequently reactor performance deteriorated.



### 3.5. Tables

Table 3.1. Sequence, coverage, specificity, and annealing temperature for each primer set designed in this study.

Target (16S rRNA gene)	F/R	Systematic Name <sup>1,2</sup>	Abbreviated Name	Sequence (5' to 3')	Coverage in clone library #1 <sup>3</sup>	Coverage in clone library #2 <sup>3</sup>	Specificity <sup>4</sup>	Anneal- ing temp. (°C) <sup>5</sup>
<i>Dechloromonas</i>	F	S-G-Dchm-0991-a-S-24	Dchm0991F	TTG ACA TGT CCA GAA GCC CGA AGA	23/26	7/7	12/29	58.5
	R	S-G-Dchm-1146-a-A-24	Dchm1146R	TGT CAC CGG CAG TCT CGT TAA AGT	21/26	6/7	68/196	
<i>Zoogloea</i>	F	S-G-Zoog-0487-a-S-24	Zoog0487F	ACC GTA AGA AGA AGC ACC GGC TAA	40/44	13/26	32/277	68.0
	R	S-G-Zoog-0627-a-A-24	Zoog0627R	TGA TGC AGT CAC AAA CGC AGT TCC	35/44	20/26	23/24	
<i>Curvibacter</i>	F	S-G-Curvib-1001-a-S-21	Curvib1001F	CGG AAG TTA CCA GAG ATG GTT	21/21	73/77	71/110	64.0
	R	S-G-Curvib-1107-a-A-21	Curvib1107R	CAA CTA ATG ACA AGG GTT GCG	20/21	74/77	203/7190	

<sup>1</sup> The primers were named according to standardized nomenclature by Alm and coworkers (Alm et al., 1996).

<sup>2</sup> The location of the primers were determined based on *Escherichia coli* numbering (Brosius et al., 1981).

<sup>3</sup> Coverage = “Number of target clones with perfect match to the corresponding primer” / “Number of target clones in the clone library”. Clone library #1 was built on the biomass collected on Day 0 of daily weak backwash experiment, while clone library #2 on Day 5 of daily strong backwash experiment.

<sup>4</sup> Specificity = “Number of target sequences in database with perfect match to the corresponding primer” / “Number of sequences in database with perfect match to the corresponding primer”. The specificity results were obtained using the Probe Match function on RDP in May 2007 (Cole et al., 2007).

<sup>5</sup> Experimentally determined in this study.

Table 3.2. Target and non-target used in the characterization of each real-time PCR primer set, and the amplification efficiencies for each real-time PCR primer set.

Primer set	Target	Non-target <sup>1</sup>	Amplification efficiency	Slope <sup>3</sup>	y-Intercept <sup>3</sup>	R <sup>2</sup>	Linear range (copies/μL)
Dchm0991F/1146R	<i>Dechloromonas</i>	<i>Zoogloea</i> (>7, 1)	0.952	-3.442	37.46	0.995	10 <sup>1</sup> -10 <sup>9</sup>
Zoog0487F/0627R	<i>Zoogloea</i>	<i>Curvibacter</i> (1, 4) <i>Dechloromonas</i> (2, 7)	0.990	-3.346	36.97	0.993	10 <sup>1</sup> -10 <sup>9</sup>
Curvib1001F/1107R	<i>Curvibacter</i>	<i>Zoogloea</i> (2, 2)	0.805	-3.898	41.86	0.995	10 <sup>1</sup> -10 <sup>8</sup>
Bact1369F/1492R	All bacteria <sup>2</sup>	NA	0.627	-4.730	52.67	0.995	10 <sup>3</sup> -10 <sup>9</sup>

<sup>1</sup>. The numbers in parentheses are the numbers of mismatches of non-targets with forward and reverse primers, respectively.

<sup>2</sup>. Plasmid DNA containing *Dechloromonas* 16S rDNA was used as real-time PCR standards for the bacterial primer set.

<sup>3</sup>. Cross reference to Figure 3.4. The equation for each standard curve follows the format of  $C_{\text{threshold}} = \text{Slope} \times \lg(\text{copy\# per } \mu\text{L}) + y\text{-Intercept}$ .

Table 3.3. Relative abundance of bacterial population determined using clone library sequence analyses in biomass samples collected on Day 0 of the weak backwash experiment (total of 182 clones) and Day 5 of the strong backwash experiment (total of 184 clones).<sup>1</sup>

Class	Genus	Day 0 <sup>2</sup> of daily weak backwash experiment (%)	Day 5 of daily strong backwash experiment (%)
<i>Acidobacteria</i>	<i>Holophage</i>	1.1	ND
	Unclassified <i>Acidobacteriaceae</i>	1.1	ND
<i>Sphingobacteria</i>	Unclassified <i>Flexibacteraceae</i> <sup>3</sup>	5.5	ND
	Unclassified <i>Sphingobacteriales</i>	6.0	7.1
	<i>Niastella</i>	ND	2.7
<i>Alphaproteobacteria</i>	<i>Terrimonas</i>	ND	1.1
	<i>Sphingomonas</i>	ND	1.1
<i>Betaproteobacteria</i>	<i>Methylophilus</i>	0.5	3.8
	<i>Dechloromonas</i> <sup>3</sup>	13.2	2.7
	<i>Zoogloea</i> <sup>3</sup>	26.4	13.6
	<i>Azospira</i>	ND	0.5
	Unclassified <i>Rhodocyclaceae</i>	3.3	1.1
	<i>Curvibacter</i> <sup>3</sup>	7.7	50.0
	Unclassified <i>Comamonadaceae</i>	7.1	1.1
	Unclassified <i>Betaproteobacteria</i>	1.6	2.2
<i>Gammaproteobacteria</i>	<i>Methylomonas</i>	6.6	3.3
	Unclassified <i>Methylococcaceae</i>	7.1	4.9

<sup>1</sup> The criterion used in selecting taxa to be included in the table: taxa that contained more than one clone in at least one of the two libraries, with the exception of the genus *Azospira*.

<sup>2</sup> Day 388 since the start of the reactor. Before the start of the daily weak backwash experiment, the reactor has been mainly operated using the baseline operating condition.

<sup>3</sup> Taxa whose relative abundances are significantly different in the two clone libraries with *p* values less than 0.01 according to the Library Comparison function on RDP.

Table 3.4. Values of  $p$  estimating the similarity between the two bacterial clone libraries using  $\int$ -LIBSHUFF.

<b>Bacterial clone library (X)</b>	<b><math>p</math> value comparison of clone library (Y) with X<sup>1</sup></b>	
	<b>Day 0 of Daily Weak BW</b>	<b>Day 5 of Daily Strong BW</b>
Day 0 of Daily Weak BW	0.0000	0.0000
Day 5 of Daily Strong BW	0.0428	0.0000

<sup>1</sup>.  $p$  values compare either X to Y or Y to X, and indicate the clone libraries were sampled from significantly different ( $p < 0.05$ ) communities.

### 3.6. Figures

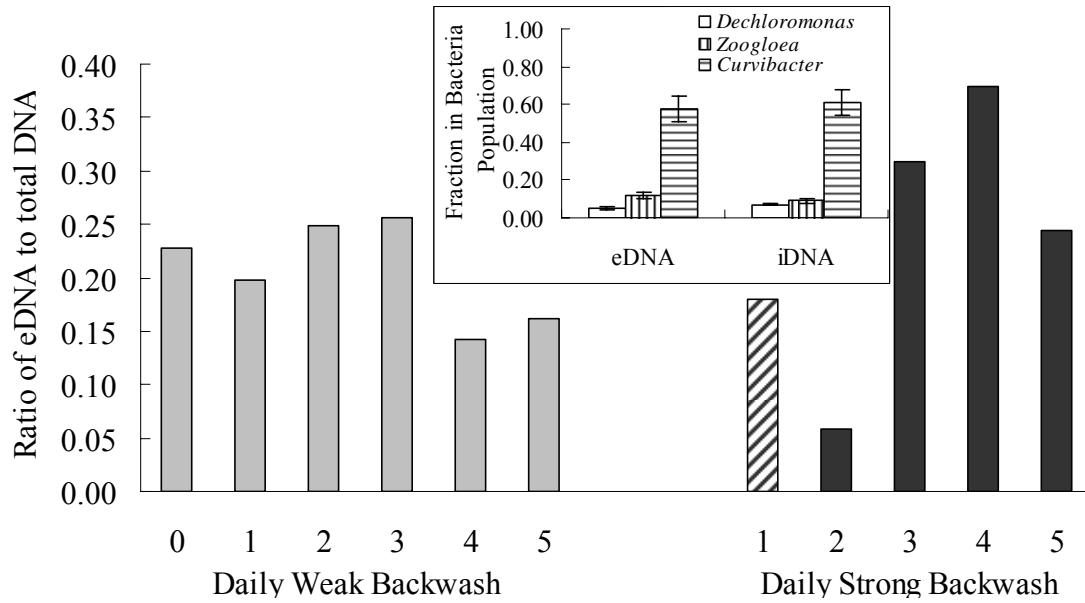


Figure 3.1. The ratios of eDNA to total DNA in biomass samples collected from the daily weak backwash (grey) and daily strong backwash experiments (dark). For the sample from Day 1 of the daily strong backwash experiment, the eDNA extracts likely were contaminated with iDNA: about 12.6% of the iDNA ended up in the eDNA extract. The ratio for this specific sample was not included in the reported average percentages in the text. The insert shows the relative abundances for the three dominant genera for the iDNA and “eDNA” extracts for the sample from Day 1 of the daily strong backwash experiment.

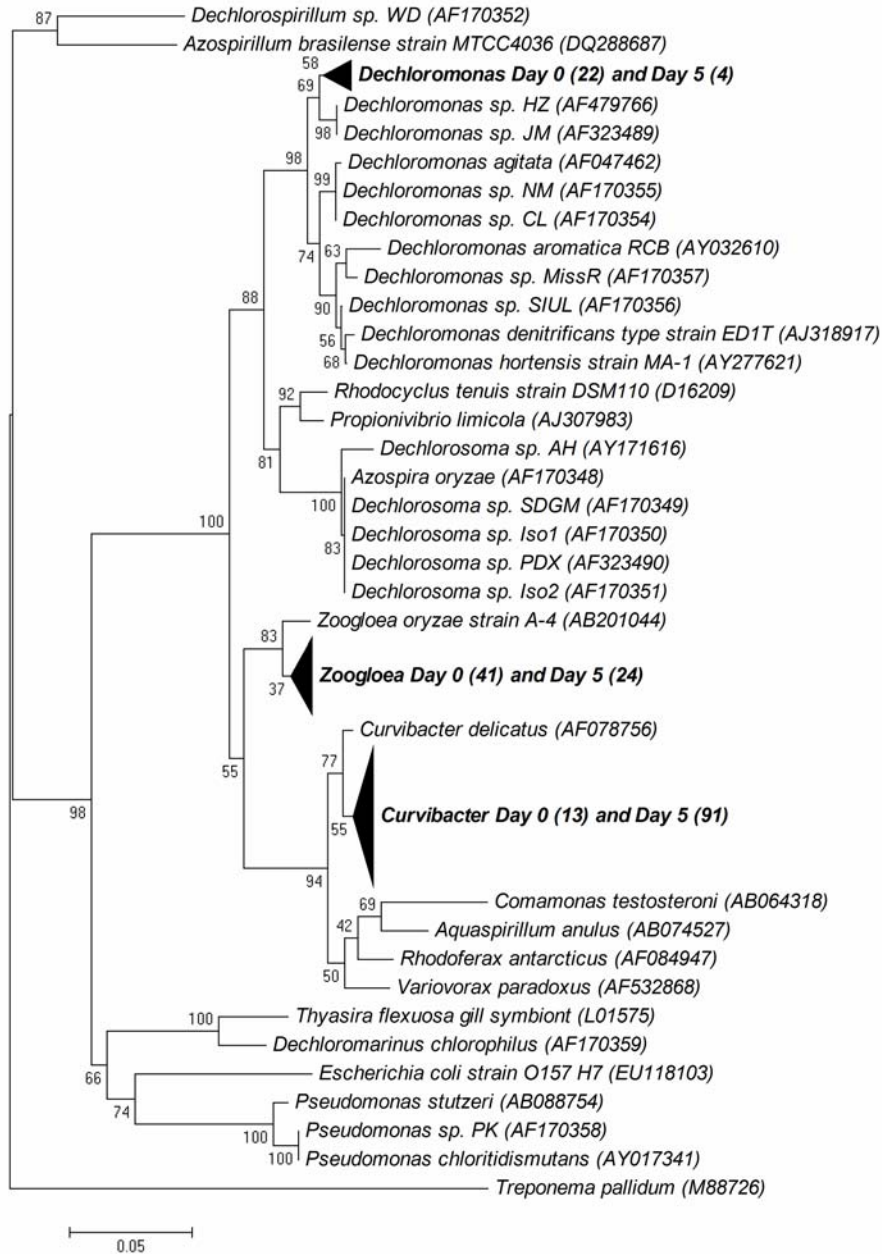
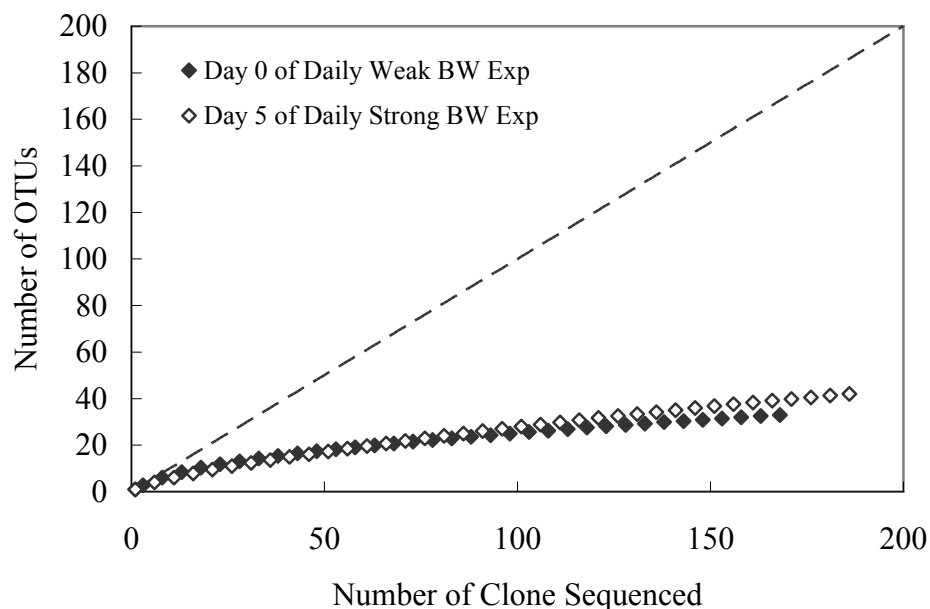


Figure 3.2. A phylogenetic tree of the clones that were closely associated with the three major bacterial genera present in the biofilm reactor. “Day 0” and “Day 5” refer to Day 0 of the daily weak backwash experiment and Day 5 of the daily strong backwash experiment, respectively. The numbers in parentheses are the numbers of clones.



Sampling time	No. of seq.	No. of OTUs <sup>1</sup>	Chao 1 <sup>2</sup>	ACE <sup>2</sup>	Shannon-Weiner Index	Inverse Simpson's index
Day 0 of dailyweak BW	168	33	60 (41, 122)	75 (49, 142)	2.77	11.51
Day 5 of daily strong BW	186	42	81 (57, 145)	92 (62, 168)	2.40	4.73

<sup>1</sup>. OTUs defined as 5% difference in 16S rRNA gene sequences.

<sup>2</sup>. Mean values with upper and lower 95% confidence intervals given in parentheses.

Figure 3.3. Rarefaction curves indicating bacterial 16S rRNA richness within the two clone libraries. The dashed line represents 1:1, indicating infinite diversity. The table lists the bacterial 16S rRNA sequence diversity indices. OTUs were defined as groups of sequences sharing 95% 16S rRNA sequence identity. The estimates of phylotype richness were calculated according to the abundance-based coverage estimate (ACE) and the bias-corrected Chao1 estimator. The Shannon-Weiner diversity index and the Inverse Simpson's diversity index, which consider species richness as well as evenness, were also calculated.

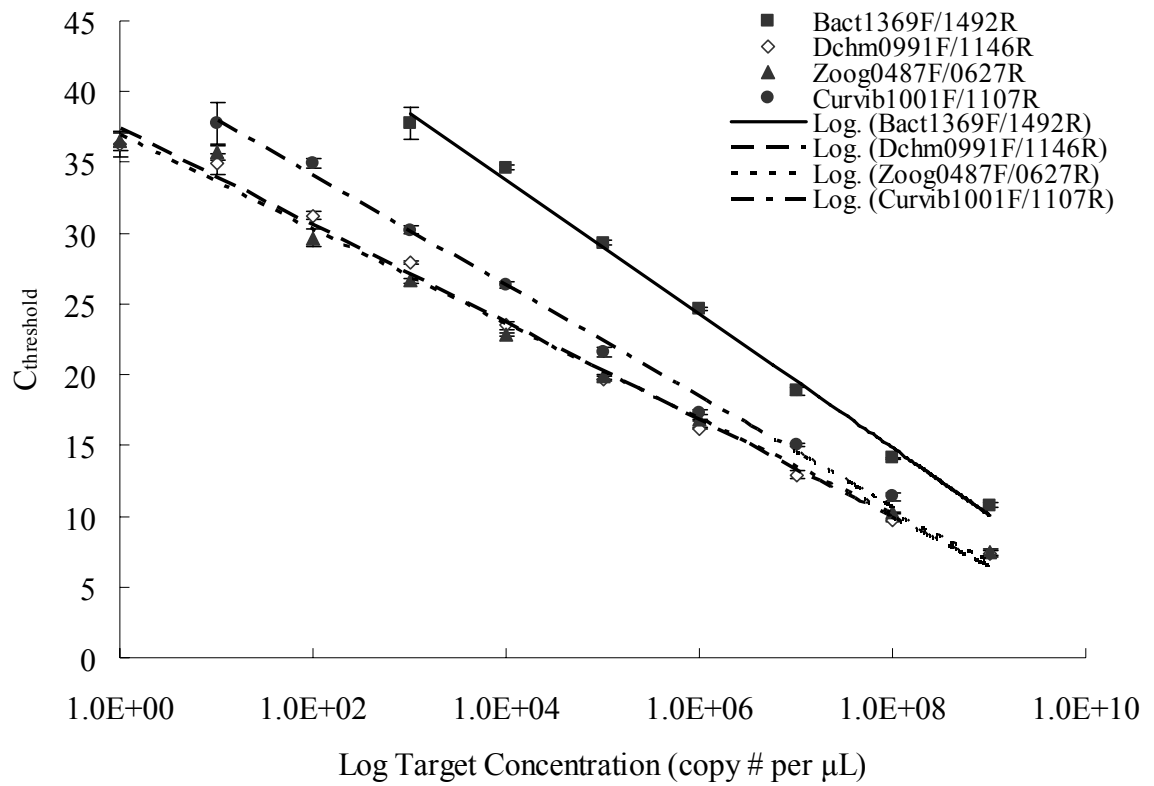


Figure 3.4. Standard curves for the primer sets designed for *Dechloromonas*, *Zoogloea*, and *Curvibacter* clones, and the standard curve for the bacterial primer set.



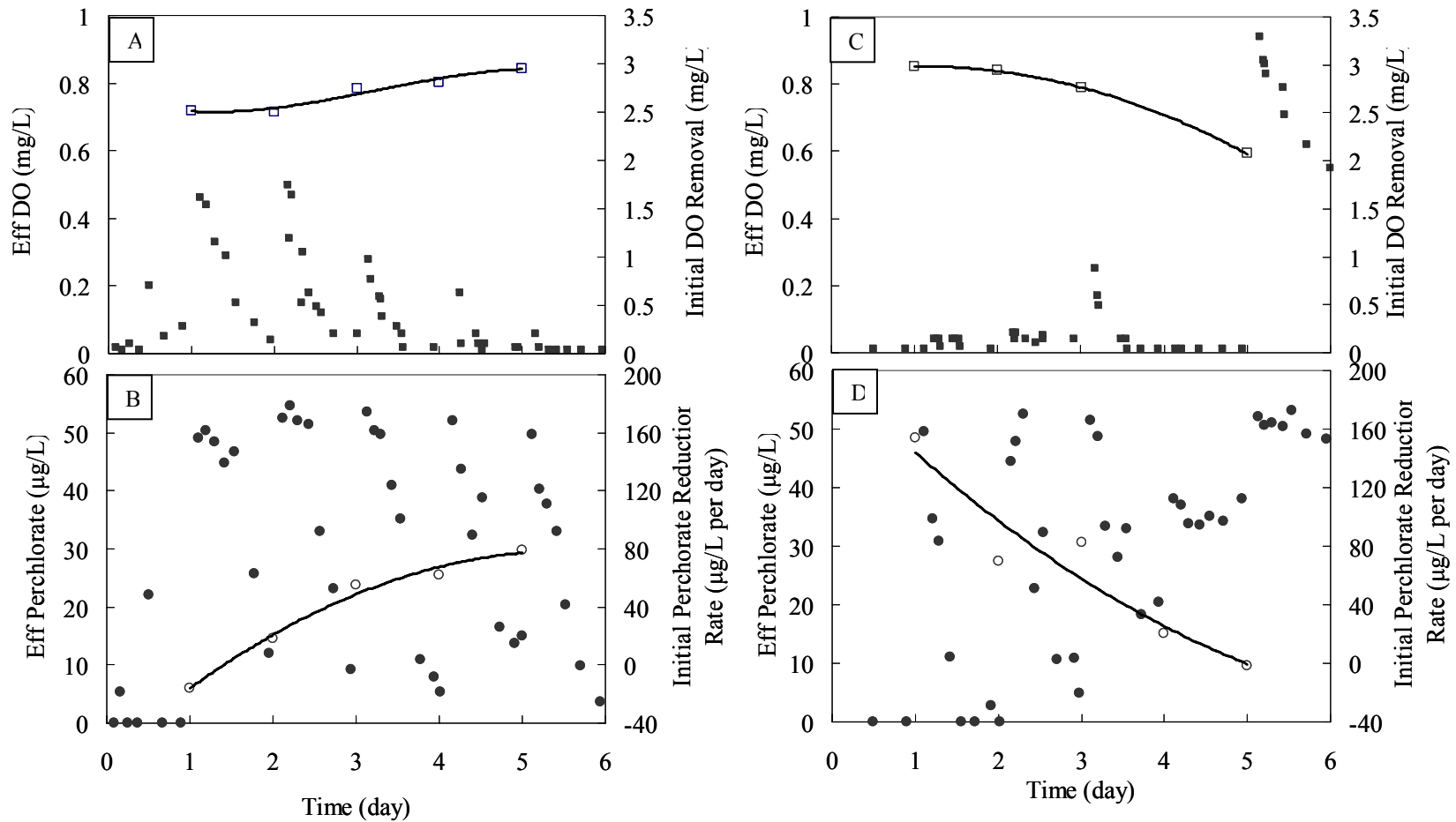


Figure 3.5. The effluent DO (top row) and perchlorate (bottom row) concentrations during the daily weak backwash experiment (left column) and the daily strong backwash experiment (right column). (■) Effluent DO level; (□) Initial DO removal; (●) Effluent perchlorate concentration; (○) Initial perchlorate reduction rate.

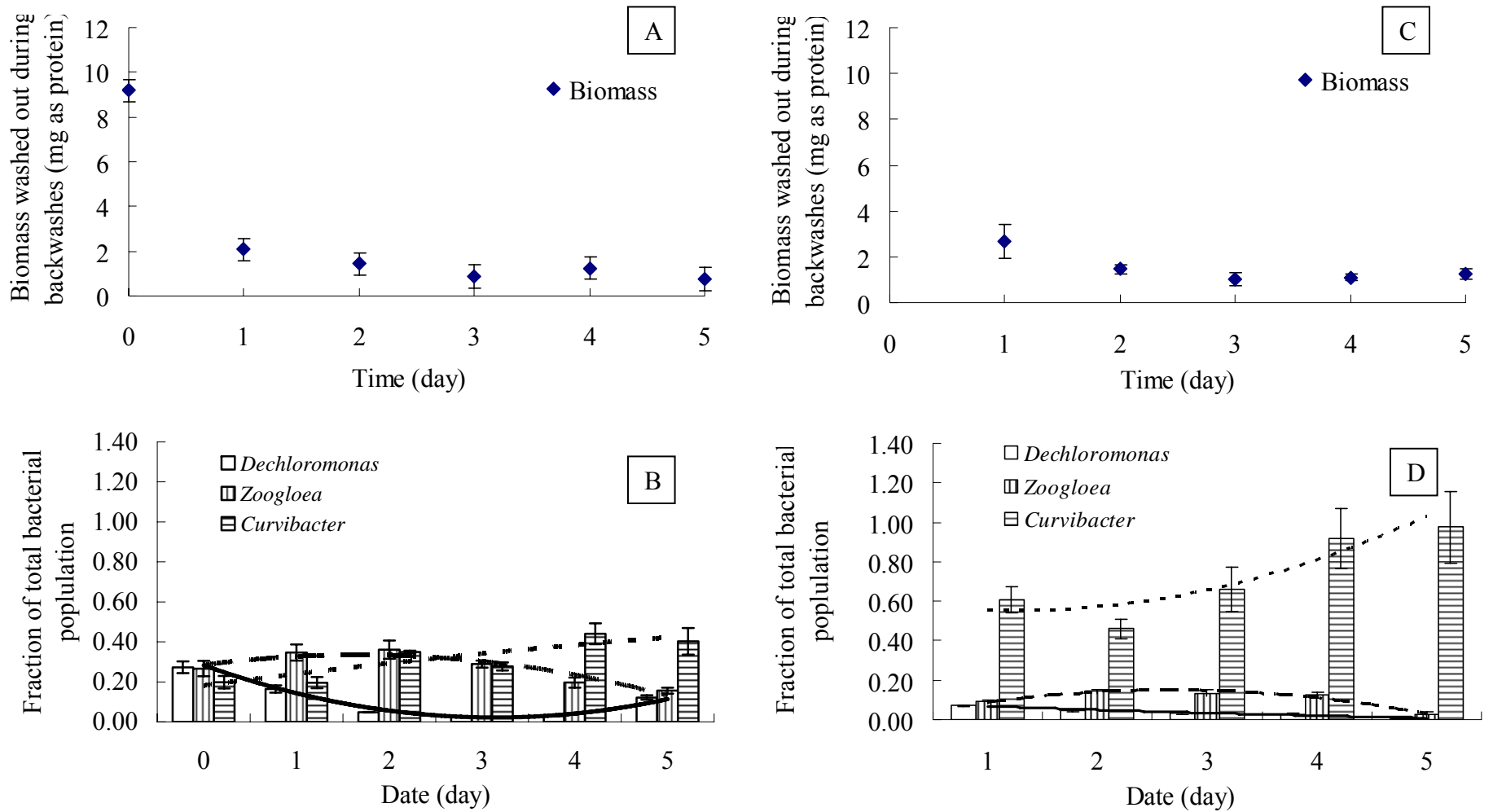
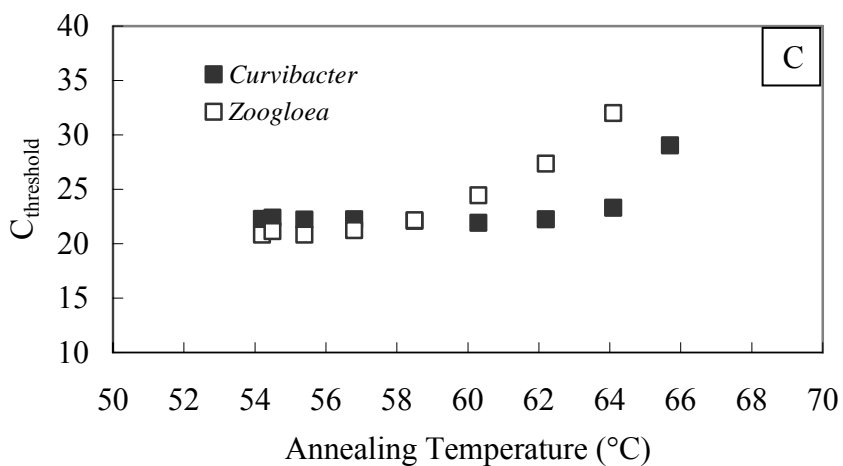
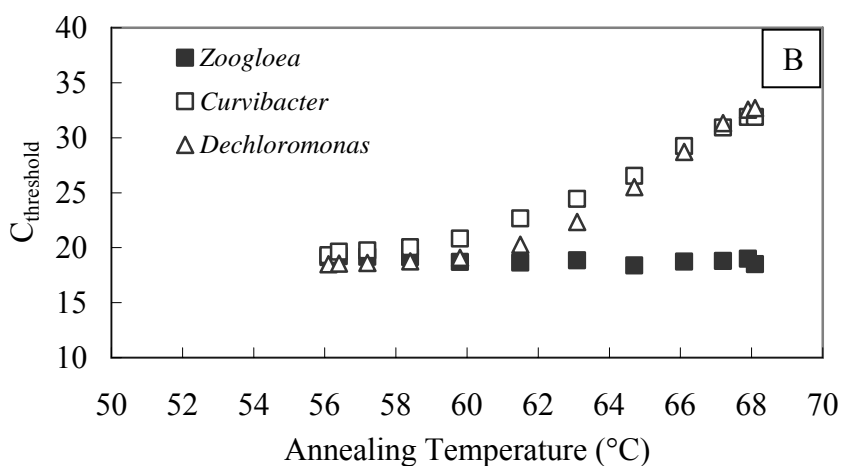
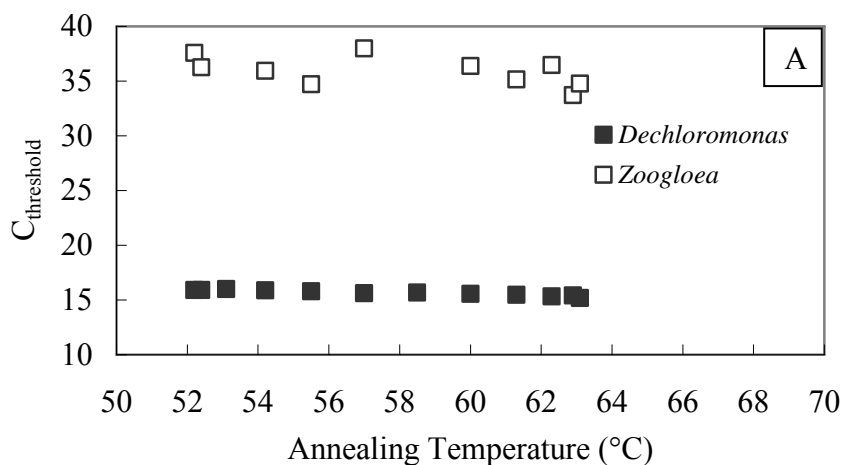
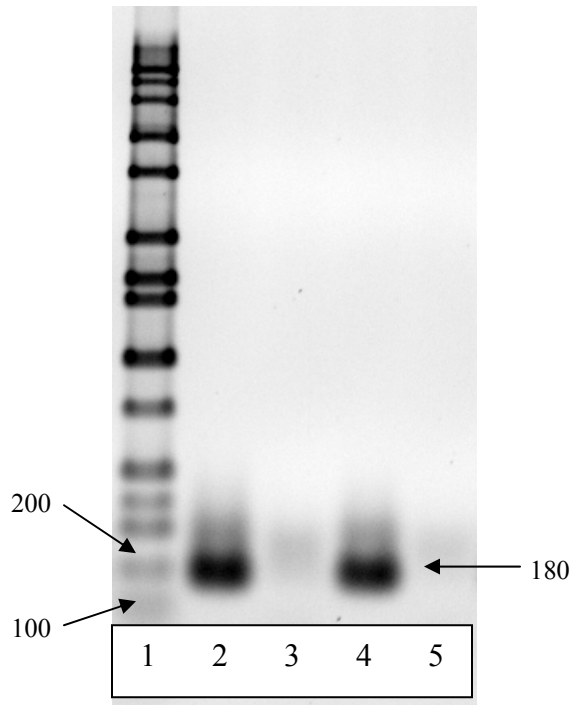


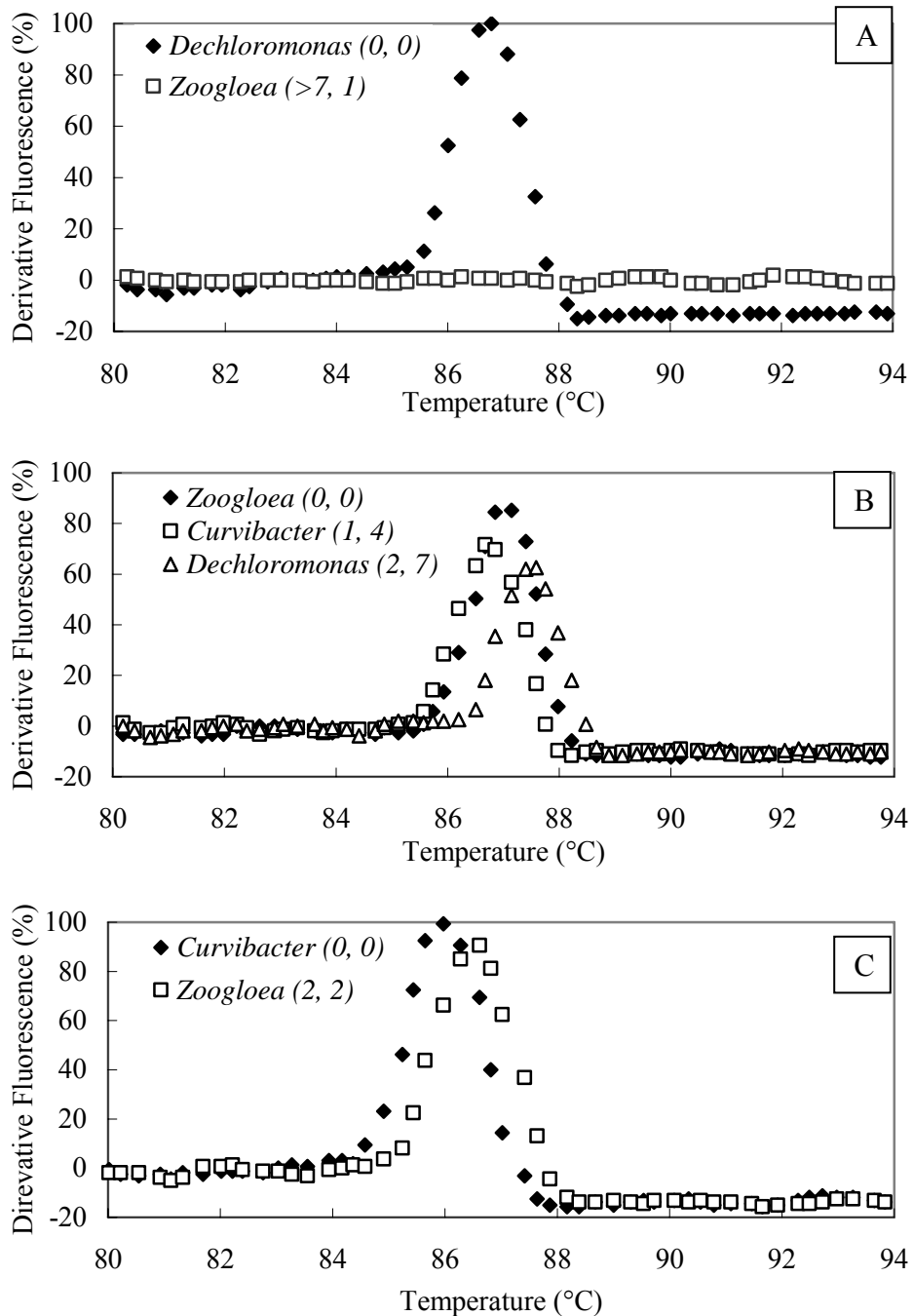
Figure 3.6. Protein measurements (top row) and the relative abundance of the three major bacterial genera in total bacterial population (bottom row) during the daily weak (left column) and strong (right column) backwash experiments. Trendlines: (solid) *Dechloromonas*; (dashed) *Zoogloea*; (dotted) *Curvibacter*.



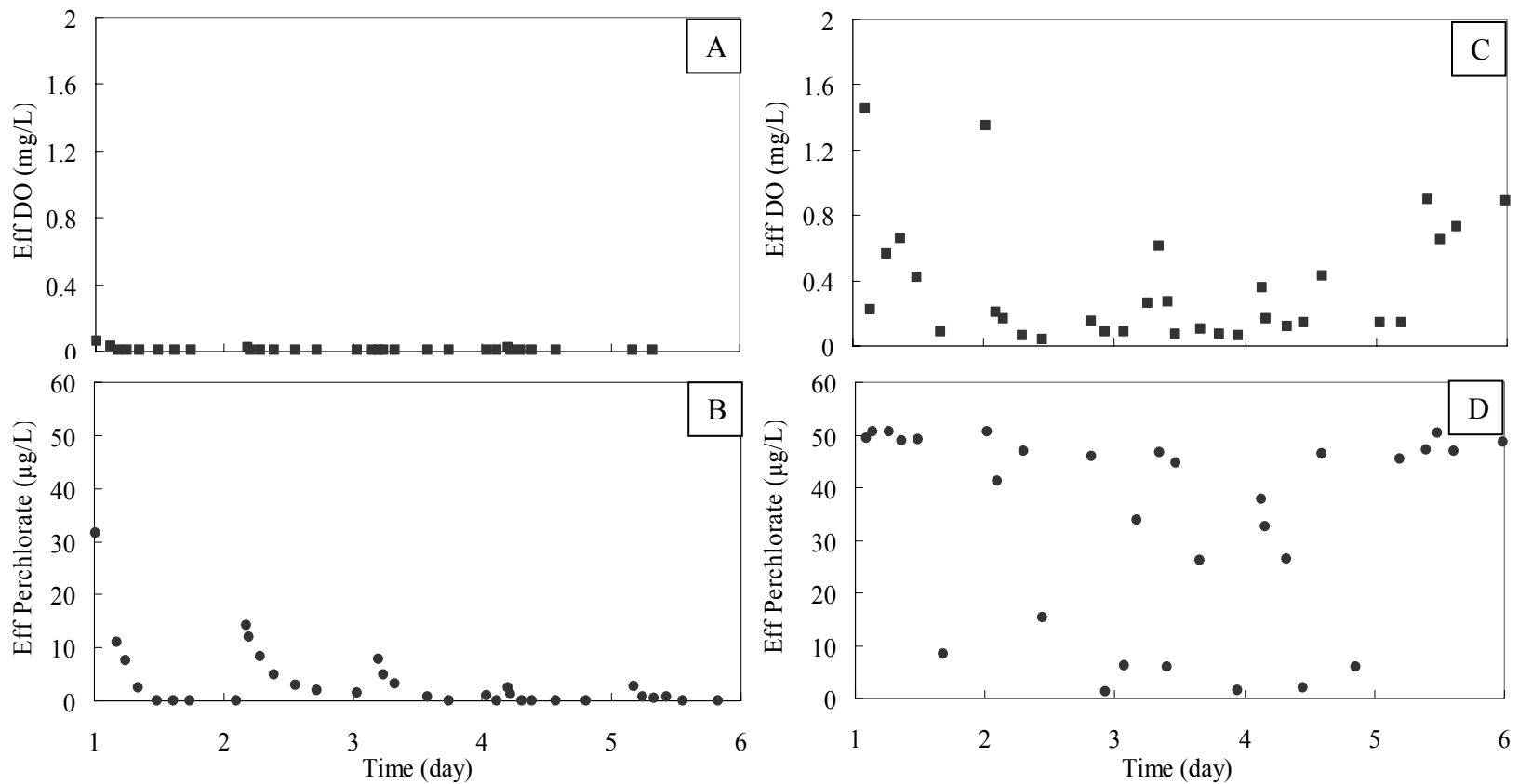
Supplemental Figure 3.1. Characterization on primer sets with various annealing temperatures: (A) Dchm0991F/1146R, (B) Zoog0487F/0627R, and (C) Curvib1001F/1107R. Filled symbols: target. Open symbols: non-target. The numbers of mismatches of the non-targets are listed in Table 3.2.



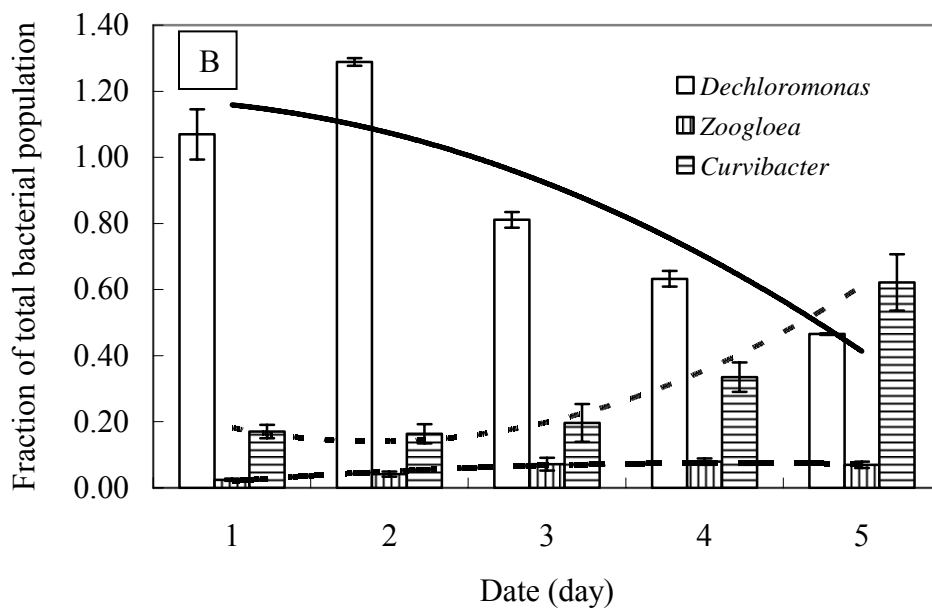
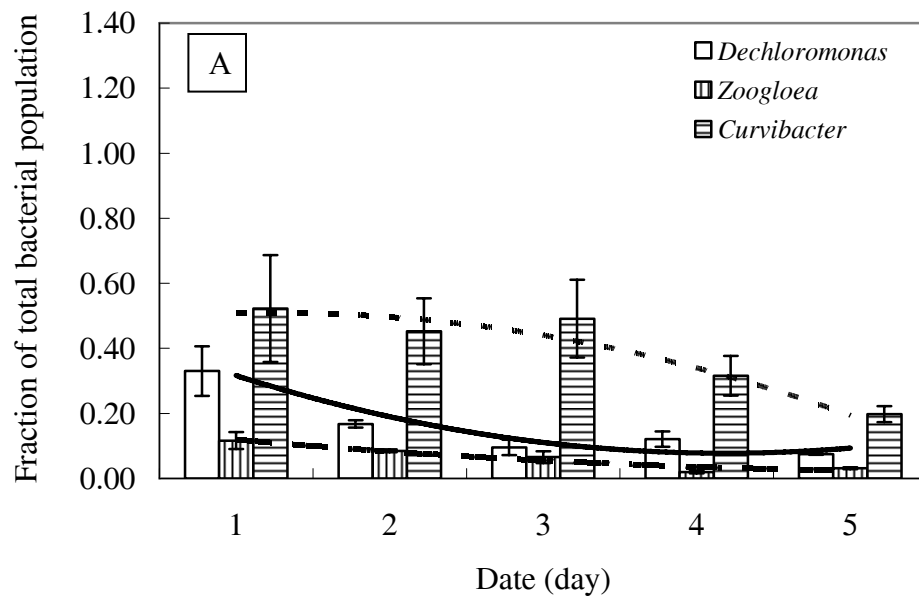
Supplemental Figure 3.2. An electrophoresis gel image of real-time PCR products using the Dchm0991F/1146R primer set. Lane 1: DNA ladder; Lane 2 and 3: *Dechloromonas* (target) and *Zoogloea* (non-target) with an annealing temperature of 58.4°C; Lane 4 and 5: *Dechloromonas* (target) and *Zoogloea* (non-target) with an annealing temperature of 64.7°C.



Supplemental Figure 3.3. Representative melting curves for the targets and non-targets of the three real-time PCR primer sets designed in this study: (A) Dchm0991F/1146R ( $T_m=86.90\pm 0.15^\circ\text{C}$  for *Dechloromonas*, N/A for *Zoogloea*); (B) Zoog0487F/0627R ( $T_m=86.63\pm 0.18^\circ\text{C}$  for *Zoogloea*,  $T_m=86.36\pm 0.17^\circ\text{C}$  for *Curvibacter*,  $T_m=87.10\pm 0.17^\circ\text{C}$  for *Dechloromonas*); (C) Curvib1001F/1107R ( $T_m=85.93\pm 0.21^\circ\text{C}$  for *Curvibacter*,  $T_m=86.50\pm 0.16^\circ\text{C}$  for *Zoogloea*). The numbers in parentheses are the numbers of mismatches with the corresponding primers. The averages and standard deviations were from n replicates ( $n>10$ ).



Supplemental Figure 3.4. The effluent DO (top row) and perchlorate (bottom row) concentrations during the daily weak backwash experiment (left column) and the daily strong backwash experiment (right column), which were replicate experiments of the ones in Figure 3.5. (■) Effluent DO level; (●) Effluent perchlorate concentration. These plots were reproduced from the work by Choi and coworkers (Choi et al., 2007).



Supplemental Figure 3.5. Fractions of three major bacterial genera in total bacterial population during the weak (A) and strong (B) backwash experiments. Trendlines: (solid) *Dechloromonas*; (dashed) *Zoogloea*; (dotted) *Curvibacter*.

### 3.7. References

Ahmad, R., Amirtharajah, A., Al-Shawwa, A. and Huck, P.M. (1998) Effects of Backwashing on Biological Filters. *Journal American Water Works Association* 90(12), 62-73.

Alm, E.W., Oerther, D.B., Larsen, N., Stahl, D.A. and Raskin, L. (1996) The Oligonucleotide Probe Database. *Applied and Environmental Microbiology* 62(10), 3557-3559.

American Public Health Association (APHA), A.W.W.A.A., Water Environment Federation (WEF) (1992) *Standard Methods for the Examination of Water and Wastewater*, American Public Health Association, Washington, DC.

Bardiya, N. and Bae, J.H. (2008) Isolation and Characterization of Dechlorospirillum Anomalous Strain Jb116 from a Sewage Treatment Plant. *Microbiological Research* 163(2), 182-191.

Briones, A. and Raskin, L. (2003) Diversity and Dynamics of Microbial Communities in Engineered Environments and Their Implications for Process Stability. *Current Opinion in Biotechnology* 14(3), 270-276.

Brosius, J., Dull, T.J., Sleeter, D.D. and Noller, H.F. (1981) Gene Organization and Primary Structure of a Ribosomal-Rna Operon from Escherichia-Coli. *Journal of Molecular Biology* 148(2), 107-127.

Brown, J.C., Snoeyink, V.L., Raskin, L. and Lin, R. (2003) The Sensitivity of Fixed-Bed Biological Perchlorate Removal to Changes in Operating Conditions and Water Quality Characteristics. *Water Research* 37(1), 206-214.

CA-DHS (2005) Perchlorate Drinking Water Action Level and Regulation. , California Department of Health Services, <http://www.dhs.ca.gov/ps/ddwem/chemicals/perchl/perchlindex.htm>.

Chenna, R., Sugawara, H., Koike, T., Lopez, R., Gibson, T.J., Higgins, D.G. and Thompson, J.D. (2003) Multiple Sequence Alignment with the Clustal Series of Programs. *Nucleic Acids Research* 31(13), 3497-3500.

Choi , Y.C., Li, X., Raskin, L. and Morgenroth, E. (2007) Effect of Backwashing on Perchlorate Removal in Fixed Bed Biofilm Reactors. *Water Research* 41(9), 1949-1959.

Choi, Y.C., Li, X., Raskin, L. and Morgenroth, E. (2007) Effect of Backwashing on Perchlorate Removal in Fixed Bed Biofilm Reactors. *Water Research* 41(9), 1949-1959.



- Choi, Y.C., Li, X., Raskin, L. and Morgenroth, E. (2008) Chemisorption of Oxygen onto Activated Carbon Can Enhance the Stability of Biological Perchlorate Reduction in Fixed Bed Biofilm Reactors. *Water Research* 42(13), 3425-3434.
- Coates, J.D. and Achenbach, L.A. (2004) Microbial Perchlorate Reduction: Rocket-Fuelled Metabolism. *Nature Reviews Microbiology* 2(7), 569-580.
- Coates, J.D., Michaelidou, U., Bruce, R.A., O'Connor, S.M., Crespi, J.N. and Achenbach, L.A. (1999) Ubiquity and Diversity of Dissimilatory (Per)Chlorate-Reducing Bacteria. *Applied and Environmental Microbiology* 65(12), 5234-5241.
- Cole, J.R., Chai, B., Farris, R.J., Wang, Q., Kulam-Syed-Mohideen, A.S., McGarrell, D.M., Bandela, A.M., Cardenas, E., Garrity, G.M. and Tiedje, J.M. (2007) The Ribosomal Database Project (Rdp-II): Introducing Myrddp Space and Quality Controlled Public Data. *Nucleic Acids Research* 35, D169-D172.
- Corinaldesi, C., Danovaro, R. and Dell'Anno, A. (2005) Simultaneous Recovery of Extracellular and Intracellular DNA Suitable for Molecular Studies from Marine Sediments. *Applied and Environmental Microbiology* 71(1), 46-50.
- Curtis, T.P., Head, I.M. and Graham, D.W. (2003) Theoretical Ecology for Engineering Biology. *Environmental Science & Technology* 37(3), 64a-70a.
- Dias, F.F. and Bhat, J.V. (1964) Microbial Ecology of Activated Sludge .I. Dominant Bacteria. *Applied Microbiology* 12(5), 412-&.
- Ding, L.X. and Yokota, A. (2004) Proposals of *Curvibacter Gracilis* Gen. Nov., Sp Nov and *Herbaspirillum Putei* Sp Nov for Bacterial Strains Isolated from Well Water and Reclassification of [*Pseudomonas*] *Huttiensis*, [*Pseudomonas*] *Lanceolata*, [*Aquaspirillum*] *Delicatum* and [*Aquaspirillum*] *Autotrophicum* as *Herbaspirillum Huttense* Comb. Nov., *Curvibacter Lanceolatus* Comb. Nov., *Curvibacter Delicatus* Comb. Nov and *Herbaspirillum Autotrophicum* Comb. Nov. *International Journal of Systematic and Evolutionary Microbiology* 54, 2223-2230.
- Dojka, M.A., Hugenholtz, P., Haack, S.K. and Pace, N.R. (1998) Microbial Diversity in a Hydrocarbon- and Chlorinated-Solvent-Contaminated Aquifer Undergoing Intrinsic Bioremediation. *Applied and Environmental Microbiology* 64(10), 3869-3877.
- Felsenstein, J. (1985) Confidence-Limits on Phylogenies - an Approach Using the Bootstrap. *Evolution* 39(4), 783-791.
- Fields, M.W., Yan, T.F., Rhee, S.K., Carroll, S.L., Jardine, P.M., Watson, D.B., Criddle, C.S. and Zhou, J.Z. (2005) Impacts on Microbial Communities and Cultivable Isolates from Groundwater Contaminated with High Levels of Nitric Acid-Uranium Waste. *FEMS Microbiology Ecology* 53(3), 417-428.
- Gentile, G., Giuliano, L., D'Auria, G., Smedile, F., Azzaro, M., De Domenico, M. and Yakimov, M.M. (2006) Study of Bacterial Communities in Antarctic Coastal Waters by a

Combination of 16s Rrna and 16s Rdna Sequencing. *Environmental Microbiology* 8(12), 2150-2161.

Greer, M.A., Goodman, G., Pleus, R.C. and Greer, S.E. (2002) Health Effects Assessment for Environmental Perchlorate Contamination: The Dose Response for Inhibition of Thyroidal Radioiodine Uptake in Humans. *Environmental Health Perspectives* 110(9), 927-937.

Griffiths, R.I., Whiteley, A.S., O'Donnell, A.G. and Bailey, M.J. (2000) Rapid Method for Coextraction of DNA and Rna from Natural Environments for Analysis of Ribosomal DNA- and Rrna-Based Microbial Community Composition. *Applied and Environmental Microbiology* 66(12), 5488-5491.

Hall, T.A. (1999) Bioedit: A User-Friendly Biological Sequence Alignment Editor and Analysis Program for Windows 95/98/Nt. *Nucleic Acids Symposium Series* 41, 95-98.

Hozalski, R.M. and Bouwer, E.J. (1998) Deposition and Retention of Bacteria in Backwashed Filters. *Journal American Water Works Association* 90(1), 71-85.

Jukes, T. and Cantor, C.R. (1969) Mammalian Protein Metabolism. HN, M. (ed), pp. 21-132, Academic Press, New York.

Lahav, O., Artzi, E., Tarre, S. and Green, M. (2001) Ammonium Removal Using a Novel Unsaturated Flow Biological Filter with Passive Aeration. *Water Research* 35(2), 397-404.

Logan, B., Zhang, H., Mulvaney, P., Milner, M., Head, I. and Unz, R. (2001) Kinetics of Perchlorate- and Chlorate-Respiring Bacteria. *Applied and Environmental Microbiology* 67(6), 2499-2506.

MA-DEP (2006) Drinking Water Status on Perchlorate by Ma Department of Environmental Protection, <http://www.mass.gov/dep/water/drinking/percinfo.htm#stds>.

Miller, J.P. and Logan, B.E. (2000) Sustained Perchlorate Degradation in an Autotrophic, Gas-Phase, Packed-Bed Bioreactor. *Environmental Science & Technology* 34(14), 3018-3022.

Min, B., Evans, P.J., Chu, A.K. and Logan, B.E. (2004) Perchlorate Removal in Sand and Plastic Media Bioreactors. *Water Research* 38(1), 47-60.

Nerenberg, R. and Rittmann, B.E. (2004) Hydrogen-Based, Hollow-Fiber Membrane Biofilm Reactor for Reduction of Perchlorate and Other Oxidized Contaminants. *Water Science and Technology* 49(11-12), 223-230.

Richardson, R.E., Bhupathiraju, V.K., Song, D.L., Goulet, T.A. and Alvarez-Cohen, L. (2002) Phylogenetic Characterization of Microbial Communities That Reductively Dechlorinate Tce Based Upon a Combination of Molecular Techniques. *Environmental Science & Technology* 36(12), 2652-2662.

- Ritalahti, K.M., Amos, B.K., Sung, Y., Wu, Q.Z., Koenigsberg, S.S. and Löffler, F.E. (2006) Quantitative Pcr Targeting 16s Rna and Reductive Dehalogenase Genes Simultaneously Monitors Multiple Dehalococcoides Strains. *Applied and Environmental Microbiology* 72(4), 2765-2774.
- Rittmann, B.E. and McCarty, P.L. (2001) *Environmental Biotechnology: Principles and Applications*, McGraw-Hill, New York, NY.
- Rossellomora, R.A., Wagner, M., Amann, R. and Schleifer, K.H. (1995) The Abundance of Zoogloea-Ramigera in Sewage-Treatment Plants. *Applied and Environmental Microbiology* 61(2), 702-707.
- Rozen, S. and Skaletsky, H. (2000) *Primer3 on the Www for General Users and for Biologist Programmers*, Humana Press, Totowa, NJ.
- Saitou, N. and Nei, M. (1987) The Neighbor-Joining Method - a New Method for Reconstructing Phylogenetic Trees. *Molecular Biology and Evolution* 4(4), 406-425.
- Schloss, P.D. and Handelsman, J. (2005) Introducing Dotur, a Computer Program for Defining Operational Taxonomic Units and Estimating Species Richness. *Applied and Environmental Microbiology* 71(3), 1501-1506.
- Schloss, P.D., Larget, B.R. and Handelsman, J. (2004) Integration of Microbial Ecology and Statistics: A Test to Compare Gene Libraries. *Applied and Environmental Microbiology* 70(9), 5485-5492.
- Servais, P., Billen, G., Ventresque, C. and Bablon, G.P. (1991) Microbial Activity in Gac Filters at the Choisy-Le-Roi Treatment Plant. *Journal American Water Works Association* 83(2), 62-68.
- Steinberger, R.E., Allen, A.R., Hansma, H.G. and Holden, P.A. (2002) Elongation Correlates with Nutrient Deprivation in Pseudomonas Aeruginosa-Unsaturated Biofilms. *Microbial Ecology* 43(4), 416-423.
- Steinberger, R.E. and Holden, P.A. (2005) Extracellular DNA in Single- and Multiple-Species Unsaturated Biofilms. *Applied and Environmental Microbiology* 71(9), 5404-5410.
- Suzuki, M.T., Taylor, L.T. and DeLong, E.F. (2000) Quantitative Analysis of Small-Subunit Rna Genes in Mixed Microbial Populations Via 5 '-Nuclease Assays. *Applied and Environmental Microbiology* 66(11), 4605-4614.
- Tamura, K., Dudley, J., Nei, M. and Kumar, S. (2007) Mega4: Molecular Evolutionary Genetics Analysis (Mega) Software Version 4.0. *Molecular Biology and Evolution* 24(8), 1596-1599.
- Thomsen, T.R., Kong, Y. and Nielsen, P.H. (2007) Ecophysiology of Abundant Denitrifying Bacteria in Activated Sludge. *Fems Microbiology Ecology* 60(3), 370-382.

Unz, R.F. (1984) *Bergey's Manual of Systematic Bacteriology*. Krieg, N.R. and Holt, J.G. (eds), pp. 214-219, Williams & Wilkins, Baltimore.

Urbansky, E.T. (2002) Perchlorate as an Environmental Contaminant. *Environmental Science and Pollution Research* 9(3), 187-192.

Urfer, D., Huck, P.M., Booth, S.D.J. and Coffey, B.M. (1997) Biological Filtration for Bom and Particle Removal: A Critical Review. *Journal American Water Works Association* 89(12), 83-98.

US-EPA (2005) State Perchlorate Advisory Levels and Other Resources, [http://www.epa.gov/fedfac/documents/perchlorate\\_links.htm](http://www.epa.gov/fedfac/documents/perchlorate_links.htm).

US-EPA (2008) Drinking Water Contaminant Candidate List 3 US-EPA, <http://www.epa.gov/safewater/ccl/ccl3.html>.

Waller, A., Cox, E. and Edwards, E. (2004) Perchlorate-Reducing Microorganisms Isolated from Contaminated Sites. *Environmental Microbiology* 6(5), 517-527.

Xie, C.H. and Yokota, A. (2006) *Zoogloea Oryzae* Sp Nov., a Nitrogen-Fixing Bacterium Isolated from Rice Paddy Soil, and Reclassification of the Strain Atcc 19623 as *Crabtreeella Saccharophila* Gen. Nov., Sp Nov. *International Journal of Systematic and Evolutionary Microbiology* 56, 619-624.

Xu, J., Song, Y., Min, B., Steinberg, L. and Logan, B. (2003) Microbial Degradation of Perchlorate: Principles and Applications. *Environmental engineering Science* 20(5), 405-422.

Zhang, H., Bruns, M. and Logan, B. (2002) Perchlorate Reduction by a Novel Chemolithoautotrophic, Hydrogen-Oxidizing Bacterium. *Environmental Microbiology* 4(10), 570-576.

Zhang, H., Logan, B.E., Regan, J.M., Achenbach, L.A. and Bruns, M.A. (2005) Molecular Assessment of Inoculated and Indigenous Bacteria in Biofilms from a Pilot-Scale Perchlorate-Reducing Bioreactor. *Microbial Ecology* 49(3), 388-398.

## **Chapter 4**

### **Effects of Phosphorus Addition on Reactor Performance and Microbial Communities of Biologically Active Carbon (BAC) Reactors for Drinking Water Treatment**

#### **4.1. Introduction**

Biological processes have been utilized in drinking water treatment to remove natural organic matter (Charnock and Kjonno, 2000), taste/odor/color-causing compounds (Nerenberg et al., 2000; Rittmann et al., 2002), and several inorganic contaminants (Andersson et al., 2001; Li and Chu, 2003). In some of these processes, pre-ozonation is applied to improve the biodegradability of refractory organic matter (Kim et al., 1997; Nishijima and Speitel, 2004). In other processes, defined as active biological treatment in the current study, electron donors are added to facilitate the removal of contaminants, such as nitrate (Fuchs et al., 1997), perchlorate (Miller and Logan, 2000; Brown et al., 2003), and other oxidized anions (Nerenberg and Rittmann, 2004). Although concerns have been raised regarding the applicability of biological processes for drinking water treatment, such as the possibility of microbial contamination (Camper et al., 1986) and the generation of soluble microbial products (Carlson and Amy, 2000), biological

treatment has been proven effective to remove multiple contaminants from water sources and deserves further investigation.

A key step in evaluating biological drinking water treatment is to characterize the microbial communities involved in the treatment process. Microbial communities in drinking water treatment systems previously have been surveyed using phospholipids fatty acid (Moll et al., 1999), culture-based methods (Moll et al., 1998; Norton and LeChevallier, 2000), and nucleic acid-based methods (Emtiazi et al., 2004; Nerenberg et al., 2008). These studies showed that the microbial community structures varied at different locations in treatment systems and shifted in composition in response to system operation, such as pre-chlorination, pre-ozonation, and temperature. However, few studies are available to elucidate how reactor operation determines the structures of microbial communities that are responsible for contaminant removal in active biological treatment systems for drinking water production.

Phosphorus is an essential element in cell growth and functioning (Madigan et al., 2003), and phosphorus addition to engineered systems can lead to increases in total biomass amount and subsequently benefit reactor performance (Nishijima et al., 1997; Sang et al., 2003). In addition to affecting biomass density, phosphorus addition can also change microbial community structures, by changing the relative abundances of certain populations (Chenier et al., 2006; Allers et al., 2007). On the other hand, phosphorus limitation can decrease the overall diversity of a microbial community by lowering the intensity of horizontal gene transfer (Souza et al., 2008). These studies suggest phosphorus addition is an operational parameter that can affect the microbial populations

responsible for contaminant removal and the overall microbial community structure in active biological drinking water treatment systems.

In the current study, efforts were made to elucidate how phosphorus addition can affect reactor performance and microbial community structure inside biologically active carbon (BAC) reactors operated for drinking water treatment. Two BAC reactors, one bench-scale and one pilot-scale, were operated to remove perchlorate and nitrate from contaminated groundwater. Phosphorus was added to the reactors approximately three months after the start of the reactors. Reactor performance and microbial community structure were monitored and compared both before and after phosphorus addition. Furthermore, the microbial community structure results were used to make implications on how active biological treatment may affect downstream treatment such as disinfection.

## **4.2. Materials and Methods**

### **4.2.1. Reactor Operation**

A bench-scale fixed-bed BAC reactor consisted of a glass column with an inner diameter of 4.9 cm and a height of 26.0 cm (Figure 4.1). The height of the granular activated carbon (GAC) bed (bituminous F816, Galgon Carbon Corp., Pittsburgh, PA) was 10.6 cm resulting in an empty bed volume of 200 mm<sup>3</sup>, and the rest of the height of the glass column was reserved for bed expansion during backwashing. A synthetic groundwater was pumped into the BAC reactor in a down flow mode at a flow rate of 10 mL/min, resulting in an empty bed contact time (EBCT) of 20 min. The synthetic groundwater composition was designed according to the composition determined for a real

groundwater (Rialto, CA, see below) and consisted of deionized water supplemented with 17.75 (12) mg/L Na<sub>2</sub>SO<sub>4</sub>, 6.90 (3) mg/L K<sub>2</sub>CO<sub>3</sub>, 289.18 (210) mg/L NaHCO<sub>3</sub>, 13.68 (8.3) mg/L NaCl, 2.81 (1.8) mg/L CaCl<sub>2</sub>, 3.88 (2.9) mg/L MgCl<sub>2</sub>, 34.27 (25) mg/L NaNO<sub>3</sub>, and 92.34 (75) µg/L NaClO<sub>4</sub> (the values in parentheses refer to the corresponding anion concentrations). The dissolved oxygen (DO) level of the synthetic groundwater remained ~7 mg/L throughout the study. Based on stoichiometric calculations (Rittmann and McCarty, 2001) with an assumed net yield value of 0.4 g COD<sub>biomass</sub>/g COD<sub>acetate</sub>, 13 mg/L of acetic acid as C was needed to completely remove all three electron acceptors (i.e., DO, NO<sub>3</sub><sup>-</sup>, and ClO<sub>4</sub><sup>-</sup>). With a safety factor of 1.5 applied, concentrated acetic acid was added to the reactor using a syringe pump and resulted in a final concentration of 20 mg/L as C in the influent. The pH values of influent and effluent varied between 7.5 and 7.9. On day 115, phosphoric acid was added to the synthetic groundwater with a final concentration of 145 µg/L as P. In order to remove excess biomass, the bench-scale BAC reactor was backwashed every 48 hours with a mixture of water (i.e., 50 mL/min) and air for 4 min followed by high flow-rate water flush (i.e., 500 mL/min) for 3 min. The BAC system was operated in a temperature control room set at 18°C. These operating conditions are designated as the baseline operating condition for the bench-scale BAC reactor.

A pilot-scale fixed-bed BAC reactor was constructed and operated by Carollo Engineers in Rialto, California (Figure 4.1 and Supplemental Figure 4.1). The pilot-scale BAC reactor was made of epoxy-coated steel with an inner diameter of 61.0 cm and a height of 228.6 cm, and contained the same type of GAC as the bench-scale BAC system. The height of the GAC bed was 143.3 cm and the rest of the reactor volume was reserved



for bed expansion during backwash. The raw groundwater feed was of the same concentrations of anions as those of the bench-scale BAC system, except the perchlorate concentration was 50 µg/L. The groundwater was pumped to the reactor at a flow rate of 41.6 L/min which resulted in an EBCT of 10 min. Acetic acid addition was determined according to the method described above, except that a safety factor of 1.13 was applied. On day 97, phosphoric acid was added to the groundwater with a final concentration of ~150 µg/L as P. The reactor was backwashed every 17-24 hours by following the procedure: fluidization (with surface wash) at 4.8 gpm/ft<sup>2</sup> for 69 s, 12.7 gpm/ft<sup>2</sup> for 180 s, 3.2 gpm/ft<sup>2</sup> for 120 s, 6.7 gpm/ft<sup>2</sup> for 480 s, and 1.3 gpm/ft<sup>2</sup> for 30 s, and during the fluidization step 2-3.2 standard cubic feet per minute per square feet air scour was pulsed for a total of 24 s.

#### **4.2.2. Chemical Measurements**

For the bench-scale system, influent and effluent DO concentrations were measured using WTW multi340 meters with Cellox325 sensors in WTW D201 flow cells (Weilheim, Germany) connected to the inlet and outlet of the reactor. For the pilot-scale system, DO concentrations were measured on site using HACH sc100 LDO probe (Loveland, CO). Water samples from the pilot-scale reactor were sent regularly to the University of Michigan using overnight service and stored according to Standard Methods (American Public Health Association (APHA), 1992) until measurement. For all chemical parameters, water samples from the bench- and pilot-scale BAC reactors were filtered through 0.45-µm filters, and concentrations were determined according to the following methods. Concentrations of acetic acid, nitrate, and nitrite were measured on an ion

chromatograph system with a conductivity detector (Dionex DX100, Sunnyvale, CA) according to Standard Methods (American Public Health Association (APHA), 1992). An AS-14 analytical column and an AG-14 guard column were used, and the eluent contained 1.0 mM bicarbonate and 3.5 mM carbonate. Perchlorate concentrations were measured using another ion chromatography system (Agilent Chemstation, Santa Clara, CA) according to the EPA Standard Method 314.1 (Hautman et al., 1999). A Dionex AS-16 analytical column and an AG-16 guard column were used, and the eluent was 65 mM NaOH. The detection limits for DO, nitrate, acetic acid, and perchlorate were determined to be 0.01 mg/L, 0.2 mg/L, 0.2 mg/L, and 2 µg/L. Effluent nitrite concentrations were always below the detection limits of 0.2 mg/L. Phosphorus concentrations were measured using induced coupled plasma and mass spectrometry (ICP-MS, PerkinElmer ALEN DRC-e, Waltham, MA) with a detection limit of 5 µg/L.

#### **4.2.3. Clone Library**

Biomass samples from the pilot-scale BAC reactor were collected from a vertical core of the BAC bed using a 1-inch PVC pipe, and shipped overnight on dry ice to the University of Michigan. Biomass samples from both the bench- and the pilot-scale BAC reactors were stored at -80°C until analyses. Four BAC samples were collected for clone library analyses, two from the bench-scale BAC reactor (Day 100 and 244) and two from the pilot-scale BAC reactor (Day 84 and Day 210). DNA was extracted from the BAC samples using FastDNA SPIN Kit (Qbiogene Inc., Irvine, CA) and quantified using a NanoDrop ND1000 (NanoDrop Technology, Wilmington, DE). DNA quality was evaluated by electrophoresis on a 0.8% agarose gel. 16S rRNA genes were amplified in

triplicate using the polymerase chain reaction (PCR) on a Mastercycler thermocycler (Eppendorf International, Hamburg, Germany) with the forward primer 8F (5'-AGA GTT TGA TCC TGG CTC AG-3') (Dojka et al., 1998) and the reverse primer 1387R (5'-GGG CGG [A/T]GT GTA CAA GGC-3') (Wobus et al., 2003). The composition of the PCR reaction mixture was adopted from the work by Wobus and coworkers (Wobus et al., 2003). The PCR reaction involved 30 cycles and started with 5 min of denaturation at 95°C and ended with a final extension at 72°C for 18 min. Each cycle consisted of denaturation at 95°C for 30 s, annealing at 50°C for 45 s, and extension at 72°C for 2 min. Pooled PCR products were purified by electrophoresis on a 1% agarose gel and extracted using the MinElute Gel Extraction Kit (QIAGEN Inc., Valencia, CA). Purified PCR products were cloned into TOPO vector (Invitrogen Inc., Carlsbad, CA) and transformed into chemically competent *Escherichia coli*. The transformed *E. coli* cells were plated on Luria-Bertani agar that contained 50 µg/mL kanamycin and incubated at 37°C overnight. Colonies were picked randomly and used to inoculate three 96-well microplates. Two of the three 96-well microplates were sent to the Genomic Center at Washington University (St. Louis, MO) in glycerol stocks for sequencing.

#### **4.2.4. Microbial Sequence Analyses**

A total of 768 clones (eight 96-well microplates, two for each library) were sequenced bidirectionally using vector primers T3 and T7 (Invitrogen Inc., Carlsbad, CA). Nucleotide sequences were analyzed and edited using BioEdit (Hall, 1999). Alignment of closely related sequences identified via the Ribosomal Database Project (RDP) (Cole et al., 2007) was conducted using ClustalW (Chenna et al., 2003) for bacterial 16S rRNA

genes. The phylogenetic tree was constructed according to a ca. 600-bp region of the 16S rRNA gene, starting at the 8F primer region, to illustrate the phylogenetic relationship of the *Dechloromonas*- and *Azospira*-like clones with other perchlorate reducing bacteria (PRB). The phylogenetic tree was created based on the evolutionary history inferred using a neighbor-joining method (Saitou and Nei, 1987) and the evolutionary distance computed using the Jukes-Cantor methods (Jukes and Cantor, 1969) incorporated in the software program MEGA (Tamura et al., 2007). The robustness of the tree topologies was tested by bootstrap test (1,000 replicates) (Felsenstein, 1985). All positions containing gaps and missing data were eliminated from the dataset (Complete deletion option). There were a total of 524 positions in the final dataset for the phylogenetic tree. Clones were considered to be part of an operational taxonomic unit (OTU) if they shared  $\geq 95\%$  identity to 16S rRNA genes (Fields et al., 2005). OTUs, diversity statistics, and rarefaction curves were calculated using DOTUR (Schloss and Handelsman, 2005). The similarities of the bacterial 16S rRNA gene clone libraries were evaluated using  $\beta$ -LIBSHUFF (Schloss et al., 2004).

#### **4.2.5. Real-Time PCR**

Real-time PCR primer sets were designed based on the representative sequences from the clones of interests using the Primer3 program made available by Integrated DNA Technologies ([www.idtdna.com](http://www.idtdna.com)) (Rozen and Skaletsky, 2000) and were synthesized by Invitrogen (Carlsbad, CA). The specificities of the designed primer sets were evaluated using the Probe Match function of RDP (Cole et al., 2007), while the coverage of the designed primer sets was evaluated against the clones of interests in relevant clone

libraries (Supplemental Table 4.1). The specificities of the primer sets were further characterized with various ranges of annealing temperatures using the gradient function of a real-time PCR Mastercycler *realplex* thermocycler (Eppendorf International, Hamburg, Germany). Target and non-target templates were plasmid DNA extracted from relevant clones using QIAprep Miniprep Kit (QIAGEN Inc., Valencia, CA). The target templates contained the representative sequences based on which the primer sets were designed, while the non-target templates contained sequences with the least number of mismatches with the designed primer sets in the relevant clone libraries. The chosen annealing temperatures for the two designed primer sets (Table 4.1) could differentiate the fluorescence signals between equal amounts of target and non-target templates (i.e.,  $10^6$  copies per  $\mu\text{L}$ ) by at least 15  $C_{\text{threshold}}$  units (Supplemental Figure 4.2).

Real-time PCR experiments were performed on the Mastercycler *realplex* thermocycler using RealMasterMix SYBR Green Kit (Eppendorf International, Hamburg, Germany), which has a self-adjusting chelating mechanism for controlling the  $\text{Mg}^{2+}$  concentration. The reaction mixtures in 25  $\mu\text{L}$  final volume contained 11.25  $\mu\text{L}$  of 2.5X RealMasterMix SYBR Green solution (including 0.05 U/ $\mu\text{L}$  HotMaster *Taq* DNA Polymerase, 10 mM magnesium acetate, 1.0 mM dNTPs, and 2.5X SYBR Green solution), 150 nM of forward and reverse primers, Sigma water (Sigma-Aldrich, St. Louis, MO), and templates of known concentrations or 10 ng of DNA template from environmental samples.

As suggested in the manual of the RealMasterMix SYBR Green kit, amplification involved one cycle of 95°C for 10 min for initial denaturation and then 40 cycles of 95°C for 15 s followed by annealing at the temperature shown in Table 4.1 for 20 s and

extension at 68°C for 30 s. SYBR Green fluorescence was detected during the extension step of each cycle. Melting profiles were collected after the 40 cycles of amplification to check the specificity of the amplification (Supplemental Figure 4.2). Dilutions of purified *E. coli* plasmid DNA containing the 16S rRNA genes of *Dechloromonas* and *Azospira* were used to construct standard curves for real-time PCR in the quantification of specific populations and bacterial domain (Supplemental Figure 4.3).

### **4.3. Results**

#### **4.3.1. Bench- and Pilot-scale BAC Reactor Performance**

Prior to Day 115, acetic acid was the only chemical added to the synthetic groundwater fed to the bench-scale BAC reactor (Figure 4.1). ICP-MS measurement on the synthetic groundwater showed that the phosphorus concentration in the influent to the reactor was between 5 to 10 µg/L as P. During this period, the reactor was able to nearly completely remove DO, and remove 17 mg/L of nitrate (68% removal) and 25 µg/L of perchlorate (33% removal) (Figure 4.2 A). After the phosphorus addition on Day 115 (145 µg/L phosphoric acid as P), the effluent dissolved oxygen (DO) immediately dropped below the detection limit, and effluent nitrate and perchlorate started to decrease nearly simultaneously and dropped below the detection limits within 5 and 15 days, respectively.

Similarly, before Day 97 in the operation of the pilot-scale BAC reactor, acetic acid was the only chemical added to the contaminated groundwater. During this period, the phosphorus concentration in the groundwater ranged between 30 and 60 µg/L as P. The reactor was able to completely remove DO (data not shown), nearly completely

remove nitrate, and remove about 38 µg/L perchlorate (75% removal) (Figure 4.2, B). Because of the experience with the bench-scale BAC reactor, phosphorus was added to the pilot-scale BAC reactor beginning on Day 97 (150 µg/L phosphoric acid as P). The effluent nitrate concentration immediately dropped below the detection limit, and the effluent perchlorate concentrations fell below the detection limit within about 16 days.

#### **4.3.2. Microbial Communities in the Bench- and Pilot-scale BAC Reactors**

*Betaproteobacteria* was the dominant bacterial phylum in the bench-scale BAC reactor both before (Day 100, 70.3%) and after (Day 244, 91.7%) the phosphorus addition on Day 115 (Table 4.2 and Figure 4.3). In contrast, significant shifts in microbial community structure occurred at the genus level after the phosphorus addition. The clone library results in Table 4.2 showed that, after phosphorus addition, the relative abundance of clones closely related to *Dechloromonas* and *Azospira* increased from 15.2 and 0.6% to 54.2 and 11.7%, respectively. Because most members of these two genera can use oxygen, nitrate, and perchlorate as electron acceptors (Coates and Achenbach, 2004), it is believed that phosphorus addition enhanced nitrate and perchlorate removal (Figure 4.2 A) by promoting and maintaining high levels of *Dechloromonas* and *Azospira*. Clones closely related to the genus *Zoogloea* made up 7.3 and 7.5% of the total bacterial clones before and after phosphorus addition. The changes in *Dechloromonas* and *Azospira* were considered significant ( $p < 0.01$ ), whereas the change in *Zoogloea* was not significant ( $p = 0.54$ ).

*Betaproteobacteria* was also the dominant phylum in the pilot-scale BAC reactor (Table 4.2 and Figure 4.3). Eight bacterial phyla were detected before phosphorus

addition, while only four remained after phosphorus addition, indicating a decrease in microbial richness at the phylum level (Table 4.2). The clone library results showed that *Dechloromonas* strains were the only known PRB in the pilot-scale BAC reactor, and the relative abundance of the clones closely related to *Dechloromonas* decreased from 7.1% to 0.6% after phosphorus addition. Different from the bench-scale BAC reactor, the pilot-scale BAC reactor did not contain any *Azospira*-like clones. Opposite to the trend for the *Dechloromonas* clones, the relative abundance of the clones closely related to *Zoogloea* increased from 17.9% to 52.0% after phosphorus addition. Both changes were statistically significant ( $p < 0.01$ ).

The phlotypes of the *Dechloromonas* clones were different in the two BAC reactors. All the *Dechloromonas* clones detected in the bench-scale BAC reactor (i.e., both before and after phosphorus addition) belonged to the CKB type (Figure 4.4) (Coates and Achenbach, 2004). In contrast, the *Dechloromonas* clones in the pilot-scale BAC reactor belonged to both CKB and RCB type (Figure 4.4).

### **4.3.3. Comparison of Microbial Community Structures**

Genus level analyses revealed the effects of phosphorus addition on bacterial community structures in the two BAC reactors. In Figure 4.5, the Chao 1 and ACE indices for the bench-scale BAC reactor dropped from 209 and 161 to 82 and 95, respectively, suggesting decreases in microbial richness after phosphorus addition. The Shannon-Weiner and Inverse Simpson's indices decreased from 3.77 and 38 to 2.93 and 12, indicating the microbial diversities had decreased after phosphorus addition. Similar trends were observed for the pilot-scale BAC reactor, although less profound. The



rarefaction curves in Figure 4.5 showed that, for the levels of sampling effort used, the microbial richness was similar in the bench- and the pilot-scale BAC reactors before phosphorus addition, and the microbial richness had decreased in both reactors after phosphorus addition. Note that none of the four rarefaction curves leveled off completely, suggesting that further sequencing would have resulted in more OTUs. In addition, changes in microbial composition after phosphorus addition were observed for both reactors in Table 4.2, and this observation was statistically confirmed by the results using  $\beta$ -LIBSHUFF. In Table 4.3, all the comparisons had  $p$  values less than 0.05, indicating that phosphorus addition caused significant microbial community shifts in both reactors.

#### **4.3.4. Microbial Population Dynamics in the Bench-scale BAC**

Real-time PCR measurements showed that the relative abundance of *Dechloromonas* spp. in the bench-scale BAC reactor started to increase immediately after the phosphorus addition and continued to increase for about 20 days (11.3% on Day 0 and 150.3% at Day 20, Figure 4.6 A). The relative abundance of *Azospira* spp. also started to increase immediately after phosphorus addition and followed an increasing trend during the course of the experiment (<0.1% on Day 0 and 1.2% on Day 20, Figure 4.6 B). On two occasions, Day 10 and 16, the relative abundances of *Azospira* were higher than the predominant trend.

The total amount biomass in the bench-scale BAC reactor increased after phosphorus addition. With the assumption of a net yield of 0.4 g COD<sub>biomass</sub> / g COD<sub>acetate</sub> (Choi et al., 2007), the total biomass yield inside the reactor during one backwash cycle (i.e., 48 h) was estimated to be 153.4 mg before phosphorus addition

(average from Day 72 to 115) and 311.3 mg after phosphorus addition (average from Day 130 to 156).

#### 4.4. Discussion

The PRB that have been isolated so far are phylogenetically diverse and include species within the *Alpha-*, *Beta-*, and *Epsilonproteobacteria* (Coates and Achenbach, 2004). In this study, two genera within the phylum of *Betaproteobacteria*, *Dechloromonas* and *Azospira*, were detected in the bench-scale BAC reactor, while *Dechloromonas* strains were the only known PRB observed in the pilot-scale BAC reactor. The dominance of these two genera in bioreactors fed acetic acid has also been reported in a previous study, in which approximately 23% and <1% of the bacterial domain belonged to the genera *Dechloromonas* and *Azospira*, respectively (Zhang et al., 2005).

After phosphorus addition, while the perchlorate removal efficiency of the pilot-scale BAC reactor increased from 33% to 100%, the relative abundance of *Dechloromonas*, the only known PRB in the system, decreased from 7.1 to 0.6%. One explanation for this unanticipated result is that the pilot-scale BAC reactor did not need a large population of PRB in its microbial community, given the fraction of perchlorate as part of the total concentration of electron acceptors was low (75  $\mu\text{g/L}$  perchlorate vs. 7 mg/L DO and 25 mg/L nitrate). If so, other bacterial populations in the microbial community would have been responsible for removing oxygen and nitrate, while *Dechloromonas* spp., even at a very low abundance, completely removed perchlorate. The genus *Zoogloea* was the most abundant population (52.0%) in the pilot-scale BAC

reactor after phosphorus addition. The genus *Zoogloea* has been found to be able to utilize oxygen and nitrate as electron acceptors (Xie and Yokota, 2006). Therefore, the increase in *Zoogloea* abundance may have contributed to the improvement of perchlorate removal by removing competing electron acceptors in the pilot-scale BAC reactor.

The difference in influent microbial composition between bench- and pilot-scale BAC reactors possibly was responsible for the different responses of the two reactors to phosphorus addition. The bench-scale BAC reactor was fed synthetic groundwater made of deionized water, while the pilot-scale BAC reactor was fed real California groundwater. The synthetic groundwater likely contained a lower level of bacterial diversity than the real groundwater. Therefore, when fed the synthetic groundwater, the functionally versatile bacterial genera *Dechloromonas* and *Azospira*, both of which can utilize all three electron acceptors, thrived in the bench-scale BAC reactor. In comparison, with the continuous influent of the real groundwater, which likely contained the genus *Zoogloea* (Hendrickx et al., 2005; Takahata et al., 2006), the constantly replenished *Zoogloea* population inside the pilot-scale BAC reactor outcompeted other bacterial populations and became the most dominant species after phosphorus addition.

Although the ability of *Zoogloea* to reduce perchlorate has not been demonstrated, the possibility of this genus being capable of doing so cannot be ruled out. A recent environmental genomic study reveals that functional chlorite dismutase, a key enzyme in the microbial pathway of perchlorate reduction, exists in a nitrite-oxidizing bacterial species (Maixner et al., 2008). Up to date, *Zoogloea* genomes have not been sequenced, so it is not possible to check whether genes related to (per)chlorate reductase and chlorite dismutase are present in the species of this genus. If the *Zoogloea* spp. can utilize

perchlorate as an electron acceptor, then the elevated relative abundance of *Zoogloea* spp. could account for the improved perchlorate removal in the pilot-scale reactor, through a mechanism similar to the increases in *Dechloromonas* and *Azospira* spp. in the bench-scale BAC reactor after phosphorus addition. Furthermore, the trends in the change of the total PRB populations, including all three genera (i.e., *Dechloromonas*, *Azospira*, and *Zoogloea*), would be similar for the two reactors.

The results obtained with real-time PCR experiments did not quantitatively agree with those from clone library experiments, although the same qualitative trend was observed with both methods. It is not uncommon to have discrepancy between quantitative results obtained with two very different molecular methods (Segawa et al., 2005). The relative abundance higher than unit observed for the bench-scale reactor on Day 20 was likely due to the coverage of the bacterial primer (Supplemental Table 4.1).

Similar to what was reported for a natural system (Cebren et al., 2007), a decrease in microbial diversity in response to nutrient addition (i.e., phosphorus) was observed in the two BAC reactors. This observation may be relevant when evaluating the quality of finished drinking water produced by these systems. The microbial community structures inside the BAC reactors determine the microbial community structure in the reactor effluents. Low microbial diversities in reactor effluents may benefit the downstream disinfection step, because lower microbial diversity is likely associated with lower probability of the presence of strains resistant to disinfection. After phosphorus addition, the relative abundance of *Betaproteobacteria* further increased, consistent with findings in another study (Salcher et al., 2007); *Gammaproteobacteria*, a phylum that contains many pathogenic bacteria (Mrazek et al., 2006), almost completely disappeared. In

addition, gram-positive bacteria (i.e., *Firmicutes*) were not detected in the bench-scale system and were found only at very low levels in the pilot-scale system. Because gram-positive bacteria are usually more resistant to disinfectants than gram-negative bacteria (Lechevallier et al., 1980), the low abundance of gram-positive bacteria suggested that efficient disinfection of BAC reactor effluent is possible.

Many drinking water treatment plants allow their GAC filters to be biologically active by utilizing limited electron donors indigenous to source waters. These biologically active GAC beds are considered nutrient-poor environments in terms of carbon and phosphorus, two controlling factors for many biological systems. Although such environments can limit the quantity of biomass accumulated and therefore may result in lower bacterial abundance in reactor effluents, they may select for a higher microbial diversity, increasing the chance for resistant bacteria to survive disinfection and thrive in distribution systems. Pang and Liu compared the bacteria that developed in meso- and low-substrate environments, and found the latter selected for microorganisms that are more adapted to survive in similar environments (e.g., distribution systems) (Pang and Liu, 2006). The results and discussion presented in this work suggested that properly controlled addition of electron donor and nutrients to bioreactors can promote beneficial microbial activities (i.e., contaminant removal) and result in low-diversity microbial communities that may allow more efficient downstream treatment (i.e., disinfection).

## 4.5. Tables

Table 4.1. Sequences and annealing temperatures of the real-time PCR primer sets used in this study.

Target	Primer	Name <sup>1,2</sup>	Sequence (5' to 3')	Annealing temp. (°C)	Source
<i>Dechloromonas</i>	Forward	S-G-Dchm-0146-a-S-24	TAT-CGG-AAC-GTA-CCT-TTC-AGT-GGG	67.0	This study
	Reverse	S-G-Dchm-0248-a-A-24	GCT-AAT-CTG-ATA-TCG-GCC-GCT-CAA		This study
<i>Azospira</i>	Forward	S-G-Azsp-1009-a-S-24	TAC-CCT-TGA-CAT-GCC-AGG-AAC-TTT	68.0	This study
	Reverse	S-G-Azsp-1163-a-A-24	CGG-CAG-TCT-CAT-TAA-AGT-GCC-CAA		This study
<i>Bacteria</i>	Forward	S-D-Bact-1369-a-S-18	CGG-TGA-ATA-CGT-TCY-CGG	56.0	(Suzuki et al., 2000)
	Reverse	S-D-Bact-1492-a-A-19	GGW-TAC-CTT-GTT-ACG-ACT-T		(Suzuki et al., 2000)

<sup>1</sup> The primers were named according to standardized nomenclature by Alm and coworkers (Alm et al., 1996).

<sup>2</sup> The target locations of the primers in the 16S rRNA gene were determined based on *Escherichia coli* numbering (Brosius et al., 1981).

Table 4.2. Phylogenetic affiliation of the clones in the four clone libraries (%).

	Bench-scale BAC Reactor		Pilot-scale BAC Reactor	
	Before P Addition (Day 100)	After P Addition (Day 244)	Before P Addition (Day 84)	After P Addition (Day 210)
<i>Alphaproteobacteria</i>	6.7	3.3	14.1	-
<i>Betaproteobacteria</i>	70.3	91.7	70.5	96.0
<i>Dechloromonas</i>	15.2	54.2	7.1	0.6
<i>Azospira</i>	0.6	11.7		
<i>Zoogloea</i>	7.3	7.5	17.9	52.0
<i>Propionivibrio</i>				1.1
<i>Ferribacterium</i>	2.4	5.0	7.1	2.8
Unclassified <i>Rhodocyclaceae</i>	26.1	10.0	3.2	0.6
Unclassified <i>Oxalobacteraceae</i>	6.1			
<i>Acidovorax</i>	7.9			
<i>Hydrogenophaga</i>	1.2		0.6	2.3
<i>Simplicispira</i>				0.6
<i>Curvibacter</i>		1.7		
Unclassified <i>Comamonadaceae</i>	1.2		5.1	25.4
<i>Aquabacterium</i>			9.6	
<i>Pelomonas</i>		0.8		
<i>Ideonella</i>			1.9	
Unclassified Incertae sedis 5			15.4	2.3
Unclassified <i>Burkholderiales</i>	1.2		1.3	3.4
Unclassified <i>Betaproteobacteria</i>	1.2	0.8	1.3	5.1
<i>Deltaproteobacteria</i>	12.7	1.7	3.2	
<i>Gammaaproteobacteria</i>	9.1		1.3	0.6
Unclassified <i>Proteobacteria</i>			3.2	0.6
<i>Acidobacteria</i>		0.8	1.3	
<i>Bacteroidetes</i>			1.9	1.1
<i>Chloroflexi</i>			0.6	
<i>Firmicutes</i>			1.3	0.6
<i>Spirochaetes</i>	0.6			
Unclassified <i>Bacteria</i>	0.6 <sup>1</sup>	2.5 <sup>2</sup>	2.6 <sup>3</sup>	1.1
Total Clones	165	120	156	177

<sup>1</sup>: included one clone that was classified as “unrooted”.

<sup>2</sup>: included two clones that were classified as “unrooted”.

<sup>3</sup>: included one clone that was classified as “unrooted”.

Table 4.3. Values of  $p$  estimating the similarity between the two bacterial clone libraries using  $\int$ -LIBSHUFF.

<b>Bacterial clone library (X)</b>	<b><math>p</math> value comparison of clone library (Y) with X<sup>1</sup></b>			
	<b>Bench Pre-P</b>	<b>Bench Post-P</b>	<b>Pilot Pre-P</b>	<b>Pilot Post-P</b>
Bench-scale BAC Pre-P		0.0000	0.0000	0.0000
Bench-scale BAC Post-P	0.0073		0.0000	0.0000
Pilot-scale BAC Pre-P	0.0000	0.0000		0.0000
Pilot-scale BAC Post-P	0.0000	0.0000	0.0105	

<sup>1</sup> $p$  values compare either X to Y or Y to X, and indicate the clone libraries were sampled from significantly different communities ( $p < 0.05$ ).



Supplemental Table 4.1. Sequence, coverage, specificity, and annealing temperature for each primer set used in this study.

Target (16S rRNA gene)	F/R	Systematic Name <sup>1,2</sup>	Abbreviated Name	Coverage in the clone library for bench-scale BAC Day 100 <sup>3</sup>	Coverage in the clone library for bench-scale BAC Day 244 <sup>3</sup>	Specificity <sup>4</sup>
<i>Dechloromonas</i>	F	S-G-Dchm-0146-a-S-24	Dchm0146F	24/25	67/67	184/351
	R	S-G-Dchm-0248-a-A-24	Dchm0248R	25/25	66/67	227/426
<i>Azospira</i>	F	S-G-Azsp-1009-a-S-24	Azsp1009F	1/1	10/13	45/185
	R	S-G-Azsp-1163-a-A-24	Azsp1163R	1/1	10/13	45/1046
<i>Bacteria</i>	F	S-D-Bact-1369-a-S-18	Bact1369F	138/163	101/129	-- <sup>6</sup>
	R	S-D-Bact-1492-a-A-19	Bact1492R	N/A <sup>5</sup>	N/A <sup>5</sup>	-- <sup>6</sup>

<sup>1</sup> The primers were named according to standardized nomenclature by Alm and co-workers (Alm et al., 1996).

<sup>2</sup> The location of the primers were determined based on *Escherichia coli* numbering (Brosius et al., 1981).

<sup>3</sup> Coverage = “Target Hit” / “Total Target”. “Total Targets” are the total numbers of target clones in corresponding clone libraries. The denominator for the *Azospira* primer set (i.e., 13) is different from the number calculated from Table 4.2 (i.e., 14), because Table 4.2 was based on the early half of the 16S rRNA gene sequence, whereas the *Azospira* primer set is targeting the late half of the 16S rRNA gene sequence. The denominator for the *Dechloromonas* primer set (i.e., 67) is slightly different from the number calculated from Table 4.2 (i.e., 65).

<sup>4</sup> Specificity = “Target Hit” / “Total Hit”. “Total Hits” are the number of hits obtained from the Probe Match function on RDP (Cole et al., 2007) in August 2008.

<sup>5</sup> Not available. The PCR primers used to construct the clone libraries were 8F and 1387R, which does not cover the region around 1492. Therefore, the coverage of the 1492R primer in the clone libraries is not available.

<sup>6</sup> For the bacterial primer set, specificity is not measured.

## 4.6. Figures

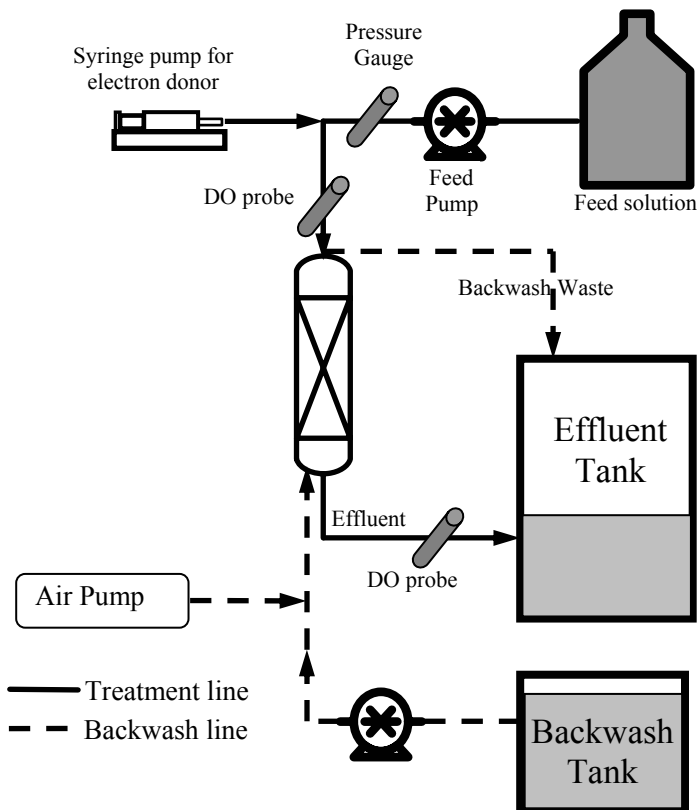


Figure 4.1. Schematics of both the bench- and the pilot-scale biological drinking water treatment systems.

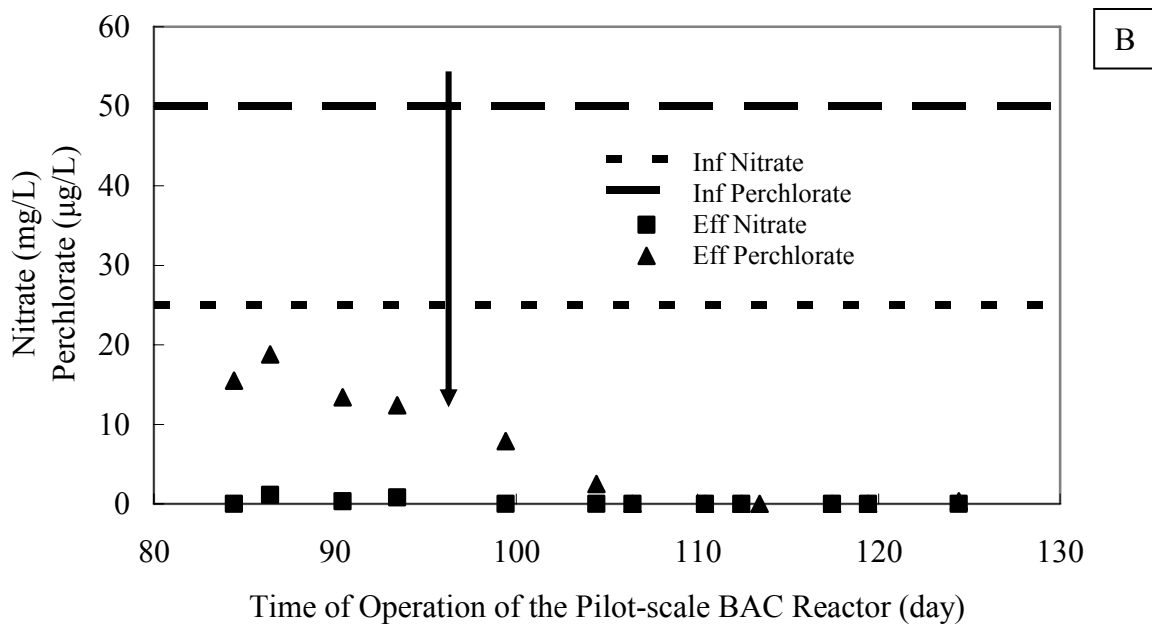
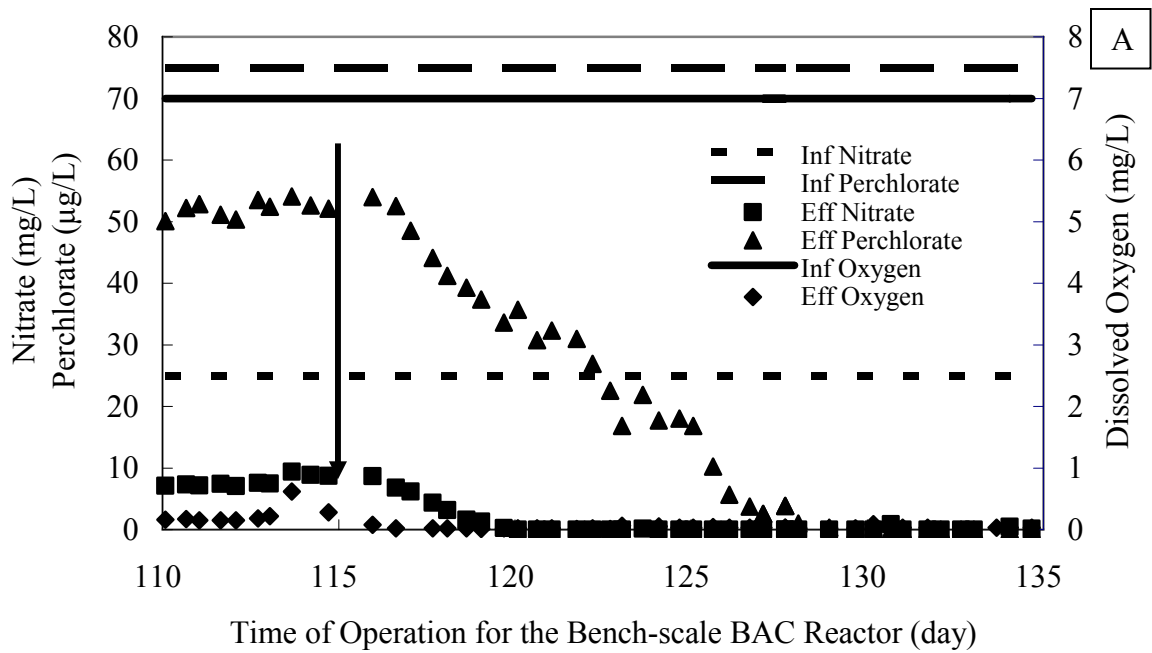


Figure 4.2. Reactor performance of the bench-scale BAC reactor (A) and the pilot-scale BAC reactor (B).

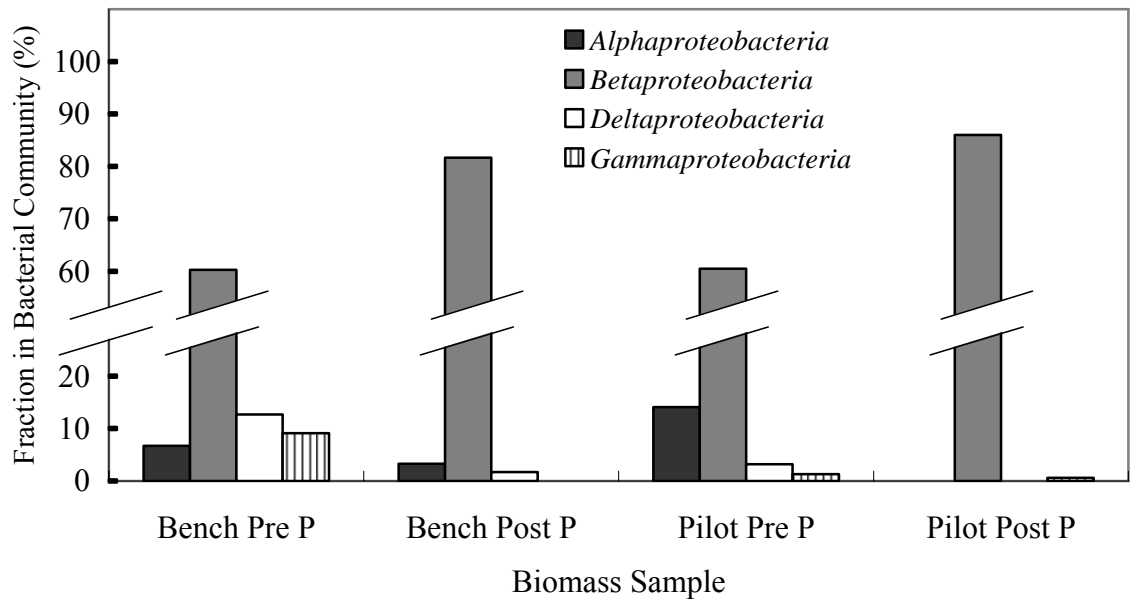


Figure 4.3. Fractions of the four subclasses of the *Proteobacteria* in the bench- and pilot-scale BAC reactors before and after phosphorus addition.

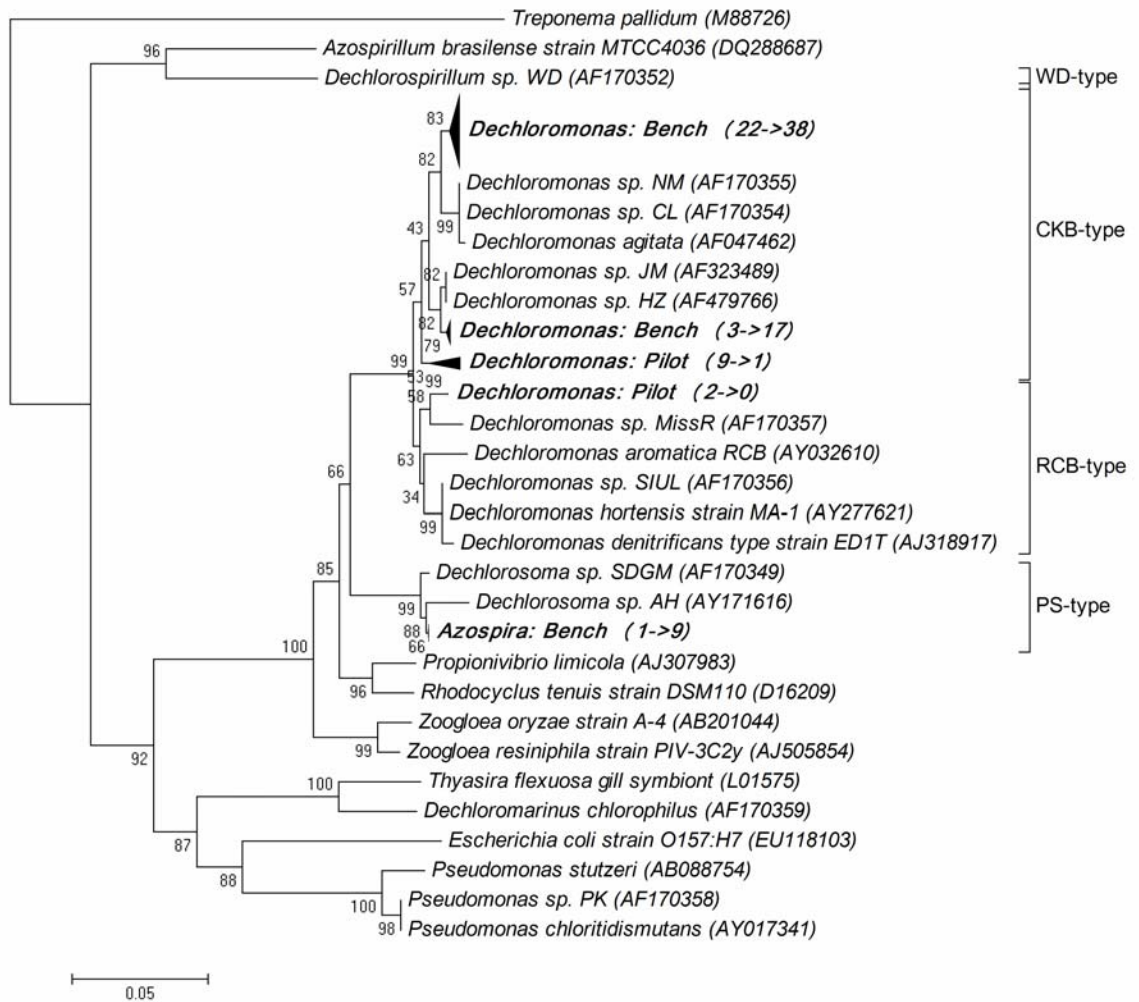
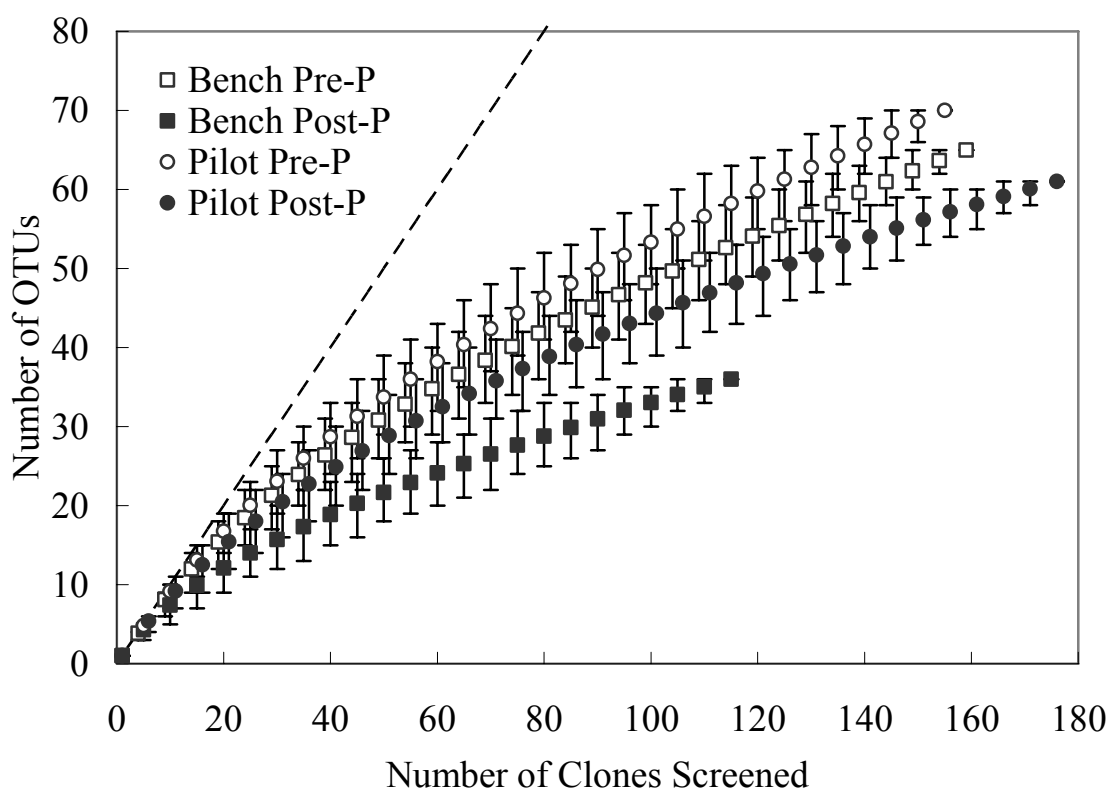


Figure 4.4. Phylogenetic tree of perchlorate reducing bacteria in the two systems before and after phosphorus addition. The two numbers in each parenthesis represent the numbers of the clones before and after phosphorus addition.



Reactor	Sampling time	No. of seq.	No. of OTUs <sup>a</sup>	Chao1 <sup>b</sup>	ACE <sup>b</sup>	Shannon-Weiner Index	Inverse Simpson's index
Bench-scale	Pre-P	159	65	209 (122, 423)	161 (113, 259)	3.77	38
	Post-P	115	36	82 (51, 175)	95 (59, 186)	2.93	12
Pilot-scale	Pre-P	155	70	152 (106, 256)	161 (117, 245)	3.90	47
	Post-P	176	61	105 (79, 167)	120 (90, 183)	3.59	25

<sup>a</sup>. OTUs defined as 5% difference in 16S rRNA gene sequences.

<sup>b</sup>. Mean values with upper and lower 95% confidence intervals given in parentheses.

Figure 4.5. Rarefaction curves indicating bacterial 16S rRNA richness within clone libraries from the bench- and the pilot-scale BAC reactors before and after phosphorus addition. The dashed line represents 1:1, indicating infinite diversity. The table lists the bacterial 16S rRNA sequence diversity indices. OTUs were defined as groups of sequences sharing 95% 16S rRNA sequence identity. The estimates of phylotype richness were calculated according to the abundance-based coverage estimate (ACE) and the bias-corrected Chao1 estimator. The Shannon-Weiner diversity index and the Inverse Simpson's diversity index, which take into account species richness and evenness, were also calculated.

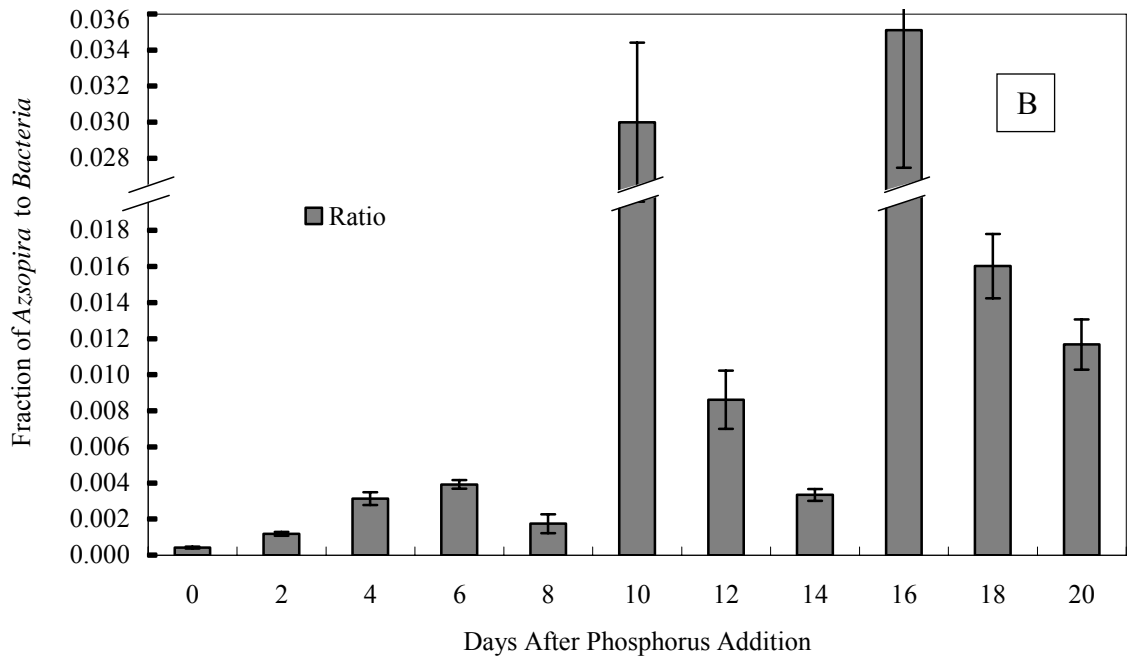
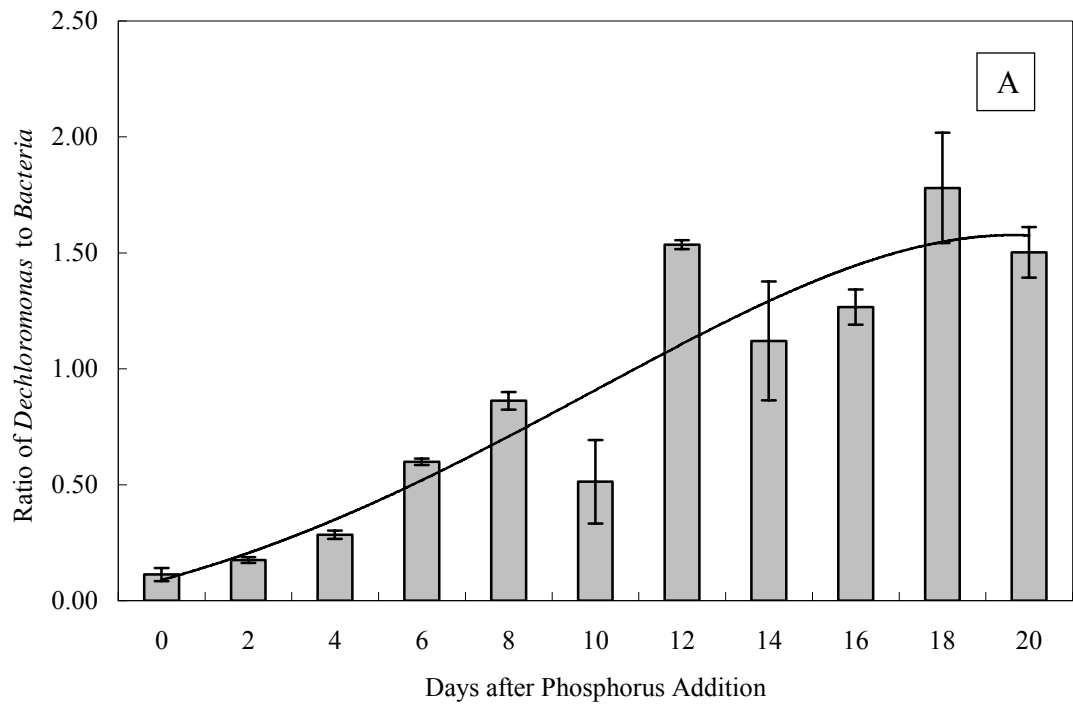
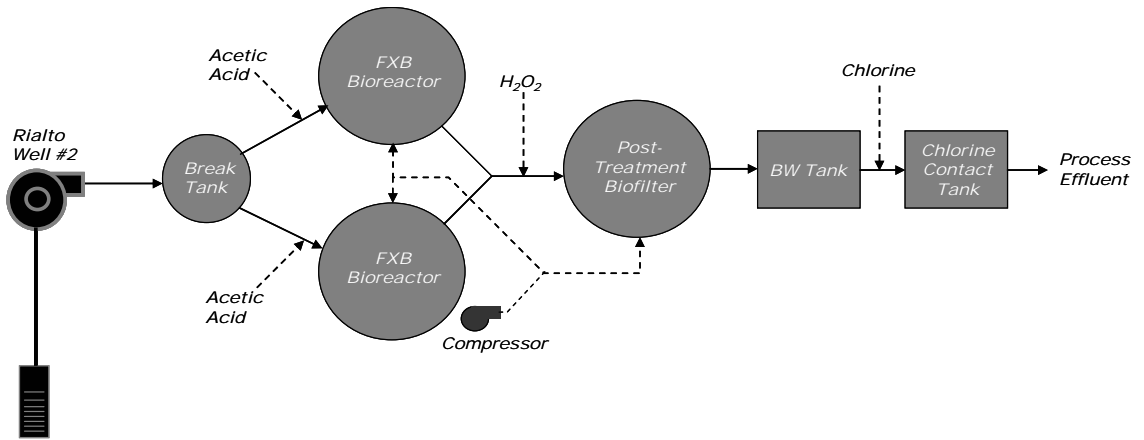
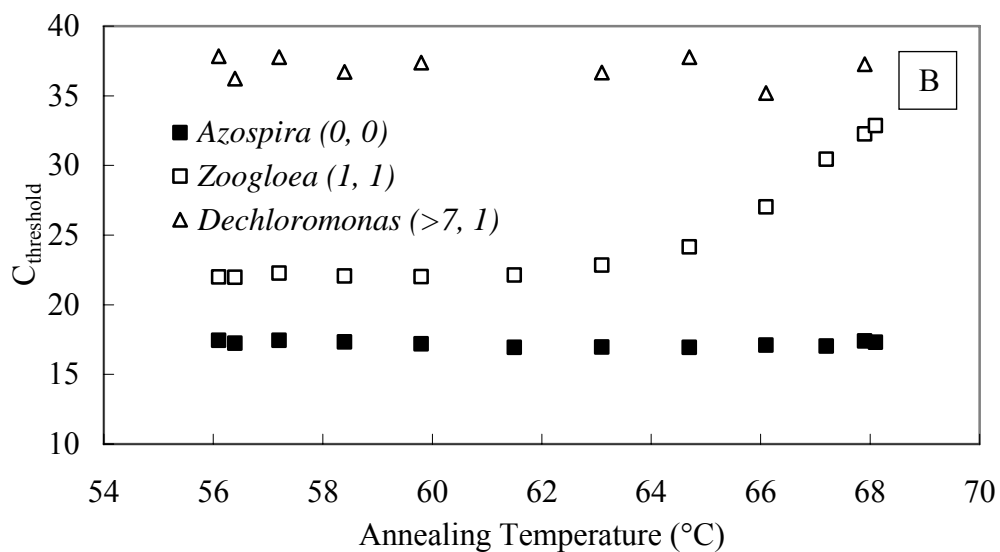
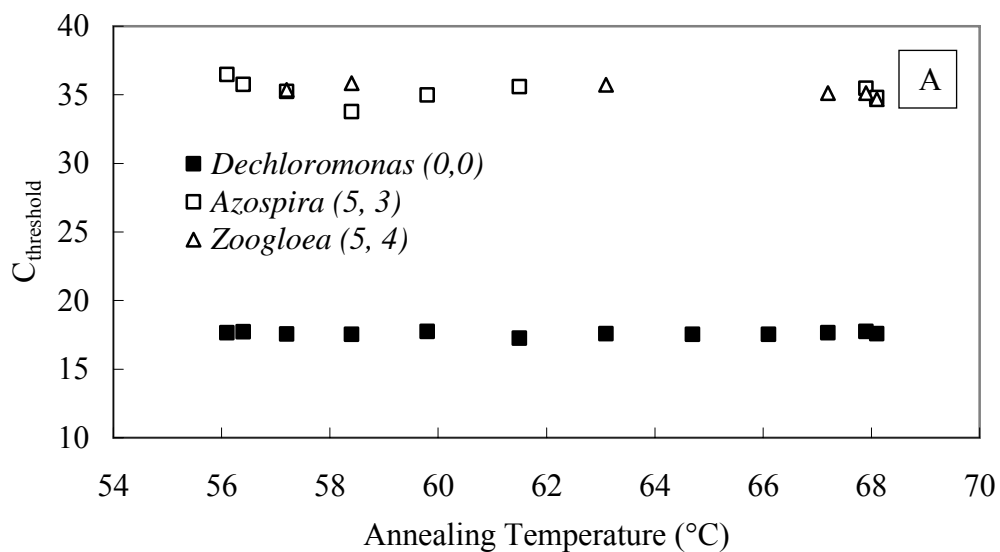


Figure 4.6. Changes in relative abundance of *Dechloromonas* spp. (A) and *Azospira* spp. (B) in the bacterial community of the bench-scale BAC reactor relative to the day that phosphorus was added (Day 0).

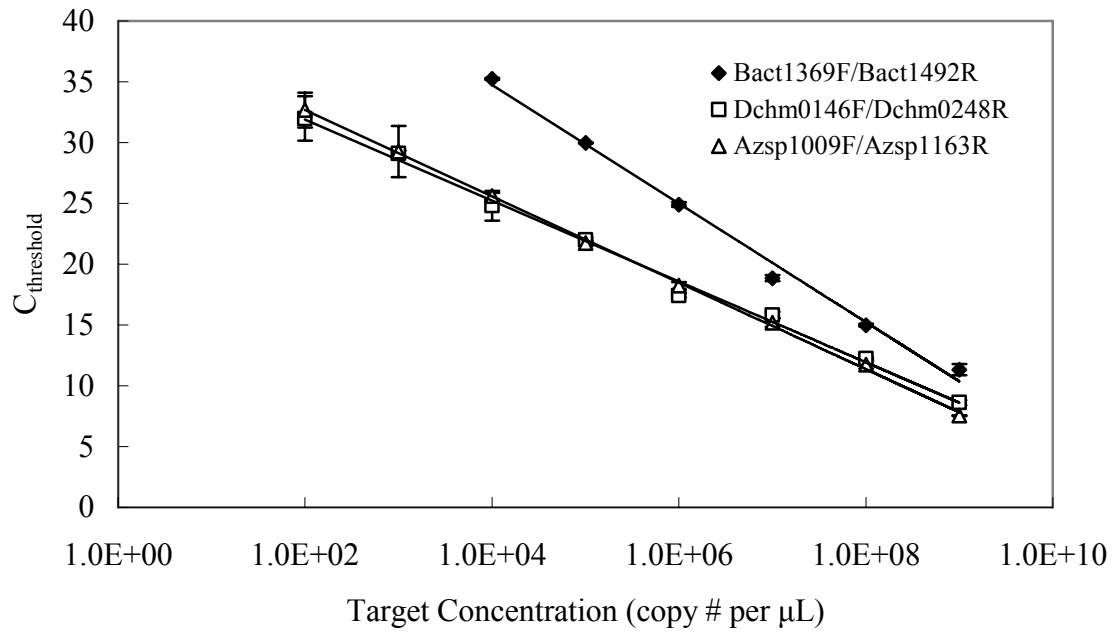


Supplemental Figure 4.1. The schematic of the entire pilot-scale system in California. The pilot-scale BAC reactor included in this work is one of the two FXB Bioreactors in the schematic.





Supplemental Figure 4.2 Characterizations on the primer sets for *Dechloromonas* (A) and *Azospira* (B). The numbers in parentheses represents the numbers of mismatches of each template with the corresponding forward and reverse primers, respectively. For the non-targets, at some annealing temperatures the PCR reaction did not generated enough fluorescence to pass the threshold, therefore, the corresponding  $C_{\text{threshold}}$  value was not available.



Supplemental Figure 4.3. Standard curves for the primer sets designed for *Dechloromonas* and *Azospira*, and for the bacterial primer set. Error bars represent standard deviation from triplicates.

## 4.7. References

- Allers, E., Gomez-Consarnau, L., Pinhassi, J., Gasol, J.M., Simek, K. and Pernthaler, J. (2007) Response of Alteromonadaceae and Rhodobacteriaceae to Glucose and Phosphorus Manipulation in Marine Mesocosms. *Environmental Microbiology* 9(10), 2417-2429.
- Alm, E.W., Oerther, D.B., Larsen, N., Stahl, D.A. and Raskin, L. (1996) The Oligonucleotide Probe Database. *Applied and Environmental Microbiology* 62(10), 3557-3559.
- American Public Health Association (APHA), A.W.W.A.A., Water Environment Federation (WEF) (1992) Standard Methods for the Examination of Water and Wastewater, American Public Health Association, Washington, DC.
- Andersson, A., Laurent, P., Kihn, A., Prevost, M. and Servais, P. (2001) Impact of Temperature on Nitrification in Biological Activated Carbon (Bac) Filters Used for Drinking Water Treatment. *Water Research* 35(12), 2923-2934.
- Brosius, J., Dull, T.J., Sleeter, D.D. and Noller, H.F. (1981) Gene Organization and Primary Structure of a Ribosomal-Rna Operon from Escherichia-Coli. *Journal of Molecular Biology* 148(2), 107-127.
- Brown, J.C., Snoeyink, V.L., Raskin, L. and Lin, R. (2003) The Sensitivity of Fixed-Bed Biological Perchlorate Removal to Changes in Operating Conditions and Water Quality Characteristics. *Water Research* 37(1), 206-214.
- Camper, A.K., Lechevallier, M.W., Broadaway, S.C. and Mcfeters, G.A. (1986) Bacteria Associated with Granular Activated Carbon Particles in Drinking-Water. *Applied and Environmental Microbiology* 52(3), 434-438.
- Carlson, K.H. and Amy, G.L. (2000) The Importance of Soluble Microbial Products (Smps) in Biological Drinking Water Treatment. *Water Research* 34(4), 1386-1396.
- Cebon, A., Bodrossy, L., Stralis-Pavese, N., Singer, A.C., Thompson, I.P., Prosser, J.I. and Murrell, J.C. (2007) Nutrient Amendments in Soil DNA Stable Isotope Probing Experiments Reduce the Observed Methanotroph Diversity. *Applied and Environmental Microbiology* 73(3), 798-807.
- Charnock, C. and Kjonno, O. (2000) Assimilable Organic Carbon and Biodegradable Dissolved Organic Carbon in Norwegian Raw and Drinking Waters. *Water Research* 34(10), 2629-2642.
- Chenier, M.R., Beaumier, D., Fortin, N., Roy, R., Driscoll, B.T., Lawrence, J.R. and Greer, C.W. (2006) Influence of Nutrient Inputs, Hexadecane and Temporal Variations

on Denitrification and Community Composition of River Biofilms. *Applied and Environmental Microbiology* 72(1), 575-584.

Chenna, R., Sugawara, H., Koike, T., Lopez, R., Gibson, T.J., Higgins, D.G. and Thompson, J.D. (2003) Multiple Sequence Alignment with the Clustal Series of Programs. *Nucleic Acids Research* 31(13), 3497-3500.

Choi, Y.C., Li, X., Raskin, L. and Morgenroth, E. (2007) Effect of Backwashing on Perchlorate Removal in Fixed Bed Biofilm Reactors. *Water Research* 41(9), 1949-1959.

Coates, J.D. and Achenbach, L.A. (2004) Microbial Perchlorate Reduction: Rocket-Fuelled Metabolism. *Nature Reviews Microbiology* 2(7), 569-580.

Cole, J.R., Chai, B., Farris, R.J., Wang, Q., Kulam-Syed-Mohideen, A.S., McGarrell, D.M., Bandela, A.M., Cardenas, E., Garrity, G.M. and Tiedje, J.M. (2007) The Ribosomal Database Project (Rdp-II): Introducing Myrddp Space and Quality Controlled Public Data. *Nucleic Acids Research* 35, D169-D172.

Dojka, M.A., Hugenholtz, P., Haack, S.K. and Pace, N.R. (1998) Microbial Diversity in a Hydrocarbon- and Chlorinated-Solvent-Contaminated Aquifer Undergoing Intrinsic Bioremediation. *Applied and Environmental Microbiology* 64(10), 3869-3877.

Emtiazi, F., Schwartz, T., Marten, S.M., Krolla-Sidenstein, P. and Obst, U. (2004) Investigation of Natural Biofilms Formed During the Production of Drinking Water from Surface Water Embankment Filtration. *Water Research* 38(5), 1197-1206.

Felsenstein, J. (1985) Confidence-Limits on Phylogenies - an Approach Using the Bootstrap. *Evolution* 39(4), 783-791.

Fields, M.W., Yan, T.F., Rhee, S.K., Carroll, S.L., Jardine, P.M., Watson, D.B., Criddle, C.S. and Zhou, J.Z. (2005) Impacts on Microbial Communities and Cultivable Isolates from Groundwater Contaminated with High Levels of Nitric Acid-Uranium Waste. *FEMS Microbiology Ecology* 53(3), 417-428.

Fuchs, W., Schatzmayr, G. and Braun, R. (1997) Nitrate Removal from Drinking Water Using a Membrane-Fixed Biofilm Reactor. *Applied Microbiology and Biotechnology* 48(2), 267-274.

Hall, T.A. (1999) Bioedit: A User-Friendly Biological Sequence Alignment Editor and Analysis Program for Windows 95/98/Nt. *Nucleic Acids Symposium Series* 41, 95-98.

Hautman, D.P., Munch, D.J., Eaton, A.D. and Haghani, A.W. (1999) Method 314.0 Determination of Perchlorate in Drinking Water Using Ion Chromatography. EPA National Exposure Research Laboratory (ed).

Hendrickx, B., Dejonghe, W., Boenne, W., Brennerova, M., Cernik, M., Lederer, T., Bucheli-Witschel, M., Bastiaens, L., Verstraete, W., Top, E.M., Diels, L. and Springael, D. (2005) Dynamics of an Oligotrophic Bacterial Aquifer Community During Contact

with a Groundwater Plume Contaminated with Benzene Toluene, Ethylbenzene, and Xylenes: An in Situ Mesocosm Study. *Applied and Environmental Microbiology* 71(7), 3815-3825.

Jukes, T. and Cantor, C.R. (1969) *Mammalian Protein Metabolism*. HN, M. (ed), pp. 21-132, Academic Press, New York.

Kim, W.H., Nishijima, W., Shoto, E. and Okada, M. (1997) Pilot Plant Study on Ozonation and Biological Activated Carbon Process for Drinking Water Treatment. *Water Science and Technology* 35(8), 21-28.

Lechevallier, M.W., Seidler, R.J. and Evans, T.M. (1980) Enumeration and Characterization of Standard Plate-Count Bacteria in Chlorinated and Raw Water-Supplies. *Applied and Environmental Microbiology* 40(5), 922-930.

Li, X.Y. and Chu, H.P. (2003) Membrane Bioreactor for the Drinking Water Treatment of Polluted Surface Water Supplies. *Water Research* 37(19), 4781-4791.

Madigan, M.T., Martinko, J.M. and Parker, J. (2003) *Brock Biology of Microorganisms*, Pearson Education, Upper Saddle River, NJ.

Maixner, F., Wagner, M., Lucker, S., Pelletier, E., Schmitz-Esser, S., Hace, K., Spieck, E., Konrat, R., Paslier, D.L. and Daims, H. (2008) Environmental Genomics Reveals a Functional Chlorite Dismutase in the Nitrite-Oxidizing Bacterium '*Candidatus Nitrospira Defluvii*'. *Environmental Microbiology*.

Miller, J.P. and Logan, B.E. (2000) Sustained Perchlorate Degradation in an Autotrophic, Gas-Phase, Packed-Bed Bioreactor. *Environmental Science & Technology* 34(14), 3018-3022.

Moll, D.M., Summers, R.S. and Breen, A. (1998) Microbial Characterization of Biological Filters Used for Drinking Water Treatment. *Applied and Environmental Microbiology* 64(7), 2755-2759.

Moll, D.M., Summers, R.S., Fonseca, A.C. and Matheis, W. (1999) Impact of Temperature on Drinking Water Biofilter Performance and Microbial Community Structure. *Environmental Science & Technology* 33(14), 2377-2382.

Mrazek, J., Spormann, A.M. and Karlin, S. (2006) Genomic Comparisons among Gamma-Proteobacteria. *Environmental Microbiology* 8(2), 273-288.

Nerenberg, R., Kawagoshi, Y. and Rittmann, B.E. (2008) Microbial Ecology of a Perchlorate-Reducing, Hydrogen-Based Membrane Biofilm Reactor. *Water Research* 42(4-5), 1151-1159.

Nerenberg, R. and Rittmann, B.E. (2004) Hydrogen-Based, Hollow-Fiber Membrane Biofilm Reactor for Reduction of Perchlorate and Other Oxidized Contaminants. *Water Science and Technology* 49(11-12), 223-230.

- Nerenberg, R., Rittmann, B.E. and Soucie, W.J. (2000) Ozone/Biofiltration for Removing Mib and Geosmin. *Journal American Water Works Association* 92(12), 85-+.
- Nishijima, W., Shoto, E. and Okada, M. (1997) Improvement of Biodegradation of Organic Substance by Addition of Phosphorus in Biological Activated Carbon. *Water Science and Technology* 36(12), 251-257.
- Nishijima, W. and Speitel, G.E. (2004) Fate of Biodegradable Dissolved Organic Carbon Produced by Ozonation on Biological Activated Carbon. *Chemosphere* 56(2), 113-119.
- Norton, C.D. and LeChevallier, M.W. (2000) A Pilot Study of Bacteriological Population Changes through Potable Water Treatment and Distribution. *Applied and Environmental Microbiology* 66(1), 268-276.
- Pang, C.M. and Liu, W.T. (2006) Biological Filtration Limits Carbon Availability and Affects Downstream Biofilm Formation and Community Structure. *Applied and Environmental Microbiology* 72(9), 5702-5712.
- Rittmann, B.E. and McCarty, P.L. (2001) *Environmental Biotechnology: Principles and Applications*, McGraw-Hill, New York, NY.
- Rittmann, B.E., Stilwell, D., Garside, J.C., Amy, G.L., Spangenberg, C., Kalinsky, A. and Akiyoshi, E. (2002) Treatment of a Colored Groundwater by Ozone-Biofiltration: Pilot Studies and Modeling Interpretation. *Water Research* 36(13), 3387-3397.
- Rozen, S. and Skaletsky, H. (2000) *Primer3 on the Www for General Users and for Biologist Programmers*, Humana Press, Totowa, NJ.
- Saitou, N. and Nei, M. (1987) The Neighbor-Joining Method - a New Method for Reconstructing Phylogenetic Trees. *Molecular Biology and Evolution* 4(4), 406-425.
- Salcher, M.M., Hofer, J., Hornak, K., Jezbera, J., Sonntag, B., Vrba, J., Simek, K. and Posch, T. (2007) Modulation of Microbial Predator-Prey Dynamics by Phosphorus Availability: Growth Patterns and Survival Strategies of Bacterial Phylogenetic Clades. *Fems Microbiology Ecology* 60(1), 40-50.
- Sang, J.Q., Zhang, X.H., Li, L.Z. and Wang, Z.S. (2003) Improvement of Organics Removal by Bio-Ceramic Filtration of Raw Water with Addition of Phosphorus. *Water Research* 37(19), 4711-4718.
- Schloss, P.D. and Handelsman, J. (2005) Introducing Dotur, a Computer Program for Defining Operational Taxonomic Units and Estimating Species Richness. *Applied and Environmental Microbiology* 71(3), 1501-1506.
- Schloss, P.D., Larget, B.R. and Handelsman, J. (2004) Integration of Microbial Ecology and Statistics: A Test to Compare Gene Libraries. *Applied and Environmental Microbiology* 70(9), 5485-5492.

- Segawa, T., Miyamoto, K., Ushida, K., Agata, K., Okada, N. and Kohshima, S. (2005) Seasonal Change in Bacterial Flora and Biomass in Mountain Snow from the Tateyama Mountains, Japan, Analyzed by 16s Rrna Gene Sequencing and Real-Time Pcr. *Applied and Environmental Microbiology* 71(1), 123-130.
- Souza, V., Eguiarte, L.E., Siefert, J. and Elser, J.J. (2008) Microbial Endemism: Does Phosphorus Limitation Enhance Speciation? *Nature Review Microbiology* 6(7), 559-564.
- Suzuki, M.T., Taylor, L.T. and DeLong, E.F. (2000) Quantitative Analysis of Small-Subunit Rrna Genes in Mixed Microbial Populations Via 5'-Nuclease Assays. *Applied and Environmental Microbiology* 66(11), 4605-4614.
- Takahata, Y., Kasai, Y., Hoaki, T. and Watanabe, K. (2006) Rapid Intrinsic Biodegradation of Benzene, Toluene, and Xylenes at the Boundary of a Gasoline-Contaminated Plume under Natural Attenuation. *Applied Microbiology and Biotechnology* 73(3), 713-722.
- Tamura, K., Dudley, J., Nei, M. and Kumar, S. (2007) Mega4: Molecular Evolutionary Genetics Analysis (Mega) Software Version 4.0. *Molecular Biology and Evolution* 24(8), 1596-1599.
- Wobus, A., Bleul, C., Maassen, S., Scheerer, C., Schuppler, M., Jacobs, E. and Roske, I. (2003) Microbial Diversity and Functional Characterization of Sediments from Reservoirs of Different Trophic State. *FEMS Microbiology Ecology* 46(3), 331-347.
- Xie, C.H. and Yokota, A. (2006) *Zoogloea Oryzae* Sp Nov., a Nitrogen-Fixing Bacterium Isolated from Rice Paddy Soil, and Reclassification of the Strain Atcc 19623 as *Crabtreeella Saccharophila* Gen. Nov., Sp Nov. *International Journal of Systematic and Evolutionary Microbiology* 56, 619-624.
- Zhang, H., Logan, B.E., Regan, J.M., Achenbach, L.A. and Bruns, M.A. (2005) Molecular Assessment of Inoculated and Indigenous Bacteria in Biofilms from a Pilot-Scale Perchlorate-Reducing Bioreactor. *Microbial Ecology* 49(3), 388-398.

## Chapter 5

### Operation of a Biologically Active Carbon Reactor to Treat Nitrate and Perchlorate Contaminated Drinking Water

#### 5.1 Introduction

During the last decade, the presence of perchlorate ( $\text{ClO}_4^-$ ) in drinking water sources (Richardson, 2003) has received much attention because of its adverse health effects (Greer et al., 2002). Perchlorate is introduced to the environment through human activities (Urbansky, 2002) and natural processes (Dasgupta et al., 2005). It has been added to US EPA's drinking water contaminant candidate list (US-EPA, 2008) and is regulated by some states (CA-DHS, 2005; US-EPA, 2005; MA-DEP, 2006) at various levels ranging from 1 to 18  $\mu\text{g/L}$ . Abiotic and biological treatment methods have been developed to remove perchlorate from drinking water. Abiotic treatment options include the use of ion exchange resins (Venkatesh et al., 2000; Gu et al., 2001), granular activated carbon (GAC) (Chen et al., 2005), and zero valent iron nanoparticles (Xiong et al., 2007). Biological treatment methods rely on perchlorate reducing bacteria (Coates and Achenbach, 2004) to convert perchlorate into non-toxic chloride (Nerenberg et al., 2002; Brown et al., 2003; Min et al., 2004). Compared to ion exchange and GAC adsorption, biological treatment can achieve consistent perchlorate removal without the need for



regeneration of ion exchange resins or GAC and avoid the need to treat or dispose concentrated waste streams (Brown et al., 2002; Xu et al., 2003). Another advantage of biological treatment methods is their potential to remove multiple pollutants simultaneously (Nerenberg and Rittmann, 2004).

Compared to other bioreactor configurations, biologically active carbon (BAC) reactors have the advantages of easy implementation and reliable performance. These systems are readily accepted and can be easily implemented by the drinking water industry because many drinking water treatment plants already employ GAC filters for advanced treatment. If bacterial proliferation on the GAC surface is allowed or promoted, then GAC filters can become biologically active and evolve to BAC treatment systems (Bouwer and Crowe, 1988). Many drinking water treatment plants employ pre-ozonation to transform refractory natural organic matter (NOM) into biodegradable dissolved organic carbon (BDOC) before GAC filtration, thus promote bacteria to grow on GAC surfaces by providing them with BDOC as electron donor substrates (Urfer et al., 1997). However, the BAC system used in the current study is different from the filters that become biologically active when ozonation precedes GAC filtration: the former system is supplied with an external electron donor to support microbial activity, while the latter type utilizes the BDOC produced through oxidation of NOM present in the source water. In addition to the wide acceptance by the drinking water industry, the adsorption capacity of the GAC surface is beneficial and provides additional treatment capacity that results in reliable performance, primarily due to three reasons: (1) contaminants that cannot be removed biologically can be removed by adsorption (Weber, 1974); (2) contaminants that are toxic or inhibitory to microbial activity can be adsorbed so that the microbes on the

GAC surface are exposed to lower concentrations (Ehrhardt and Rehm, 1985); and (3) during dynamic or unfavorable operating conditions (e.g., pulse increase in the concentration of competing electron acceptors or accidental interruption of electron donor addition), removal of contaminants can be maintained temporarily because of adsorption (Choi et al., 2008).

Most previous studies on biological perchlorate removal from drinking water have concentrated primarily on system optimization with a focus on the removal of perchlorate, and have not considered other aspects of effluent water quality. However, some aspects of biological drinking water treatment, such as the addition of electron donor to promote microbial growth, have direct and indirect impacts on the chemical and biological properties of finished water. Excess electron donor ends up in reactor effluents, which raises concerns about the biological stability of the finished water in drinking water distribution systems. Therefore, the benefits of high influent electron donor concentrations to promote biological activity inside the bioreactors need to be balanced with the need of having low effluent electron donor concentrations to minimize the impact on microbial growth in distribution systems. In addition, because microbes from the bioreactors may end up in reactor effluents, microbial safety is a concern without adequate post-treatment. Brown recognized these concerns and initiated a study to evaluate the need for post-treatment after BAC treatment of perchlorate contaminated drinking water (Brown, 2002), however, additional work is needed.

The current study evaluates the operation of a bench-scale BAC system for perchlorate and nitrate removal with respect to chemical and biological properties of reactor effluent. Specifically, intermittent electron donor addition was tested to evaluate

the robustness of perchlorate and nitrate removal by this BAC reactor and to minimize the electron donor residual in the effluent. Furthermore, bacterial inactivation kinetics using monochloramine as the disinfectant were determined to study if regular disinfection practice can inactivate bacteria in BAC reactor effluents.

## **5.2 Materials and Methods**

### **5.2.1 Intermittent Electron Donor Addition Experiment**

The configuration of the bench-scale BAC reactor, the baseline operating conditions of the reactor, and the analytical method for liquid samples have been introduced in Chapter 4. Intermittent addition of acetic acid (HAc) to the BAC reactor was tested by dividing one backwash cycle (i.e., 48 hours) into four periods. Each 12-hour period consisted of a 6-hour acetic acid addition at a concentration twice the stoichiometric requirement (i.e., 26 mg/L acetic acid as C) followed by acetic acid addition at a concentration half the stoichiometric requirement (i.e., 6.5 mg/L as C) for 6 hours. Effluent samples were taken 1, 3, and 5 hours each time after each change in influent acetic acid concentration.

The decision to use an acetic acid concentration twice the stoichiometric requirement was determined experimentally using batch tests in sealed serum bottles which separated air exchange with ambient atmosphere and contained synthetic groundwater with various concentrations of electron donor in a final volume of 100 mL. In order to elucidate the correlation between nitrate/perchlorate removal rates and electron donor concentration, it was critical to ensure that the same amount of biomass was added to each serum bottle. To this end, four replicate serum bottles each containing

5 g wet weight of BAC particles and 100 mL influent of the BAC system (i.e., 20 mg/L of acetic acid in synthetic groundwater) were monitored with respect to nitrate and perchlorate concentrations. The resulting concentration profiles were nearly identical (data not shown), indicating that the same amount of biomass was added to each serum bottle, and demonstrating that controlling BAC wet weight was an effective means to control biomass. Therefore, 10 g wet weight of BAC was added to each of the eight batch tests with electron donor concentrations of 0, 0.3, 0.6, 1, 1.5, 2, 2.5 and 3 times the stoichiometric requirement. The nitrate and perchlorate concentration profiles in each batch test were plotted and fitted in the software Kaleidagraph (Synergy Software, Reading, PA) using an exponential decay model with  $R^2$  values higher than 0.95 (Figure 5.1). The fitted curves were used to calculate the initial nitrate and perchlorate removal rates, which were also the maximum removal rates, at time zero (Figure 5.1). The initial removal rates were plotted against electron donor concentrations tested.

### **5.2.2 Adsorption Isotherm Experiment**

Prior to the experiment, GAC was dried at 105°C overnight and all experimental devices were sterilized using an autoclave. Because the adsorbate (i.e., acetic acid) is an acid, the adsorption solutions that contained various concentrations of acetic acid were buffered using a 0.03 M phosphate buffered saline (PBS) at pH 7.40-7.65, a range close to the pH of the bench-scale BAC reactor (i.e. 7.5-7.9). Among eight 125 mL amber glass bottles, six were used to determine an adsorption isotherm (i.e., 4, 10, 20, 40, 100, and 200 mg/L acetic acid as C), one to verify that adsorption equilibrium had been reached (K bottle), and one to serve as a negative control with no GAC (B bottle). Eight grams of dried

GAC was added to the amber bottles except the one for the negative control. Each bottle was completely filled with adsorption solution. 1 mL adsorption solution was collected at time zero from each amber bottle for IC measurement. 1 mL sample was taken from the K bottle each day. After equilibrium was reached on day 8, 1 mL sample was taken from each bottle to measure the final acetic acid concentrations.

A Freundlich adsorption isotherm was used to describe the adsorption behavior of acetic acid to fresh GAC at the pH range of 7.40-7.65.

$$q_e = K \times C_e^{1/n} \quad (1)$$

where  $C_e$  is the equilibrium concentration of adsorbate in solution, and  $q_e$  is the equilibrium adsorbent-phase concentration of adsorbate (mg HAc as C / g of GAC dry weight),  $K$  is Freundlich adsorption capacity parameter (mg/g)(L/mg)<sup>1/n</sup>, and  $1/n$  is dimensionless Freundlich adsorption intensity parameter.

### 5.2.3 Mass Balance Calculation

The assumptions made in calculating acetic acid adsorption/desorption on the GAC surface inside the BAC reactor are the following:

- Instantaneous equilibrium was reached after the influent acetic acid concentration was changed in the intermittent electron donor experiment, and  $C_e=13$  mg/L HAc as C.
- The adsorption capacity of BAC is half of that for GAC:  $K_{BAC}=0.5 \times K_{GAC}$ , and the adsorption intensity of BAC approximately equals that of GAC:  $(1/n)_{BAC} \approx (1/n)_{GAC}$  (Zhao et al., 1999).

- The acetic acid adsorbed on the GAC surface during the stages of high influent acetic acid concentrations was 100% desorbed for microbial utilization during the succeeding stages of low influent acetic acid concentrations.

The assumptions made in calculating polyhydroxybutyrate (PHB) formation/consumption and the parameters adopted from the literature are the following:

- During the feast phase, the ratio of PHB formation to acetic acid supply is 0.68 g COD-PHB/g COD-HAc, which is equivalent to 0.43 g PHB/g HAc (Beccari et al., 1998; Beun et al., 2002).
- During the famine phase, about 81% of the PHB formed in the feast phase is consumed for cell synthesis (Beun et al., 2002).

#### **5.2.4 Disinfection Experiment**

Monochloramine was prepared using sodium hypochlorite and ammonium chloride by following the protocol presented in (Driedger et al., 2001), quantified using the DPD titrimetric method (American Public Health Association (APHA), 1992), and added to disinfection experiments at a final concentration of 4 mg/L as Cl<sub>2</sub>. Disinfection experiments were performed in 250 mL Erlenmeyer flasks wrapped with aluminum foil and placed in a recirculating water bath set at 20 °C. The pH of the solution used in the disinfection experiments was maintained at 8.0 using phosphate buffered saline (PBS). Samples were taken from the disinfection experiment at various time points. The samples were added to dilution water (American Public Health Association (APHA), 1992), which contained sodium thiosulfate to stop the inactivation reaction by quenching the monochloramine residual. Heterotrophic plate count (HPC) using R2A agar

(American Public Health Association (APHA), 1992) was used to determine the viable microbial counts.

The inactivation kinetic curve was constructed based on a two population model, first reported by (Luh and Marinas, 2007) who used it to describe the inactivation of *Mycobacterium avium* using free chlorine:

$$\frac{N}{N_0} = \frac{N_{1,0}}{N_0} \times e^{(-k_1CT)} + \frac{N_{2,0}}{N_0} \times e^{(-k_2CT)} \quad (2)$$

where  $N_0$  and  $N$  are HPC values in colony forming units (CFU) at time zero and time  $t$ , respectively, after a disinfection experiment occurs. Luh and Marinas used  $N_{1,0}/N_0$  and  $N_{2,0}/N_0$  to denote the fractions of susceptible and resistant *M. avium* cells, respectively. In this study, we used these two symbols to denote the fractions of individual cells and cell aggregates in the BAC reactor effluent.  $k_1$  and  $k_2$  are the rates of inactivation for the individual cells and cell aggregates, respectively, and  $CT$  is the product of the monochloramine concentration and the time of disinfection in  $\text{min} \times \text{mg/L}$ .

## 5.3 Results

### 5.3.1 Intermittent Electron Donor Addition

The batch tests indicated that nitrate and perchlorate removal rates increased with the concentration of electron donor. In Figure 5.2, the electron donor concentrations are expressed in “times the stoichiometric requirement”. For example, in the batch test with a value of 2, the electron donor concentration was twice the concentration that was needed to stoichiometrically reduce all electron acceptors. As shown in Figure 5.2, the nitrate removal rate averaged 7.48 mg/L per hour when the electron donor concentrations

were between 0 and 1 time the stoichiometric requirement. The rate was slightly higher at 1.5 and substantially higher at 2 and above. A similar trend was observed for the perchlorate removal rate. The electron donor concentration corresponding to 2 times the stoichiometric requirement was chosen for the feast stage of the intermittent electron donor addition experiment, because (i) both nitrate and perchlorate removal rates were substantially higher than those at lower concentrations; (ii) a concentration higher than 2 may result in too much electron donor in excess exceeding the capacity of the electron donor reservoirs, i.e., adsorption on the GAC surface and formation of storage material in cells.

The intermittent electron donor addition pattern was evaluated using the bench-scale BAC reactor within one 48-hour backwash cycle. Before the intermittent addition experiment, which started at time zero in Figure 5.3, the BAC reactor was operated using the baseline operating conditions (i.e., 20.0 mg/L acetic acid as C). During this time, the reactor completely reduced the three electron acceptors and had an effluent acetic acid residual concentration close to the expected value (i.e., 3.9 vs. 6.5 mg/L acetic acid as C). During the intermittent experiment, each time the influent acetic acid concentration was switched from half the stoichiometric concentration to twice the stoichiometric requirement (i.e., 6.5 to 26 mg/L acetic acid as C), the effluent acetic acid concentration *gradually*, rather than *immediately*, increased from 0 towards 13 mg/L acetic acid as C. 13 mg/L was the expected effluent acetic acid concentration when the influent acetic acid concentration was twice the stoichiometric requirement and when no reservoir for electron donor was present in the system. During the feast periods when acetic acid was added in excess, effluent nitrate and perchlorate concentrations remained below the



detection limits. When the influent acetic acid concentration was switched to half the stoichiometric requirement, the effluent acetic acid concentration quickly dropped to below the detection limit. The effluent nitrate and perchlorate concentrations remained zero for one hour after the switch, and then gradually increased. After the intermittent experiment ended, reactor operation was returned to the baseline operating conditions and the performance was similar to that observed before the intermittent experiment.

### 5.3.2 Adsorption Isotherm

In order to explain the effluent acetic acid and nitrate/perchlorate concentration profiles in Figure 5.3, the GAC adsorption capacity of acetic acid was investigated by obtaining an adsorption isotherm of acetic acid at a pH relevant for this study. Because of the limited amount of BAC (200 mm<sup>3</sup>) available in the bench-scale reactor, the adsorption isotherm was obtained using virgin F816 GAC, the same type of GAC from which BAC was developed. The adsorption isotherm experiment revealed that acetic acid was able to adsorb onto the GAC surface at pH values between 7.40 and 7.65, as shown in Figure 5.4. The range of the tested concentrations for the adsorption isotherm was relevant to the operating conditions of the bench-scale BAC reactor. The Freundlich adsorption isotherm equation calculated from the experimental data is:

$$q_e = 1.50 \times 10^{-3} \times C_e^{0.8771} \quad (3)$$

An effort was made to use the information from the Freundlich adsorption isotherm to explain the profiles in Figure 5.3. However, even with the most aggressive assumptions, which were reported in Materials and Methods, GAC adsorption alone cannot fully explain the phenomenon. Therefore, the possibility that some bacteria in the

BAC reactor produce storage materials, such as polyhydroxybutyrate (PHB), during the feast stages was investigated as another possible mechanism by which acetic acid can be temporarily “stored” when it is provided in excess and be consumed when its concentration becomes limiting.

### **5.3.3 Calculation on Formation of Storage Materials and Overall Mass Balance**

Calculations show that cellular storage material production and consumption could play a significant role in leading to the profiles shown in Figure 5.3, when acetic acid was provided in an intermittent pattern. As shown in Figure 5.5, when the influent acetic acid concentration was twice the stoichiometrically required concentration during a 6-hour feast period, half of the influent acetic acid was used to reduce three electron acceptors and synthesize cell mass, about 14.63 mg acetic acid ended up in the reactor effluent, and the rest of the acetic acid was either adsorbed onto the GAC surface or transformed by bacteria into cellular storage materials, likely PHB (Eynde et al., 1984). When the influent acetic acid concentration was half the stoichiometrically required concentration, the amount of acetic acid needed, based on the amount of electron acceptors reduced, was about 33.04 mg. We assume that acetic acid was provided from three sources: 17.55 mg from the acetic acid provided in the influent, 14.70 mg from intracellular storage material, and 0.79 mg from desorption from the GAC surface (Figure 5.5). The values of acetic acid corresponding to PHB production/consumption were balanced values. To verify the mass balance, conversions between acetic acid and PHB during feast/famine conditions were calculated. Based on assumptions provided in the Materials and Methods, 19.67 mg acetic acid as C could be converted to 21.15 mg PHB during the feast stage. In the

famine stages, 17.13 mg PHB – 81% (Beun et al., 2002) of the 21.15 mg PHB produced previously – should approximate 14.70 mg acetic acid as C. Given that the bacterial growth rate on PHB is usually lower than that on the original substrate (van Loosdrecht et al., 1997), the approximation seemed reasonable.

#### 5.3.4 Inactivation Kinetics

Microscopic observation of the biomass in BAC reactor effluents showed that the majority of the microbes were free cells, while cell aggregates as large as a couple of hundred  $\mu\text{m}$  in dimension also existed (data not shown). The total cell number determined using the HPC method was  $2.6 \times 10^5$  colony forming units (CFU).

The inactivation kinetics experiment showed that there were two populations which responded differently with respect to kinetics when 4 mg/L monochloramine was used as the disinfectant (Figure 5.6). The first population (filled symbols) was inactivated efficiently: 2-log decrease was achieved using a  $CT$  value less than 40 mg $\times$ min/L. In contrast, the second population (open symbols) was inactivated at a lower rate. The overall disinfection kinetics of the community (two populations) was simulated using Equation 2. The simulated result is

$$\frac{N}{N_0} = 0.989 \times e^{-0.166CT} + 0.011 \times e^{-0.030CT} \quad (4)$$

where the values 0.989 and 0.011 are the estimates of the fractions of free cells and cell aggregates in the microbial community in the BAC reactor effluent, respectively.

## 5.4 Discussion

In order to evaluate the robustness of biological perchlorate/nitrate reduction activities inside BAC reactors and to minimize the electron donor residual in the effluent, an intermittent electron donor experiment was conducted. Originally, GAC adsorption was believed to be the major reservoir for electron donor in the BAC reactor during dynamic operating conditions, such as in the intermittent experiment. We hypothesized that when acetic acid was added in excess, the GAC could adsorb the acetic acid in excess and lower the concentration of electron donor in the reactor effluent; when acetic acid was added below the stoichiometric requirement, the acetic acid previously stored in the reservoir (i.e., the one adsorbed previously on the GAC) would be utilized by bacteria to achieve complete removal of nitrate and perchlorate, and the adsorption sites on GAC would be regenerated. In addition, we expected that the perchlorate reducing bacteria mainly resided at the bottom of the biofilm, while the other heterotrophic bacteria dominated the surface of the biofilm. Such model has been proposed in a mathematical simulation in which denitrifiers and other heterotrophic bacteria were classified as two groups (Kim et al., 2004). The model has also been demonstrated in a fluorescence *in situ* hybridization analysis on biomass samples collected from a pilot-scale BAC reactor in which most *Dechlorosoma* spp. and a fraction of the *Dechloromonas* resided at the bottom of biofilm in a bioreactor, which was run to remove perchlorate with acetic acid as the sole electron donor (Zhang et al., 2005). For our BAC system, if the PRB populations indeed mainly resided closer to the GAC surface, then the adsorbed acetic acid would be first utilized by PRB for perchlorate reduction.

The calculation from the GAC adsorption isotherm could not fully explain the concentration profiles in Figure 5.3, so another mechanism, production and consumption of intracellular storage materials by certain bacteria, was considered. Storage has been studied in both pure cultures of bacteria (van Aalst-van Leeuwen et al., 1997) and in mixed bacterial cultures (Beccari et al., 1998). The formation of storage materials usually occurs simultaneously with the conversion of electron donor in excess, and the consumption of the storage materials starts immediately after the depletion of electron donor in the bulk liquid phase (Krishna and Van Loosdrecht, 1999; Beun et al., 2002). The time scale of the intermittent addition experiment in this study is similar to those reported in other studies. Estimates shown in Figure 5.5 indicate that the electron donor reservoir by formation of cellular storage material may play an important role in forming the profiles in Figure 5.3.

Electron donor reservoirs (i.e., adsorption/desorption on GAC and production/consumption of cellular storage materials) promote robustness to biological processes and allow for lower electron donor concentrations in reactor effluent. When acetic acid was added below the stoichiometric requirement, low effluent nitrate and perchlorate concentrations resulted from the utilization of electron donor stored in those reservoirs. In fact, the non-zero nitrate and perchlorate removal rates at zero electron donor addition in Figure 5.2 likely resulted from the utilization of stored electron donor. Once stored electron donor was depleted, the emptied reservoirs became ready for the storage of electron donor during the next stage when acetic acid was added at twice the stoichiometric requirement. However, the breakthrough of acetic acid during high stage

and the breakthrough of nitrate/perchlorate during low stage indicated that the capacity of the reservoirs, GAC adsorption and cellular storage materials, was limited.

Disinfection of finished water from biological drinking water treatment has been studied previously (Pernitsky et al., 1995; Norton and LeChevallier, 2000). In these earlier studies, biological treatment did not involve addition of external electron donor. In the current study, acetic acid was added as the electron donor to promote microbial growth in the BAC reactor. The inactivation kinetics experiment showed two populations that responded to monochloramine disinfection differently. The population with the slow inactivation kinetics was likely associated with cell aggregates in the reactor effluent. In order to inactivate cell aggregates, all viable cells in the aggregates need to be inactivated, because any viable cells in an aggregate can lead to the formation of a colony in the HPC method. Therefore, we speculate that it took a longer time to inactivate cell aggregates due to the diffusion of disinfectant into the centers of cell aggregates. It is worth noting that, at the *CT* value of 150 min×mg/L, the HPC reading of the reactor effluent met the EPA drinking water standard for HPC (i.e., < 500 CFU/mL), which is regulated for drinking water facilities treating surface waters.

## 5.5 Figures

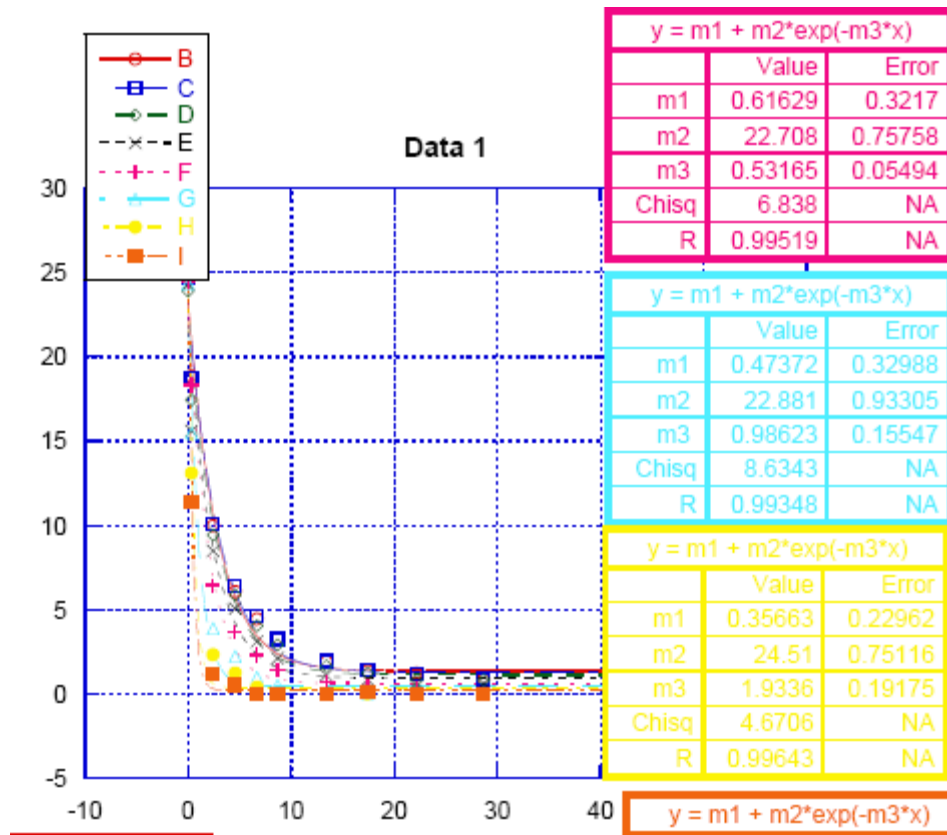


Figure 5.1. A sample figure showing the nitrate concentration profiles with simulated curves using an exponential decay model.

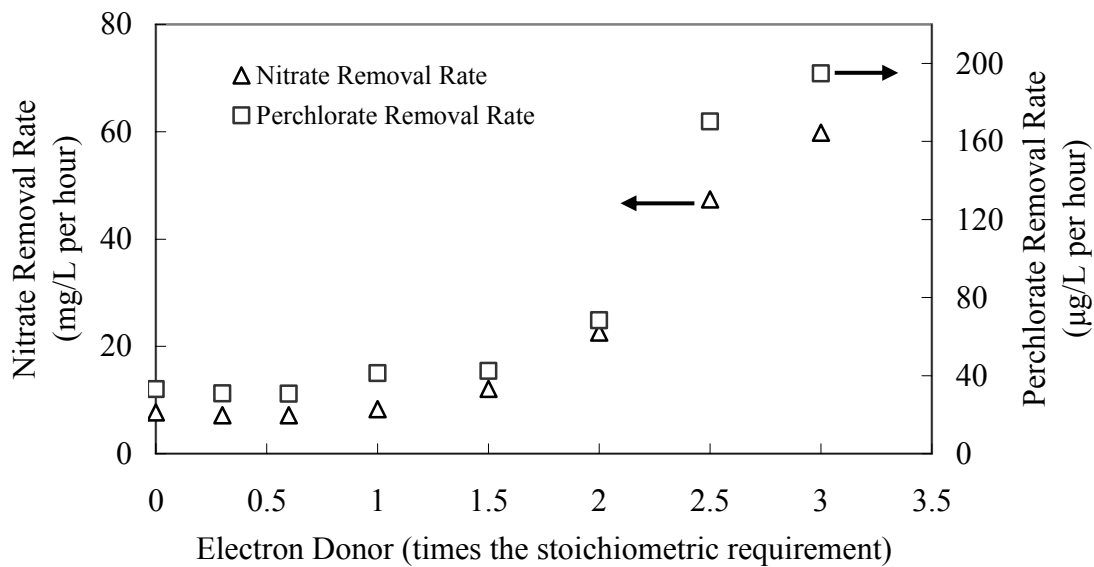


Figure 5.2. Nitrate and perchlorate removal rates as functions of electron donor in the batch tests. The wet weight of BAC particles added to each batch test was identical.



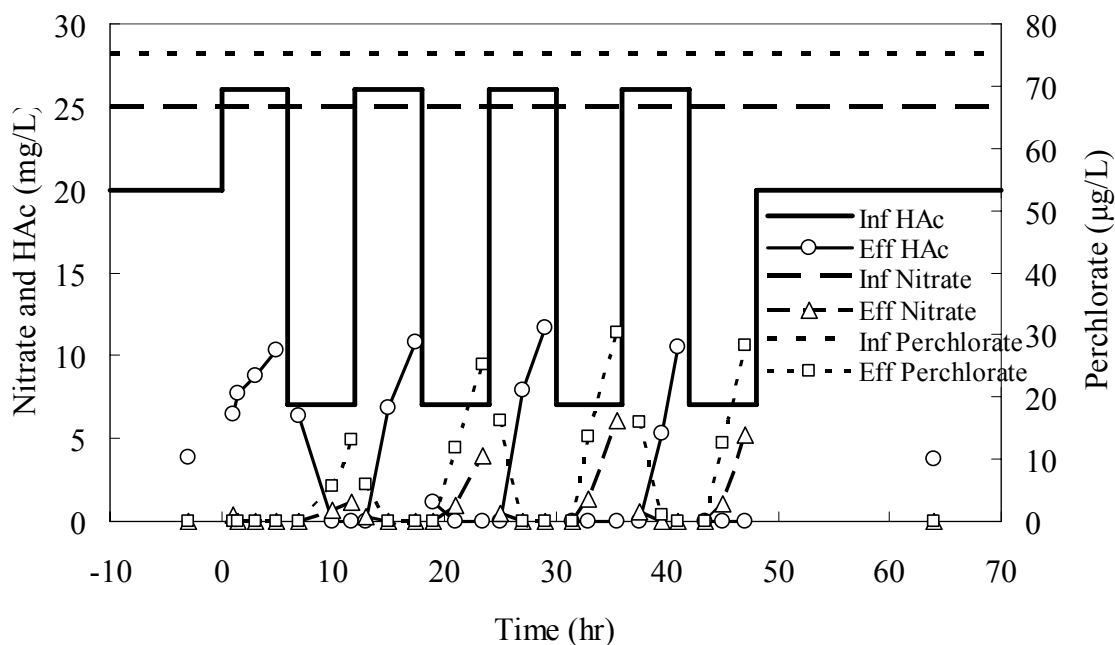


Figure 5.3. Results of effluent nitrate, perchlorate, and acetic acid from the intermittent electron donor addition experiment. For simplicity, influent and effluent DO levels, which respectively remained at 7 mg/L and below the detection limit throughout the experiment, were not included in the figure.

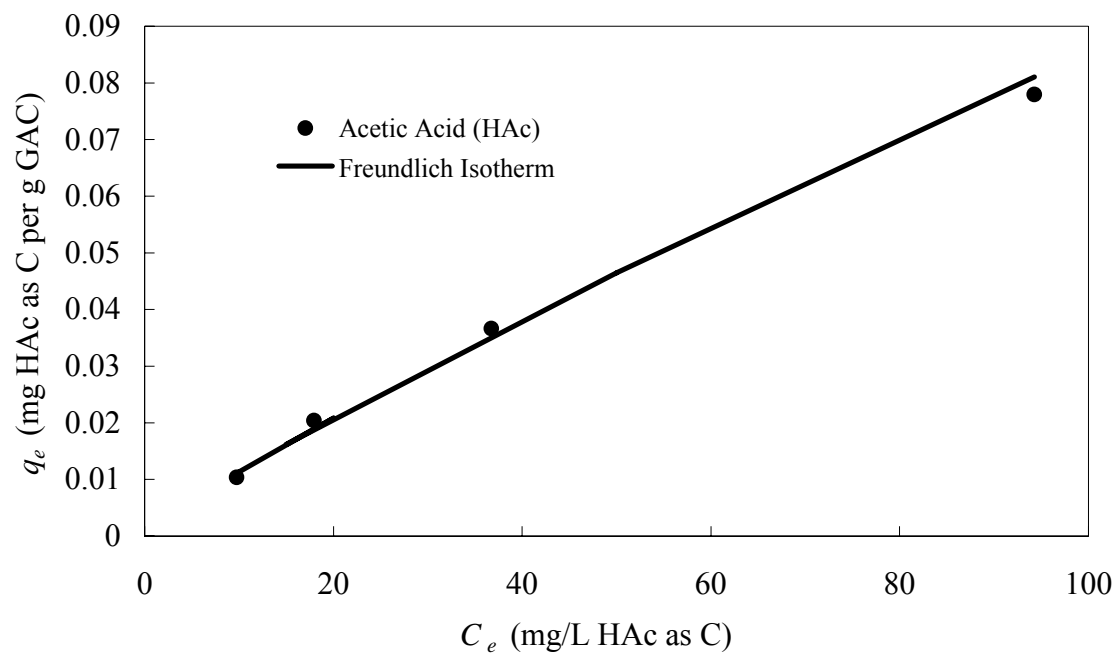


Figure 5.4. Adsorption isotherm for acetic acid adsorption on GAC (pH 7.40-7.65). The curve is constructed based on Equation 3.

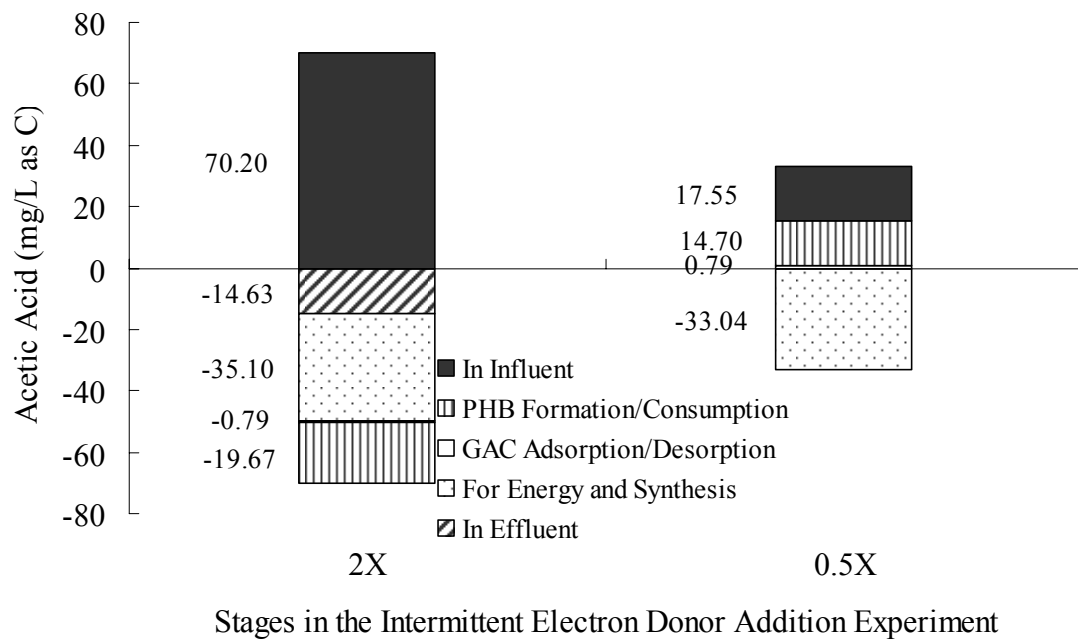


Figure 5.5. Breakdown of source (positive values) and sink (negative values) of acetic acid within one feast and one famine stage in the intermittent electron donor addition experiment. Values of acetic acid corresponding to PHB formation/consumption (▨) are balanced values.

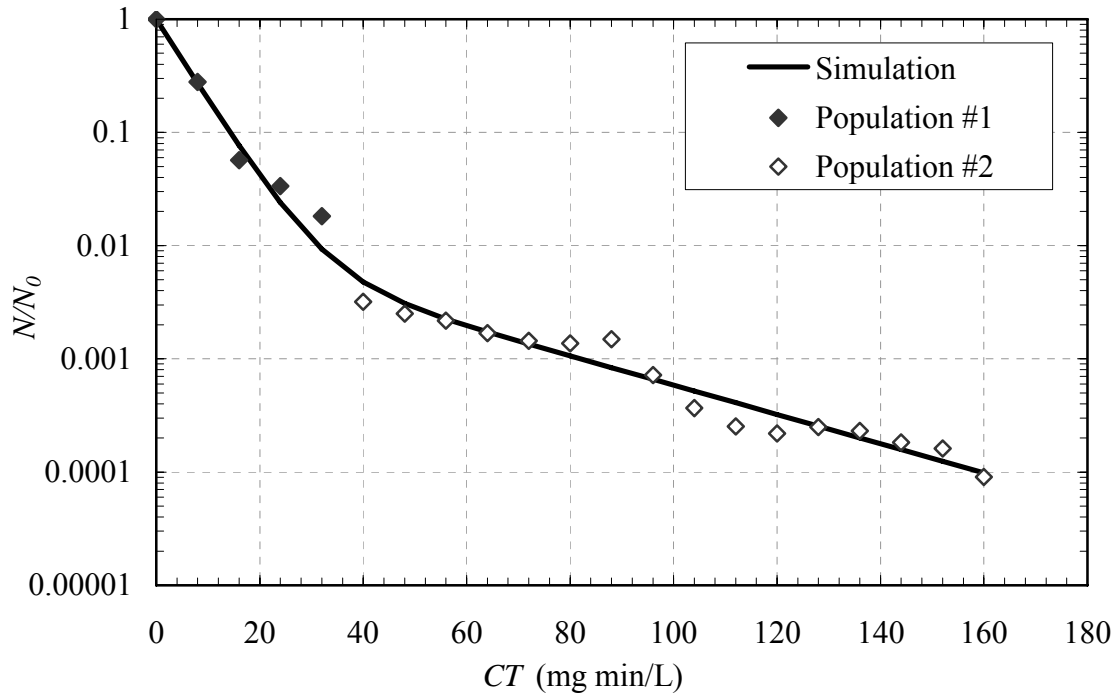


Figure 5.6. Inactivation kinetics of BAC reactor effluent using ( $C_{\text{monochloramine}}=4$  mg/L, pH=8, at 20°C). The curve corresponds to Equation 4. The reported data points are the averages of four replicates.

## 5.6 References

- American Public Health Association (APHA), A.W.W.A.A., Water Environment Federation (WEF) (1992) Standard Methods for the Examination of Water and Wastewater, American Public Health Association, Washington, DC.
- Beccari, M., Majone, M., Massanisso, P. and Ramadori, R. (1998) A Bulking Sludge with High Storage Response Selected under Intermittent Feeding. *Water Research* 32(11), 3403-3413.
- Beun, J.J., Dircks, K., Van Loosdrecht, M.C.M. and Heijnen, J.J. (2002) Poly-Beta-Hydroxybutyrate Metabolism in Dynamically Fed Mixed Microbial Cultures. *Water Research* 36(5), 1167-1180.
- Bouwer, E.J. and Crowe, P.B. (1988) Biological Processes in Drinking Water Treatment. *Journal American Water Works Association* 80(9), 82-93.
- Brown, J. (2002) Abiotic and Biotic Perchlorate Removal in an Activated Carbon Filter, University of Illinois, Urbana-Champaign.
- Brown, J.C., Snoeyink, V.L. and Kirisits, M.J. (2002) Abiotic and Biotic Perchlorate Removal in an Activated Carbon Filter. *Journal American Water Works Association* 94(2), 70-79.
- Brown, J.C., Snoeyink, V.L., Raskin, L. and Lin, R. (2003) The Sensitivity of Fixed-Bed Biological Perchlorate Removal to Changes in Operating Conditions and Water Quality Characteristics. *Water Research* 37(1), 206-214.
- CA-DHS (2005) Perchlorate Drinking Water Action Level and Regulation. , California Department of Health Services, <http://www.dhs.ca.gov/ps/ddwem/chemicals/perchl/perchlindex.htm>.
- Chen, W.F., Cannon, F.S. and Rangel-Mendez, J.R. (2005) Ammonia-Tailoring of Gac to Enhance Perchlorate Removal. II: Perchlorate Adsorption. *Carbon* 43(3), 581-590.
- Choi, Y.-c., Li, X., Raskin, L. and Morgenroth, E. (2008) Chemisorption of Oxygen onto Activated Carbon Can Enhance the Stability of Biological Perchlorate Reduction in Fixed Bed Biofilm Reactors. *Water Research* Accepted.
- Coates, J.D. and Achenbach, L.A. (2004) Microbial Perchlorate Reduction: Rocket-Fuelled Metabolism. *Nature Reviews Microbiology* 2(7), 569-580.
- Dasgupta, P.K., Martinelango, P.K., Jackson, W.A., Anderson, T.A., Tian, K., Tock, R.W. and Rajagopalan, S. (2005) The Origin of Naturally Occurring Perchlorate: The Role of Atmospheric Processes. *Environmental Science & Technology* 39(6), 1569-1575.
- Driedger, A.M., Rennecker, J.L. and Marinas, B.J. (2001) Inactivation of *Cryptosporidium Parvum* Oocysts with Ozone and Monochloramine at Low Temperature. *Water Research* 35(1), 41-48.
- Ehrhardt, H.M. and Rehm, H.J. (1985) Phenol Degradation by Microorganisms Adsorbed on Activated Carbon. *Applied Microbiology and Biotechnology* 21(1-2), 32-36.

- Eynde, E.v.d., Vriens, L., Wynants, M. and Verachtert, H. (1984) Transient Behaviour and Time Aspects of Intermittently and Continuously Fed Bacterial Cultures with Regard to Filamentous Bulking of Activated Sludge. *Applied Microbiology and Biotechnology* 19, 44-52.
- Greer, M.A., Goodman, G., Pleus, R.C. and Greer, S.E. (2002) Health Effects Assessment for Environmental Perchlorate Contamination: The Dose Response for Inhibition of Thyroidal Radioiodine Uptake in Humans. *Environmental Health Perspectives* 110(9), 927-937.
- Gu, B.H., Brown, G.M., Maya, L., Lance, M.J. and Moyer, B.A.A. (2001) Regeneration of Perchlorate (ClO<sub>4</sub><sup>-</sup>)-Loaded Anion Exchange Resins by a Novel Tetrachloroferrate (FeCl<sub>4</sub><sup>-</sup>) Displacement Technique. *Environmental Science & Technology* 35(16), 3363-3368.
- Kim, H.S., Jaffe, P.R. and Young, L.Y. (2004) Simulating Biodegradation of Toluene in Sand Column Experiments at the Macroscopic and Pore-Level Scale for Aerobic and Denitrifying Conditions. *Advances in Water Resources* 27(4), 335-348.
- Krishna, C. and Van Loosdrecht, M.C.M. (1999) Effect of Temperature on Storage Polymers and Settleability of Activated Sludge. *Water Research* 33(10), 2374-2382.
- Luh, J. and Marinas, B.J. (2007) Inactivation of Mycobacterium Avium with Free Chlorine. *Environmental Science & Technology* 41(14), 5096-5102.
- MA-DEP (2006) Drinking Water Status on Perchlorate by Ma Department of Environmental Protection, <http://www.mass.gov/dep/water/drinking/percinfo.htm#stds>.
- Min, B., Evans, P.J., Chu, A.K. and Logan, B.E. (2004) Perchlorate Removal in Sand and Plastic Media Bioreactors. *Water Research* 38(1), 47-60.
- Nerenberg, R. and Rittmann, B.E. (2004) Hydrogen-Based, Hollow-Fiber Membrane Biofilm Reactor for Reduction of Perchlorate and Other Oxidized Contaminants. *Water Science and Technology* 49(11-12), 223-230.
- Nerenberg, R., Rittmann, B.E. and Najm, I. (2002) Perchlorate Reduction in a Hydrogen-Based Membrane-Biofilm Reactor. *Journal American Water Works Association* 94(11), 103-114.
- Norton, C.D. and LeChevallier, M.W. (2000) A Pilot Study of Bacteriological Population Changes through Potable Water Treatment and Distribution. *Applied and Environmental Microbiology* 66(1), 268-276.
- Pernitsky, D.J., Finch, G.R. and Huck, P.M. (1995) Disinfection Kinetics of Heterotrophic Plate-Count Bacteria in Biologically Treated Potable Water. *Water Research* 29(5), 1235-1241.
- Richardson, S.D. (2003) Disinfection by-Products and Other Emerging Contaminants in Drinking Water. *Trends in Analytical Chemistry* 22(10), 666-684.
- Urbansky, E.T. (2002) Perchlorate as an Environmental Contaminant. *Environmental Science and Pollution Research* 9(3), 187-192.

- Urfer, D., Huck, P.M., Booth, S.D.J. and Coffey, B.M. (1997) Biological Filtration for BOM and Particle Removal: A Critical Review. *Journal American Water Works Association* 89(12), 83-98.
- US-EPA (2005) State Perchlorate Advisory Levels and Other Resources, [http://www.epa.gov/fedfac/documents/perchlorate\\_links.htm](http://www.epa.gov/fedfac/documents/perchlorate_links.htm).
- US-EPA (2008) Drinking Water Contaminant Candidate List 3 US-EPA, <http://www.epa.gov/safewater/ccl/ccl3.html>.
- van Aalst-van Leeuwen, M.A., Pot, M.A., van Loosdrecht, M.C.M. and Heijnen, J.J. (1997) Kinetic Modeling of Poly(Beta-Hydroxybutyrate) Production and Consumption by *Paracoccus Pantotrophus* under Dynamic Substrate Supply. *Biotechnology and Bioengineering* 55(5), 773-782.
- van Loosdrecht, M.C.M., Pot, M.A. and Heijnen, J.J. (1997) Importance of Bacterial Storage Polymers in Bioprocesses. *Water Science and Technology* 35(1), 41-47.
- Venkatesh, K.R., Cobe, E.R., Jennings, D.L. and Wagner, N.J. (2000) Process for the Removal and Destruction of Perchlorate and Nitrate from Aqueous Streams, U.S. patent 6,066,257, U.S.A.
- Weber, W.J. (1974) Adsorption Processes. *Pure and Applied Chemistry* 37(3), 375-392.
- Xiong, Z., Zhao, D.Y. and Pan, G. (2007) Rapid and Complete Destruction of Perchlorate in Water and Ion-Exchange Brine Using Stabilized Zero-Valent Iron Nanoparticles. *Water Research* 41(15), 3497-3505.
- Xu, J., Song, Y., Min, B., Steinberg, L. and Logan, B. (2003) Microbial Degradation of Perchlorate: Principles and Applications. *Environmental Engineering Science* 20(5), 405-422.
- Zhang, H., Logan, B.E., Regan, J.M., Achenbach, L.A. and Bruns, M.A. (2005) Molecular Assessment of Inoculated and Indigenous Bacteria in Biofilms from a Pilot-Scale Perchlorate-Reducing Bioreactor. *Microbial Ecology* 49(3), 388-398.
- Zhao, X.D., Hickey, R.F. and Voice, T.C. (1999) Long-Term Evaluation of Adsorption Capacity in a Biological Activated Carbon Fluidized Bed Reactor System. *Water Research* 33(13), 2983-2991.

## **Chapter 6**

### **Conclusions and Future Research**

#### **6.1 Conclusions**

The main goal of this work was to apply environmental biotechnology complemented with studies on microbial communities to provide a feasible solution for the removal of oxy-anion contaminants from drinking water. To reach the main goal, two objectives were established: (i) to optimize biofilm reactor operation using knowledge obtained from microbial community characterization, and (ii) to study the potential of biofilm reactors to produce high quality drinking water from water sources contaminated with perchlorate and nitrate. The two objectives were approached through two lines of experiments that were conducted concurrently. A series of biofilm reactors were studied with respect to the following factors: (i) design parameters (i.e., biofilm support material and reactor size); (ii) operating conditions (i.e., backwash, addition of nutrient and electron donor); and (iii) post-treatment (i.e., disinfection). A number of microbial community studies were conducted using molecular techniques targeting the 16S rRNA and 16S rRNA gene (i.e., clone library and sequencing, real time PCR, and a solution-based hybridization assay): (i) to elucidate how the microbial communities inside these



biofilm reactors responded to changes in design and operation factors; (ii) to determine how the microbial responses correlated to reactor performance; and (iii) to predict how the microbial composition inside bioreactors may affect post-treatment. Results presented in this work demonstrated the potential of biological treatment for drinking water purposes. Further research should head to achieve the ultimate goal of maximizing beneficial functions and minimize possible negative effects of microbial communities in engineered systems to provide high quality water.

This study of biofilm reactors started with a comparison of two types of support materials for biofilm attachment: glass beads vs. GAC. The former has an inert surface, while the latter can adsorb a variety of compounds that are relevant to biological processes. To compare these two support materials, two reactors containing glass beads and GAC, respectively, were evaluated in terms of perchlorate reduction under dynamic influent compositions (i.e., short- and long-term high influent DO) (Appendix B). During these dynamic phases, GAC could adsorb DO, a competing electron acceptor for perchlorate, and allowed biological perchlorate reduction to take place in the attached biofilm. In contrast, biological perchlorate reduction stalled in the glass bead biofilm reactors under similar conditions. In addition, in a separate experiment in which electron donor was added in an intermittent pattern, the GAC surface served as a reservoir for a fraction of the excess electron donor (Chapter 5). In short, biofilm reactors using GAC as a support material for biofilm growth (i.e., BAC reactors) showed advantages under dynamic influent conditions due to the adsorption capacity of GAC.

Changes in reactor operating conditions had short- and long-term impacts on the structure of microbial communities inside biofilm reactors, and consequently microbial

communities affected reactor performance at different time scales. When the backwash frequency was increased (i.e., monthly to daily), the glass bead biofilm reactor initially lost a significant amount of biomass, and then the three most abundant bacterial genera exhibited different trends in relative abundance as a result of adjusting to the new backwash method (Chapter 3 and Appendix A). In the meantime, reactor performance dropped in correspondence to the initial biomass loss, and then a gradual improvement was observed, likely resulting from the adjustment of the microbial community. In contrast, when backwash intensity was elevated (i.e., normal to high intensity), the PRB population failed to adjust to the new operation, and its relative abundance dropped. Correspondingly, the reactor performance deteriorated.

Phosphorus addition enhanced the performance of two BAC reactors; however, its impacts on the microbial communities of the two reactors were different (Chapter 4). For the bench-scale BAC reactor, phosphorus addition improved perchlorate and nitrate reduction, which was coupled with the increases in the relative abundance of *Dechloromonas* and *Azospira*, two known perchlorate reducing bacterial genera. In comparison, for the pilot-scale BAC reactor, phosphorus addition had a similar impact on reactor performance, but it caused a decrease in the relative abundance of *Dechloromonas*, the only PRB detected, and an increase in the relative abundance of *Zoogloea*. The observed opposite trends in microbial responses of the two BAC reactors suggested that lab-scale experiments may not always be able to accurately describe or predict what happens in systems of a larger scale.

The solution-based hybridization assay using PNA MB probes showed its potential to quantify 16S rRNA in environmental samples (Chapter 2). The hybridization

kinetic experiments showed faster kinetics in the hybridization of PNB MB with non-target template, presumably due to faster dissociation kinetics. For some PNA MB sequences, hybridization temperature was sufficient to control hybridization stringency, whereas for other sequences, formamide concentration in hybridization buffers was more suitable. Applications of PNA MB to quantify specific microbial groups were successful for artificial mixtures and environmental samples under optimized hybridization conditions.

In conclusion, this work contributes to the knowledge base to apply environmental biotechnology to drinking water treatment, and complements the understanding of engineering practice with scientific knowledge from microbial community studies. The engineering part of the work focused on both the removal of the contaminants and the overall impacts of the biofilm reactors on the quality of finished waters, which provides a more complete picture of biological drinking water treatment in removing inorganic contaminants. The microbial studies provide a framework of studying the correlation between reactor operation/performance and microbial community. Although the microbial knowledge was primarily used to explain the reactor performance, efforts were made to apply the knowledge to guide system operation.

## **6.2 Future Research**

To make biological treatment a practical solution for drinking water treatment, further optimization of reactor operation and detailed evaluation of post treatment options are

needed. In the meantime, microbial community studies can provide insights in system optimization.

1. Multiple Contaminants

Compared to abiotic counterparts, biological drinking water treatment can consistently remove multiple contaminants without generating concentrated waste streams. This work and the previous studies from our lab demonstrated the advantage of possessing GAC adsorption as an additional treatment mechanism in BAC reactors. Therefore, BAC-based biological treatment technology deserves further investigation for drinking water treatment. As the next step, their potential of simultaneously removing inorganic and organic contaminants, including natural organic matter, should be explored.

2. Comparison with Currently Operated BAC filters

Many drinking water treatment plants operate their GAC filters as biofilters, on which biofilm develops by utilizing natural organic matter present in source waters. Based on this work, it was hypothesized that despite lower biomass quantity, such biofilters may contain microbial communities that are more diverse than those in BAC reactors fed external electron donors, and consequently have a higher likelihood of containing strains resistant to disinfection. To test the hypothesis, comparison between the two types of systems is necessary with respect to microbial composition and disinfection kinetics.

3. Other Post-treatment Approaches

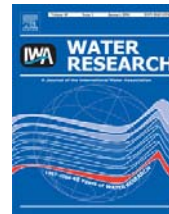
This work has demonstrated the disinfection efficiency of monochloramine for biologically treated finished water. However, inactivated biomass can still be of aesthetic concerns for drinking water supplies and need to be removed. Therefore, post-treatment processes that can remove biomass, live or dead, need to be investigated, e.g., membrane units, membrane units plus disinfection, and longer filter depth.

#### 4. Application of Microbial Knowledge to Guide Reactor Operation

One major goal of studying the structure of microbial communities during engineering studies is to use microbial knowledge to guide the design and operation of engineered systems. In this work, implications on disinfection kinetics were made based on microbial community studies. As the next step, these engineering implications should be verified. In addition, efforts should be made to combine the knowledge from microbial community studies and newly obtained genomic information of individual species to predict the potential of bioreactors to remove emerging contaminants.

## **Appendix A**

### **Effect of Backwashing on Perchlorate Removal in Fixed Bed Biofilm Reactors**

Available at [www.sciencedirect.com](http://www.sciencedirect.com)journal homepage: [www.elsevier.com/locate/watres](http://www.elsevier.com/locate/watres)

## Effect of backwashing on perchlorate removal in fixed bed biofilm reactors

Young Chul Choi<sup>a,1</sup>, Xu Li<sup>a,2</sup>, Lutgarde Raskin<sup>a,2</sup>, Eberhard Morgenroth<sup>a,b,\*</sup>

<sup>a</sup>Department of Civil and Environmental Engineering, University of Illinois at Urbana-Champaign, 205 N. Mathews Ave., Urbana, IL 61801, USA

<sup>b</sup>Department of Animal Sciences, University of Illinois at Urbana-Champaign, 205 N. Mathews Ave., Urbana, IL 61801, USA

### ARTICLE INFO

#### Article history:

Received 29 September 2006

Received in revised form

8 January 2007

Accepted 10 January 2007

Available online 26 March 2007

#### Keywords:

Perchlorate

Fixed bed biofilm reactor

Backwash

Oxygen

Competing electron acceptor

### ABSTRACT

The influence of backwashing on biological perchlorate reduction was evaluated in two laboratory scale fixed bed biofilm reactors using 1- or 3-mm glass beads as support media. Influent perchlorate concentrations were 50 µg/L and acetate was added as the electron donor at a concentration of 2 mg C/L. Perchlorate removal was evaluated at various influent dissolved oxygen (DO) concentrations. Complete perchlorate removal was achieved with an influent DO concentration of 1 mg/L resulting in bulk phase DO concentrations below the detection limit of 0.01 mg/L. The influence of increasing influent DO concentrations for 12 h periods was evaluated before and after individual backwash events. Partial perchlorate removal was achieved with an influent DO concentration of 3.5 mg/L before a strong backwash (bulk phase DO concentrations of approximately 0.2 mg/L), while no perchlorate removal was observed after the strong backwash at the same influent DO level (bulk phase DO concentrations of approximately 0.8 mg/L). The immediate effect of backwashing depended on influent DO concentrations. With influent DO concentrations of 1 mg/L, strong backwashing resulted in a brief (<12 h) increase of effluent perchlorate concentrations up to 20 µg/L; more pronounced effects were observed with influent DO concentrations of 3 mg/L. Daily weak backwashing had a small and, over time, decreasing negative influence on perchlorate reduction, while daily strong backwashing ultimately resulted in the breakdown of perchlorate removal with influent DO concentrations of 3 mg/L.

© 2007 Elsevier Ltd. All rights reserved.

### 1. Introduction

Nine states in the US have recently defined state perchlorate advisory levels ranging from 1 to 18 µg/L for drinking water (USEPA, 2006). Several studies have shown that biological treatment is an effective technology to remove perchlorate from drinking water (Brown et al., 2002; Giblin et al., 2000;

Herman and Frankenberger, 1999; Min et al., 2004). For example, for a typical groundwater concentration of 50 µg/L, biologically active carbon (BAC) fixed bed reactors consistently removed perchlorate to below 2 µg/L (Brown et al., 2002, 2005). Despite these encouraging studies, the reliability of biological drinking water treatment is sometimes questioned, in particular under dynamic loading conditions and during

\*Corresponding author. Department of Civil and Environmental Engineering, University of Illinois at Urbana-Champaign, 3219 Newmark Civil Engineering Laboratory, MC-250, 205 N. Mathews Ave., Urbana, IL 61801, USA. Tel.: +1 217 333 6965, fax: +1 217 333 6968.

E-mail address: [emorgenr@uiuc.edu](mailto:emorgenr@uiuc.edu) (E. Morgenroth).

<sup>1</sup> Current address: Department of Microbiology, University of Massachusetts Amherst, Amherst, MA 01003, USA.

<sup>2</sup> Current address: Department of Civil and Environmental Engineering, University of Michigan, 1351 Beal Ave., Ann Arbor, MI 48109, USA.

0043-1354/\$ - see front matter © 2007 Elsevier Ltd. All rights reserved.

doi:10.1016/j.watres.2007.01.025

changes in reactor operation, such as after backwashing (Kim and Logan, 2001). The current study evaluates the influence of backwashing on perchlorate removal in fixed bed biofilm reactors.

Regular backwashing is a key process for fixed bed biofilm reactors that is necessary to prevent clogging, to reduce excessive head loss across the filter, to maintain an active biofilm, to prevent the proliferation of filamentous bacteria and eukaryotic organisms, such as fungi and protozoa, and to enhance the mass transfer of contaminants to the biofilm (Brown et al., 2002; Hozalski and Bouwer, 1998; Laurent et al., 2003). However, backwashing also reduces the amount of active biomass in the reactor, which could potentially lead to unstable reactor performance (Lahav et al., 2001; Nakhla and Farooq, 2003). Optimal strategies for backwashing of biofilm reactors used for drinking water treatment are not well defined (Ahmad et al., 1998; Chaudhary et al., 2003; Laurent et al., 2003; Liu et al., 2001). For a perchlorate removing fluidized bed biofilm reactor, McCarty and Meyer (2005) demonstrated that, using a model based sensitivity analysis, biofilm detachment was a key factor influencing effluent perchlorate concentration. In their system, detachment was achieved by removing the most buoyant BAC particles from the top of the reactor, cleaning them externally, and then returning cleaned BAC into the fluidized bed. In fixed bed reactors the main process to remove biomass is backwashing by air scouring and filter bed expansion. Backwashing is typically performed in intervals ranging from 1 to 7 days (Boller et al., 1997). However, in some cases, backwashing intervals can be months (Brown et al., 2003). Backwashing intervals are usually determined by setting a fixed filter run time and a maximum head loss across the filter bed (Boller et al., 1997; Niquette et al., 1998). Using fixed bed reactors packed with plastic or sand media, Min et al. (2004) were able to reduce 77 µg/L perchlorate in groundwater to below 4 µg/L. Regular weekly backwashing was necessary to prevent short-circuiting, especially in their reactor packed using sand as a biofilm support medium. However, Kim and Logan (2000) observed that perchlorate removal in BAC reactors was not stable after backwashing. They suggested that perchlorate previously adsorbed to the granular activated carbon desorbed after backwashing, which caused fluctuating effluent perchlorate concentrations.

Evaluating the effect of backwashing on fixed bed biofilm reactor performance is complicated by the fact that backwashing influences a range of process conditions including fluid flow in the fixed bed, the amount of biomass, and biofilm

structure. Biomass in fixed bed reactors is retained both in the form of biofilms attached to the surfaces of the support medium and in the form of large microbial aggregates that accumulate in the inter-particle space (Delahaye et al., 1999; Laurent et al., 2003). Backwashing removes the majority of the loosely attached, large microbial aggregates and a smaller fraction of the tightly attached biofilms (Servais et al., 1991). Mass transfer limitations of dissolved oxygen (DO) into large microbial aggregates reduce process efficiencies for aerobic processes (e.g., oxidation of organic carbon or nitrification) (Laurent et al., 1999, 2003). However, for perchlorate and nitrate removal, such microbial aggregates can be beneficial as DO mass transfer limitations can result in local anaerobic or anoxic zones allowing for perchlorate and nitrate reduction despite the presence of DO in the bulk phase. Kim et al. (2004) showed that oxygen and nitrate can be reduced simultaneously using a column reactor containing an aerobic and a denitrifying bacterial strain. Neither of these two populations were facultative aerobes and the bulk phase DO concentration was too high for denitrification to occur in the bulk liquid. They attributed their observation to the existence of anoxic zones allowing denitrifiers to reduce nitrate even when the bulk phase DO concentration was high. The impact of such mass transfer limitations on perchlorate removal in fixed bed reactors is not well understood.

The purpose of this study was to evaluate the influence of the frequency and intensity of backwash on perchlorate removal in biofilm reactors under varying influent DO levels for two fixed bed reactors with two different diameter glass beads (1 or 3 mm) as biofilm support media. Responses of these biofilm reactors to increasing influent DO levels were monitored before and after individual backwash events. In addition, repeated daily backwash experiments were conducted with weak or strong backwashing.

## 2. Materials and methods

### 2.1. Reactors and reactor operation

Two laboratory-scale fixed bed column reactors with an inner diameter of 2.4 cm and a length of 14 cm were filled, respectively, with 1- and 3-mm diameter glass beads as packing materials and were operated in parallel. Physical parameters for both reactors are summarized in Table 1. The surface of the glass beads was etched for 1 h using 0.25% HF to enhance the adhesion of bacteria. The influent flow was

**Table 1 – Physical dimensions of the biofilm systems**

	1-mm glass bead reactor	3-mm glass bead reactor
Empty bed volume (mL)	63.4	63.4
Reactor volume occupied by the glass bead (mL)	38.7	37.0
Measured porosity of the glass bead bed	0.429	0.454
Surface area of the reactor wall (m <sup>2</sup> )	0.011	0.011
Surface area of the glass beads (m <sup>2</sup> )	0.133	0.040
Total surface area (m <sup>2</sup> )	0.144	0.051



introduced in the bottom of the reactor at a rate of 2.7 mL/min ( $Q_{\text{influent}}$ ), resulting in an empty bed contact time of 23.4 min. A recirculation loop ( $Q_{\text{recirculation}} = 5 \times Q_{\text{influent}}$ ) was added to approximate completely mixed conditions of the bulk liquid. Flow distribution in the column may have been influenced to some extent by wall-effects with column to glass bead ratios of 24 and 8 for the 1 and 3-mm glass bead reactors, respectively (Cohen and Metzner, 1981). The 3-mm glass bead reactor was inoculated with biomass from a BAC filter previously operated with deionized, distilled water amended with 2 mg C/L acetate and 50  $\mu\text{g/L}$  perchlorate (Brown et al., 2002) and then with groundwater amended with 50  $\mu\text{g/L}$  perchlorate (Lin, 2004). The 1-mm glass bead reactor was inoculated with biomass collected from the 3-mm glass bead reactor which had been previously operated for 7 months.

Acetate was used as the sole electron donor at an influent concentration of 2 mg C/L. The electron donor was delivered with a syringe pump and was mixed immediately before entering the reactor with a feed solution containing perchlorate and oxygen. The feed solution was prepared with deionized water and contained 50  $\mu\text{g/L}$  perchlorate, 0.15 mg N/L  $\text{NH}_4\text{Cl}$ , and 0.5 mM phosphate buffer resulting in pH 7.5. The influent DO level was adjusted to concentrations ranging from 1 to 4 mg/L by purging the feed solution with  $\text{N}_2$  gas. The feed solution was isolated from the atmosphere after purging using a floating cover to prevent oxygen transfer.

Both reactors were operated with a baseline influent DO level of 1 mg/L without backwashing for 4 weeks. The influent

DO level was increased from 1 to 4 mg/L for a 12-h period on day 28. A strong backwash (see below for details) was performed on day 29, followed by another 12-h period of operation with an influent DO level of 4 mg/L on day 30. The transient exposure to increased DO levels and backwashing was repeated with an influent DO concentration of 3.5 mg/L, beginning on day 62. The effect of daily backwashing was evaluated after increasing the influent DO level to 3 mg/L on day 68. Five daily weak backwash events (starting on day 68) were followed by six daily strong backwash events (starting on day 73). After the period with daily strong backwash events, the reactors were monitored for 1 week without backwashing followed by another strong backwash on day 85. The influent DO level was reduced from 3 to 1 mg/L on day 102. Influent DO levels and timing of backwash events are schematically represented at the top of Figs. 1 and 3–6.

Backwashing was performed with two different intensities. A “weak backwash” was performed by placing the contents of the reactor into a 600-mL beaker and adding 100 mL of previously collected effluent. The reactor contents were stirred for 1 min with a 7.5 cm long magnetic stir bar using a stir plate at 75 revolutions per minute (RPM). The supernatant containing the detached biomass was decanted. A “strong backwash” was performed by placing the contents of the reactor into a 600-mL beaker, adding 125 mL of collected effluent, stirring at 150 RPM for 1 min, and decanting the supernatant containing the detached biomass. For the strong backwash, this process was repeated once. The biomass

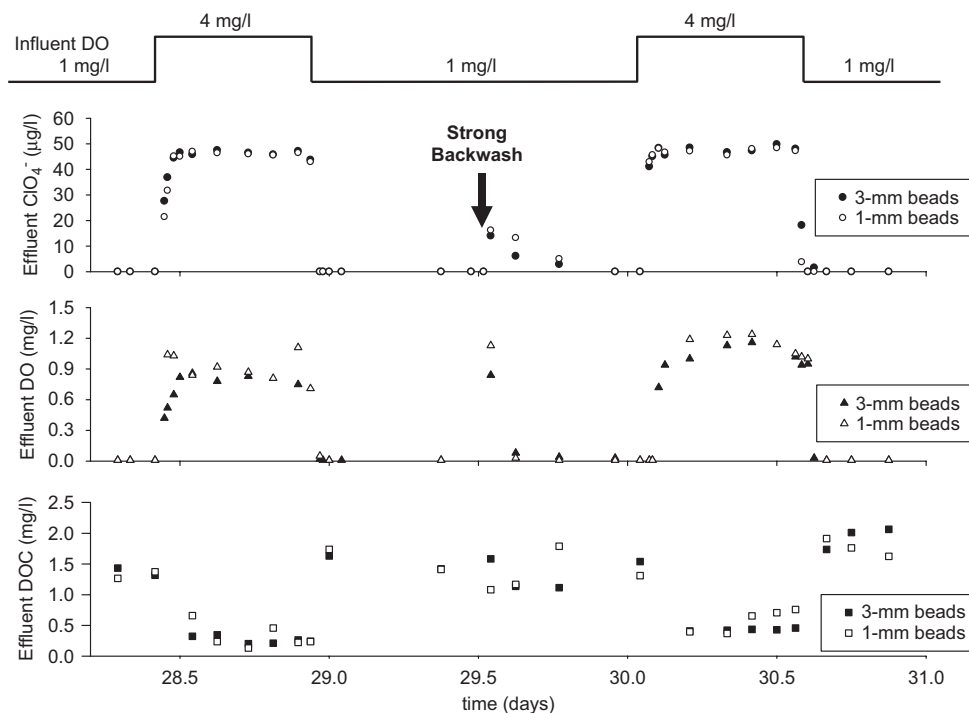


Fig. 1 – Reactor performance for 1-mm (open symbols) and 3-mm glass bead reactors (closed symbols) in response to increasing influent DO concentrations from 1 to 4 mg/L before and after backwash events.

detached during backwashing was quantified as volatile suspended solids (VSS).

## 2.2. Analytical methods

DO was measured using a galvanic oxygen sensor (WTW CelloX 325 with Oxi 340i, Weilheim, Germany) with a detection limit of 0.01 mg/L in a flow cell (WTW model D201, Weilheim, Germany) connected directly to the reactor effluent. Perchlorate was measured using an ion chromatograph (Dionex ICS-2000, Sunnyvale, CA, USA) with an AS50 autosampler and a conductivity detector. An AS16 column and an AG16 guard column were used and the detection limit was 1 µg/L. The eluent was 65 mM KOH at a flow rate of 1.2 mL/min and the injection volume was 990 µL. Dissolved organic carbon (DOC) was measured using a UV-Persulfate TOC Analyzer (Tekmar-Dohrmann Phoenix 8000, Mason, OH, USA) with a detection limit of 0.2 mg/L as C. All samples were filtered using a 0.45 µm filter (Nalgene SFCA 25 mm, Nalge Nunc International, Rochester, NY, USA) prior to analysis. VSS were measured according to Standard Methods (APHA et al., 1999). A stereomicroscope (Zeiss Stemi 2000-C, Oberkochen, Germany) was used to image the biofilm growth patterns directly through the glass wall of the reactors without disturbing the biomass structure.

## 3. Results

### 3.1. Influent DO variations and individual backwash events

During the initial baseline operation with an influent DO level of 1 mg/L, effluent perchlorate concentrations for both reactors were consistently below the detection limit of 1 µg/L (days 0–28). When the influent DO level was increased to 4 mg/L for a period of 12 h on day 28, perchlorate removal immediately ceased and effluent perchlorate concentrations increased to 50 µg/L (Fig. 1). During that period, effluent DO concentrations increased from below the detection limit of 0.01 mg/L to approximately 1 mg/L and effluent DOC concentrations decreased from approximately 1.5 to below 0.5 mg C/L in both reactors (Fig. 1). Based on the observed DOC removal (2 mg C/L = 5.33 mg COD/L) and DO removal (3.2 mg/L), a net yield ( $Y_H$ ) of 0.4 g COD<sub>biomass</sub>/g COD<sub>acetate</sub> can be calculated assuming that all acetate in the influent was metabolized and that the DOC in the effluent only consisted of soluble microbial products. This observed net yield is reasonable for heterotrophic growth (Henze et al., 2002). With relatively high bulk phase (= effluent) DO concentrations of approximately 1 mg/L, mass transfer limited anaerobic zones were likely not present, explaining the absence of perchlorate removal during this 12-h period of increased influent DO concentrations. As soon as the influent DO level was returned to baseline conditions, both reactors removed perchlorate completely (Fig. 1).

A strong backwash was performed 12 h after the end of the period with increased influent DO concentrations (Fig. 1). Immediately following the backwash event, the effluent perchlorate concentrations increased to approximately

15 µg/L in both reactors followed by a complete recovery of perchlorate removal within 12 h. On day 30 (12 h after the backwash event), the influent DO level was increased again to 4 mg/L for a period of 12 h. Similar to the previous results, effluent perchlorate concentrations reached almost 50 µg/L, effluent DO concentrations increased, and DOC concentrations decreased in both reactors. However, both DO and DOC concentrations were slightly higher than during the previous period with the same 4 mg/L influent DO levels, suggesting that, after backwashing, aerobic acetate oxidation was biomass limited. As soon as baseline operation was resumed, again, both reactors removed perchlorate completely.

In this study, glass beads were selected as the support medium for biofilm growth, instead of a sorptive material such as granular activated carbon, to allow evaluation of the effect of biomass growth and detachment patterns without interference from sorption or desorption of perchlorate and oxygen. The amounts of biomass detached during backwashing on day 29 were 28.3 and 18.8 mg VSS for the 1- and 3-mm glass bead reactors, respectively. The reactors had been operated for 4 weeks without backwashing prior to backwashing on day 29. Assuming an average effluent acetate concentration of 1.5 mg C/L during baseline operation with an influent DO level of 1 mg/L and a net yield of 0.4 g COD<sub>biomass</sub>/g COD<sub>acetate</sub>, the estimated biomass production for this 4-week period is 41 mg VSS. The amount of biomass removed during the backwashing accounted for 69% and 46% of the estimated biomass production during this period in the 1- and 3-mm glass bead reactors, respectively. However, backwash efficiencies vary and the amount of VSS removed in a single backwash event may be smaller or larger than the net biomass accumulation between backwash events. In addition, biomass may have been lost through detachment during normal operation. The larger amount of biomass removed in the 1-mm glass bead reactor suggests that more biomass accumulated in the 1-mm glass bead reactor, which can be attributed to a larger surface area and an improved ability to retain biomass during normal operation compared to the 3-mm glass bead reactor.

Accumulation of large biomass aggregates in the size range of several hundred micrometers was observed during operation in both reactors (Fig. 2), but they were removed during backwash events. While a quantitative analysis of size and amount of aggregates was beyond the scope of this study, this qualitative observation supports the feasibility of localized mass transport limited zones allowing for perchlorate

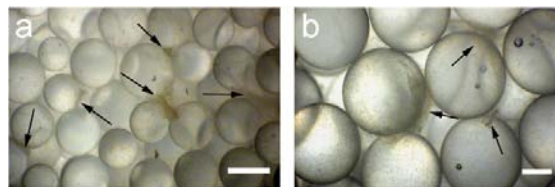


**Fig. 2 – Stereomicroscope image of media from the 1-mm (a) and 3-mm (b) glass bead reactor. Arrows indicate large microbial aggregates. Scale bars denote 1 mm.**

removal to occur in the reactors in spite of increased bulk phase DO concentrations.

The next experimental phase evaluated the influence of short-term increases of influent DO levels to 3.5 mg/L, which is only slightly higher than the estimated DO concentration of 3.2 mg/L required to completely oxidize the 2 mg C/L of acetate present in the influent. Unlike the previous experiment, the response of the reactors during 12-h periods with an influent DO level of 3.5 mg/L was substantially different before and after backwashing (Fig. 3). During the first 12-h period (before backwashing), effluent perchlorate concentrations temporarily increased to 5 and 20 µg/L in the 1- and 3-mm glass bead reactors, respectively. During the second 12-h period (after backwashing), effluent perchlorate concentrations increased to the influent level of 50 µg/L in both reactors. Bulk phase DO concentrations increased to approximately 0.2 mg/L in the first and approximately 0.8 mg/L during the second 12-h period. Bulk phase DOC concentrations decreased in both periods to approximately 0.2 mg C/L. The immediate effect of backwashing under baseline conditions (day 65) was similar to the effect observed for the previous backwash and the effluent perchlorate concentrations temporarily increased to 7.3 and 13.7 µg/L in the 1- and 3-mm glass bead reactors, respectively. The amounts of VSS removed during this second backwash event were 58 and 37.5 mg VSS for the 1- and 3-mm glass bead reactors, respectively. The amount of removed VSS is close to the

theoretically expected amount of 53 mg VSS (assuming an average effluent acetate concentration of 1.5 mg C/L for the 36 days of operation since the previous backwash).

### 3.2. Daily backwash events

The effect of daily backwashing was evaluated with an influent DO level of 3 mg/L, which is just below the theoretical stoichiometric requirement for the complete oxidation of the acetate present in the influent. Increasing the influent DO concentration from 1 to 3 mg/L did not result in increased effluent perchlorate concentrations (day 68, before backwashing in Fig. 4). Effluent perchlorate concentrations increased following each of five weak backwash events. In the 1-mm glass bead reactor, effluent perchlorate concentrations decreased to below the detection limit within 24 h, while the recovery in the 3-mm glass bead reactor remained incomplete after the first three backwashes. Daily weak backwashing prevented large microbial aggregates from developing in both glass bead reactors based on visual examination of biomass removed during backwash events and of the filter beds. Over time, backwashing had less influence on perchlorate removal in both reactors: the initial weak backwashing caused effluent perchlorate concentrations to increase up to 30 µg/L while perchlorate concentrations after subsequent backwash events remained below 10 µg/L at all times.

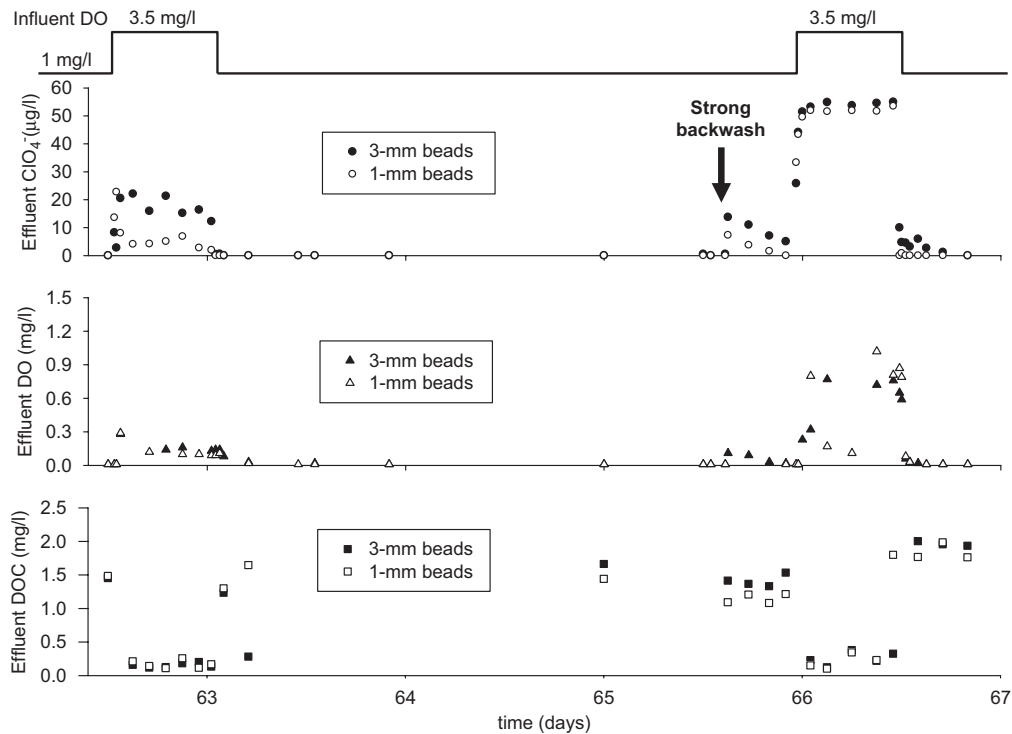
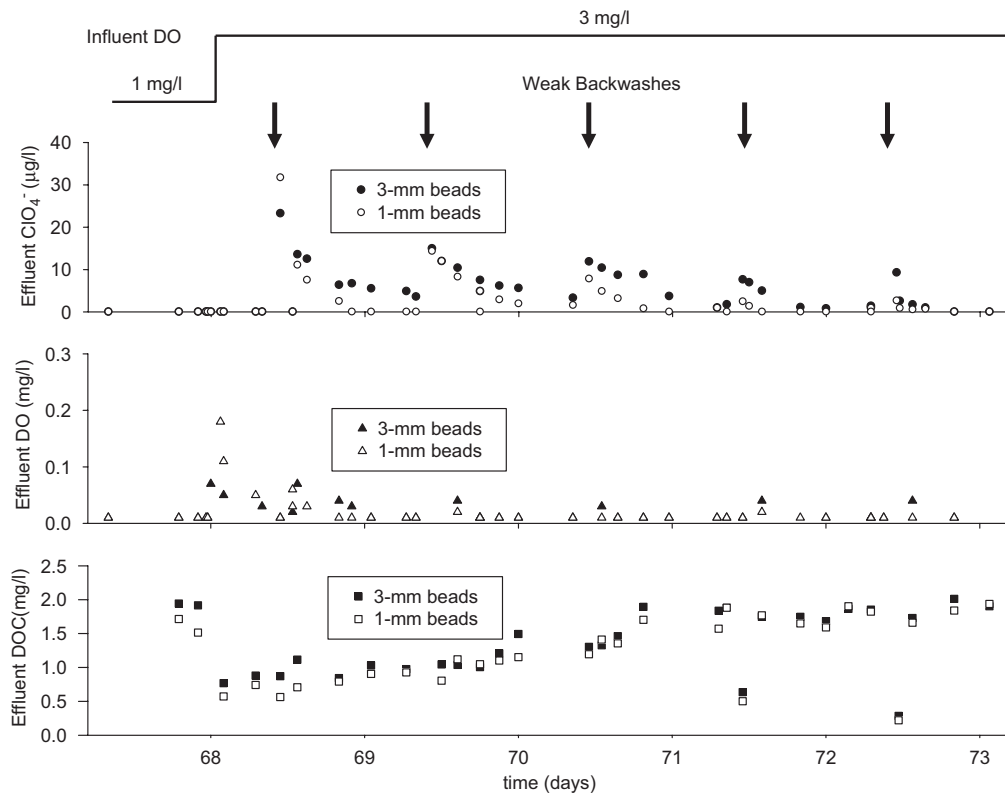


Fig. 3 – Reactor performance for 1-mm (open symbols) and 3-mm glass bead reactors (closed symbols) in response to increasing influent DO concentrations from 1 to 3.5 mg/L before and after backwash events.



**Fig. 4 – Reactor performance for 1-mm (open symbols) and 3-mm glass bead reactors (closed symbols) in response to weak daily backwash events with influent DO concentrations of 3 mg/L.**

Daily strong backwashing began on day 73 and had a much larger impact on perchlorate removal compared to weak backwashing (Fig. 5). Following five strong backwashing events, effluent perchlorate concentrations in both reactors increased to 50 µg/L and only decreased slowly. In most cases, effluent perchlorate concentrations did not decrease below the detection limit between daily strong backwash events. During the period of daily strong backwashing, effluent DO concentrations were approximately 0.5 mg/L; the effluent DOC concentrations did not show a clear pattern. Lack of perchlorate removal after strong backwashing can be explained by the loss of large biomass aggregates, removal of biofilm growing on the glass bead surface, and increased bulk phase DO concentrations due to biomass limited oxygen removal. Unlike the weak daily backwashing experiment, there was no substantial difference between the performances of 1- and 3-mm glass bead reactors.

### 3.3. Recovery of system performance after strong daily backwashing

After the five daily strong backwashing events, while maintaining an influent DO level of 3 mg/L, perchlorate removal continued to deteriorate (Fig. 6). On day 85, following six strong backwashing events, the effluent perchlorate concen-

trations reached approximately 20 µg/L in both reactors. Perchlorate removal deteriorated further after another strong backwashing event on day 85 even though bulk phase DO concentrations were at times below 0.1 mg/L. Apparently, daily strong backwashing resulted in a substantial decrease in the activity of perchlorate reducing bacteria in the systems. Perchlorate reduction could not be reestablished with an influent DO level of 3 mg/L during a 2-week period without backwashing even though these conditions prior to daily backwashing had allowed for stable and complete perchlorate removal.

After decreasing influent DO levels to 1 mg/L on day 102, bulk phase DO concentrations decreased to below the detection limit and perchlorate removal recovered completely within 2 or 4 days for the 1- and 3-mm glass bead reactors, respectively. During this period, effluent DOC levels increased above influent acetate concentrations, possibly due to an increased release of soluble microbial products after decreasing the influent DO levels to 1 mg/L. The time period necessary for the recovery of perchlorate removal was longer than the time required for system recovery after short-term exposure to increased influent DO levels, but shorter than the time required for initial reactor start-up of 2 weeks (data not shown). The time required for recovery can be explained by the need for regrowth of perchlorate reducing bacteria. The

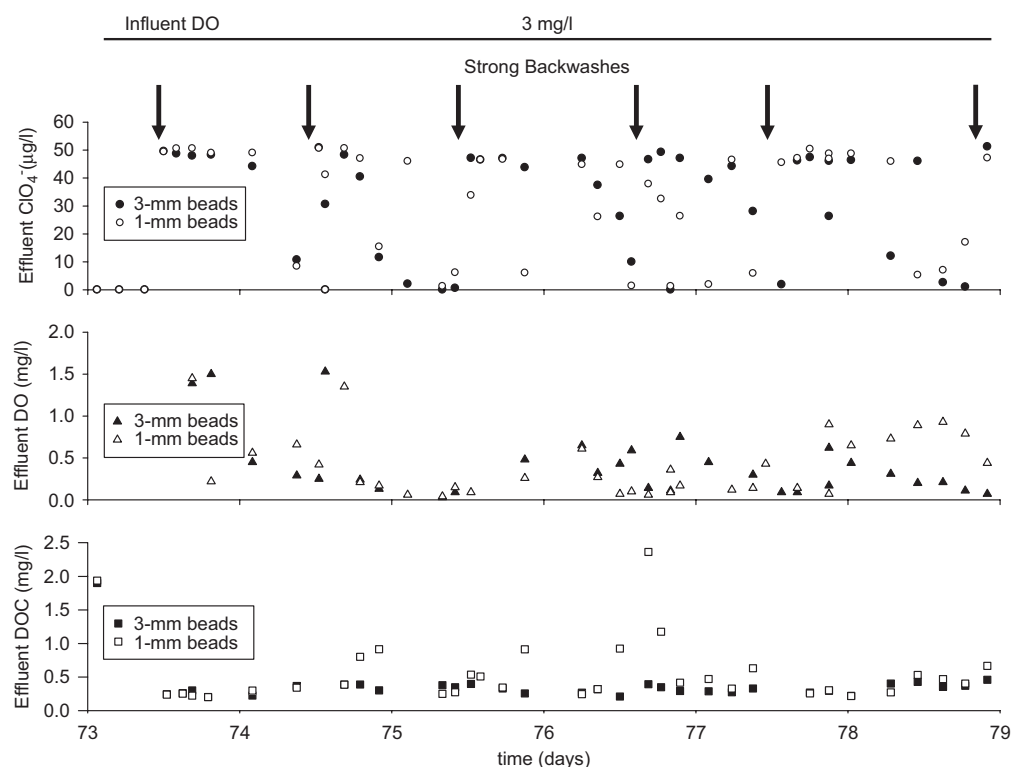


**Fig. 5** – Reactor performance for 1-mm (open symbols) and 3-mm glass bead reactors (closed symbols) in response to strong daily backwash events with influent DO concentrations of 3 mg/L.

faster recovery of the 1-mm compared to the 3-mm glass bead reactor is consistent with the larger surface area in the 1-mm glass bead reactor, which may have retained a larger amount of perchlorate reducing bacteria even during the period of reduced perchlorate removal.

## 4. Discussion

### 4.1. Influence of oxygen

Perchlorate reduction is inhibited by oxygen for all known perchlorate reducing bacteria (Kengen et al., 1999; Song and Logan, 2004; Xu et al., 2003). Inhibition by oxygen also was observed in the current study; an influent DO level of 4 mg/L resulted in bulk phase DO concentrations of approximately 1 mg/L and the breakdown of perchlorate removal (Fig. 1). However, for an influent DO level of 3.5 mg/L, bulk phase DO concentrations were approximately 0.2 mg/L (following a period of more than 4 weeks without backwashing) and with these conditions partial perchlorate removal was observed (day 62 in Fig. 3). The effect of oxygen on perchlorate removal observed in this study is different from previously reported observations. Song (2004) determined a threshold DO concentration to inhibit perchlorate reduction of 0.04 mg/L (only 4% of the influent perchlorate was reduced in a chemostat by

a pure suspended culture of *Dechlorosoma* sp. KJ). Song and Logan (2004) showed that a 12-h exposure to DO concentrations of 6–7 mg/L inhibited perchlorate removal in a suspended culture of *Dechlorosoma* sp. KJ even after oxygen had been removed. In the current study, while no perchlorate removal was achieved with influent DO levels of 4 mg/L (bulk phase DO concentrations of approximately 1 mg/L), complete perchlorate removal was achieved within 30 min after decreasing the influent DO concentrations to 1 mg/L (bulk phase DO concentrations below the detection limit of 0.01 mg/L) (Fig. 1). There are two possible explanations for these differences: (1) inhibition threshold levels and long-term effects of oxygen are species dependent and differ between *Dechlorosoma* sp. KJ and the perchlorate reducing bacteria present in the mixed community in the current study; (2) mass transfer limitations in the current study caused the DO concentrations inside the biofilm to be substantially lower than in the bulk phase. The relevance of mass transfer limitations due to the accumulation of biomass has been well documented for BAC filters (Laurent et al., 2003). With bulk phase DO concentrations of 0.2 mg/L (day 62, Fig. 3), DO concentrations in part of the biofilm conceivably were below the 0.04 mg/L threshold reported by Song (2004). It is interesting to note that on day 62, with an influent DO level of 3.5 mg/L, perchlorate removal was greater in the 1-mm glass bead reactor compared to the removal in the 3-mm glass bead reactor even though the bulk

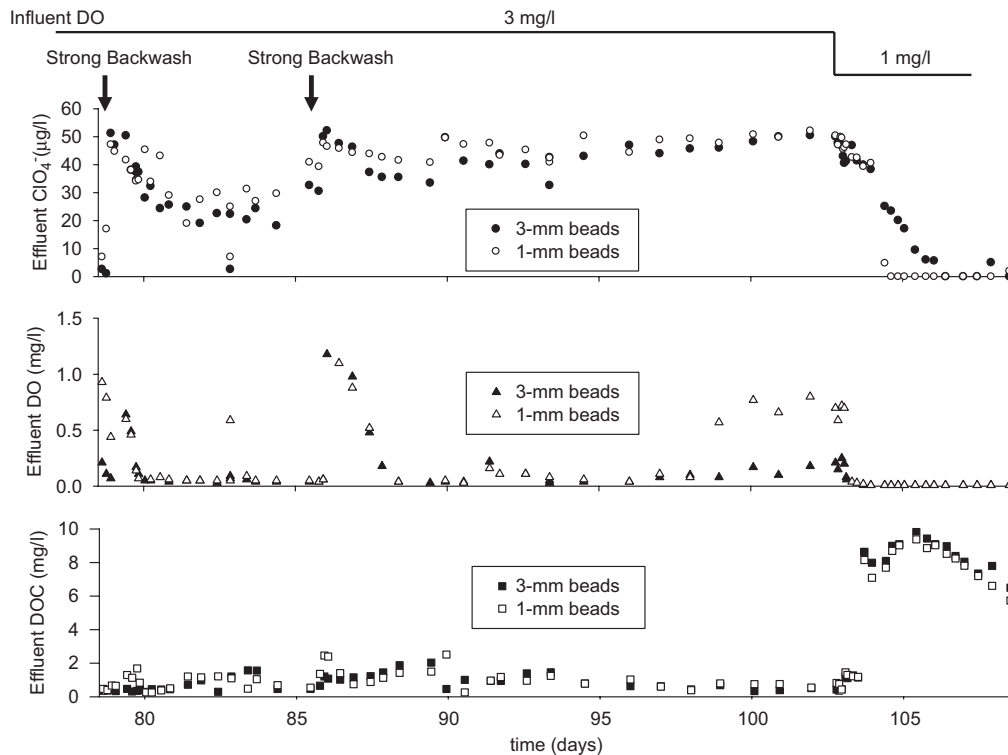


Fig. 6 – Reactor performance for 1-mm (open symbols) and 3-mm glass bead reactors (closed symbols) following a period of strong daily backwashing with influent DO concentrations of 3 or 1 mg/L.

phase DO and DOC were very similar. This result can be explained since the 1-mm glass bead reactor had accumulated more biomass compared to the 3-mm glass bead reactor (based on 58 vs. 37.5 mg VSS that were removed during backwashing, respectively) and presumably a larger fraction of the biomass was anaerobic. This apparent beneficial effect of mass transfer limitations was observed only for relatively low bulk phase DO concentrations of less than 0.2 mg/L. In a deep biofilm anaerobic zones can develop if the biofilm is sufficiently thick and if electron acceptor concentrations relative to electron acceptor concentrations are sufficiently high (Wanner et al., 2006). Oxygen is likely to be limiting for  $\gamma \gg 1$  where

$$\gamma = (1 - Y_H) \frac{D_S S_S}{D_{O_2} S_{O_2}} \quad (1)$$

and where  $D_S$  and  $D_{O_2}$  are diffusion coefficients for the electron donor and oxygen in the biofilm and  $S_S$  and  $S_{O_2}$  are bulk phase electron donor and DO concentrations. For bulk phase DO concentrations of approximately 0.2 mg/L, anaerobic zones are likely to develop for bulk phase acetate concentrations larger than 0.27 mg DOC/L (assuming  $D_S$  and  $D_{O_2}$  of 0.8 and 1.7 cm<sup>2</sup>/d, respectively). Thus, it is feasible that oxygen utilization in the biofilm resulted in anaerobic zones. Problems with the direct application of Eq. (1) to the experimental results in this study are that the effluent DOC most likely accounts for a mixture of organic substrates

including non-biodegradable soluble microbial products and that Eq. (1) does not take into account endogenous respiration. For an influent DO level of 4 mg/L (bulk phase DO concentrations of approximately 1 mg/L), mass transfer limitations were apparently not sufficient to reduce DO concentrations within the biofilm to below the inhibitory threshold (Fig. 1).

#### 4.2. Influence of backwashing

The short-term effect of backwashing on perchlorate removal depended both on influent DO levels and backwash intensity. With an influent DO level of 1 mg/L, a time period of up to 12 h was required for the effluent perchlorate concentration to decrease to below the detection limit following a backwashing event (Figs. 1 and 3). This lag period was longer than the lags observed after short-term increases of influent DO levels, which were typically less than 1 h. Since exposure of biomass from the reactors to DO concentrations of up to 40 mg/L did not result in a lag in perchlorate reduction (data not shown), short-term exposures to the atmosphere during backwashing should not have had an impact on the length of the lag period after backwashing. One explanation for the observed lag could be that some biomass growth was required before complete perchlorate removal could be achieved after backwashing.

With an influent DO concentration of 3 mg/L, the recovery of perchlorate removal after backwashing was even slower. For a single weak backwash, partial perchlorate reduction recovered within approximately 12 h (day 68 in Fig. 4), while after strong backwashing full recovery was not achieved within 24 h (day 73 in Fig. 5). This difference between observed perchlorate removal after weak or strong backwash could be explained by the weak backwash removing mainly loosely attached large microbial aggregates while the strong backwash also removes significant amounts of the strongly attached biofilm. As suggested above, perchlorate reduction in the presence of detectable bulk phase DO concentrations can be achieved in localized anaerobic zones within large microbial aggregates. Removing these aggregates has a larger effect on perchlorate removal for higher bulk phase DO concentrations. With an influent DO level of 1 mg/L, bulk phase DO concentrations were below the detection limit and mass transfer resistance may not be necessary to provide conditions suitable for perchlorate reduction. Brown et al. (2003) reported a different effect of backwashing on perchlorate removal. They observed improved perchlorate removal following backwashing presumably due to reduced clogging and channeling following months of operation without backwashing. In the current study, backwashing never resulted in improved system performance.

In full-scale fixed bed biofilm reactors backwashing intervals are typically much shorter (ranging from 1 to 7 days) than in most research studies. However, backwashing is costly as it causes downtime of the reactors during backwashing and since the wash water needs to be treated. Results from this and other laboratory scale studies (e.g., Brown et al., 2003) indicate that longer intervals between backwashing can be feasible, at least if biological performance is the criterion used for evaluation. In full-scale reactors, shorter intervals between backwashing are often based on process requirements other than the biological performance (e.g., backwashing is performed to prevent localized lumping of filter medium or to distribute active biomass evenly over the height of the reactors). The feasibility of longer backwashing intervals between backwashing for fixed bed biofilm reactors used for drinking water treatment should be further evaluated in pilot or full-scale applications.

The positive effect of localized anaerobic zones on perchlorate reduction was observed only for a narrow range of influent DO levels, while influent DO and electron donor were present in approximately stoichiometric ratios resulting in  $\gamma \approx 1$ . Brown et al. (2005) suggested dosing electron donor at approximately stoichiometric requirements to reduce competing electron acceptors in the influent.<sup>3</sup> In research applications, however, electron donor is often added in much larger concentrations (Brown et al., 2003; Min et al., 2004). It should be noted that conclusions drawn on the influence of

<sup>3</sup> Note that Brown et al. (2005) expressed their acetate dosage as the amount of acetate needed to reduce influent electron acceptors but neglected acetate used for cell synthesis. Taking into account cell synthesis with a net yield of 0.4 g COD<sub>biomass</sub>/g COD<sub>acetate</sub> the acetate dosing of 150–183% of the stoichiometric requirement in their paper corresponds to 90–110% of the actual stoichiometric requirement.

backwashing are applicable only when similar electron donor and acceptor ratios are considered. For practical reactor operation, one goal is to minimize electron donor addition in order to minimize cost. While it is possible to achieve stable performance by adding near-stoichiometric amounts of electron donor, it needs to be considered that minimizing electron donor addition can result in less stable system performance following backwashing.

#### 4.3. Influence of biofilm history

Perchlorate removal depended not only on influent DO and electron donor concentrations but also on the history of the reactor. For daily weak backwashing, the system adjusted to these frequent backwashes after some time. The weak backwash events on days 71 and 72 had a much smaller impact on perchlorate removal than those performed on days 68, 69, and 70 (Fig. 4). This observation may be explained by the development of tightly attached biofilms of perchlorate reducing and other heterotrophic bacteria on the support medium, and the reduced role of loosely attached large aggregates that are easily removed during backwashing. For daily strong backwashing, however, perchlorate removal deteriorated and did not recover even after 17 days without backwashing with influent and operating conditions that had previously allowed for complete perchlorate removal (Fig. 6). Perchlorate removal recovered only after decreasing influent DO levels to 1 mg/L. These results raise questions regarding the extent by which shifts in specific microbial populations and changes in biofilm structure determine reactor performance and how reactor operation can be used to control such shifts. McCarty and Meyer (2005) applied a model to predict perchlorate removal based on the relative penetration of competing electron acceptors (oxygen, nitrate, and perchlorate) into biofilms. In their model, it was assumed that the appropriate bacteria (i.e., aerobic heterotrophic, denitrifying, and perchlorate reducing bacteria) establish themselves in different redox zones, and that perchlorate and nitrate removal are limited by the availability of electron donors rather than by the availability of appropriate bacteria. Our results agree with other studies in which reactor performance was not only determined by current operating conditions but also by the history of reactor operation (Kirisits et al., 2001; Wolf et al., 2005).

Further research should evaluate to what extent perchlorate reducing bacteria can establish themselves in a biofilm under optimal or suboptimal operating conditions.

#### 4.4. Scale up

Glass beads are frequently used when a well defined and non-porous support medium is necessary for laboratory-scale biofilm reactor studies (e.g., Logan and LaPoint, 2002; Zhang and Huck, 1996). When interpreting results from such laboratory-scale systems, similarities and differences to full-scale systems need to be considered. In the current study, effluent perchlorate concentrations were similar to bulk phase concentrations in the reactors since recirculation of the effluent provided near completely mixed conditions in the bulk phase. Full-scale biofilm reactors are usually operated

without recycling, which leads to concentration gradients along the length of the reactor. Whether backwashing results in complete mixing of the biofilm support media and avoid a heterogeneous distribution of biomass along the length of the reactor depends on factors such as reactor geometry and filter bed expansion during backwashing (Laurent et al., 2003). The completely mixed biofilm reactor used in the current study may not be representative of all types of fixed bed BAC reactors depending on mixing characteristics.

Suitable methods need to be developed to directly monitor biofilm growth and the accumulation of large microbial aggregates in filter media. In the current study, the significance of mass transfer limited zones is suggested based only on indirect inference. Large microbial aggregates were observed inside the reactors and during backwashing (Fig. 2) and mass transfer limitations in such aggregates help to explain the observed perchlorate removal during periods with relatively high bulk phase DO concentrations. However, further studies are necessary to quantify the amount, distribution, and significance of these large microbial aggregates and their contribution to overall reactor performance.

Backwashing in the current study was performed after removing the reactor content from the reactor. The energy input and shear or abrasion forces during this backwashing procedure are different from those associated with backwashing in full-scale applications for which air scouring and increased water flow rates are typically used to expand the filter bed. However, the net result of backwashing, i.e., removal of the majority of the accumulated large microbial aggregates and a smaller fraction of the biofilm directly attached to the support medium, likely is similar in full-scale applications and in the current study (Laurent et al., 2003). Nevertheless, mixing conditions and backwashing of fixed bed biofilm reactors depend on scale and reactor geometry (Min et al., 2004) and mechanisms derived from laboratory-scale studies need to be evaluated further in pilot- and full-scale studies.

## 5. Conclusions

The effect of backwashing on perchlorate removal was studied in fixed bed biofilm reactors using 1- or 3-mm glass beads as support media. It was shown that:

- The response of fixed bed biofilm reactors to transient increases in influent DO levels depended on the history of backwashing. For an influent DO level of 3.5 mg/L and a slight electron donor deficit, no perchlorate removal was observed after strong backwashing, while the same influent conditions before backwashing resulted in 60% perchlorate removal. Presumably, the accumulation of large microbial aggregates resulted in local anaerobic zones that allowed for perchlorate reduction even with detectable DO concentrations in the bulk phase. Backwashing removed these aggregates and resulted in poor perchlorate removal in the presence of DO in the bulk liquid.
- The influence of backwashing on perchlorate removal depended on the electron donor to acceptor ratio in the influent. With electron donor addition in excess of stoichiometric requirements (3.2 times the stoichiometric requirement based on a net yield of 0.4 g COD<sub>biomass</sub>/g COD<sub>acetate</sub>), strong backwashing resulted in a brief (<12 h) and small increase in effluent perchlorate concentrations. With the addition of electron donor close to stoichiometric requirement, perchlorate removal did not recover within 24 h after strong backwashing.
- The response to daily backwashing depended on the backwashing intensity. Weak daily backwashing had a small and, over time, decreasing negative effect on perchlorate removal. Strong daily backwashing had a substantial influence and ultimately lead to the complete breakdown of perchlorate removal.
- For practical applications, increasing the electron donor addition above the stoichiometric requirement would result in lower bulk phase DO concentrations, which would lead to more stable biofilm reactor performance following backwashing.

## Acknowledgements

The authors would like to thank Vernon Snoeyink and Jess Brown for helpful discussions. This research was supported by the US National Science Foundation, Grant No. BES-0123342.

## REFERENCES

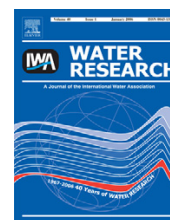
- Ahmad, R., Amirtharajah, A., Al-Shawwa, A., Huck, P.M., 1998. Effects of backwashing on biological filters. *J. Am. Water Works Assoc.* 90 (12), 62–73.
- APHA, AWWA and WEF, 1999. *Standard Methods for the Examination of Water and Wastewater*, 20th ed. American Public Health Association, Washington, DC.
- Boller, M., Kobler, D., Koch, G., 1997. Particle separation, solids budgets and headloss development in different biofilters. *Water Sci. Technol.* 36 (4), 239–247.
- Brown, J.C., Snoeyink, V.L., Kirisits, M.J., 2002. Abiotic and biotic perchlorate removal in an activated filter. *J. Am. Water Works Assoc.* 94 (2), 70–79.
- Brown, J.C., Snoeyink, V.L., Raskin, L., Lin, R., 2003. The sensitivity of fixed-bed biological perchlorate removal to changes in operating conditions and water quality characteristics. *Water Res.* 37 (1), 206–214.
- Brown, J.C., Anderson, R.D., Min, J.H., Boulos, L., Prasifka, D., Juby, G.J.G., 2005. Fixed bed biological treatment of perchlorate-contaminated drinking water. *J. Am. Water Works Assoc.* 97 (9), 70–81.
- Chaudhary, D.S., Vigneswaran, S., Ngo, H.H., Shim, W.G., Moon, H., 2003. Biofilter in water and wastewater treatment. *Korean J. Chem. Eng.* 20 (6), 1054–1065.
- Cohen, Y., Metzner, A.B., 1981. Wall effects in laminar-flow of fluids through packed-beds. *AIChE J.* 27 (5), 705–715.
- Delahaye, A.P., Gilmore, K.R., Husovitz, K.J., Love, N.G., Holst, T., Novak, J.T., 1999. Distribution and characteristics of biomass in pilot-scale upflow biological aerated filters treating domestic wastewater. In: *IWAQ Conference on Biofilm Systems*, New York, October 17–20.
- Giblin, T., Herman, D., Deshusses, M.A., Frankenberger, W.T., 2000. Removal of perchlorate in ground water with a flow-through bioreactor. *J. Environ. Qual.* 29 (2), 578–583.



- Henze, M., Harremoës, P., Jansen, J.L.C., Arvin, E., 2002. *Waste-water Treatment*, third ed. Springer, Berlin.
- Herman, D.C., Frankenberger, W.T., 1999. Bacterial reduction of perchlorate and nitrate in water. *J. Environ. Qual.* 28 (3), 1018–1024.
- Hozalski, R.M., Bouwer, E.J., 1998. Deposition and retention of bacteria in backwashed filters. *J. Am. Water Works Assoc.* 90 (1), 71–85.
- Kengen, S.W.M., Rikken, G.B., Hagen, W.R., van Ginkel, C.G., Stams, A.J.M., 1999. Purification and characterization of (per)chlorate reductase from the chlorate-respiring strain GR-1. *J. Bacteriol.* 181 (21), 6706–6711.
- Kim, H.S., Jaffe, P.R., Young, L.Y., 2004. Simulating biodegradation of toluene in sand column experiments at the macroscopic and pore-level scale for aerobic and denitrifying conditions. *Adv. Water Resour.* 27 (4), 335–348.
- Kim, K., Logan, B.E., 2000. Fixed-bed bioreactor treating perchlorate-contaminated waters. *Environ. Eng. Sci.* 17 (5), 257–265.
- Kim, K., Logan, B.E., 2001. Microbial reduction of perchlorate in pure and mixed culture packed-bed bioreactors. *Water Res.* 35 (13), 3071–3076.
- Kirisits, M.J., Snoeyink, V.L., Inan, H., Chee-Sanford, J.C., Raskin, L., Brown, J.C., 2001. Water quality factors affecting bromate reduction in biologically active carbon filters. *Water Res.* 35 (4), 891–900.
- Lahav, O., Artzi, E., Tarre, S., Green, M., 2001. Ammonium removal using a novel unsaturated flow biological filter with passive aeration. *Water Res.* 35 (2), 397–404.
- Laurent, P., Prevost, M., Cigana, J., Niquette, P., Servais, P., 1999. Biodegradable organic matter removal in biological filters: Evaluation of the CHABROL model. *Water Res.* 33 (6), 1387–1398.
- Laurent, P., Kihn, A., Andersson, A., Servais, P., 2003. Impact of backwashing on nitrification in the biological activated carbon filters used in drinking water treatment. *Environ. Technol.* 24 (3), 277–287.
- Lin, R., 2004. Bacterial community analysis and optimization of biologically active carbon filters used to remove perchlorate from groundwater. M.S. Thesis, Civil and Environmental Engineering, University of Illinois at Urbana-Champaign.
- Liu, X.B., Huck, P.M., Slawson, R.M., 2001. Factors affecting drinking water biofiltration. *J. Am. Water Works Assoc.* 93 (12), 90–101.
- Logan, B.E., LaPoint, D., 2002. Treatment of perchlorate- and nitrate-contaminated groundwater in an autotrophic, gas phase, packed-bed bioreactor. *Water Res.* 36 (14), 3647–3653.
- McCarty, P.L., Meyer, T.E., 2005. Numerical model for biological fluidized-bed reactor treatment of perchlorate-contaminated groundwater. *Environ. Sci. Technol.* 39 (3), 850–858.
- Min, B., Evans, P.J., Chu, A.K., Logan, B.E., 2004. Perchlorate removal in sand and plastic media bioreactors. *Water Res.* 38 (1), 47–60.
- Nakhla, G., Farooq, S., 2003. Simultaneous nitrification-denitrification in slow sand filters. *J. Hazard. Mater.* 96 (2–3), 291–303.
- Niquette, P., Prevost, M., Maclean, R.G., Thibault, D., Coallier, J., Desjardins, R., Lafrance, P., 1998. Backwashing first-stage sand—BAC filters. *J. Am. Water Works Assoc.* 90 (1), 86–97.
- Servais, P., Billen, G., Ventresque, C., Bablon, G.P., 1991. Microbial activity in Gac filters at the Choisy-Le-Roi treatment-plant. *J. Am. Water Works Assoc.* 83 (2), 62–68.
- Song, Y., 2004. Respiratory pathways used by perchlorate respiring bacteria. Ph.D. Thesis, Pennsylvania State University, University Park.
- Song, Y.G., Logan, B.E., 2004. Effect of O<sub>2</sub> exposure on perchlorate reduction by *Dechlorosoma* sp KJ. *Water Res.* 38 (6), 1626–1632.
- USEPA, 2006. US Environmental Protection Agency Perchlorate Links, <[http://www.epa.gov/fedfac/documents/perchlorate\\_links.htm](http://www.epa.gov/fedfac/documents/perchlorate_links.htm)>.
- Wanner, O., Eberl, H.J., Morgenroth, E., Noguera, D.R., Picioreanu, C., Rittmann, B.E., van Loosdrecht, M.C.M., 2006. *Mathematical Modeling of Biofilms*. IWA Publishing, London, UK.
- Wolf, G., Almeida, J.S., Reis, M.A.M., Crespo, J.G., 2005. Non-mechanistic modelling of complex biofilm reactors and the role of process operation history. *J. Biotechnol.* 117 (4), 367–383.
- Xu, J.L., Song, Y.U., Min, B.K., Steinberg, L., Logan, B.E., 2003. Microbial degradation of perchlorate: principles and applications. *Environ. Eng. Sci.* 20 (5), 405–422.
- Zhang, S.L., Huck, P.M., 1996. Parameter estimation for biofilm processes in biological water treatment. *Water Res.* 30 (2), 456–464.

## **Appendix B**

### **Chemisorption of Oxygen Onto Activated Carbon Can Enhance the Stability of Biological Perchlorate Reduction in Fixed Bed Biofilm Reactors**

Available at [www.sciencedirect.com](http://www.sciencedirect.com)journal homepage: [www.elsevier.com/locate/watres](http://www.elsevier.com/locate/watres)

## Chemisorption of oxygen onto activated carbon can enhance the stability of biological perchlorate reduction in fixed bed biofilm reactors

Young Chul Choi<sup>a,1</sup>, Xu Li<sup>c</sup>, Lutgarde Raskin<sup>c</sup>, Eberhard Morgenroth<sup>a,b,\*</sup>

<sup>a</sup>Department of Civil and Environmental Engineering, University of Illinois at Urbana-Champaign, 3219 Newmark Civil Engineering Laboratory, MC-250, 205 North Mathews Avenue, Urbana, IL 61801, USA

<sup>b</sup>Department of Animal Sciences, University of Illinois at Urbana-Champaign, 205 North Mathews Avenue, Urbana, IL 61801, USA

<sup>c</sup>Department of Civil and Environmental Engineering, University of Michigan, 1351 Beal Avenue, Ann Arbor, MI 48109, USA

### ARTICLE INFO

#### Article history:

Received 12 February 2008

Received in revised form

5 May 2008

Accepted 5 May 2008

Available online 16 May 2008

#### Keywords:

Granular activated carbon

Biologically active carbon

Chemisorption

Oxygen

Perchlorate

Biofilm

Clone library

### ABSTRACT

Fixed bed biofilm reactors with granular activated carbon (GAC) or glass beads as support media were used to evaluate the influence of short-term (12 h) and long-term (23 days) increases of influent dissolved oxygen (DO) concentrations on biological perchlorate removal. The goal was to evaluate the extent by which chemisorption of oxygen to GAC can enhance the stability of biological perchlorate reduction. Baseline influent concentrations were 50 µg/L of perchlorate, 2 mg/L of acetate as C, and 1 mg/L of DO. Perchlorate removal in the glass bead reactor seized immediately after increasing influent DO concentrations from 1 to 4 mg/L since glass beads have no sorptive capacity. In the biologically active carbon (BAC) reactor, chemisorption of oxygen to GAC removed a substantial fraction of the influent DO, and perchlorate removal was maintained during short-term increases of influent DO levels up to 8 mg/L. During long-term exposure to influent DO concentrations of 8.5 mg/L, effluent perchlorate and DO concentrations increased slowly. Subsequent exposure of the BAC reactor bed to low DO concentrations partially regenerated the capacity for oxygen chemisorption. Microbial analyses indicated similar microbial communities in both reactors, which confirmed that the differences in reactor performance during dynamic loading conditions could be attributed to the sorptive properties of GAC. Using a sorptive biofilm support medium can enhance biological perchlorate removal under dynamic loading conditions.

© 2008 Elsevier Ltd. All rights reserved.

## 1. Introduction

Perchlorate (ClO<sub>4</sub><sup>-</sup>) is an oxidizing anion, which is commonly used in the form of ammonium perchlorate in rocket fuels, air bags, road flares, and other industrial applications (Urbansky, 1998). Since the introduction of an analytical method that can

measure perchlorate accurately at µg/L levels (USEPA, 1997), perchlorate has been reported to be present in many drinking water sources (Gullick et al., 2001). Removal of perchlorate from drinking water sources can be achieved using abiotic processes, such as ion exchange (Roquebert et al., 2000; Urbansky, 1998), reverse osmosis (Urbansky, 1998),

\*Corresponding author at: Department of Civil and Environmental Engineering, University of Illinois at Urbana-Champaign, 3219 Newmark Civil Engineering Laboratory, MC-250, 205 North Mathews Avenue, Urbana, IL 61801, USA.  
Tel.: +1 217 333 6965; fax: +1 217 333 6968.

E-mail address: [emorgenr@uiuc.edu](mailto:emorgenr@uiuc.edu) (E. Morgenroth).

<sup>1</sup> Current address: Doosan Hydro Technology Inc., Tampa, FL, USA.  
0043-1354/\$ - see front matter © 2008 Elsevier Ltd. All rights reserved.  
doi:10.1016/j.watres.2008.05.004

electrodialysis (Roquebert et al., 2000), and tailored activated carbon (Chen et al., 2005; Parette and Cannon, 2005), in addition to a range of biological processes. Biological reduction of perchlorate is carried out by perchlorate-reducing bacteria which can use perchlorate as an electron acceptor (Achenbach et al., 2001; Coates et al., 1999; Rikken et al., 1996). Compared to abiotic processes, biological processes can convert perchlorate to non-toxic chloride without generating waste streams that contain high concentrations of perchlorate or brines from regenerating ion exchange resins. Another advantage of biological treatment is that, in addition to perchlorate, other contaminants such as nitrate and bromate can be reduced in the same system (Nerenberg and Rittmann, 2004). While the reduction of these other contaminants is desirable, these oxidized compounds will compete with perchlorate for electron donors. In perchlorate-contaminated drinking water, the dominant competing electron acceptors are typically oxygen and nitrate. Microbial reduction of perchlorate is inhibited by high concentrations of oxygen and nitrate (Coates and Achenbach, 2004) and the application of biological processes for drinking water treatment may be problematic in case of variable influent oxygen or nitrate concentrations.

Biological removal of perchlorate has been evaluated in biofilm reactors using different carrier media including plastic (Min et al., 2004), sand (Min et al., 2004), Celite (Losi et al., 2002), and granular activated carbon (GAC) (Brown et al., 2002) for fixed bed reactors, and sand and GAC for fluidized bed reactors (McCarty and Meyer, 2005; Sutton, 2006). Other reactor configurations include membrane diffuser biofilm reactors (Nerenberg et al., 2002) and ion exchange membrane bioreactor (Matos et al., 2006). Advantages of using GAC as a carrier medium include the widespread application of GAC in drinking water treatment plants where existing GAC filters can easily be retrofitted to operate as biologically active carbon (BAC) reactors. In 2004, the California Department of Health Services issued a conditional approval of biological removal of perchlorate from drinking water sources using fixed bed BAC (CADHS, 2004).

Not only can GAC be used to support the growth of biofilms, but sorption by GAC has been shown to complement biological removal in BAC reactors under dynamic loading conditions (Hanaki et al., 1997; Herzberg et al., 2003; Jaar and Wilderer, 1992; Sutton, 2006). Based on mathematical modeling, Herzberg et al. (2003) showed that the sorptive capacity of GAC can be beneficial by serving as a temporary sink for contaminants and then allowing biological degradation of the sorbed contaminants. They demonstrated that sorption, intraparticle diffusion, and desorption resulted in increased biofilm activity on the GAC compared to non-absorbing carrier media. Kim and Logan (2000), however, pointed out a potential problem related to using GAC as a temporary sink. They observed increased effluent perchlorate concentrations after backwash and redistribution of the GAC within the reactor, and attributed increased effluent concentrations to the desorption of perchlorate from GAC. A better understanding of the interactions between sorption, desorption, biological processes, and reactor operation is needed to make use of the sorptive capacity to improve reactor performance (Sutton, 2006).

In addition to the direct benefits of acting as a temporary sink of target contaminants, the sorptive capacity of GAC should be able to enhance biological perchlorate removal indirectly by lowering the concentration of oxygen, the competing electron acceptor, through chemisorption. Molecular oxygen can be irreversibly removed by interacting with the GAC surface (Abuzaid and Nakhla, 1994; Prober et al., 1975): one oxygen molecule and two carbon atoms form two C—O bonds (Zhu et al., 2000). Also, oxygen can be removed by reacting with surface C=O groups to form carboxylic acid groups (Prober et al., 1975). Prober and coworkers showed that chemisorption of oxygen can sustain as much as 6000 bed volumes with 10–40 mg oxygen removed per g of carbon. However, it is not clear to what extent this capacity can be regenerated through physical, chemical, or biological processes. The purpose of the current study was to examine how chemisorption of oxygen on GAC affects biological perchlorate reduction in a BAC filter. To study the specific effects of chemisorption, two identical laboratory-scale biofilm reactors were operated using GAC or glass beads as sorptive or non-sorptive carrier media, respectively. The effects of the sorption capacity of the GAC were evaluated by comparing oxygen and perchlorate removal during short- and long-term exposure to increased influent dissolved oxygen (DO) concentrations and during electron donor failure conditions.

## 2. Materials and methods

### 2.1. Reactor setup and influent composition

The two laboratory-scale fixed bed biofilm reactors had an inner diameter of 2.4 cm and a length of 14 cm, which resulted in an empty bed volume of 63.4 mL. One reactor was filled with GAC (Norit model RO 0.8, Amersfoort, The Netherlands); the other reactor was filled with glass beads (1-mm glass beads, etched using 0.25% HF for 1 h to allow for a better adhesion of bacteria). Both reactors were operated in an upflow mode with completely mixed bulk-phase conditions by adding a recirculation loop with a flow rate ( $Q_{\text{recirculation}}$ ) five times of the influent flow rate ( $Q_{\text{influent}} = 2.7$  mL/min). This corresponds to an empty bed contact time of 23.5 min. The BAC reactor was seeded using biomass collected from two other BAC reactors: one had been fed Urbana (IL) tap water amended with acetate at a concentration of 2 mg/L as C and 50  $\mu\text{g/L}$  perchlorate (Brown et al., 2002), the other had been fed Urbana groundwater amended with 50  $\mu\text{g/L}$  perchlorate (Lin, 2004). Sorption capacities of the GAC for perchlorate and oxygen were exhausted before initial start-up by recirculating water containing 50  $\mu\text{g/L}$  of perchlorate and saturated by oxygen through the reactor. The glass bead reactor was seeded using biomass from a previously operated 3-mm glass bead reactor, which had been seeded with biomass from the BAC reactor used in the current study.

The synthetic influent was prepared with deionized water and contained 50  $\mu\text{g/L}$  perchlorate, 0.15 mg/L of  $\text{NH}_4\text{Cl}$  as N, and 0.5 mM phosphate buffer to maintain a pH of 7.5. The influent DO level was adjusted to values between 1 and 8.5 mg/L by purging the influent with  $\text{N}_2$  gas. After purging, the influent was isolated from ambient air using a floating lid.

Acetate, the sole electron donor, was provided with a syringe pump and mixed with the synthetic influent immediately before it entered the reactors. The final concentration of acetate entering the reactors was 2 mg/L as C.

## 2.2. Reactor operation

Backwash was performed by pouring the content of each reactor into a 600 mL beaker, adding 125 mL of collected effluent, and stirring with a 7.5 cm long magnetic stir bar at 150 revolutions per minute (RPM) for 1 min. After the supernatant was decanted, another 125 mL effluent was added to the beaker and the rest of the procedure was repeated. Then the reactor contents were poured back to the reactors. This type of backwash was defined as a “normal backwash”. For a strong backwash, the contents of the reactors were stirred at 200 RPM for 1 min, followed by decanting of the supernatant; this process was repeated four times.

Prior to this study, both the BAC and the glass bead reactors were operated with influent acetate and DO concentrations of 2 mg/L as C and 1 mg/L, respectively. Experiments were initiated (= day 0) after both reactors had been consistently removing perchlorate to below 1 µg/L for at least 1 month. The influent DO level for the BAC reactor was increased from 1 to 4, 6, and 8 mg/L for 12-h periods on days 8, 9, and 14, respectively. On day 15, a normal backwash was conducted and then the influent DO level was increased again to 8 mg/L for a 12-h period. On day 17, a strong backwash was conducted. Finally, the influent DO level was increased again to 8 mg/L for 12 h. The glass bead reactor also was exposed to transient DO increases from 1 to 4, 6, and 8 mg/L for 12-h periods on days 256, 279, and 22, respectively. GAC and glass bead reactors were not operated side-by-side and the sequences of experiments in both reactors were different. However, the reactors were operated according to the stated baseline operating conditions and complete perchlorate removal was accomplished for at least 7 days prior to each experiment. Following a normal backwash of the glass bead reactor on day 25, the influent DO concentration was increased again to 8 mg/L for 12 h on day 26.

To study the responses of the BAC reactor to long-term exposures to high DO concentrations, the influent DO level was increased from 1 to 8.5 mg/L for 23 days starting on day 22. Then the influent DO level was decreased to 1 mg/L on day 45, and increased again to 8.5 mg/L on day 48 for 6 days. A normal backwash was performed on day 53 to test if detachment of biomass would influence the chemisorption capacity. To verify that perchlorate removal was the result of microbial activity, acetate addition was stopped for 4.5 days starting on day 60 for the BAC reactor and on day 364 for the glass bead reactor.

## 2.3. Chemical analyses

DO concentrations were measured using galvanic oxygen sensors (WTW CellOx 325 with Oxi 340i, Weilheim, Germany) and flow cells (WTW model D201, Weilheim, Germany) connected to reactor effluents. The detection limit for DO measurement was 0.01 mg/L. Perchlorate was measured using an ion chromatograph (Dionex ICS-2000, Sunnyvale, CA) with

an AS50 autosampler and a conductivity detector. An AS16 column and an AG16 guard column were used and the detection limit was 1 µg/L. The eluent was 65 mM KOH at a flow rate of 1.2 mL/min and the injection volume was 990 µL. Dissolved organic carbon (DOC) was measured using a UV-Persulfate TOC Analyzer (Tekmar-Dohrmann Phoenix 8000, Mason, OH) with a detection limit of 0.2 mg/L as C. Volatile suspended solids (VSS) were measured according to Standard Methods (APHA et al., 1998). The pressure drop across the BAC bed was measured using glycerin-filled pressure gauges (Lenz Inc., Dayton, OH).

## 2.4. Clone libraries and phylogenetic analysis

Biomass samples were collected during backwashing from the BAC reactor on days 17 and 53, and from the glass bead reactor on day 388. For both reactors, biomass was first sampled after the reactors had achieved complete perchlorate removal for at least 7 days. DNA was extracted from these samples using a Mo Bio Ultra Clean Soil DNA Extraction Kit (Mo Bio Laboratories, Carlsbad, CA), quantified using a NanoDrop 1000 (NanoDrop Technology, Wilmington, DE), and checked for DNA integrity by electrophoresis on a 1% agarose gel. Each DNA extract was PCR amplified in triplicate using bacterial primer 8F (5'-AGAGTTTGATCCTGGCTCAG-3') and universal primer 1492R (5'-GG(C/T)TACCTGTTCAGACTT-3') (Richardson et al., 2002), which were synthesized by Invitrogen (Carlsbad, CA). The protocol of the PCR reaction was adopted from the work by Dojka et al. (1998). The reagents used in the PCR reaction were from Takara (Takara Inc., Japan). Pooled PCR products were loaded on an agarose gel and bands of the appropriate size were cut. Purified PCR products were extracted from the gel bands using MinElute Gel Extraction Kit (QIAGEN Inc, Valencia, CA), cloned into vectors, and transformed into competent *Escherichia coli* cells using TOPO TA Cloning Kit for Sequencing (Invitrogen, Carlsbad, CA). A total of 192 clones in glycerol stocks were submitted for each clone library for bi-directional sequencing (Genome Sequencing Center at Washington University, St. Louis, MO). Raw data from sequencing in both forward and backward direction were evaluated using the Ribosomal Database Project II (RDP) Pipeline to remove vector sequences (Cole et al., 2007). Either forward or backward sequences were used in this analysis, depending on which direction resulted in a higher number of sequences of good quality. The phylogenetic classification of the clones was conducted using the “Classification” function under “MyRDP” in RDP. Comparisons between two libraries were made using the “Library Compare” function in RDP.

## 3. Results

### 3.1. Short-term increase of influent DO levels

For the baseline condition with an influent DO concentration of 1 mg/L and an acetate concentration of 2 mg/L as C, the BAC reactor reliably reduced perchlorate to below the detection limit of 1 µg/L for more than 1 month (data not shown) before the start of the experiment. When the influent DO level was

increased to 4, 6, and 8 mg/L for 12-h periods, effluent DO concentrations increased to 0.1, 0.2, and 0.4 mg/L, respectively, and effluent perchlorate concentrations increased to 10–13  $\mu\text{g/L}$  (Fig. 1). Thus, even with increased influent DO concentrations, the BAC reactor was able to remove more than 90% of the influent DO and 75–80% of the influent perchlorate. When the influent DO level was lowered to 1 mg/L following each 12-h period, effluent DO concentrations rapidly decreased to non-detectable levels and perchlorate was removed to below detection limit within 2 h.

Assuming a net yield of  $0.4 \text{ g COD}_{\text{biomass}}/\text{g COD}_{\text{acetate}}$ , an acetate concentration of 2 mg/L as C can reduce 3.2 mg/L of DO. Thus, if chemisorption is not considered, for influent DO levels of 4, 6, and 8 mg/L the expected effluent (or bulk liquid) DO concentrations should be 0.8, 2.8, and 4.8 mg/L, respectively. However, the observed effluent DO concentrations were much lower than these expected values. Control experiments using virgin GAC demonstrated that more than 4.7 mg of  $\text{O}_2$  can be removed abiotically per gram of GAC through chemisorption (data not shown). Based on this capacity, chemisorption could in fact account for the observed increased removal of DO from bulk liquid.

For the glass bead reactor, similar short-term (12 h) increases in influent DO levels to 4, 6, and 8 mg/L resulted

in effluent DO concentrations of approximately 0.8, 2.6, and 3.5 mg/L, respectively (Fig. 2). These observed effluent DO concentrations were much closer to the expected effluent DO values, assuming biological reduction as the only sink for oxygen. Furthermore, during these short-term increases in influent DO levels, perchlorate removal was compromised and the effluent perchlorate levels were close to the influent concentrations of 50  $\mu\text{g/L}$ .

Regular backwash is necessary in operating fixed bed biofilm reactors, as it can remove biomass in excess and to avoid clogging (Niquette et al., 1998). A normal backwash was conducted in the BAC reactor on Day 15 (Fig. 1). The amount of biomass detached was 63.6 mg VSS and the pressure drop across the bed decreased from 48 kPa before to below the detection limit of 0.7 kPa after backwash. Even though the amount of biomass was reduced during backwashing, no perchlorate was observed in the effluent of the BAC reactor after the backwash or even during the 12-h period when the influent DO level was raised again to 8 mg/L. During the strong backwash on day 17, the amount of biomass removed was too low to be quantified using VSS measurements. Despite the additional removal of biomass, no perchlorate was observed in the effluent after the strong backwash and after the DO level was increased to 8 mg/L (Fig. 1). Effluent DO

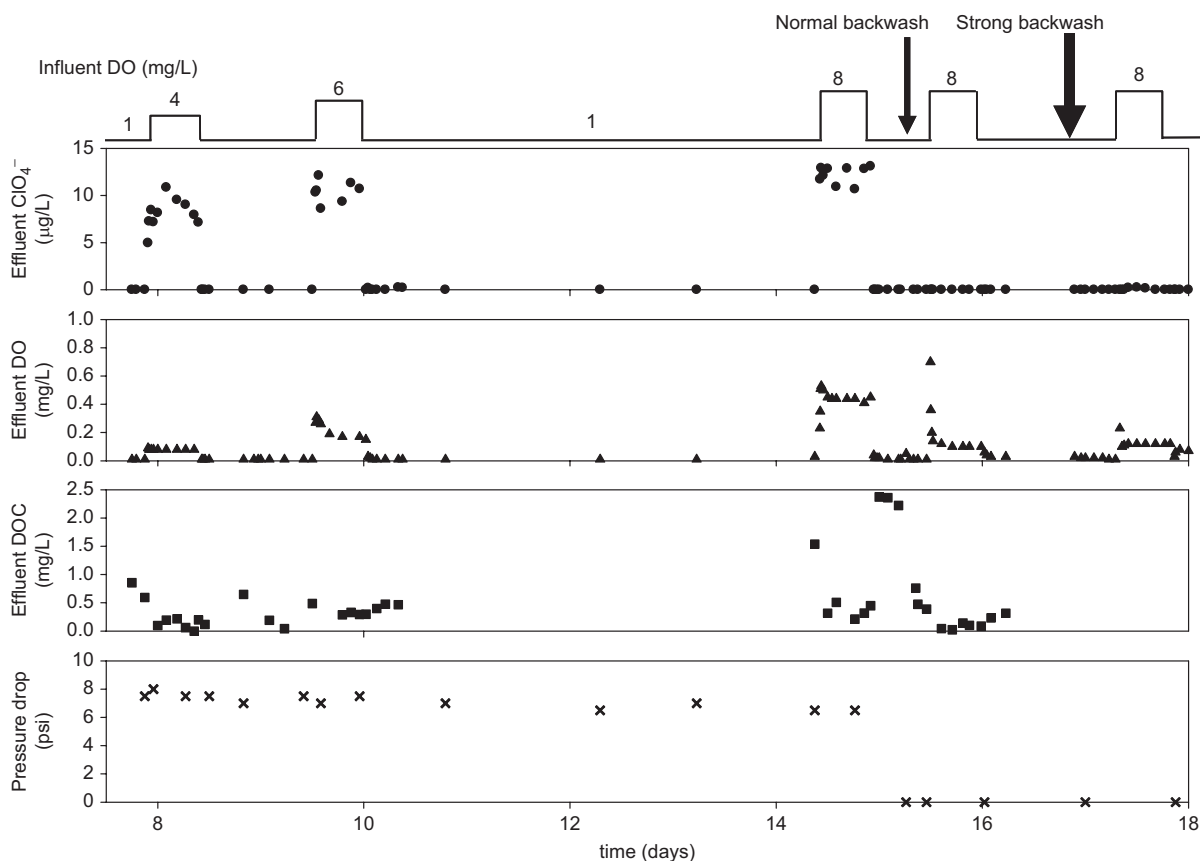
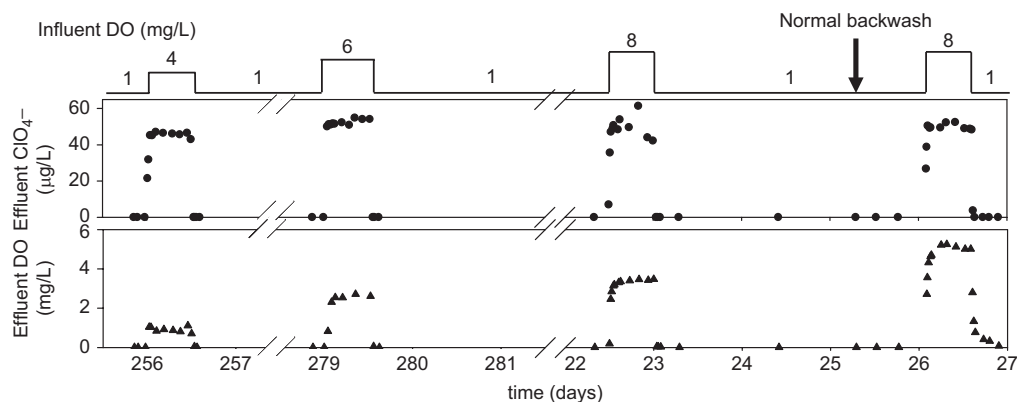


Fig. 1 – Effect of short-term (12 h) increases of influent DO levels to 4, 6, and 8 mg/L and backwashing on the performance of the BAC reactor. The influent acetate concentration was kept constant at 2 mg/L as C.



**Fig. 2 – Effect of short-term (12 h) increases of influent DO levels to 4, 6, and 8 mg/L and backwashing on the performance of the glass bead reactor. The influent acetate concentration was kept constant at 2 mg/L as C. Results are from three different experimental periods. Experiments were performed after steady-state removal of perchlorate had been achieved.**

concentrations were approximately 0.12 mg/L during the last two 12-h periods when the influent DO level was at 8 mg/L. These effluent DO concentrations were much lower than those observed during the first 12-h period of 8 mg/L influent DO, but they were similar to those observed during the 12-h period of 4 mg/L influent DO on day 8 (Fig. 1) when incomplete perchlorate reduction was observed. The improved removal of both oxygen and perchlorate after backwashing indicates that perchlorate removal may have been accomplished through a combination of direct adsorption of perchlorate and biological perchlorate reduction under low bulk-phase DO levels that were the result of oxygen removal through chemisorption. Backwashing likely resulted in a decrease in biofilm coverage on GAC surface (patchy biofilms), and thus more GAC surface became available for sorption of oxygen and perchlorate, which resulted in improved perchlorate removal after backwashing (Herzberg et al., 2003).

Backwashing of the glass bead reactor resulted in increases of both perchlorate and oxygen concentrations in the effluent (Fig. 2). During the 12-h increase in influent DO levels to 8 mg/L on day 22, the effluent DO concentration was approximately 3.5 mg/L. During the 12-h increase in influent DO level to 8 mg/L on day 26, after the normal backwash on day 25, effluent DO concentrations were approximately 5 mg/L, close to the expected value of 4.5 mg/L. For the glass bead reactor, a larger amount of biomass in the reactor before backwashing resulted in greater DO removal (day 22) compared to the DO removal after backwashing (day 26), which is opposite to what was observed for the BAC reactor.

### 3.2. Long-term increase of influent DO levels

Long-term effects of increased influent DO levels were evaluated by operating the BAC reactor with an influent DO concentration of 8.5 mg/L for a period of 23 days (Fig. 3). During this time, effluent perchlorate concentrations increased steadily and reached about 30 µg/L. Effluent DO concentrations remained low (<0.12 mg/L) during the first 8 days of this period and began to increase after day 31. The increase in effluent DO concentrations correlated with a

decrease in effluent DOC concentrations. The correlation can be explained by the depletion of GAC sorptive capacity, which resulted in an increased amount of DO in the bulk liquid that was available for biological oxidation of dissolved organics. The observed increase in effluent perchlorate concentrations over time did not appear to be affected by the changes in effluent DO and DOC levels. The pressure drop across the bed also gradually increased, from below the detection limit to 48 kPa as a result of biofilm growth within the reactor.

When the influent DO level was decreased to 1 mg/L on day 46 (baseline conditions), the effluent perchlorate concentrations dropped immediately to 20 µg/L and then decreased slowly. It required 2.5 days to lower the effluent perchlorate concentration to below the detection limit. This is in contrast with the results obtained after the short-term exposure to increased influent DO level at 8 mg/L when perchlorate reduction was fully restored within 2 h (Fig. 1).

As soon as complete perchlorate reduction was restored on day 48, the influent DO level was increased again to 8.5 mg/L to test if the oxygen chemisorption capacity was restored during the 2.5 days of low (1 mg/L) influent DO levels (Fig. 3). Unlike the gradual increase observed after the increase in the influent DO on day 23, the effluent perchlorate concentrations immediately increased to about 20 µg/L on day 48. This level is equal to the effluent perchlorate concentrations 13 days into the first long-term DO experiment, and perchlorate concentrations only slightly increased in the subsequent 5 days. The effluent DO concentrations increased within 2 days to 2.5 mg/L, the same level that was only reached on day 46, which corresponds to 23 days of the first period operating with high influent DO concentrations. These results demonstrate that the chemisorption capacity for both oxygen and perchlorate were depleted during the first 23 days of operation at high influent DO levels and that only part of the capacity was regenerated during the 2.5 days of operation at low DO conditions.

To examine the effects of backwashing on perchlorate removal after the chemisorption capacity of GAC was depleted, the BAC reactor was backwashed on day 53, while influent DO concentrations were maintained at

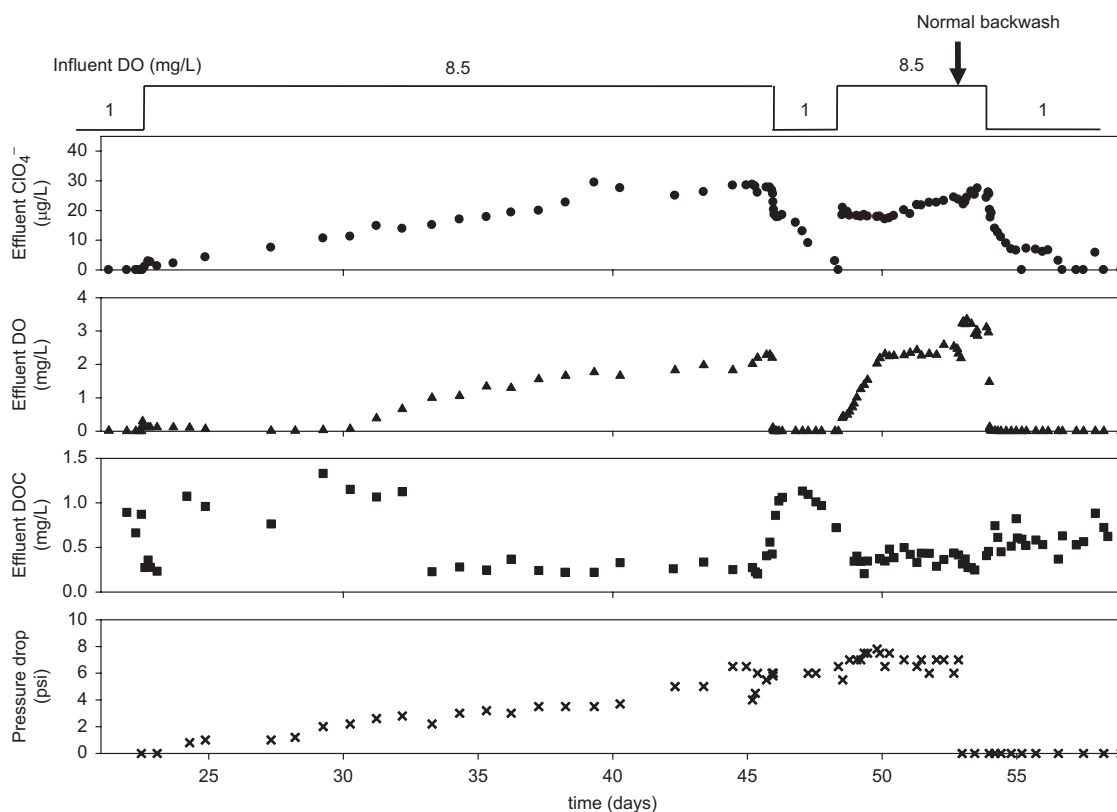


**Fig. 3 – Response of the BAC reactor to long-term operation (duration of 23.4 and 5.6 days) with increased influent DO levels of 8.5 mg/L and a backwash event. The influent acetate concentration was kept constant at 2 mg/L as C.**

8.5 mg/L (Fig. 3). After backwashing, effluent DO and perchlorate concentrations remained high. This was different from the two backwash events in Fig. 1, after which the BAC reactor was able to remove both DO and perchlorate to low levels under influent DO level at 8 mg/L. This comparison suggests that once the sorptive capacity of GAC was depleted, the reactor lost the ability to lower DO and perchlorate levels when influent DO levels were high.

### 3.3. Operation without electron donor addition

Prior to evaluating operation without electron donor addition, the BAC and glass bead reactors were operated with an influent DO level of 1 mg/L and achieved complete perchlorate removal for 7 and 6 days, respectively (Fig. 4). Eliminating acetate addition for a 4.5-day period resulted in increases of effluent perchlorate concentrations in both reactors. However, the increase was much slower for the BAC reactor compared to the glass bead reactor. Near the end of the 4.5-day period, effluent perchlorate concentrations were about 30 and 45 µg/L in BAC and glass bead reactors, respectively. There was no increase in effluent DO concentrations for the BAC reactor (except for one outlier), while there was an immediate increase in the glass bead reactor and the effluent DO level reached 0.4 mg/L at the end of

the experiment. Following electron donor addition, effluent perchlorate concentrations decreased rapidly in both reactors.

### 3.4. Clone library results for the BAC and glass bead reactors

The composition of the microbial communities in the BAC and glass bead reactors was compared based on clone library results (Table 1). For the baseline operating conditions, the microbial communities contained large numbers of *Betaproteobacteria* (62.2% and 64.3% of total identified clones in the BAC and the glass bead reactor, respectively). *Dechloromonas* was the only known genus of perchlorate-reducing bacteria found in the clone libraries, and accounted for 11.7% and 13.2% of the total clones in the BAC and the glass bead reactors, respectively. The genus *Zoogloea*, which also belongs to the *Betaproteobacteria*, was the most abundant bacterial genus in both reactors.

The structure of the bacterial community in the BAC reactor changed after the reactor had been exposed to increased influent DO concentrations for an extended period of time (day 53 in Fig. 3). The abundance of the *Betaproteobacteria* decreased substantially. During the same time period, the numbers of clones that were associated with the phyla *Bacteroidetes* and *Verrucomicrobia* increased. Within the



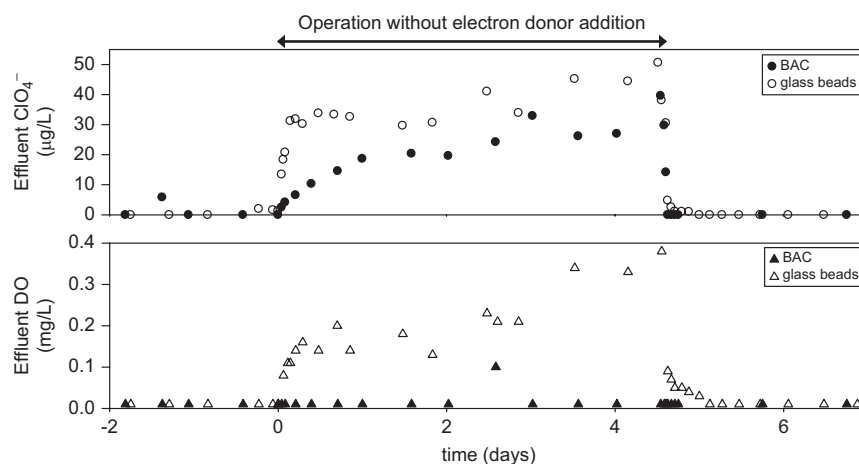


Fig. 4 – Effluent perchlorate and DO concentrations for the BAC and glass bead reactors in response to operation without electron donor addition, while maintaining the influent DO level at 1 mg/L. Day 0 corresponds to day 60 and day 364 for the BAC and glass bead reactors, respectively.

Table 1 – Dominant bacterial populations (in % of total clones) in biomass samples collected from backwash water of the BAC and glass bead reactors

Source of biomass	BAC reactor		Glass bead reactor
	Day 17	Day 53	Day 388
Number of clones sequenced	n = 180	n = 179	n = 182
<i>Betaproteobacteria</i> <sup>a</sup>	62.2	34.1	64.3
<i>Dechloromonas</i>	11.7	1.7	13.2
<i>Zoogloea</i>	30.6	10.1	25.8
Other <i>Betaproteobacteria</i>	20.0	22.3	25.3
Other <i>Proteobacteria</i>	19.4	6.1	17.0
<i>Acidobacteria</i>	1.7	0.6	2.2
<i>Actinobacteria</i>	0.6	N/D <sup>b</sup>	N/D
<i>Bacteroidetes</i>	5.6	34.6	12.6
<i>Chloroflexi</i>	0.6	N/D	N/D
<i>Deinococcus-Thermus</i>	5.0	1.7	N/D
<i>Planctomycetes</i>	N/D	2.2	N/D
<i>Verrucomicrobia</i>	0.6	9.5	N/D
Candidate phylum OP10	2.2	0.6	N/D
Unknown Bacteria	2.2	10.6	3.8

<sup>a</sup> *Betaproteobacteria* are subdivided into *Dechloromonas*, *Zoogloea*, and other *Betaproteobacteria*.  
<sup>b</sup> N/D = not detected.

*Betaproteobacteria*, the clones related to the genera *Dechloromonas* and *Zoogloea* decreased from 11.7% to 1.7% and from 30.6% to 10.1%, respectively.

## 4. Discussion

### 4.1. Combined effects of oxygen chemisorption and direct sorption of perchlorate

Comparing the performances of the BAC and the glass bead reactors demonstrated that a sorptive carrier medium can

enhance perchlorate removal substantially when reactors are exposed to increased DO concentrations. Under optimized operating conditions, the overall performance and the composition of the microbial community were similar in both reactors. Complete perchlorate and oxygen removal was achieved with acetate added as the electron donor in excess, 3.2 times the stoichiometric requirement. Different from the glass bead reactor, the BAC reactor maintained substantial perchlorate and oxygen removal rate during periods of increased influent DO concentrations when acetate addition was below the stoichiometric requirement (40–80% of the requirement). This study demonstrated that sorption could

support biological processes during dynamic reactor operations, such as increased influent DO concentrations and operation without electron donor addition—conditions that both resulted in substrate limitation for biological perchlorate removal.

Sorptive properties of GAC supported perchlorate removal most likely through a combination of oxygen chemisorption, which reduces bulk-phase DO concentrations and thus enhances biological perchlorate removal, and direct sorption of perchlorate. In the glass bead reactor, without any sorptive capacity, both the increase of influent DO concentrations and the operation without electron donor addition resulted in the complete breakthrough of perchlorate. The situation was different for the BAC reactor. Operation without electron donor addition resulted in increased effluent perchlorate concentrations up to 30 µg/L and no increase in effluent DO concentrations (Fig. 4). These results demonstrate that sorption within the BAC, without biological perchlorate reduction, cannot remove perchlorate completely to below the detection limit. With baseline acetate addition and influent DO concentrations of 8 mg/L, complete removal of both DO and perchlorate was achieved (Fig. 1). The addition of a limited amount of electron donor (40% of the stoichiometric requirement) combined with oxygen removal through chemisorption resulted in sufficient biological perchlorate removal to achieve effluent concentrations below the detection limit in the BAC but not in the glass bead reactor.

Reduced bulk-phase DO concentrations in the BAC reactor alone, however, cannot explain the observed perchlorate removal. Bulk-phase DO concentrations on days 8 and 17 were approximately 0.1 mg/L, but complete perchlorate removal was observed on day 17, whereas the effluent perchlorate concentration on day 8 was approximately 10 µg/L (Fig. 1). The improved perchlorate removal on day 17 can be explained by the two backwash events on days 15 and 17, which likely resulted in an increased GAC surface area that was accessible not only for oxygen chemisorption but also for direct sorptive removal of perchlorate.

#### 4.2. Advantages and disadvantages of sorptive support medium for perchlorate removal

In the literature there is no consensus on the benefits of sorptive support media and only limited information on the mechanisms of how biological perchlorate reduction can be supported by using sorptive biofilm support media is available. Sutton (2006) suggested that biological reduction should be supplemented with physico-chemical removal using for example GAC as a support medium. GAC could be beneficial both as a temporary sink and also to help increase local perchlorate concentrations on the GAC surface as the result of adsorption and desorption of perchlorate. This mechanism of temporary sorption to increase local perchlorate concentrations had been suggested by Herzberg et al. (2003). Other studies evaluating BAC reactors for perchlorate removal did not discuss possible effects of temporary sorption on reactor performance (Hatzinger, 2005; McCarty and Meyer, 2005). Kim and Logan (2000) went so far as to discourage the use of GAC due to negative effects of desorption of perchlorate in a BAC

reactor after backwashing. In their study, plug flow condition in the fixed bed reactor exposed BAC at the inlet of the reactor to high perchlorate concentrations. After backwashing and redistribution of filter media within the reactor, desorption of previously sorbed perchlorate close to the outlet of the reactor could not be reduced biologically and resulted in increased effluent perchlorate concentrations after backwashing. Thus, while plug flow conditions can be advantageous for biological processes due to higher substrate concentrations resulting in higher removal rates near the inlet of a reactor, these concentration gradients along the length of the reactor also have drawbacks. These drawbacks include the involuntary shuttling of sorbed perchlorate into the effluent, as described above, and heterogeneous biomass distributions. Choi and Silverstein (2007) have shown that completely mixed reactors (e.g., gas lift reactors or fixed bed reactors with recirculation) can provide a more even distribution of biomass and avoid the problem of increased effluent perchlorate concentrations after backwashing.

The discussion of sorption and desorption in this study was focused on macro-scale effects of the overall removal of perchlorate and oxygen from the bulk phase. This leads to interesting research questions to understand the influence of biofilm coverage, sorption, intraparticle diffusion, and mass transport within the GAC particle on the local availability of substrates for biological perchlorate removal (Herzberg et al., 2003). Another question that requires further research is the rate and extent of regeneration of the sorption capacity for both perchlorate and oxygen. Partial regeneration of oxygen chemisorption over a period of 2.5 days was observed in Fig. 3. Long-term regeneration of sorption capacities over the course of reactor operation was demonstrated, as the sorption capacities of the GAC for oxygen and perchlorate had been exhausted before start-up and were regenerated over the course of reactor operation. The rate of regeneration of the sorption capacities was, however, not evaluated in this study.

#### 4.3. Critical bulk-phase oxygen concentrations for perchlorate removal

This study demonstrated that chemisorption of oxygen resulted in reduced bulk-phase oxygen concentrations to sufficiently low levels so that biological perchlorate reduction could occur (approx. 0.05 mg DO/L). McCarty and Meyer (2005) used a fluidized bed reactor for perchlorate removal from groundwater. They observed perchlorate removal within the first 25 cm of the reactor where bulk-phase DO concentrations were greater than 2 mg/L as long as sufficient electron donor was present. McCarty and Meyer (2005) explained this perchlorate reduction in the presence of relatively high bulk-phase DO concentrations based on mass transfer-limited anaerobic zones inside the biofilm. Complete overall perchlorate removal in their reactor was, however, associated with low effluent DO and nitrate concentrations of 0.1 and 0.01 mg/L, respectively. The extent to which perchlorate removal can occur at elevated bulk-phase DO concentrations depends on the biofilm structure (i.e., the biofilm needs to be sufficiently thick to allow for the development of anaerobic zones) and the electron donor to acceptor ratio in the bulk

phase (Choi et al., 2007; McCarty and Meyer, 2005). In most reactor studies, information on biofilm structure is not reported. For fixed bed reactors, as in the current study, representative sampling of GAC with attached biofilm without disturbing the biofilm structure is usually difficult. This study focused on evaluating the feasibility of oxygen chemisorption on perchlorate removal. Further research needs to evaluate the influence of the type of reactor, reactor operation, and the resulting biofilm structure on the interactions between sorption/desorption on GAC surface and biological reduction processes.

#### 4.4. Microbial community structure

Our study showed that *Dechloromonas* spp were the only known perchlorate-reducing bacteria in the two bioreactors, both of which used acetate as the sole electron donor. The importance of *Dechloromonas* spp. in perchlorate-reducing systems had also been suggested by Zhang et al. (2005), who evaluated the microbial community in an acetate-fed pilot-scale fixed bed bioreactor. In their study, based on the results from fluorescence *in situ* hybridization, Zhang and coworkers reported that *Dechloromonas* spp. accounted for about 23% and 1% of the bacterial populations at the surface and at the bottom of the biofilm, respectively. In comparison, based on clone library results, we reported the relative abundances of *Dechloromonas* as 11.7% and 13.2% in the BAC and the glass bead reactors, respectively. Zhang and coworkers also reported *Dechlorosoma* spp. to be present at low abundance in their system, while we did not detect any *Dechlorosoma* spp. in our systems (note that the *Dechlorosoma* genus has been renamed as *Azospira*; *Dechlorosoma suillum* (Achenbach et al., 2001) is a later subjective synonym of *Azospira oryzae* (Reinhold-Hurek and Hurek, 2000)). The relative abundances of perchlorate-reducing bacteria in the BAC and the glass bead reactors should not be considered low, because the influent perchlorate concentration was low compared to the influent DO level (i.e., 50 vs. 1000 µg/L), and the microbial communities in the two reactors likely did not need to maintain large perchlorate-reducing bacterial populations to reduce the small amount of perchlorate. Finally, for the baseline operation condition, the levels of the most abundant bacterial populations were similar in the two reactors, while some less abundant bacterial populations were shown to be present in the BAC reactor only. We speculate that the roughness of the GAC surface provides a wider range of environmental niches than the glass surface, resulting in a more diverse microbial community in the GAC biofilm compared to the biofilm in the glass bead reactor.

The observation of similar major bacterial populations in the two reactors supported our conclusion that the differences in the response of both reactors to short-term exposure to increased DO levels (Figs. 1 and 2) were due to the sorptive nature of GAC rather than to differences in microbial composition. The change in the microbial community after long-term exposure to increased DO concentrations (Fig. 3) demonstrated a direct influence of reactor operation on the competition of perchlorate-reducing bacteria with other heterotrophic bacteria.

## 5. Conclusions

This is the first report demonstrating that using a sorptive biofilm support medium can enhance biological perchlorate reduction through chemisorption of oxygen (the competing electron acceptor), in addition to the removal of perchlorate by direct sorption. Substantial removal of both oxygen and perchlorate was achieved for short periods (12 h) with influent DO concentrations of up to 8 mg/L in the BAC reactor. Using a non-sorptive support medium, complete breakthrough of perchlorate was observed for increased influent DO concentrations. During long-term exposure (23 d), the sorptive removal of DO and perchlorate slowly decreased. Application of sorptive support media is advantageous for biofilm reactors exposed to transient operating conditions, such as variable influent DO levels, reactor backwashing, and periods without electron donor addition. Partial regeneration of the sorption capacity was observed after long-term exposure to increased influent DO levels but mechanisms and kinetics of this regeneration should be further evaluated.

## Acknowledgments

The authors would like to thank Vernon Snoeyink and Jess Brown for helpful discussions. This research was supported by the US National Science Foundation, Grant no. BES-0123342.

## REFERENCES

- Abuzaid, N.S., Nakhla, G.F., 1994. Dissolved-oxygen effects on equilibrium and kinetics of phenolics adsorption by activated carbon. *Environ. Sci. Technol.* 28 (2), 216–221.
- Achenbach, L.A., Michaelidou, U., Bruce, R.A., Fryman, J., Coates, J.D., 2001. *Dechloromonas agitata* gen. nov., sp nov and *Dechlorosoma suillum* gen. nov., sp nov., two novel environmentally dominant (per)chlorate-reducing bacteria and their phylogenetic position. *Int. J. Syst. Evol. Microbiol.* 51, 527–533.
- APHA, WEF and AWWA, 1998. In: Clesceri, L.S., Greenberg, A.E., Eaton, A.D. (Eds.), *Standard Methods for the Examination of Water and Wastewater*, 20th ed. American Public Health Association, Washington, DC.
- Brown, J.C., Snoeyink, V.L., Kirisits, M.J., 2002. Abiotic and biotic perchlorate removal in an activated filter. *J. Am. Water Works Assoc.* 94 (2), 70–79.
- CADHS, 2004. Conditional Acceptance of Fixed-Bed Biological Treatment for the Production of Drinking Water from Perchlorate-Contaminated Water. Letter from the California Department of Health Services to Carollo Engineers.
- Chen, W.F., Cannon, F.S., Rangel-Mendez, J.R., 2005. Ammonia-tailoring of GAC to enhance perchlorate removal. II: perchlorate adsorption. *Carbon* 43 (3), 581–590.
- Choi, H., Silverstein, J., 2007. Effluent recirculation to improve perchlorate reduction in a fixed biofilm reactor. *Biotechnol. Bioeng.* 98 (1), 132–140.
- Choi, Y.C., Li, X., Raskin, L., Morgenroth, E., 2007. Effect of backwashing on perchlorate removal in fixed bed biofilm reactors. *Water Res.* 41 (9), 1949–1959.
- Coates, J.D., Achenbach, L.A., 2004. Microbial perchlorate reduction: rocket-fuelled metabolism. *Nat. Rev. Microbiol.* 2 (7), 569–580.

- Coates, J.D., Michaelidou, U., Bruce, R.A., O'Connor, S.M., Crespi, J.N., Achenbach, L.A., 1999. Ubiquity and diversity of dissimilatory (per)chlorate-reducing bacteria. *Appl. Environ. Microbiol.* 65 (12), 5234–5241.
- Cole, J.R., Chai, B., Farris, R.J., Wang, Q., Kulam-Syed-Mohideen, A.S., McGarrell, D.M., Bandela, A.M., Cardenas, E., Garrity, G.M., Tiedje, J.M., 2007. The ribosomal database project (RDP-II): introducing myRDP space and quality controlled public data. *Nucleic Acids Res.* 35, D169–D172.
- Dojka, M.A., Hugenholtz, P., Haack, S.K., Pace, N.R., 1998. Microbial diversity in a hydrocarbon- and chlorinated-solvent-contaminated aquifer undergoing intrinsic bioremediation. *Appl. Environ. Microbiol.* 64 (10), 3869–3877.
- Gullick, R.Q., Lechvallier, M.W., Barhorst, T.A.S., 2001. Occurrence of perchlorate in drinking water sources. *J. Am. Water Works Assoc.* 93 (1), 66–77.
- Hanaki, K., Saito, T., Matsuo, T., 1997. Anaerobic treatment utilizing the function of activated carbon. *Water Sci. Technol.* 35 (8), 193–201.
- Hatzinger, P.B., 2005. Perchlorate biodegradation for water treatment. *Environ. Sci. Technol.* 39 (11), 239A–247A.
- Herzberg, M., Dosoretz, C.G., TARRE, S., Green, M., 2003. Patchy biofilm coverage can explain the potential advantage of BGAC reactors. *Environ. Sci. Technol.* 37 (18), 4274–4280.
- Jaar, M.A.A., Wilderer, P.A., 1992. Granular activated carbon sequencing batch biofilm reactor to treat problematic wastewaters. *Water Sci. Technol.* 26 (5–6), 1195–1203.
- Kim, K., Logan, B.E., 2000. Fixed-bed bioreactor treating perchlorate-contaminated waters. *Environ. Eng. Sci.* 17 (5), 257–265.
- Lin, R., 2004. Bacterial community analysis and optimization of biologically active carbon filters used to remove perchlorate from groundwater.
- Losi, M.E., Giblin, T., Hosangadi, V., Frankenberger, J., 2002. Bioremediation of perchlorate-contaminated groundwater using a packed bed biological reactor. *Bioremediation J.* 6 (2), 97.
- Matos, C.T., Velizarov, S., Crespo, J.G., Reis, M.A.M., 2006. Simultaneous removal of perchlorate and nitrate from drinking water using the ion exchange membrane bioreactor concept. *Water Res.* 40 (2), 231–240.
- McCarty, P.L., Meyer, T.E., 2005. Numerical model for biological fluidized-bed reactor treatment of perchlorate-contaminated groundwater. *Environ. Sci. Technol.* 39 (3), 850–858.
- Min, B., Evans, P.J., Chu, A.K., Logan, B.E., 2004. Perchlorate removal in sand and plastic media bioreactors. *Water Res.* 38 (1), 47–60.
- Nerenberg, R., Rittmann, B.E., 2004. Hydrogen-based, hollow-fiber membrane biofilm reactor for reduction of perchlorate and other oxidized contaminants. *Water Sci. Technol.* 49 (11–12), 223–230.
- Nerenberg, R., Rittmann, B.E., Najm, I., 2002. Perchlorate reduction in a hydrogen-based membrane-biofilm reactor. *J. Am. Water Works Assoc.* 94 (11), 103–114.
- Niquette, P., Prevost, M., Maclean, R.G., Thibault, D., Coallier, J., Desjardins, R., Lafrance, P., 1998. Backwashing first-stage sand-BAC filters. *J. Am. Water Works Assoc.* 90 (1), 86–97.
- Parette, R., Cannon, F.S., 2005. The removal of perchlorate from groundwater by activated carbon tailored with cationic surfactants. *Water Res.* 39 (16), 4020–4028.
- Prober, R., Pyena, J.J., Kiddon, W.E., 1975. Interactions of activated carbon with dissolved oxygen. *Aiche J.* 21 (6), 1200–1204.
- Reinhold-Hurek, B., Hurek, T., 2000. Reassessment of the taxonomic structure of the diazotrophic genus *Azoarcus sensu lato* and description of three new genera and new species, *Azovibrio restrictus* gen. nov., sp. nov., *Azospira oryzae* gen. nov., sp. nov. and *Azonexus fungiphilus* gen. nov., sp. nov. *Int. J. Syst. Evol. Microbiol.* 50, 649–659.
- Richardson, R.E., Bhupathiraju, V.K., Song, D.L., Goulet, T.A., varez-Cohen, L., 2002. Phylogenetic characterization of microbial communities that reductively dechlorinate TCE based upon a combination of molecular techniques. *Environ. Sci. Technol.* 36 (12), 2652–2662.
- Rikken, G.B., Kroon, A.G.M., vanGinkel, C.G., 1996. Transformation of (per)chlorate into chloride by a newly isolated bacterium: reduction and dismutation. *Appl. Microbiol. Biotechnol.* 45 (3), 420–426.
- Roquebert, V., Booth, S., Cushing, R.S., Crozes, G., Hansen, E. (Eds.), 2000. Electrodialysis reversal (EDR) and ion exchange as polishing treatment for perchlorate treatment, *Desalination* 131 (1–3), 285–291.
- Sutton, P.M., 2006. Bioreactor configurations for ex-situ treatment of perchlorate: a review. *Water Environ. Res.* 78 (13), 2417–2427.
- Urbansky, E.T., 1998. Perchlorate chemistry: implications for analysis and remediation. *Bioremediation J.* 2 (2), 81–95.
- USEPA, 1997. Method 300.1: Determination of Inorganic Anions in Water by Ion Chromatography. US EPA, Cincinnati, OH.
- Zhang, H., Logan, B.E., Regan, J.M., Achenbach, L.A., Bruns, M.A., 2005. Molecular assessment of inoculated and indigenous bacteria in biofilms from a pilot-scale perchlorate-reducing bioreactor. *Microb. Ecol.* 49 (3), 388–398.
- Zhu, X.Y., Lee, S.M., Lee, Y.H., Frauenheim, T., 2000. Adsorption and desorption of an O-2 molecule on carbon nanotubes. *Phys. Rev. Lett.* 85 (13), 2757–2760.

## Appendix C

### Membrane Hybridization Results

Table C.1. Sequences for PNA MB probes and DNA oligonucleotide probes targeting *Dechloromonas* and *Dechlorosoma*.

No	Name	Sequence (5'-3')	Target	Type	Fluo. Label for PNA MB
1	S-G-Dmonas-0121-a-A-18	AAG-GTA-CGT-TCC-GAT-ACA	<i>Dechloromonas</i>	PNA MB and DNA probe	TAMRA
2	S-G-Dmonas-0441-a-A-18	TGC-GAT-TTC-TTC-CCG-GCC	<i>Dechloromonas</i>	DNA probe	
3	S-G-Dsoma-0848-a-A-17	TAG-CTG-CGG-TAC-TAA-AA	<i>Dechlorosoma</i>	PNA MB and DNA probe	TAMRA
4	S-G-Dsoma-1015-a-A-18	TTC-GGG-CAC-CAA-TCC-ATC	<i>Dechlorosoma</i>	DNA probe	

Table C.2. Target and non-target bacterial species used in probe characterization.

No	1	2	3	4
<b>Probe name</b>	S-G-Dmonas-0121-a-A-18	S-G-Dmonas-0441-a-A-18	S-G-Dsoma-0848-a-A-17	S-G-Dsoma-1015-a-A-18
<b>Probe sequence (5'-3')</b>	AAGGTACGT TCCGATACA	TGCGATTTT TTCCCGGCC	TAGCTGCGG TACTAAAA	TTCGGGCAC CAATCCATC
<b>Target</b>	<b>Name</b>	<i>Dechloromonas agitata</i>	<i>Dechloromonas agitata</i>	<i>Dechlorosoma suillum</i>
	<b>Source</b>	DSMZ: DSM 13637		DSMZ: DSM 13638
<b>Non-target with 1 mismatch</b>	<b>Name</b>		<i>Marinospirillum minutulum</i>	<i>Duganella zoogloeoides</i>
	<b>Source</b>		ATCC 19193	ATCC 19544
<b>Non-target with 2 mismatches</b>	<b>Name</b>	<i>Methylophilus methylotrophus</i>	<i>Propionibacter pelophilus</i> strain asp 66	<i>Lactobacillus sanfranciscensis</i> strain Kline L-2
	<b>Source</b>	ATCC 53528	DSMZ: DSM 12018	ATCC 27651
				<i>Comamonas testosteroni</i> strain RH 1104 ATCC 11996
				ATCC 11996

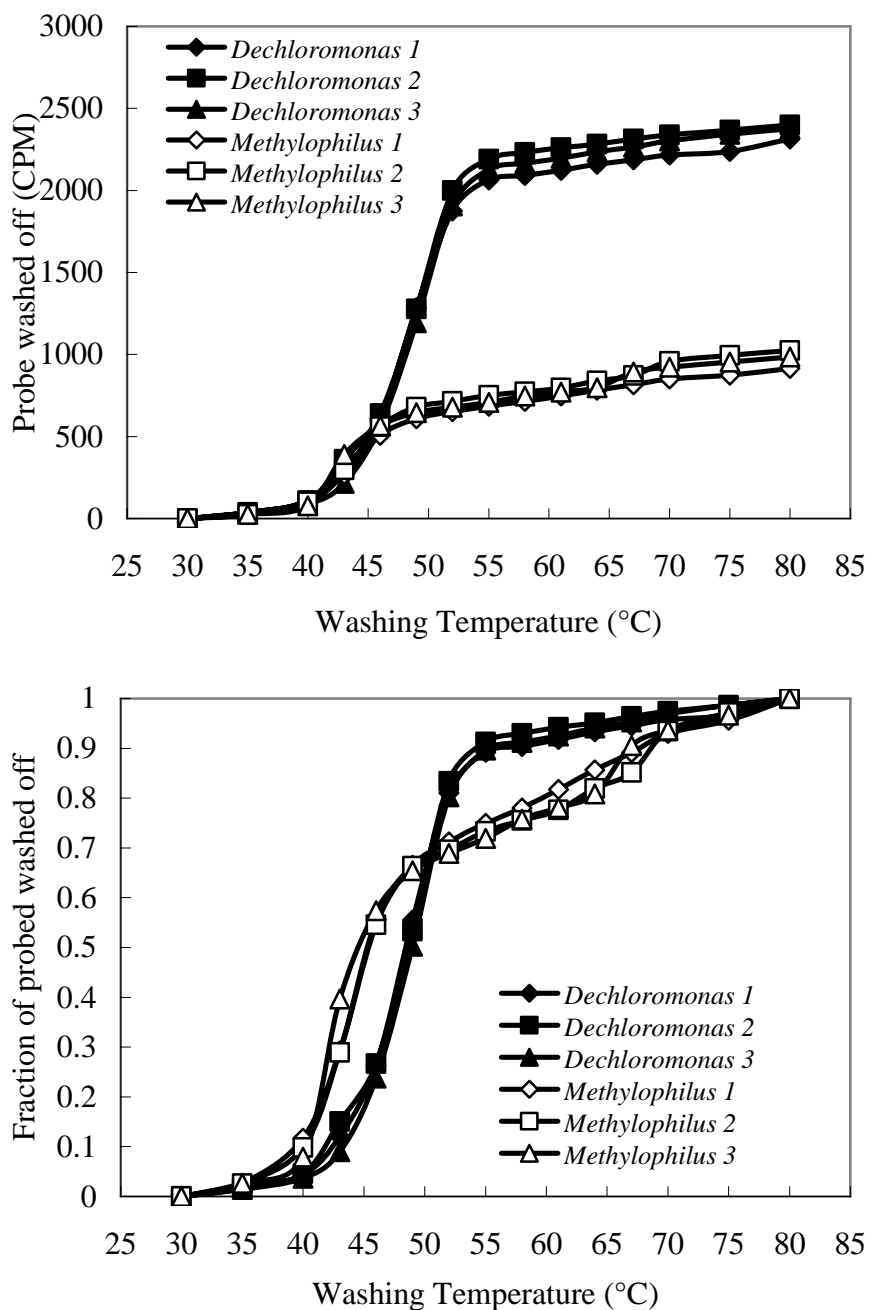


Figure C.1.  $T_d$  curves of DNA oligonucleotide probe S-G-Dmonas-0121-a-A-18 using the elution method. Target and non-target RNA extracts were from *Dechloromonas agitata* and *Methylophilus methylotrophus*, containing 0 and 2 mismatches with the probe, respectively. Top: absolute signals. Bottom: normalized signals.

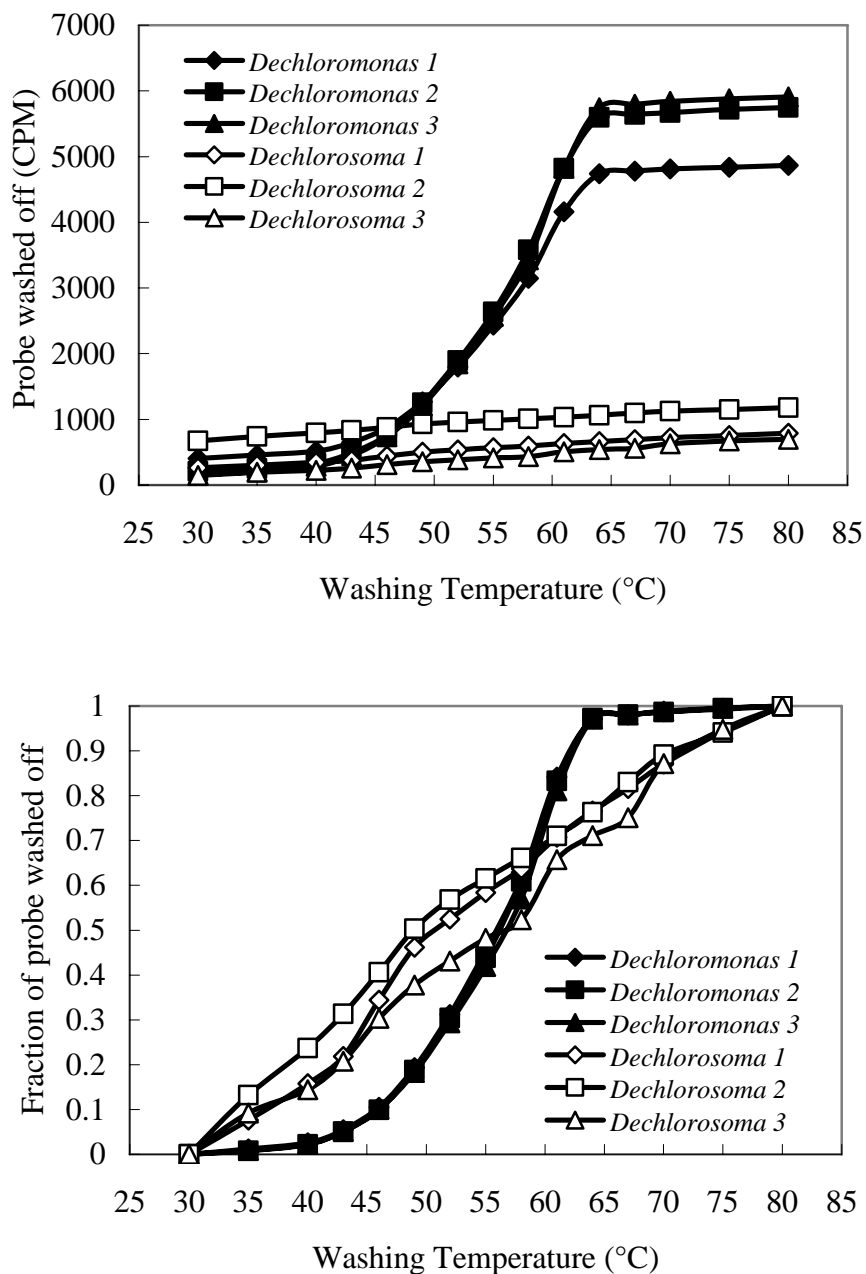


Figure C.2.  $T_d$  curves of DNA oligonucleotide probe S-G-Dmonas-0441-a-A-18 using the elution method. Target and non-target RNA extracts were from *Dechloromonas agitata* and *Dechlorosoma suillum*, containing 0 and 2 mismatches with the probe, respectively. Top: absolute signals. Bottom: normalized signals.

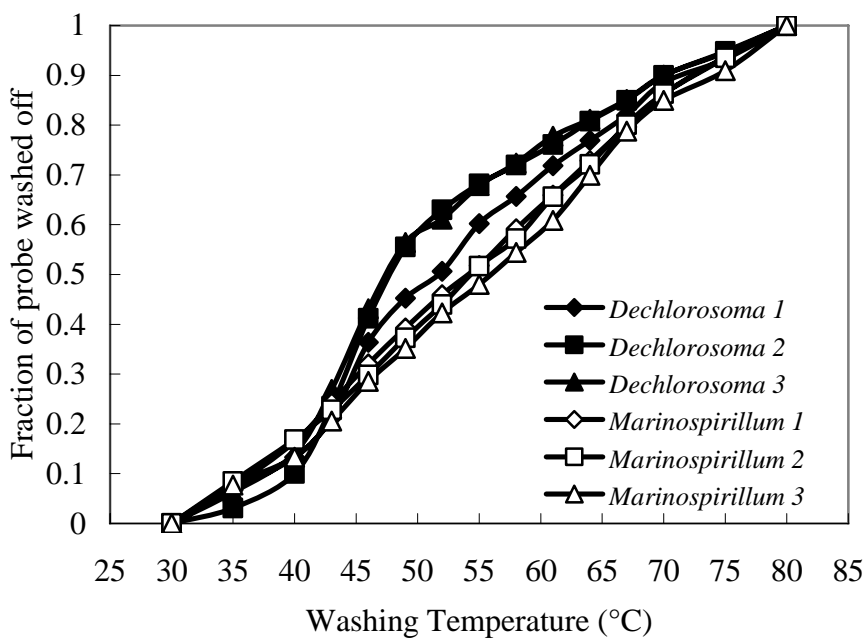
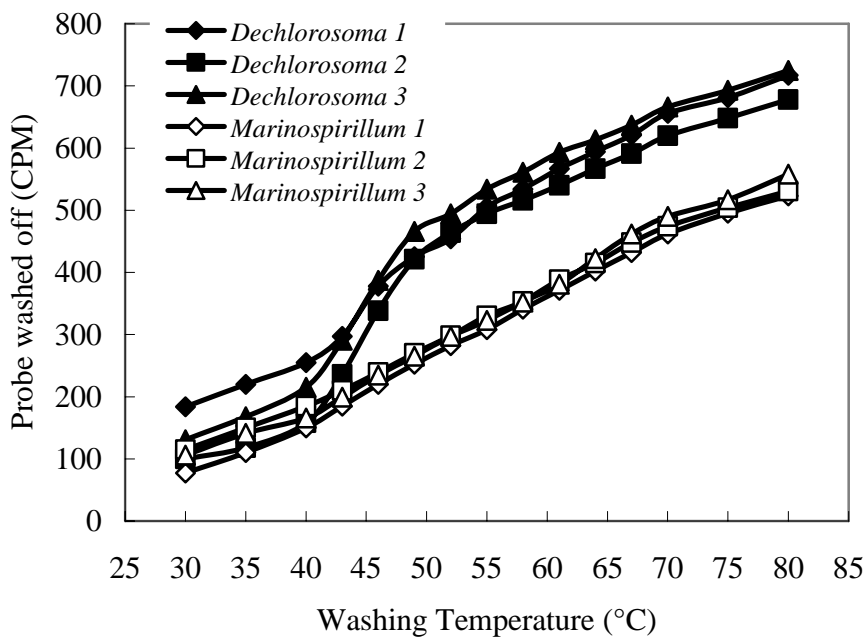


Figure C.3.  $T_d$  curves of DNA oligonucleotide probe S-G-Dsoma-0848-a-A-17 using the elution method. Target and non-target RNA extracts were from *Dechlorosoma suillum* and *Marinospirillum minutulum*, containing 0 and 1 mismatch with the probe, respectively. Top: absolute signals. Bottom: normalized signals.



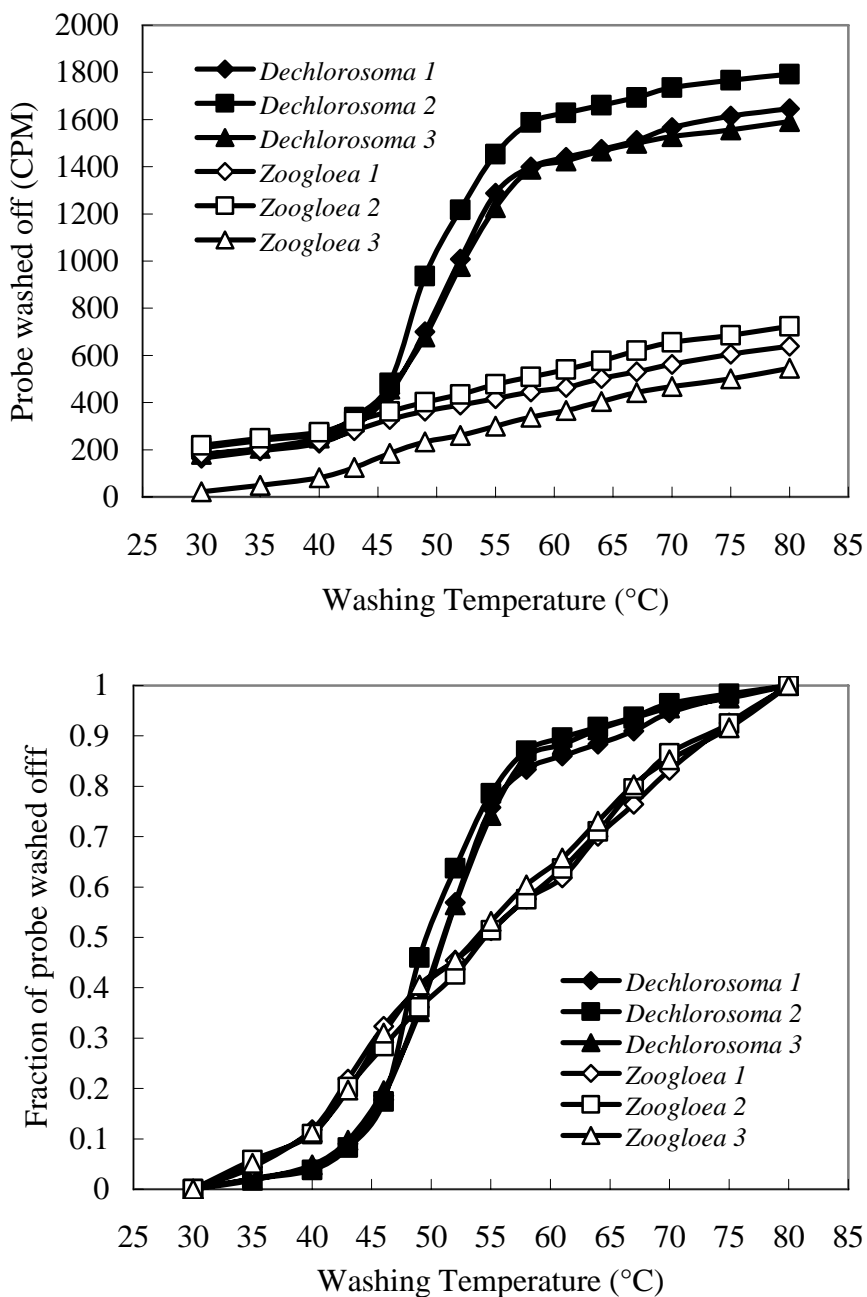


Figure C.4.  $T_d$  curves of DNA oligonucleotide probe S-G-Dsoma-1015-a-A-18 using the elution method. Target and non-target RNA extracts were from *Dechlorosoma suillum* and *Zoogloea ramigera*, containing 0 and 1 mismatch with the probe, respectively. Top: absolute signals. Bottom: normalized signals.

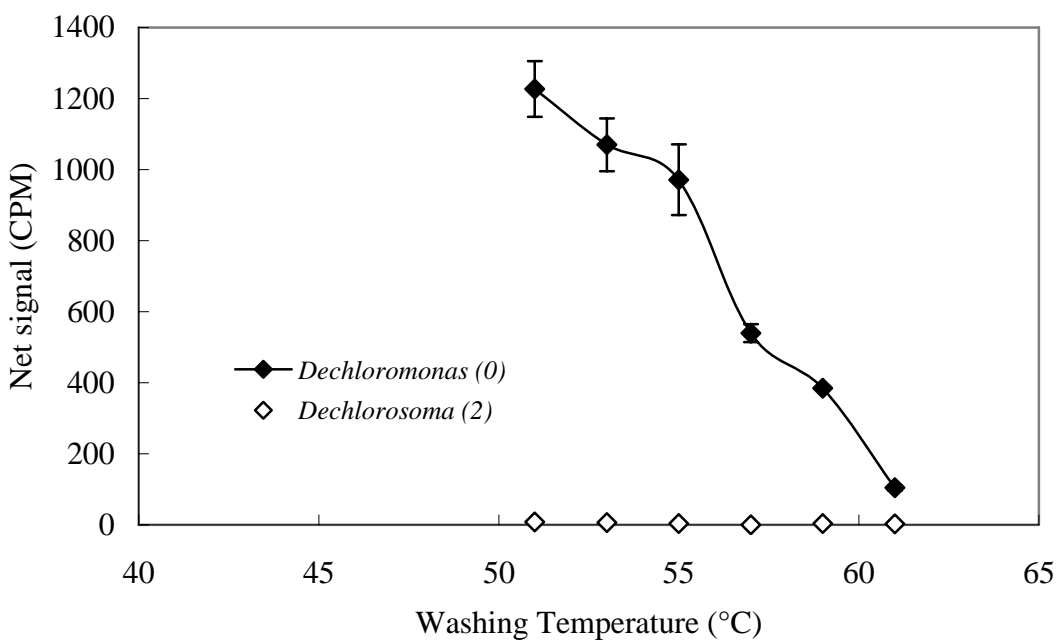
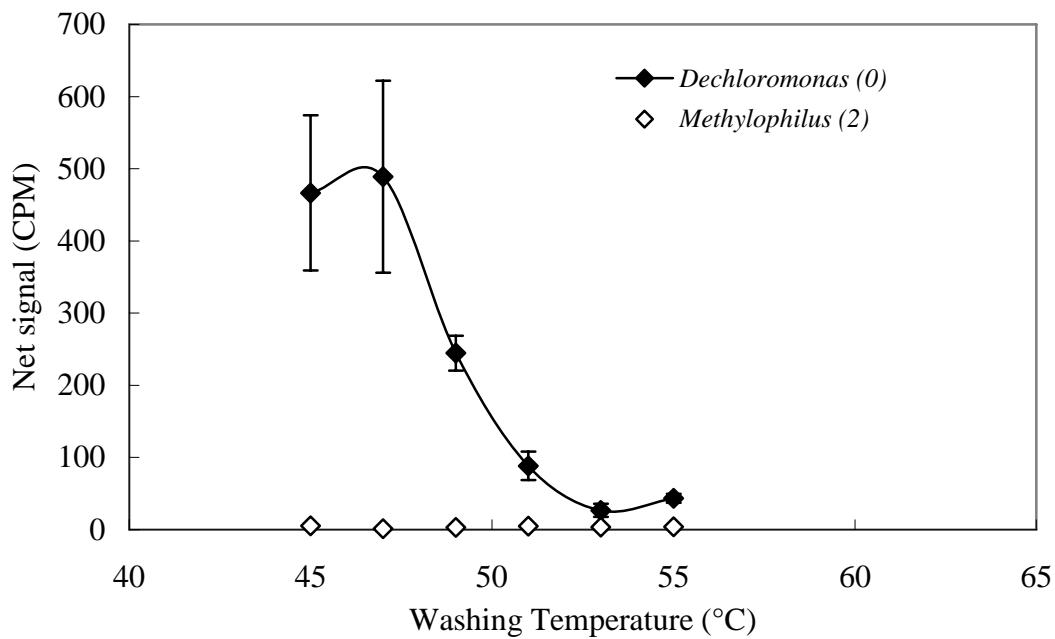


Figure C.5. Fine tune of  $T_d$  for the two DNA oligonucleotide probes targeting *Dechloromonas* spp.. The numbers in parentheses indicate the number of mismatches between 16S rRNA and corresponding DNA probes. Top: S-G-Dmonas-0121-a-A-18. Bottom: S-G-Dmonas-0441-a-A-18.

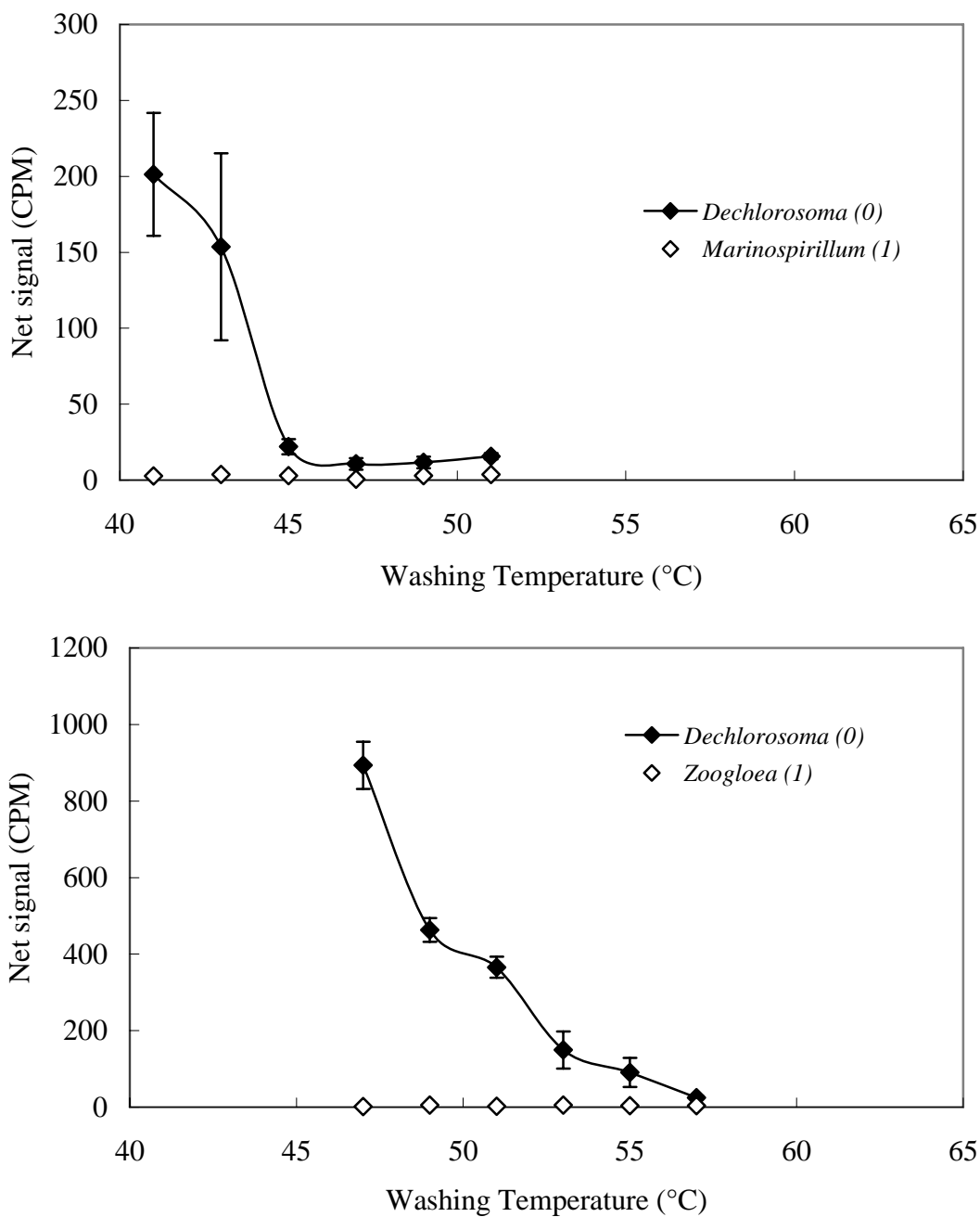


Figure C.6. Fine tune of  $T_d$  for the two DNA oligonucleotide probes targeting *Dechlorosoma* spp.. The numbers in parentheses indicate the number of mismatches between 16S rRNA and corresponding DNA probes. Top: S-G-Dsoma-0848-a-A-17. Bottom: S-G-Dsoma-1015-a-A-18.

## Appendix D

### Characterizations of PNA MB Probes Using 16S rRNA and Whole Cells

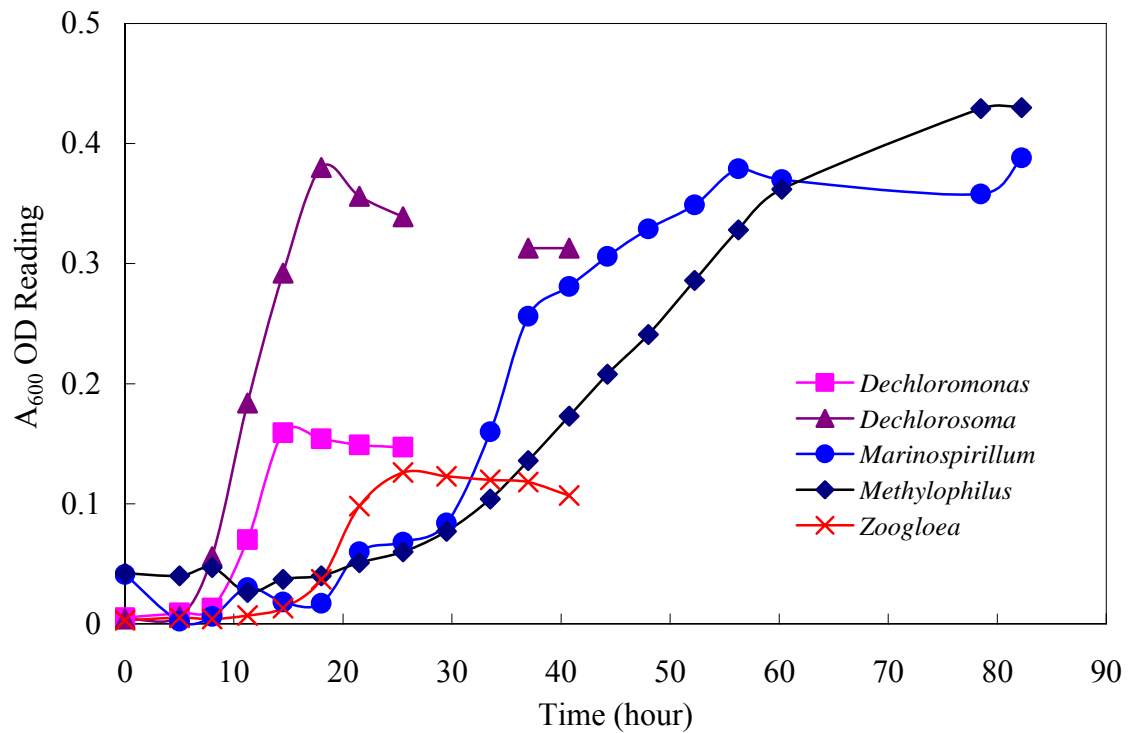


Figure D.1. Growth curves of five bacterial cultures that were used in the characterization experiments for PNA MB probes.

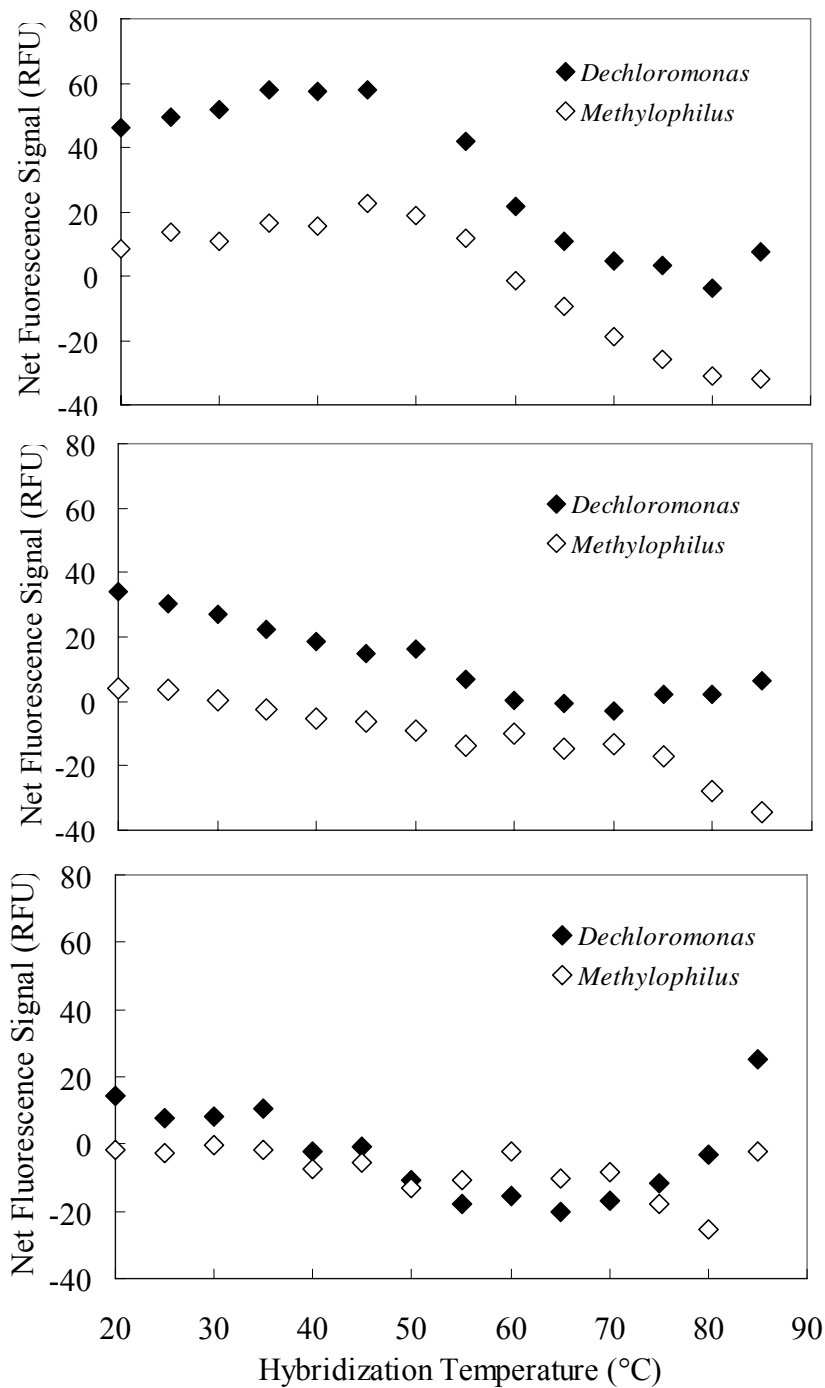


Figure D.2. Characterization of PNA MB probe S-G-Dmonas-0121-a-A-18 using the whole cells of target *Dechloromonas agitata* and non-target *Methylophilus methylotrophus*, containing 0 and 2 mismatches with the probe, respectively. 2.5  $\mu$ L of 5  $\mu$ M PNA MB were added to 100  $\mu$ L hybridization buffers that contained 30% (top), 50% (middle) and 70% (bottom) formamide. RFU: relative fluorescence unit. Background fluorescence signal from non-specific opening of PNA MB was subtracted.

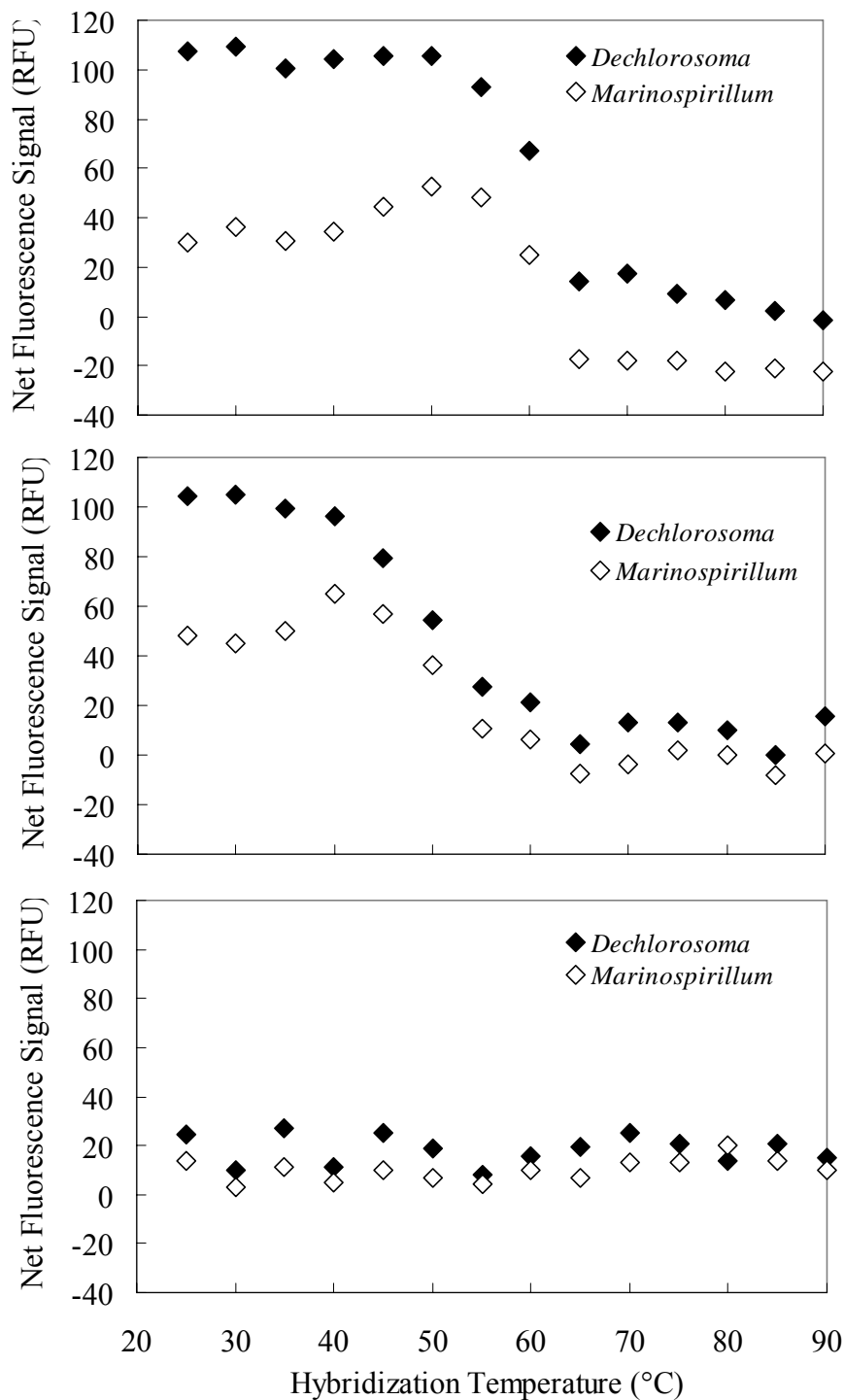


Figure D.3. Characterization of PNA MB probe S-G-Dsoma-0848-a-A-17 using the whole cells of target *Dechlorosoma suillum* and non-target *Marinospirillum minutulum*, containing 0 and 1 mismatch with the probe, respectively. 2.5  $\mu$ L of 5  $\mu$ M PNA MB were added to 100  $\mu$ L hybridization buffers that contained 30% (top), 50% (middle) and 70% (bottom) formamide. RFU: relative fluorescence unit. Background fluorescence signal from non-specific opening of PNA MB was subtracted.

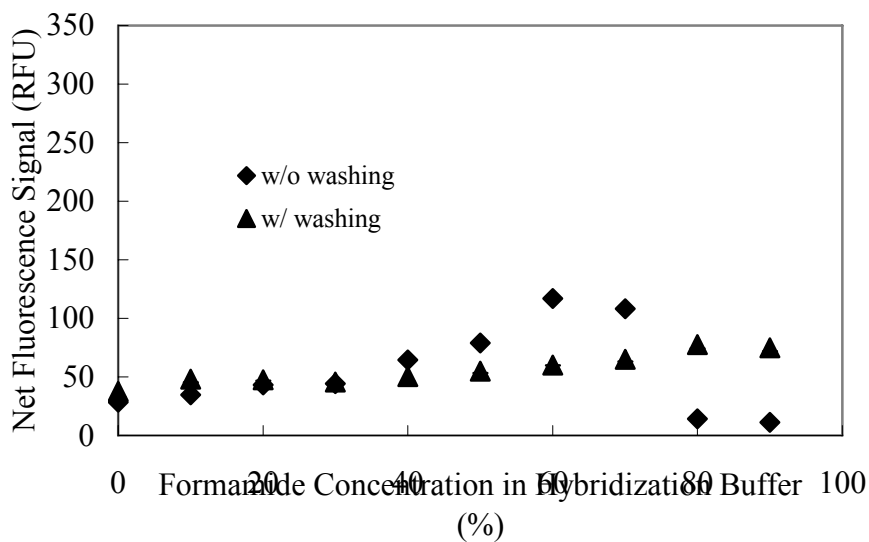
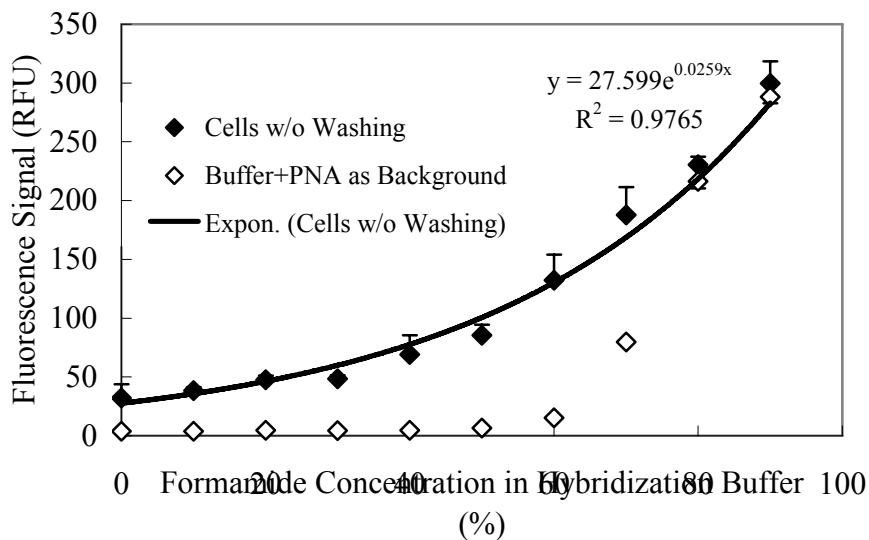


Figure D.4. Fluorescence signals as a function of the formamide concentrations in hybridization buffers for the PNA MB probe S-G-Dmonas-0121-a-A-18. The whole cells of *Dechloromonas agitata* were used as targets. Top: fluorescence signals from the hybridization between PNA MB and the whole cell as well as from the negative control that only contained PNA MB. Bottom: net fluorescence signals from the difference between the two curves in the top plot, and from the whole cell samples that were washed at 50°C for 20 minutes after hybridization.

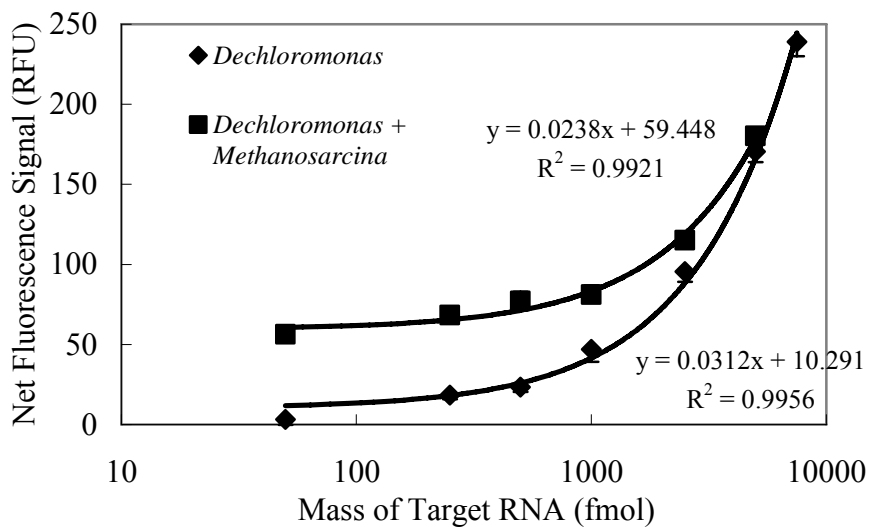


Figure D.5. Specificity test of PNA MB probe S-D-Bact-0338-a-A-16, using 16S rRNA of target *Dechloromonas* and the mixture of 16S rRNA from target *Dechloromonas* and non-target *Methanosarcina*, at a published hybridization condition. Error bars were calculated from standard deviations of triplicates, and some of them are smaller than the symbols.



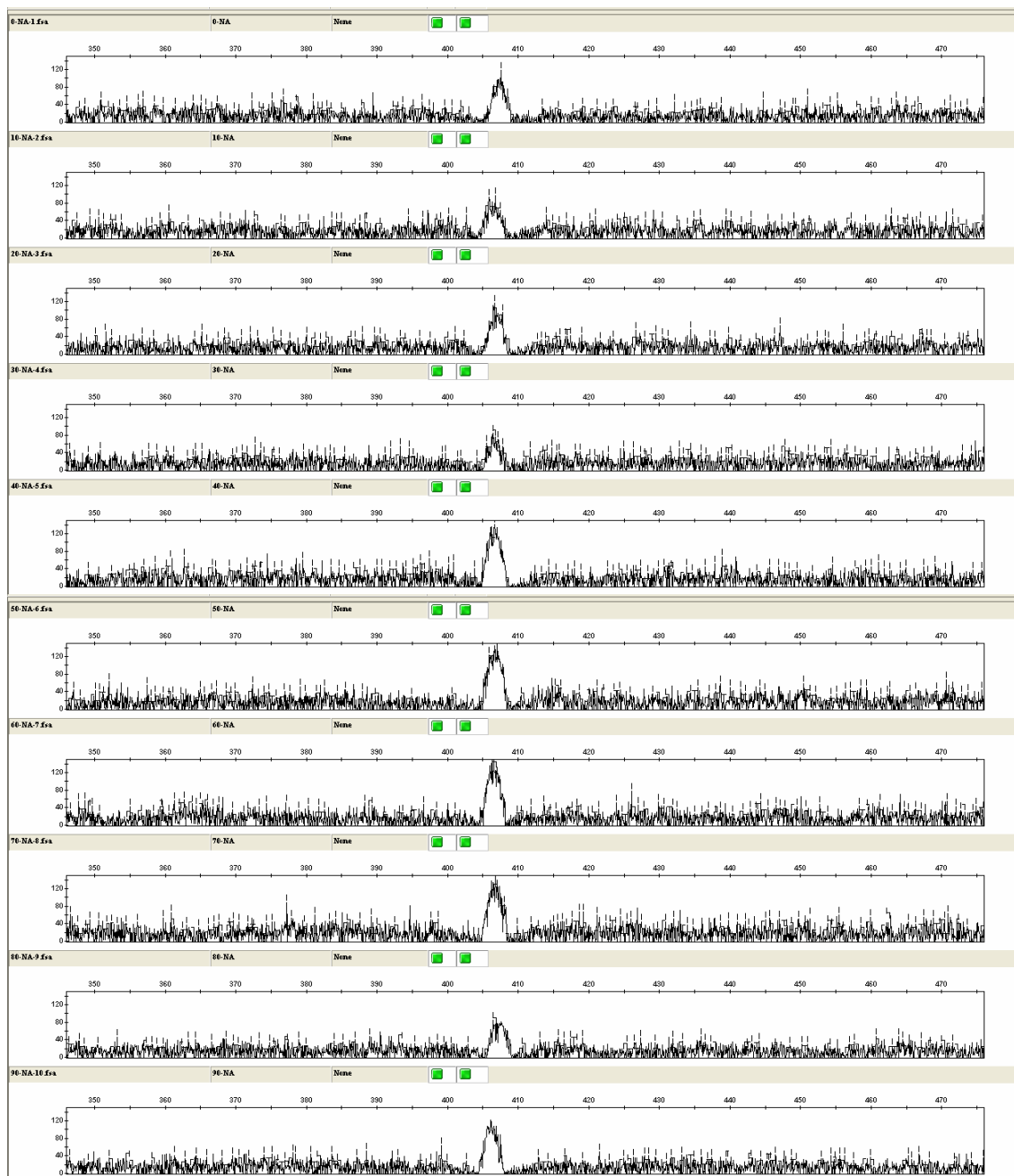


Figure D.6. Sample plots of fluorescence signal from PNA MB probe S-G-Dsoma-0848-a-A-17 hybridized to 16S rRNA of target *Dechlorosoma suillum* measured using capillary electrophoresis. In the ten panels (top to bottom) formamide concentrations in hybridization buffers ranged from 0 to 90% with 10% increment.

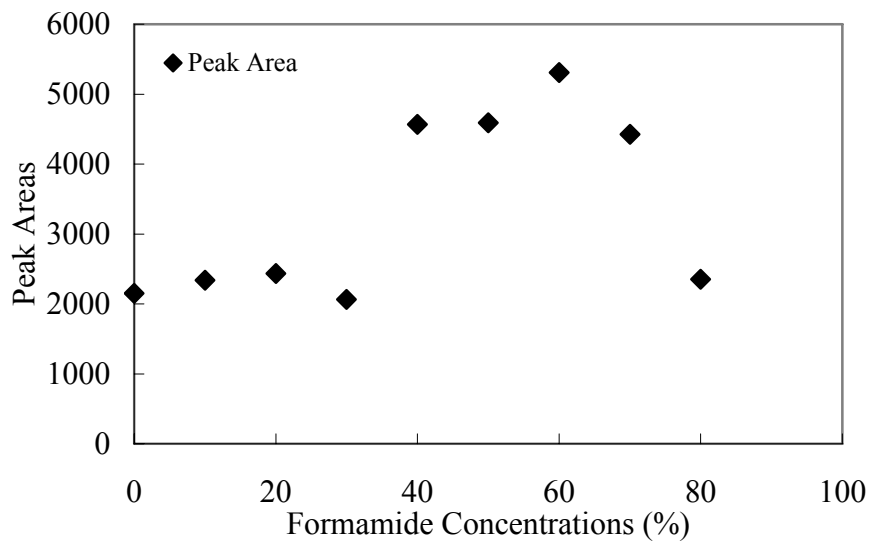


Figure D.7. Peak area collected from Figure D.6 as a function of formamide concentrations in hybridization buffers. The peak area in the test for 90% formamide concentration could not be recognized or calculated by the software.

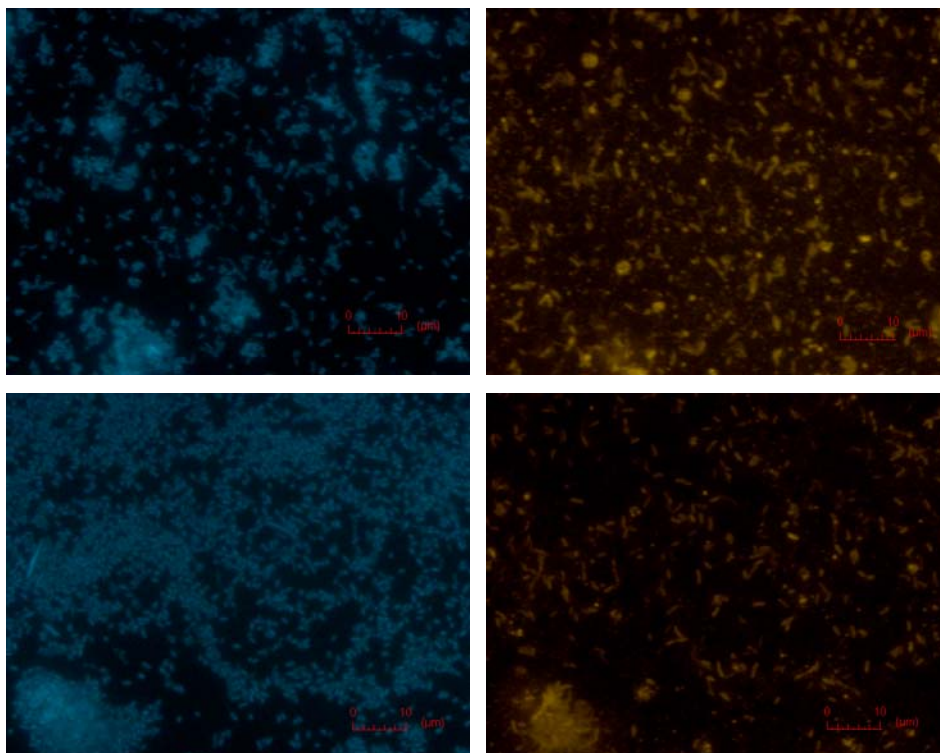


Figure D.8. Characterization of PNA MB probe S-G-Dmonas-0121-a-A-18, using a FISH protocol that did not include a washing step, on target *Dechloromonas agitata* and non-targets *Methylophilus methylotrophus* and *Escherichia coli*. Top: an artificial mixture of *D. agitata* and *M. methylotrophus*. Bottom: an artificial mixture of *D. agitate* and *E. coli*. Left: DAPI staining. Right: fluorescence signals from the PNA MB probe. The final formamide concentration in the hybridization buffers was 70% (v/v).

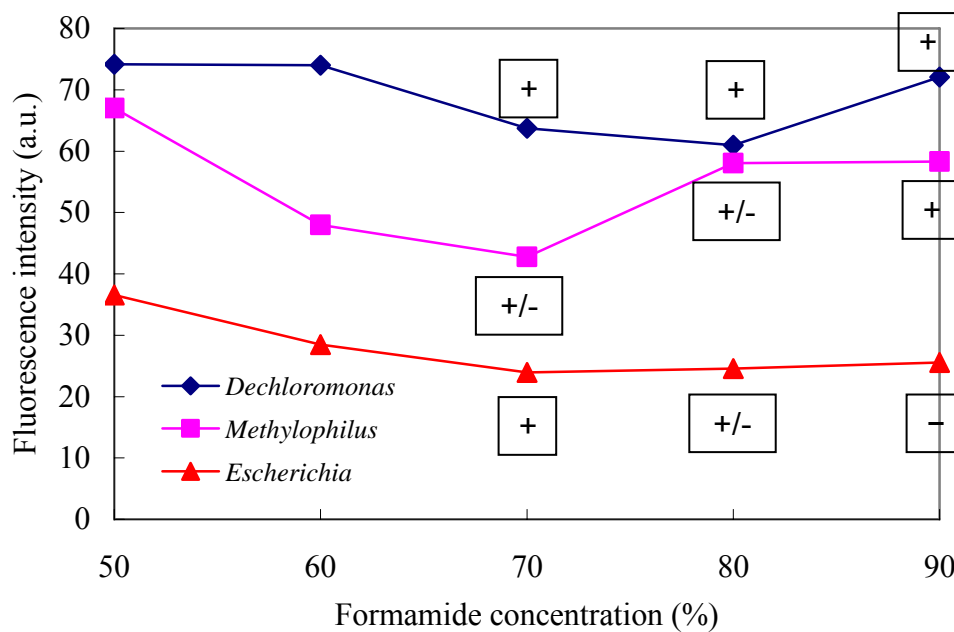


Figure D.9. Fluorescence signals from PNA MB probe S-G-Monas-0121-a-A-18 measured using a flow cytometry. Bacterial species included target *Dechloromonas agitata*, and non-target *Methylophilus methylotrophus* and *Escherichia coli*. The unit a.u. stands for arbitrary unites. “+” and “-” indicate whether the cells were visible and invisible under fluorescence microscope. “+/-” represents visibility between “+” and “-”.

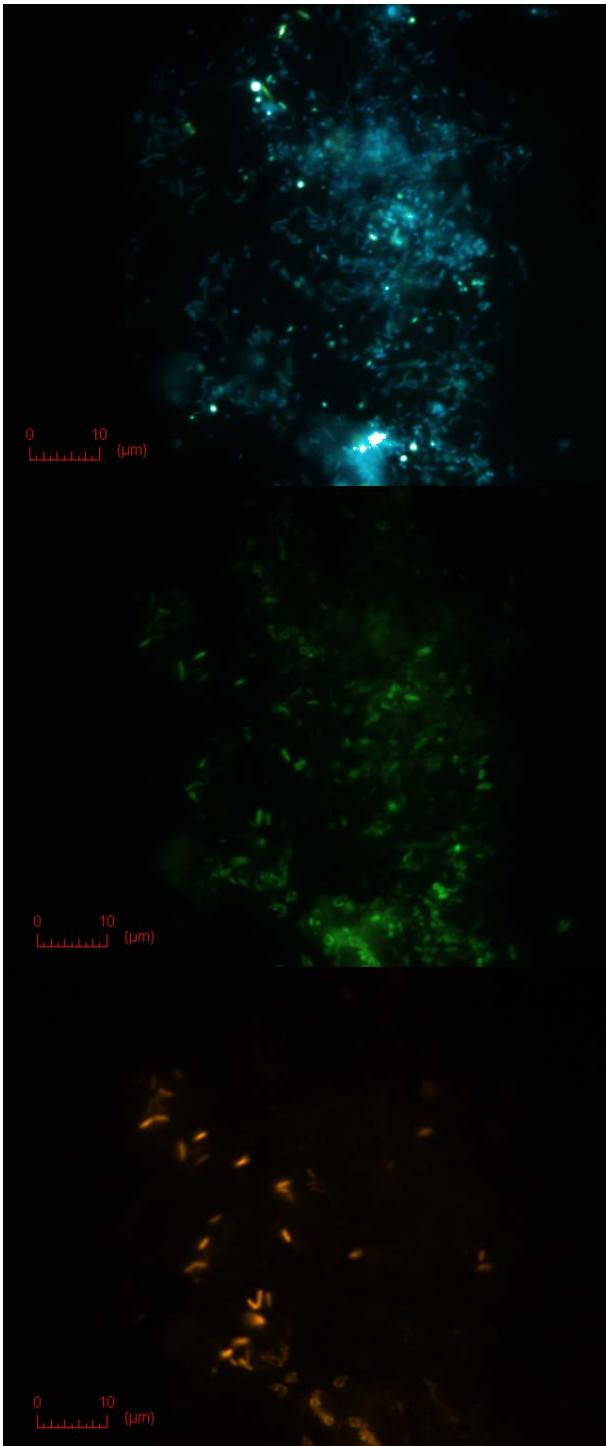


Figure D.10. FISH images, obtained by following a protocol that include a washing step, on environmental samples. Top: DAPI staining. Middle: PNA MB S-D-Bact-0338-a-A-16. Bottom: PNA MB S-G-Dmonas-0121-a-A-18.

## Appendix E

### Microbial Community Analysis of a Biologically Active Carbon Reactor Operated for Perchlorate Removal

#### 1. Abstract

A sample of biologically active carbon (BAC) was collected from a pilot-scale bioreactor operated by Carollo Engineers and transported on ice to the University of Illinois in February 2005. Two methods targeting the 16S ribosomal rRNA gene were used to identify the major bacterial populations in the sample, i.e., terminal restriction fragment length polymorphism (T-RFLP) and construction of a clone library combined with a phylogenetic analysis. The T-RFLP approach was designed to detect the two major genera of perchlorate-reducing bacteria so far identified, i.e., *Dechloromonas* and *Dechlorosoma* (*Dechlorosoma* is also called *Azospira*, Tan and Reinhold-Hurek, 2003). The T-RFLP results indicated that both *Dechloromonas* and *Dechlorosoma* species were present and comprised  $6.1 \pm 2.4\%$  and  $1.9 \pm 0.8\%$ , respectively, of the total bacteria in the sample. The clone library and phylogenetic analysis results indicated that *Beta*-, *Epsilon*-, and *Deltaproteobacteria* were the dominant groups in the sample and comprised 62%, 36%, and 2%, respectively, of the total bacteria. A detailed phylogenetic analysis determined that the closest cultured

relatives to clones identified in the sample were perchlorate-, nitrate-, and sulfate-reducing bacteria.

## **2. Materials and Methods**

### ***2.1 Sample***

A sample of biologically active carbon (BAC) was collected from a pilot-scale bioreactor operated by Carollo Engineers and transported overnight on dry ice to the University of Illinois. The sample was received on February 25, 2005. The sample was aliquotted and processed upon arrival.

### ***2.2 T-RFLP***

Total DNA was extracted from three subsamples using the Ultra Clean Soil DNA Kit (MoBio Lab Inc, Carlsbad, CA). Bacterial 16S ribosomal RNA (rRNA) genes were amplified using the polymerase chain reaction (PCR). A forward primer specific for the bacterial domain, S-D-Bact-0027-a-S-20 (AGAGTTTGATCMTGGCTCAG), labeled with the fluorescent dye Carboxyfluorescein (FAM), and a universal reverse primer, S-\*-Univ-1392-a-A-15 (ACGGGCGGTGTGTRC) (Stahl *et al.*, 1988) were used as the primer set. Reaction mixtures were set at 50  $\mu$ L and contained 2  $\mu$ L 10 ng/ $\mu$ L template (quantified using NanoDrop, Wilmington, DE), 2.5 units of ExTaq DNA Polymerase (Takara Shuzo Co., Ltd., Otsu, Japan), 5  $\mu$ L 10X reaction buffer (Takara Shuzo Co., Ltd.), 4  $\mu$ L dNTP mixture (2.5 mM each), 4  $\mu$ L 25-mM MgCl<sub>2</sub>, and primers at 10 pmol each. PCR was performed as follows: 5 min at 94°C (hot

start); 1 min at 94°C, 1 min at 55°C, and 1.5 min at 72°C (30 cycles); and a final 8-min extension step at 72°C.

PCR products were purified using a QIAquick PCR Purification Kit (Qiagen Inc., Chatsworth, CA), and the purified DNA was digested using restriction enzymes *FauI* and *MaeIII* (New England Biolabs, Inc., Beverly, MA, enzymes were chosen using a program presented in Klein *et al.* 2005) at 55°C for 3 hours followed by inactivation at 65°C for 20 min. A desalting procedure was performed to further purify the digested DNA fragment. In every 10 µL digested DNA sample, 0.25 µL of 20 mg/mL glycogen (Roche Applied Science, Penzberg, Germany) and 1 µL of 3 M sodium acetate (pH=5.2) were added and gently mixed. 25 µL of ice-cold 95% ethanol was added, and the samples were stored at -20°C for 30 min followed by a centrifugation at 16,100 g for 15 min. The supernatants were removed and 200 µL of ice-cold 70% ethanol was added followed by a centrifugation at 16,100 g for 2 min. The supernatant was removed and the DNA fragment was re-suspended in 10 µL distilled deionized water after air drying for 15 min.

Purified fragments were analyzed using an ABI Prism 3730xl Analyzer (Applied Biosystem Instrument, Foster City, CA) at the W.M. Keck Center for Comparative and Functional Genomics at the University of Illinois at Urbana-Champaign Biotechnology Center (Urbana, IL). T-RFLP results were analyzed using GeneMapper v.3.7 (Applied Biosystems Instruments). The *Dechloromonas* and *Dechlorosoma* 16S rRNA genes should theoretically generate terminal restriction fragments (T-RFs) with sizes of 149 bp and 151 bp, respectively,



when digested with *MaeIII*. The corresponding T-RF sizes for digestion with *FauI* were predicted to be 926 bp and 485 bp, respectively. Using pure cultures of *Dechloromonas* and *Dechlorosoma* species as positive controls, additional fragment sizes that were not predicted by the initial *in silico* analysis were detected. These additional fragments were present due to incomplete digestion, resulting in fluorescent T-RFs of multiple sizes. For enzyme *FauI*, the presence of the reverse complementary sequence of its recognition site in the 16S rRNA gene sequences also contributed to the generation of multiple fluorescent T-RFs. Relevant fragment sizes are listed in Table 1. The abundance of *Dechloromonas* and *Dechlorosoma* was determined by dividing the sum of the peak areas for target T-RFs by the total area contributed by all peaks.

Table E.1. Actual T-RF sizes determined with pure cultures of *Dechloromonas agitata* and *Dechlorosoma suillum* after digestion with enzymes *FauI* and *MaeIII*. The sequences represent recognition sites for the enzymes and arrow heads indicate the locations where the enzymes cut. The numbers in parentheses are the theoretical fragment sizes.

	T-RF sizes (bp)		
	<i>FauI</i>		<i>MaeIII</i>
	5'..CCCGC(N) <sub>4</sub> ~..3'	5'..~(N) <sub>6</sub> GCGGG..3'	5'..~GTNAC..3'
<i>Dechloromonas</i>	929 (926)	267.1 (269) and 267.9 (269)	147.5 (149) and 627.5 (625)
<i>Dechlorosoma</i>	485 (485)	177.7 (180), 421.8 (424), and 422.7 (424)	149 (151)

## 2.2 Clone Library

The PCR reaction for the clone library was similar to the one for T-RFLP, except for the following two modifications: 1) an unlabeled forward primer,

S-D-Bact-0027-a-S-20, was used; 2) the extension time at the end of the PCR reaction was 20 min instead of 8 min. Clones of amplified 16S rRNA genes were generated using a TOPO TA Cloning Kit for Sequencing (Invitrogen Corp., Carlsbad, CA). Colony PCRs were performed on 83 single colonies with a primer set located on the plasmid used in the cloning kit (T3 and T7). Thereafter, 42 amplicons of the correct size (approximately 1,400 base pairs) were digested with enzyme *Hae*III. After visualization of the digestion products on 1.5% NuSieve 3:1 agarose (Cambrex Bio Science Inc., Rockland, ME), 11 unique clones were selected and plasmid DNA was extracted for sequencing at the W.M. Keck Center at the University of Illinois at Urbana-Champaign. A phylogenetic tree was built using MacVector 7 (by Accelrys). The tree was prepared with 386 unambiguously aligned basepairs starting from the reverse primer using the CLUSTALW method. Bootstrap values were annotated to each branch using neighbor joining method and the algebra of Tamura-Nei. The tree was rooted by using the 16S rDNA sequence from *Escherichia coli* as an outgroup.

### **3. Results**

#### ***3.1 T-RFLP***

The abundances of *Dechloromonas* and *Dechlorosoma* were expressed as percentages of the total bacterial community for each of the three sub-samples extracted. Results obtained with both enzymes (*Fau*I and *Mae*III) indicated *Dechloromonas* and *Dechlorosoma* were present in the BAC sample. When *Fau*I was used,  $6.1 \pm 2.4\%$  of the bacteria were estimated to belong to the genus *Dechloromonas*, while  $2.0 \pm 2.3\%$

were estimated to belong to *Dechlorosoma*. The corresponding numbers obtained with the enzyme *MaeIII* were  $12.9 \pm 6.6\%$  and  $1.9 \pm 0.8\%$ , respectively.

The estimates of the relative abundance of *Dechloromonas* obtained with the two enzymes were quite different. A search in the Ribosomal Database Project (RDP, <http://rdp.cme.msu.edu>) indicated that some beta-proteobacteria could contribute to false-positive signals for *MaeIII*. It is possible that these beta-proteobacteria were present in the BAC sample and contributed to the high abundance obtained with *MaeIII*. Therefore, the estimate obtained with *FauI* (lower value) is preferred over the percentage determined with *MaeIII*.

The abundance of *Dechlorosoma* was substantially lower than that of *Dechloromonas*. This observation is consistent with previous observations with samples collected from perchlorate-reducing BAC reactors (Lin *et al.*, 2005).

### **3.2 Clone Library**

Out of 42 identifiable clones, 26 (62%), 15 (36%), and one (2%) belonged to the beta-proteobacteria, epsilon-proteobacteria, and delta-proteobacteria, respectively. Further phylogenetic analysis indicated that five clones that grouped within the beta-proteobacteria (e.g., clones A10 and D5-2, representing 12% of the total bacteria) were close relatives of *Dechloromonas* species, as shown in Figure 1. Therefore, these five clones likely functioned as perchlorate-reducing bacteria. The other 21 clones in the beta-proteobacteria (e.g., clones F4, C3-2, B6-2, A11-2, and H8, representing 50% of the total bacteria) were closely related to two uncultured representatives in the Genbank database (<http://www.ncbi.nlm.nih.gov>), i.e., clones

Orbal D41 and D54. These clones were obtained from a wastewater treatment plant operated for enhanced biological phosphorus removal. Clone Orbal D41 was believed to represent a phosphorus accumulating organism (Zilles *et al.*, 2002). No clones were found to have a high similarity to the genus *Dechlorosoma*.

The 15 clones in the epsilon-proteobacteria (represented by clones E1, H6, and H10) exhibited 93% identity to *Thiomicrospira denitrificans*, a thiosulphate-oxidizing, nitrate-reducing microorganism recovered from a deep-sea hydrothermal vent sample (Muyzer *et al.*, 1995). Assuming 16S rRNA gene similarity can be used to derive physiological information, this result may indicate that the BAC reactor contained bacteria using nitrate as their electron acceptor and reduced sulfur compounds as their electron donor. The clone in the delta-proteobacteria (clone B7) is a close relative of *Desulfobacter postgatei* (95% identity, not shown in the tree). *Desulfobacter postgatei* is a sulfate-reducing bacterium (Friedrich, 2002), suggesting that sulfate reduction may have occurred in the BAC reactor.

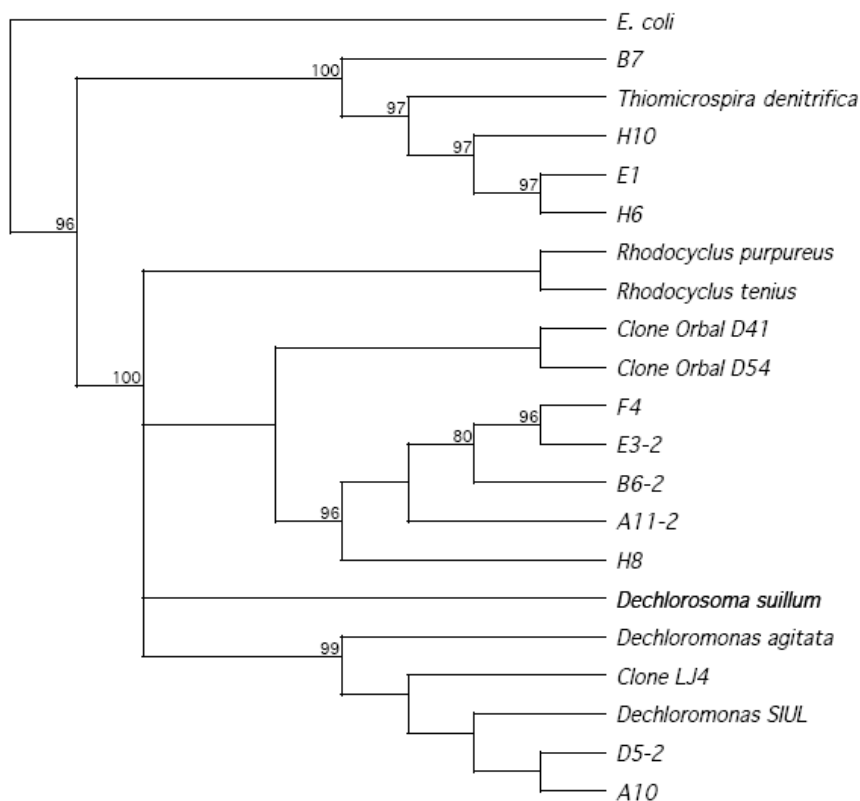


Figure E.1. Phylogenetic tree based on 384 bp of the 16S rRNA genes from the clones recovered from the BAC sample (11 unique clones were sequenced in this study and were given names with an uppercase letter followed by a number). Neighbor Joining Method with bootstrap value of 1000. Distance: Tamura-Nei.

#### 4. Discussion

Beta-, epsilon-, and delta-proteobacteria were identified to be present in the BAC sample using phylogenetic analysis of 16S rRNA gene sequences generated after construction of a clone library. Based on a detailed phylogenetic analysis and comparison of sequencing results with sequence information in public databases, it may be derived that three types of reduction reactions took place in the BAC reactor: perchlorate, nitrate, and sulfate reduction. It should be noted that it is not always

possible to derive physiological information from phylogenetic data, so this conclusion should be interpreted with caution.

The relative abundances of *Dechloromonas* species estimated with T-RFLP and clone library analyses were  $6.1 \pm 2.4\%$  and 12%, respectively. These numbers should be interpreted with caution since the methods used in this study are at best semi-quantitative. Both methods rely on PCR and therefore are subject to typical biases associated with PCR. Furthermore, only a limited number of clones was obtained and sequenced in the clone library analysis.

Using T-RFLP, about 2% of the total bacteria was identified as *Dechlorosoma* species, whereas the clone library analysis did not yield a clone representing this genus. The absence of a *Dechlorosoma* clone was not unexpected given the low relative abundance of this genus and the limited number of clones analyzed.

## References:

- Friedrich, M. W. (2002), Phylogenetic Analysis Reveals Multiple Lateral Transfers of Adenosine-5'-Phosphosulfate Reductase Genes among Sulfate-Reducing Microorganisms. *Journal of Bacteriology* 184: 278-289
- Klein, A. N, Frigon, D., Lin, R., Padmasiri, S., Crawford, J., and Raskin, L. (2005), Targeted Terminal-Restriction Fragment Length Polymorphism: A New Approach to Analyze Complex Microbial Communities. In preparation.
- Lin, R., C. Xi, J. C. Brown, Y. C. Choi, E. Morgenroth, L. Raskin (2005), Use of natural organic matter (NOM) as sole electron donor for perchlorate removal from groundwater in a biologically active carbon (BAC) filter, submitted to *Water Research*
- Muyzer, G., Teske, A., Wirsen, C. O. (1995), Phylogenetic Relationships of *Thiomicrospira* species and their identification in deep-sea hydrothermal vent samples by denaturing gradient gel electrophoresis of 16S rDNA fragments. *Arch. Microbiol.* 164: 165-172
- Stahl, D.A., B. Flesher, H.R. Mansfield, and L. Montgomery (1988), Use of phylogenetically based hybridization probes for studies of ruminal microbial ecology *Appl. Environ. Microbiol.* 54:1079-1084.
- Tan, Z. and Reinhold-Hurek, B. (2003), *Dechlorosoma suillum* Achenbach et al. 2001 is a later subjective synonym of *Azospira oryzae* Reinhold-Hurek and Hurek 2000. *Int. J. Syst. Evol. Microbiol.* 53:1139-1142.
- Zilles, J. L., Peccia, J., Kim, M-W., Hung, C-H., and Noguera, D.( 2002), Involvement of *Rhodocyclus*-Related Organisms in Phosphorus Removal in Full-Scale Wastewater Treatment Plants. *Applied and Environmental Microbiology.* 68: 2763-2769

## Appendix F

### Bench-Scale BAC

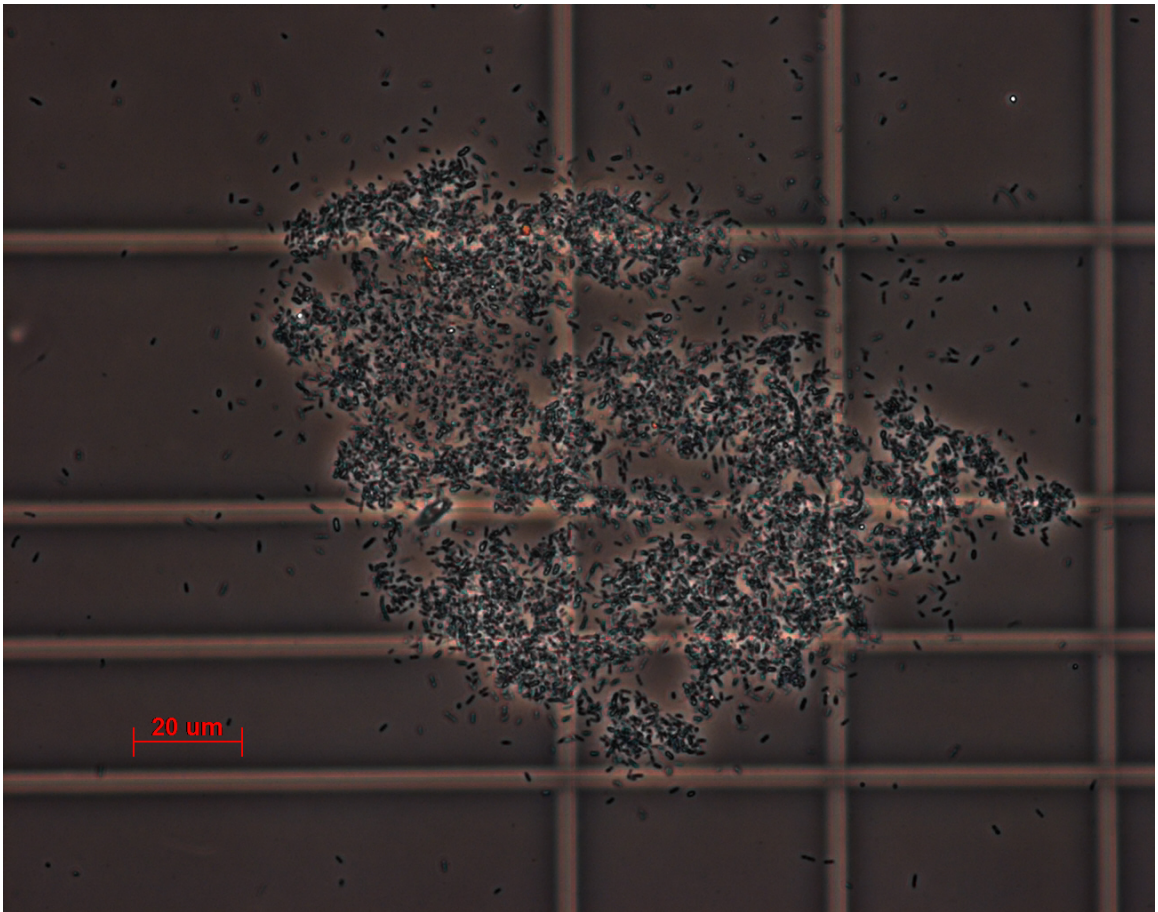


Figure F.1. A cell aggregate and free cells in the effluent of the bench-scale BAC reactor observed under a 50 $\times$  objective of a light microscope.



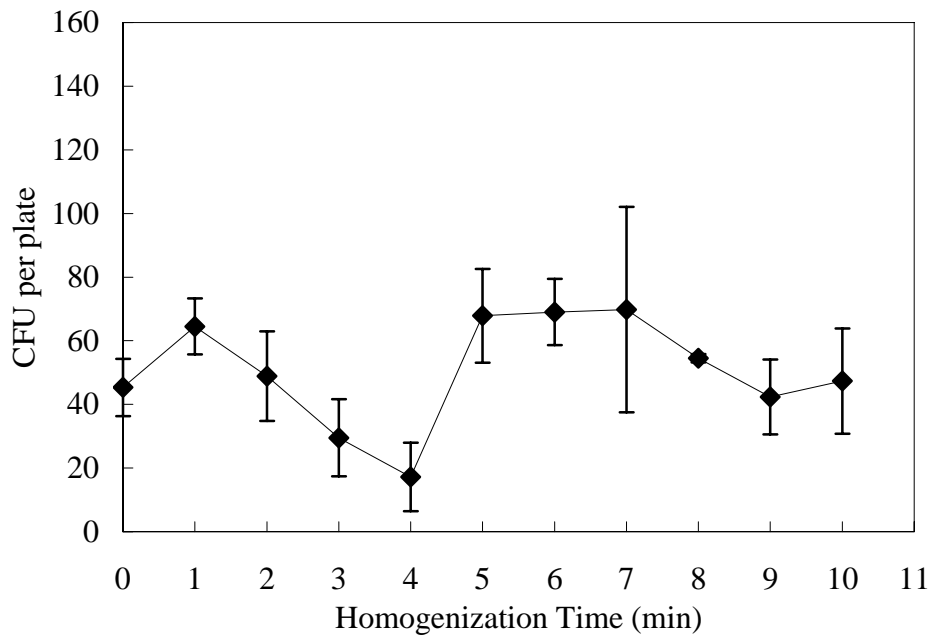
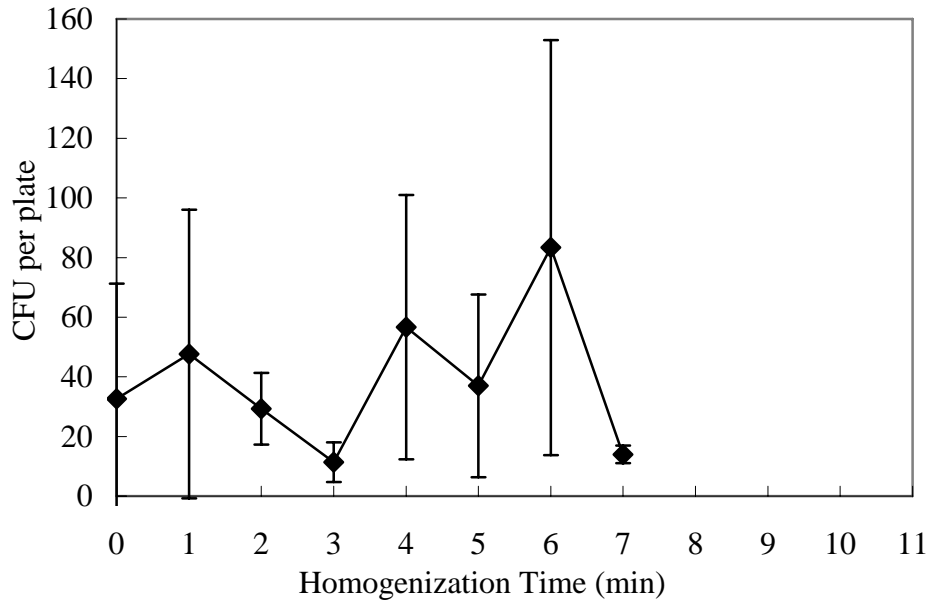


Figure F.2. Homogenization experiment results. The two plots were from two separate experiments.

## **Appendix G**

### **Curriculum Vitae**

## CURRICULUM VITAE

**Xu Li**

**Date of Birth:** July 14<sup>th</sup>, 1979

### Education

Ph.D. in Environmental Engineering, University of Michigan, 2008  
Advisors: Dr. Lutgarde Raskin (University of Michigan) and  
Dr. Eberhard Morgenroth (University of Illinois at Urbana-Champaign)  
M.S. in Environmental Engineering, Pennsylvania State University, 2003  
Advisor: Dr. Bruce E. Logan  
B.E. in Environmental Engineering, Tsinghua University, China, 2001  
Advisor: Dr. Xiaojian Zhang

### Research Experience

Graduate research assistant, DoD project “Direct fixed-bed biological perchlorate destruction”, University of Michigan, Ann Arbor, MI, 2005-2008.  
Graduate research assistant, NSF project “Process optimization, molecular microbial characterization, and biofilm modeling of a bioreactor for perchlorate removal from drinking water”, University of Illinois, Urbana, IL, 2003-2005.  
Graduate research assistant, NSF project “Molecular level analysis of macromolecule-surface interactions in bacterial adhesion”, Pennsylvania State University, University Park, PA, 2001-2003.  
Undergraduate research assistant, project “Biological treatment for micro-polluted drinking water”, Tsinghua University, Beijing, P. R. China, 2000-2001.

### Professional Memberships

American Chemical Society  
American Society for Microbiology  
American Water Works Association  
Association of Environmental Engineering and Science Professors

### Awards and Honors

- First Place, Poster Presentation  
American Water Works Association MI Section, 2007; IL Section 2005
- Fellowship for Water Quality and Treatment Study  
American Water Works Association Michigan Section, 2007
- Kuehn Fellowship  
University of Illinois, 2003-2004
- Fellow of Graduate School  
Pennsylvania State University, 2001-2002